

University of Warwick institutional repository: <http://go.warwick.ac.uk/wrap>

**A Thesis Submitted for the Degree of PhD at the University of Warwick**

<http://go.warwick.ac.uk/wrap/1127>

This thesis is made available online and is protected by original copyright.

Please scroll down to view the document itself.

Please refer to the repository record for this item for information to help you to cite it. Our policy information is available from the repository home page.

# Representing Spatial Interactions in Simple Ecological Models

Andrew John Morris

Submitted for the degree of Doctor of Philosophy

Mathematics Institute  
University of Warwick  
Coventry CV4 7AL

**September 1997**

For mum and dad.

# Contents

<b>1</b>	<b>Introduction</b>	<b>1</b>
1.1	About this Thesis . . . . .	2
1.2	Why model? . . . . .	2
1.3	The History of Modelling in Population Dynamics and Ecology . . . . .	4
1.3.1	Basic Concepts . . . . .	4
1.3.2	Density Dependence . . . . .	5
1.4	Infectious Disease Models . . . . .	8
1.4.1	The Contact Process . . . . .	8
1.4.2	SIR Equations . . . . .	9
1.4.3	SEIR Equations . . . . .	11
1.5	Game Theory . . . . .	12
1.5.1	Hawks and Doves . . . . .	15
1.5.2	The Prisoner's Dilemma . . . . .	16
1.6	Ecological Models . . . . .	17
1.7	Interactions, Events and the Spatial Environment . . . . .	19
1.7.1	The Spatial Environment . . . . .	20
1.7.2	Metapopulations and Patch Models . . . . .	21
1.7.3	Explicit Spatial Models . . . . .	23
1.7.3.1	Cellular Automata . . . . .	23
1.7.3.2	Coupled Map Lattices . . . . .	26
1.7.3.3	Reaction Diffusion Equations . . . . .	26
1.8	Mathematics . . . . .	28
1.8.1	Event rates . . . . .	28
1.8.2	Stability Analysis . . . . .	30
1.9	Summary . . . . .	32
<b>2</b>	<b>Using Pair Models to Represent Space</b>	<b>33</b>
2.1	Pair Approximations in the Literature . . . . .	34
2.2	Spatial Games . . . . .	35
2.2.1	Lattice Model . . . . .	36

2.2.2	Mean-field Model . . . . .	37
2.2.3	Pair Model . . . . .	39
2.2.4	Model Extensions . . . . .	40
2.3	The Hawk-Dove Game . . . . .	40
2.4	Analysis . . . . .	42
2.4.1	Analysis of Mean-field Dynamics . . . . .	44
2.4.2	Analysis of Pair Model Dynamics . . . . .	46
2.5	Discussion . . . . .	49
2.6	General $2 \times 2$ Games . . . . .	50
2.6.1	Stability . . . . .	53
2.7	Other Ways of Incorporating Space . . . . .	54
2.8	Summary . . . . .	58
<b>3</b>	<b>Formalisation of the Pair Approximation</b>	<b>60</b>
3.1	Chapter Aims . . . . .	61
3.2	Basic Premise and Notation . . . . .	61
3.2.1	Dynamics . . . . .	62
3.3	Averages and Errors . . . . .	64
3.3.1	Reduction . . . . .	65
3.4	The Aim of the Pair Approximation . . . . .	66
3.5	Estimating the Error Terms, $\Gamma$ . . . . .	67
3.5.1	$\Gamma^\sigma(i j i)$ . . . . .	68
3.5.2	$\Gamma^\sigma(i j k)$ . . . . .	69
3.6	Example - Spatial Game Revisited . . . . .	71
3.6.1	Regular Networks . . . . .	72
3.6.2	Irregular Networks . . . . .	75
3.6.3	Alternative Pair Approximations . . . . .	79
3.7	Discussion . . . . .	83
<b>4</b>	<b>Extensions and General Pair Models</b>	<b>85</b>
4.1	Introduction . . . . .	86
4.2	More Terminology . . . . .	86
4.2.1	Expressions for $\overline{Q}^\sigma$ . . . . .	88
4.3	An Alternative Perspective . . . . .	92
4.4	Extending the Pair Analysis . . . . .	96
4.4.1	Triple Approximation in the Two-Player Spatial Game . . . . .	97
4.4.2	Closure . . . . .	98
4.4.3	Results . . . . .	102
4.5	General Pair Models . . . . .	102

4.5.1	No explicit Network . . . . .	105
4.5.2	Clumping . . . . .	106
4.6	Discussion . . . . .	107
<b>5</b>	<b>Examples</b>	<b>109</b>
5.1	The Iterated Prisoner's Dilemma. . . . .	110
5.1.1	Stochastic Strategies . . . . .	112
5.1.2	Analysis . . . . .	112
5.1.3	A Spatial Environment . . . . .	114
5.1.4	IPD Pair Model . . . . .	115
5.1.4.1	Two Species IPD Contests . . . . .	116
5.1.4.2	More than Two Species IPD Contests . . . . .	117
5.2	Other Spatial Games . . . . .	120
5.3	Predator-Prey Systems . . . . .	121
5.3.1	Variable Population Pair Model . . . . .	123
5.3.2	Empty Site Pair Model . . . . .	127
5.4	Discussion . . . . .	131
<b>6</b>	<b>Infection Systems</b>	<b>132</b>
6.1	Introduction . . . . .	133
6.2	The Contact Process . . . . .	133
6.2.1	Spatial Structure . . . . .	134
6.2.2	No Recovery from Infection . . . . .	135
6.3	Susceptible-Infectious-Recovered . . . . .	138
6.3.1	Behaviour . . . . .	139
6.3.2	Stochastic Simulation . . . . .	140
6.3.3	Seasonal Forcing . . . . .	145
6.4	Measles . . . . .	147
6.4.1	Modelling . . . . .	148
6.4.1.1	Seasonal Forcing . . . . .	148
6.4.1.2	Age Structure . . . . .	149
6.4.1.3	Spatial Structure . . . . .	150
6.4.2	Measles Pair Model . . . . .	150
6.4.2.1	Results . . . . .	153
6.5	Discussion . . . . .	156
<b>7</b>	<b>Conclusions</b>	<b>158</b>
7.1	Review . . . . .	159
7.2	Discussion . . . . .	159
7.3	Future Work . . . . .	162

7.4 Summary . . . . .	163
<b>Appendices</b>	<b>164</b>
A Binomial Theorem . . . . .	164
B Software and Computation . . . . .	165
C Abbreviations . . . . .	167
<b>References</b>	<b>168</b>

# List of Figures

1.1	Solutions of the continuous time logistic equation . . . . .	6
1.2	Solutions of the discrete time logistic equation . . . . .	7
1.3	Damped oscillatory convergence of the SIR equations . . . . .	11
1.4	Cycles in phase space for the Lotka-Volterra predator prey model. . . . .	18
1.5	Typical spatial structure for explicit spatial models. . . . .	24
1.6	Exponential decay through multiple decay classes . . . . .	31
2.1	Neighbouring sites on a square lattice. . . . .	37
2.2	Lattice, pair and mean-field model time series for the spatial hawk-dove game. . . .	42
2.3	Effects of grid size on convergence times for the lattice hawk-dove model. . . . .	43
2.4	Spatial structure snapshots of the lattice hawk-dove model. . . . .	43
2.5	Equilibrium population composition in the hawk-dove game for the lattice, pair and mean-field models. . . . .	44
2.6	Comparison of stochastic simulations and ODE analysis for hawk-dove mean-field and pair models. . . . .	49
2.7	Regions of solution existence and stability for the general two player spatial game. .	53
2.8	Pair equation trajectories for a general two player spatial game . . . . .	57
2.9	Pair equation trajectories for the spatial hawk-dove model at $s = 0.4$ . . . . .	58
3.1	Two alternative routes for two events to occur in a network. . . . .	63
3.2	$\Gamma^\sigma(i j k)$ for the lattice hawk-dove model. . . . .	68
3.3	Initial distribution of neighbours for the lattice hawk-dove spatial game. . . . .	73
3.4	Distribution of neighbours at equilibrium with $s = 0.4$ in the lattice hawk-dove spatial game. . . . .	74
3.5	Distribution of neighbours at equilibrium with $s = 0.5$ in the lattice hawk-dove spatial game. . . . .	74
3.6	Equilibrium population composition in the hawk-dove game for the fixed network random position model. . . . .	77
3.7	Equilibrium population composition in the hawk-dove game for the dynamic network random position models. . . . .	77



3.8	Snapshots of the spatial structure in each of the three irregular network hawk-dove models. . . . .	78
3.9	Initial distribution of neighbours for the irregular network spatial hawk-dove models. . . . .	79
3.10	Equilibrium distribution of neighbours for the fixed irregular network spatial hawk-dove model. . . . .	80
3.11	Equilibrium distribution of neighbours for the dynamic irregular network spatial hawk-dove model with local birth. . . . .	80
3.12	Equilibrium distribution of neighbours for the dynamic irregular network spatial hawk-dove model with global birth. . . . .	81
4.1	Example neighbourhood with $Q_x^\sigma(ij)$ totals. . . . .	87
4.2	Neighbourhood configurations which effect $\overline{Q}^\sigma(ij kl)$ . . . . .	88
4.3	Comparison between estimates for $[ijk]$ . . . . .	95
4.4	Relative accuracy of pair model estimates for $(ijk)$ in the lattice hawk-dove game. . . . .	96
4.5	Possible orientations of a 5-path on a square grid. . . . .	101
4.6	Triple approximation prediction for the hawk-dove game population equilibrium. . . . .	103
4.7	Two neighbouring individuals a distance $d$ apart . . . . .	104
4.8	The pair approximation for $(ij)$ for various $\phi$ . . . . .	106
5.1	IPD pair model for AllD, TFT and $\gamma$ TFT. . . . .	118
5.2	IPD pair model for AllC, AllD, TFT, 0.1-TFT and 0.2-TFT. . . . .	119
5.3	Pair model trajectories for three species games. . . . .	122
5.4	Phase space trajectories in the variable population Lotka-Volterra pair model. . . . .	125
5.5	Schematic diagram for the empty-site predator prey pair model. . . . .	128
5.6	Effect of increasing migration and clumping on the predator-prey-empty site pair model. . . . .	130
6.1	Phase space trajectories for the contact process pair model with no recovery . . . . .	136
6.2	Contact process pair model with no recovery from infection. . . . .	137
6.3	Schematic diagram of sites connected with an $(m, \phi)$ spatial structure. . . . .	138
6.4	Hopf bifurcation from equilibrium for SIR pair model. . . . .	140
6.5	Snapshots for the hex grid SIR model . . . . .	142
6.6	Hexagonal lattice SIR model time series. . . . .	143
6.7	SIR equations for pair model and original non-spatial model. . . . .	144
6.8	Forced SIR pair model output. . . . .	146
6.9	Measles infection in England and Wales from 1948 to 1968 . . . . .	147
6.10	Forced Measles trajectory. . . . .	154

# List of Tables

2.1	Different spatial models in Durrett and Levin (1994a).	55
4.1	Exact expressions for the $\overline{Q}^\sigma$ average quantities in any general network $\sigma$ .	90
4.2	Notation for the neighbourhood elements	91
4.3	Triple Approximations for elements in a regular square lattice.	102
5.1	IPD payoff table in the limit $\varepsilon \rightarrow 0$ .	113
5.2	IPD payoff table to $O(\varepsilon^2)$ in the case $R = 3, T = 5, S = 0$ and $P = 1$ .	114
5.3	Parameter values for the variable population Lotka-Volterra pair model.	126
6.1	Response of oscillations to parameter changes in the measles pair model.	152

# Acknowledgements

I am grateful for the support and assistance of a great many people during my time at Warwick which has enabled me to write this thesis. I thank them all, and I hope I will be forgiven for not acknowledging them all individually: The list would be long and without a natural end.

It would, however, be unforgivable not to mention some by name.

I would like to thank my supervisor, Professor David Rand, for his encouragement and guidance.

Thanks must also go to Dr Matthew Keeling and Dr Minus van Baalen who, through many discussions and patient explanation, have taught me a great deal and pointed out my many mistakes.

Finally, two others deserve a special mention. They have suffered much more than their fair share on my behalf over the last four years, and have provided endless support and friendship. I could not have got this far without them. Thank you Andrew and Alex.

I also thank Warwick University for its hospitality and EPSRC for funding during the course of my studies.

# Declaration

This thesis is the result of original research conducted by myself, unless stated in the text or acknowledgements. The research was carried out under the supervision of Professor D. A. Rand at the University of Warwick. All sources of information have been specifically acknowledged.

No part of this thesis has been submitted for a degree at any other university.

Work from Chapters 4 and 6 has been published in:

M.J. Keeling, D.A. Rand and A.J. Morris (1997)

CORRELATION MODELS FOR CHILDHOOD EPIDEMICS

*Proc. R. Soc. Lond. B* **264** : 1-8

# Summary

The real world is a spatial world, and all living organisms live in a spatial environment. For mathematical biologists striving to understand the dynamical behaviour and evolution of interacting populations, this obvious fact has not been an easy one to accommodate. Space was considered a disposable complication to systems for which basic questions remained unanswered, and early studies ignored it. But as understanding of non-spatial systems developed, attention turned to methods of incorporating the effects of spatial structure. The essential problem is how to usefully manage the vast amounts of information that are implicit in a fully heterogeneous spatial environment. Various solutions have been proposed but there is no single best approach which covers all circumstances. High dimensional systems range from partial differential equations which model continuous population densities in space, to the more recent individual-based systems which are simulated with the aid of computers.

This thesis develops a relatively new type of model with which to explore the middle ground between spatially naive models and these fully complex systems. The key observation is to note the existence of correlations in real systems which may naturally arise, as a consequence of their dynamical interaction, amongst neighbouring individuals in a local spatial environment. Reflecting this fact - but ignoring other large scale spatial structure - the new models are developed as differential equations (pair models) which are based on these correlations. Effort is directed at a first-principles derivation, from explicit assumptions with well-stated approximations, so the origin of the models is properly understood. The first step is consideration of simple direct neighbour correlations. This is then extended to cover larger local correlations and the implications of local spatial geometry. Some success is achieved in establishing the necessary framework and notation for future development. However, complexity quickly multiplies and on occasion conjectures necessarily replace rigorous derivations. Nevertheless, useful models result.

Examples are taken from a range of simple and abstract ecological models, based on game theory, predator-prey systems and epidemiology. The motivation is always the illustration of possibilities rather than in-depth investigation. Throughout the thesis, a dual interpretation of the models unfolds. Sometimes it can be helpful to view them as approximations to more complex spatial models. On the other hand, they stand as alternative descriptions of space in their own right. This second interpretation is found to be valuable and emphasis is placed upon it in the examples. For the game theory and predator-prey examples, the behaviour of the new models is not radically different from their non-spatial equivalents. Nevertheless, quantitative behavioural consequences of the spatial structure are discerned. Results of interest are obtained in the case of infection systems, where more realistic behaviour (an improvement on non-spatial models) is observed. Cautiously optimistic conclusions are reached that this ‘middle road’ of spatial modelling has an important contribution to make to the field.

**1**

# **Introduction**

## 1.1 About this Thesis

This thesis develops a new method of representing spatial interactions for a variety of simple model systems. The systems concerned are well studied examples from ecology and population dynamics, and so a biological flavour persists throughout.

By way of an introduction, the rest of this chapter describes the range of ecological systems and accompanying models relevant to the thesis. The effect of spatial distribution on these systems, with some of the modelling techniques currently used, is also discussed. Chapter 2 introduces the technique of Pair Modelling, a method of incorporating a degree of spatial structure, from first principles by developing an example system. This is the approach which underpins the rest of the thesis, where it is studied and extended. Chapters 3 and 4 take a closer look at the derivation of pair models from a mathematical perspective, and Chapters 5 and 6 study some specific applications. Finally, conclusions are drawn together in Chapter 7.

References are included throughout the text. As with most modern scientific disciplines, there is a large volume of published research literature and it is not possible to give it comprehensive coverage. Where many references are relevant, a representative sample is given; usually the most recent, from which earlier papers can be found. All abbreviations and acronyms used in the text are listed in Appendix C.

## 1.2 Why model?

This is a thesis in the field of mathematical biology, and some words are appropriate on what this is and what it isn't; what it can and can't do.

In all areas of science, models are necessary for understanding. Lord Kelvin aptly conveyed this feeling:

I am never content until I have constructed a mechanical model of the subject I am studying. If I succeed in making one, I understand; otherwise I do not.

The process of modelling involves making and justifying assumptions about the system under study. Because biological systems are characterised by immense complexity and detail, this can be a difficult task. Indeed, it may be necessary, in practice, to make approximations which are manifestly not true. Proper consideration of the assumptions is therefore an important and difficult part of the interpretation of a model's behaviour.

Models can be detailed - incorporating many observed features of a particular system - or models can be simple and more abstract, applying to a range or class of systems. The former are often useful for prediction (as, for example, with the complex fluid equations used in weather forecasting models), whereas the latter can sometimes illustrate more general basic phenomena. The biological models studied here fall into the simple, abstract category. Nevertheless, their analysis can be far from straight forward.

One common feature of biological systems is non-uniqueness of the modelling approach. The literature contains many different models for similar systems, each having made slightly different assumptions. When the models produce different behaviour (as they sometimes do), interpreting the results can be difficult. There may not be right and wrong models to choose between, but a comparative study can be performed: Including or removing particular effects and assumptions can indicate responses common to many models, and therefore help elucidate important factors.

Mathematics is the best language available in which to formulate models, but it is not perfect and does have limitations. These seem especially relevant for biological systems. Specifically, one is often forced to take a phenomenological, non-mechanistic approach (especially with abstract biological models) to the modelling of some important processes, simply because the model assumptions and approximations that are necessary for tractability have removed the detail on which to base realistic biological or physiological mechanisms. Physicists may be more confident of the suitability of mathematical models for their desired use because of a belief that simple, neat and mathematically expressible natural laws underly the universe. Complications arise in biology because of the nature of the interactions: discrete individuals, stochastic events and a very interactive environment all take their toll. (Physicists may, of course, be wrong. For example, there is certainly no unanimous opinion holding today about the best interpretation of quantum mechanics and the corresponding implications it has for the deterministic nature of the universe.)

Finally, the role of computer simulation must be mentioned. The recent phenomenal increase in available computing power has provided another valuable tool with which to investigate model systems, and an added reason to derive them. Most models can be investigated numerically with comparative ease, and computer graphics have been particularly useful when investigating certain systems, such as the high dimensional explicit spatial models described in section (1.7.3).



## 1.3 The History of Modelling in Population Dynamics and Ecology

### 1.3.1 Basic Concepts

Thomas Malthus (1766-1834) the mathematician and clergyman is credited as being one of the first people to apply scientific thought and mathematics to the study of population dynamics. His famous essay (Malthus, 1798) notes that a breeding population will increase in size exponentially if left unchecked by factors such as disease, accidents, war or famine. This most fundamental, though crude, observation outraged many people at the time because of its accompanying commentary on social welfare, but it also inspired others to take the study of population dynamics further. Malthus' observation was, like all subsequent work, a mathematical model of the real world. Assumptions were made concerning the relevant behaviour of the population; in his case that, on average, each individual left behind a fixed number of offspring during their lifetime.

One of the first questions any modeller has to address is how to treat the individuals who comprise the population(s) in question. *i.e.* what measurable properties should be modelled. It is the individuals and their behaviour in relation to one another that are responsible for the dynamics but it is not always possible, or indeed sensible, to model each individual directly. The problem is one of complexity. If we try and understand the behaviour of a system in terms of the behaviour of each of its many constituent parts we risk being swamped in a sea of detail that is likely to obscure the underlying rules and patterns of interest. It is also likely to be an extremely difficult task. The trick is to include just enough detail to reproduce the important effects.

If all individuals are identical, a population can be represented simply by its size. Malthusian exponential growth is then described by the difference equation

$$x_{t+1} = \lambda x_t \tag{1.1}$$

where  $x_t$  is the number of individuals in the population at time  $t$  (the units of time being discrete generations), and  $\lambda$  is the number of distinct offspring per individual. Solving this equation gives  $x_t = \lambda^t x_0$ . However, this only strictly makes sense when  $\lambda$  is an integer because each (assumed identical) individual must produce exactly  $\lambda$  offspring. If  $\lambda$  is non-integer valued,  $x_t$  will itself eventually be non-integer valued for large enough  $t$ , regardless of the initial population size  $x_0$ .

In practice we do not expect all individuals to have exactly the same birth rates, in which case  $\lambda$  can be interpreted as the average birthrate per individual per generation and equation (1.1) still holds, providing we can accommodate non-integer values for  $x_t$ . There are two obvious ways of doing this. One is to round each calculated value of  $x_t$  to the nearest integer; an easy task in principle but one that makes any further mathematical analysis extremely difficult. Models that are not amenable

to any form of analysis other than direct simulation lose a lot of their appeal and so this is not a particularly useful or popular approach. The other method is essentially to ignore the problem and allow populations to have a non-integer size. Often referred to as the continuity assumption, this works very well in many circumstances, especially as the resulting real numbers are a much more natural field for mathematical analysis. Its main drawback is when population sizes are very small. Important extinctions that naturally occur with discrete individuals often can not happen with continuous individuals, where so called nanopeople (the equivalent of tiny fractions of an individual) continue to survive. For some models this presents no practical problem, but for others it can have a major influence (see for example section (1.4.2) concerning infectious disease models). Despite this drawback, the continuity assumption is widely used in population dynamics, and will be used throughout this thesis.

This problem is typical of those that arise from ignoring all the real differences between individuals in the population - an implicit assumption of representing the whole population simply by its size. In reality, all individuals are not identical and there are often many differences (heterogeneities) like those in birth rates, *e.g.* in sex, age, behaviour or environment, that may or may not be important to the dynamics. Again, broadly speaking, there are two approaches to account for the effects of any particular heterogeneity in the population. The extra structure can be explicitly modelled, at the expense of added complexity, or it can be averaged out over the population. The continuity assumption is the result of this second approach in many circumstances, as above. An example of the first, by incorporating at least some aspects of the spatial structure, is the goal of this thesis. For many systems, the interactions between individuals are important to the dynamics (section (1.7)), and the appropriate averaging assumption in this case is the mass-action principle. This assumes that all individuals in a population mix thoroughly and encounter every other individual with equal probability.

Using the continuity assumption we can also consider the case of non-discrete, overlapping generations, and model the population size at any time rather than just once every generation (in which case the age structure in the population is averaged away). Assuming a constant birthrate per individual gives rise to a different exponential growth law in the form of an ordinary differential equation (ODE):

$$\frac{dx}{dt} = \lambda x \tag{1.2}$$

This time  $x(t)$  represents the population size at any real time  $t$ , and the similarly behaved solution is  $x(t) = x(0)e^{\lambda t}$ .

### 1.3.2 Density Dependence

Neither equation (1.1) nor equation (1.2) is a particularly realistic model in the long term because ex-

ponential growth cannot continue unabated in a finite world with finite resources. (When resources are not limiting, however, *e.g.* during the initial stages of bacterial colony growth, exponential growth can be a good model). The next stage in modelling is to incorporate the effect of Malthus's growth limiting factors (disease, starvation, *etc.*) by reducing the birthrate per head of population as the total population rises, giving so called density dependent growth. There are many different ways of modifying the equations to include this in simple models for the growth of a single species but all work in a non-mechanistic fashion, in the sense that only the effect on the net birthrate is specified, and the real mechanisms responsible (increased deathrate from disease or starvation; reduced offspring survival due to predation *etc.*) are not alluded to.

As an illustration, consider logistic growth. In the continuous time case, equation (1.2) becomes

$$\frac{dx}{dt} = \lambda x(N - x) \quad (1.3)$$

when the constant birthrate per individual is replaced by the linearly decreasing function  $\lambda(N - x)$ . A negative birthrate is a positive deathrate when  $x > N$ . This is probably the simplest way of including density dependence and can be integrated using partial fractions to give

$$x(t) = \frac{x(0)N}{x(0) + (N - x(0))e^{-\lambda Nt}} \quad (1.4)$$

Figure (1.1) shows the behaviour of these solutions for various initial conditions (with the population and time scaled such that  $N = 1$  and  $\lambda = 1$  for convenience). Instead of exponential growth, the population always converges to a stable equilibrium size of  $x = N$ , where the net birthrate is zero.

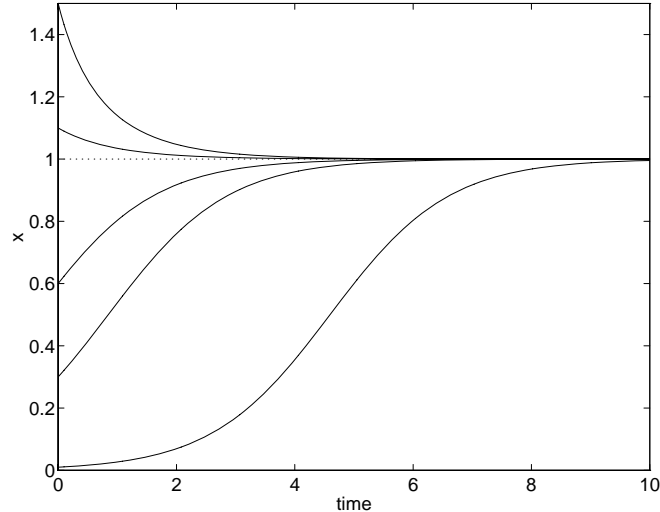


Figure 1.1: Solutions of the continuous time logistic equation for various initial population sizes (scaled to  $N = 1$  and  $\lambda = 1$ ).

When using discrete generation difference equations, however, the picture is surprisingly complicated. The analogous logistic equation here is

$$x_{t+1} = \lambda x_t(N - x_t) \quad (1.5)$$

If  $0 \leq \lambda \leq 4/N$  the population will remain between 0 and  $N$  as long as it is initially; even so, the behaviour of this system is fascinating. As is well known, for relatively low values of  $\lambda$  the sequence of population sizes ( $x_t$ ) converges to a stable fixed point, but as  $\lambda$  is increased up to  $4/N$ , the system undergoes a period doubling cascade to chaos, exhibiting wilder and wilder behaviour until the sequence is visibly indistinguishable from random noise; see figure (1.2).

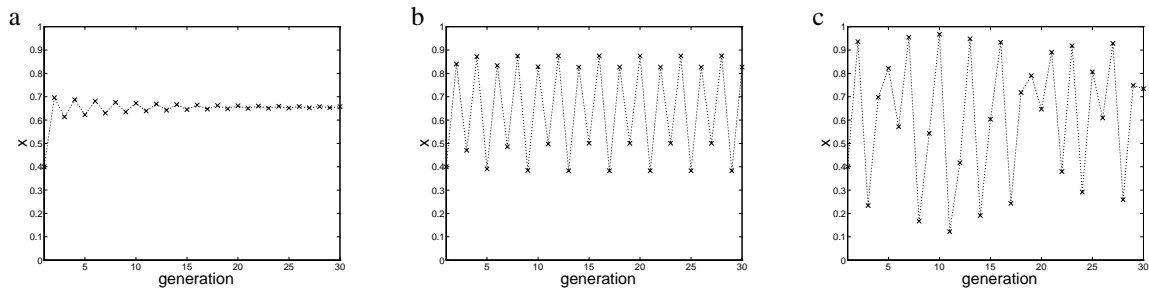


Figure 1.2: Typical solutions of the discrete time logistic equation scaled to  $N = 1$ , showing a) approach to an attracting fixed point trajectory ( $\lambda = 2.9$ ), b) a period four orbit ( $\lambda = 3.5$ ) and c) a large period orbit ( $\lambda = 3.9$ , dotted).

Such exotic behaviour from such an innocent looking equation came as a surprise to both its discoverer (May, 1974; May, 1976) and to the field of population dynamics as a whole, but this behaviour is far from unique. ODE systems too often have limit cycle dynamics (in more than one dimension) or even chaotic attractors (in more than two).

After these very basic and abstract models, adding further detail to represent particular systems was the next step. This usually involved considering more than one interacting species or species type, resulting in coupled systems of difference or differential equations. Three important classes of models, which are used as example systems in this thesis, are now briefly described. Each is a continuous time system (little more will now be said about difference equations) and each still assumes a homogeneous population with respect to age structure, spatial structure, sexual structure (*i.e.* males and females are not distinguished; all birth is asexual), and all forms of genetic structure too.

## 1.4 Infectious Disease Models

A particularly interesting category of models is those that cover infectious diseases. Much work has been done on their study, because of their importance to the understanding and control of disease in humans. Prevention and eradication programmes through the design of successful vaccination schemes, and disease prediction to target other appropriate medical resources, all depend upon such models.

Many microparasitic infections are of special theoretical concern because the life-history of the relevant pathogens allows the within body dynamics to be largely ignored. Essentially, hosts can be divided into those that have the infection, and those that do not. This is usually because the pathogens, which are typically bacteria, viruses or protozoans, rapidly multiply within the host so the size of the initial infection becomes irrelevant. Given this assumption, the simplest approach to infection modelling concentrates on disease transmission between hosts, which may include complicating factors like recovery, immunity and latent infectious periods. (By contrast, with macroparasitic infections *e.g.* helminth infections, the actual parasite burden is relevant; individuals with a light worm burden and a heavy burden generally suffer differently and behave differently).

Of course it is possible to model the details of within host dynamics or the interaction of immunology and epidemiology where appropriate (Dushoff, 1996; Anita, Koella and Perrot, 1996). Anita *et al.*, for example, consider the mycobacterial infections responsible for tuberculosis and leprosy. These diseases are characterised by extended periods of low levels of infection within the body, and modelling explicitly incorporates the host's immune response. Still other infections exist in more than one type or strain, and a host's immune response to each of these can be varied and genetically determined. Ignoring such extra structure is another approximation implicit in simple infection models, but this too can be taken into consideration with more specific and more complicated models. The coevolutionary trajectory of a multi-strain host-pathogen system, displaying a rich dynamical behaviour, is studied in Andreasen and Christiansen (1995).

### 1.4.1 The Contact Process

The simplest possible model is the contact process in which the population is divided into just two classes: those infected (I) who have the disease, and those susceptible (S) who don't. Susceptible individuals can catch the disease from contact with infected individuals, and infected individuals recover from the disease in time, becoming susceptible again (there is no immunity). A common assumption, and one made here, is that the total population remains a constant size; we do not consider births and deaths. This is often reasonable when the time scale for disease transmission is much shorter than that for population growth or decay. In an abstract model, we are free to make

this assumption.

To write down a differential equation governing  $I$ , the number of infecteds, two further assumptions are needed. The first is the mass-action principle which states that the number of contacts (per unit time) between a susceptible and an infected individual is proportional to the product  $S \times I$ . This is equivalent to assuming the population is thoroughly mixed and every individual contacts every other with equal probability. The second assumption holds that infected individuals recover from infection at a uniform rate (*i.e.* they remain infected for an exponentially distributed time - see section (1.8.1)). On scaling the total population so that  $S + I = 1$ , and scaling time to give a recovery rate of unity, this gives

$$\frac{dI}{dt} = \lambda SI - I \quad (1.6)$$

If  $\lambda > 1$ ,  $I$  always converges to an equilibrium value of  $1 - \frac{1}{\lambda}$ , representing a disease endemic in the population, providing  $I \neq 0$  originally (this is a trivial fixed point with no infection present). Otherwise, the infection can not persist, and  $I$  converges to zero.

An alternative interpretation of the contact process, more relevant to section (1.6) is as a birth and death process, with density dependence, in a single species. Individuals are assumed to require space in which to live. Instead of susceptible and infected, the classes are unoccupied space and occupied space, or dead and alive. Births replace infections; offspring of an individual (occupied space) can only survive in an unoccupied space, and constant rate death replaces recovery.

### 1.4.2 SIR Equations

With a small extension, the abstract contact process can be transformed into a much more realistic and applicable system of equations known as the SIR equations. The infection process is identical, depending upon the mass-action principle to give the crucially important number of susceptible-infected contacts. Recovery, however, is different. Instead of returning recovered individuals to the susceptible class, a third category ( $R$ ) is formed for recovered individuals (sometimes known as the removed or resistant class). Individuals move to this class (again at constant rate,  $\nu$ ) after recovering from the infection, and it is assumed that they have then acquired 100% immunity to the disease for life. To avoid the inevitability of the infection dying out, new susceptibles are introduced to the population. This is done through birth and death; individuals from all three classes die at a constant, class-independent rate  $\mu$  and new susceptibles are born at exactly the same rate, so the total population is again kept constant,  $S + I + R = N$ , as for the contact process. (For the more complicated case of a variable population size, see for example Hethcote and Driessche (1995), or Zhou and Hethcote (1994)). The equations are:

$$\begin{aligned}
\frac{dS}{dt} &= \mu N - \mu S - \beta SI \\
\frac{dI}{dt} &= -\mu I + \beta SI - \nu I \\
\frac{dR}{dt} &= -\mu R + \nu I
\end{aligned}
\tag{1.7}$$

Notice that they sum to zero. The system is second order and the  $R$  equation can be ignored. (It is given here for clarity). Despite the fact there are still major simplifications (the list is long; including the effects of host age-structure, seasonality, genetics, stochasticity, vertical transmission, maternal antibodies, sex differences, loss of immunity, disease induced mortality and the homogeneous mixing mass-action principle itself) of the biology of any particular infection, the SIR equations are directly useful to epidemiologists. One of their important predictions is that of a threshold for epidemics. The basic reproductive rate is defined as

$$R_0 = \frac{\beta N}{\nu + \mu} \tag{1.8}$$

and is interpreted as the expected number of secondary infections a lone primary infection will cause in a large population full of susceptibles. (The average life expectancy of an infection is  $1/(\nu + \mu)$  and in this time approximately  $\beta N$  susceptible contacts will be made because the number of newly infecteds or recovered is small compared to  $N$ ). For the SIR equations it is found that if  $R_0 < 1$  then any infection dies out; the population returns to an equilibrium of  $S = N, R = I = 0$ . If  $R_0 > 1$ , infections do not die out. We typically see epidemic periods in which the number of infecteds rises rapidly, spreading quickly through the population, alternating with longer, slower periods of recruitment of new susceptibles (through birth) during which the number of infecteds is very low. With all non-trivial initial conditions these oscillations eventually damp down and the population settles to an equilibrium composition of  $S = N/R_0, I = \mu(N - S)/(\mu + \nu), R = \nu(N - S)/(\mu + \nu)$ . Figure (1.3) shows the SIR equations numerically integrated for a population scaled to size  $N = 1$  with  $\beta = 50, \nu = 10$  and  $\mu = 0.02$  which imply  $R_0 \approx 4.99$ . These values do not correspond to any particular infection, but they do illustrate the rise and fall oscillatory approach to equilibrium. Note that in the infection troughs, the number of infecteds falls very low, often to much less than the equivalent of one individual in a million. This is typical of the SIR equations away from equilibrium and does strain the credibility of the continuity assumption for many ordinary-sized animal populations; at such low levels stochastic events will almost certainly be important. However, the SIR equations are some of the most studied in the whole of mathematical biology and are the foundation for many other infection models. Amongst these are stochastic versions which consider individuals and the possibility of disease extinctions. These models can be used to address questions about the probability of a particular outbreak occurring or the expected duration of an outbreak when it does occur which are not in the scope of deterministic models (van Herwaarden and Grasman, 1995).

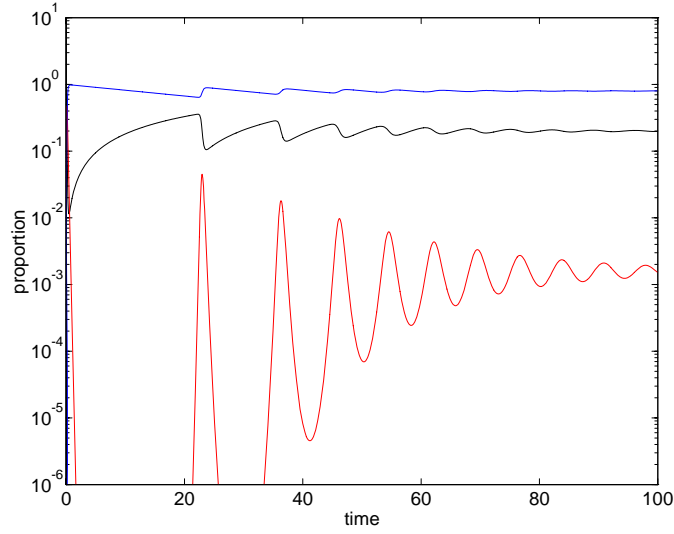


Figure 1.3: The SIR equations numerically integrated for  $\beta = 50, \nu = 10$  and  $\mu = 0.02$  from an initial condition of 99% susceptible, 1% infected and shown on a log scale. The susceptibles are shown in black, infecteds in red and recovered in blue; at equilibrium the population is approximately 20% susceptible, and only 0.15% infected. Note the damped oscillatory convergence, composed of periods of rapid spread of infection and gradual build up of susceptibles.

### 1.4.3 SEIR Equations

For some infections, notably measles, where there is a significant incubation period inside the host, it is a further improvement to split the infected class  $I$  of the SIR model into two classes labelled exposed ( $E$ ) and infectious ( $I$ ). Individuals who have just acquired the infection enter the exposed category where they remain (as usual) for an exponentially distributed time and during which they do not infect other susceptibles (a latent period). Only after this time do they move to the infectious class and contribute to making new infections. This makes the SEIR equations

$$\begin{aligned}
 \frac{dS}{dt} &= \mu N - \mu S - \beta SI \\
 \frac{dE}{dt} &= -\mu E + \beta SI - \gamma E \\
 \frac{dI}{dt} &= -\mu I + \gamma E - \nu I \\
 \frac{dR}{dt} &= -\mu R + \nu I
 \end{aligned} \tag{1.9}$$

For both the SIR and SEIR equations it is possible to estimate the parameters  $\mu, \nu, \gamma$  and  $\beta$  from data for specific infections to give realistic values. The rate parameters  $\mu, \nu$  and  $\gamma$  are simply the reciprocals (see section 1.8.1) of the expected durations of the appropriate times: life-time, infectious time and exposed time respectively; so  $\mu$  is often much smaller than  $\nu$  and  $\gamma$ . Because infection is transmitted at rate  $\beta SI$ ,  $\beta$  is really a composite of the expected number of actual contacts per unit



time multiplied by the probability of a particular contact being effective (*i.e.* transmitting the infection). Given the mass-action assumption both of these can be estimated; by further assumptions on the rate of mixing for the former and by experiment for the latter.

Anderson and May (1992) gives a detailed derivation and history of the SIR and SEIR equations, and many more besides, in relation to human infections. The specific example of measles will be returned to in Chapter 6.

## 1.5 Game Theory

Game theory models provide a simple but surprisingly useful abstract tool for modelling systems in which the behaviour of individuals towards each other determines the dynamics.

The mathematical framework for game theory, and many important results, was developed mainly by John von Neumann during the middle of the twentieth century (see von Neumann's biography by Poundstone (1992) for an interesting history). The theory was originally applied to economics, to help understand and analyse rational behaviour (*i.e.* strategies) in the context of human business decisions. Its brilliant application to biological problems was largely due to Maynard Smith who recognised that animal behaviour patterns could also be thought of as rational strategies for playing their own special games of survival. His book, Maynard Smith (1982), provides an excellent discussion. See also Maynard Smith and Price (1973) and Maynard Smith (1974).

Many traditional games, such as chess, black-jack, noughts and crosses or rock-scissors-paper qualify as a game in the game-theory sense. The aim is usually simple: each player wants to win, but the array of possible strategies can be daunting (as in chess, for example). The skill is in choosing a winning strategy. These games are examples of so called zero-sum games, where the sum of the rewards (or benefits, penalties, payoff) to all participants, measured in appropriate units, is always zero; one player's winnings is another player's loss. However, this does not always have to be the case; many games are non-zero-sum games where this is no longer true.

Biological examples of games often centre around possession of a resource, *e.g.* a piece of food, a territory, a desirable home or a sexual mate. As with the more complex traditional games, a host of different strategies are available to the protagonists (whether to fight, how to fight, when to run, ways to deceive, ...) who display a variety of attributes of interest to a behavioural biologist (how aggressive, cowardly, courageous, submissive, ...). The payoff in biological games is, in principle, as easy to define as for traditional games. Living things do not compete for food or search for mates for fun, they do it to survive and reproduce. The currency of the payoff is Darwinian fitness, the propen-

sity to successfully reproduce and further one's genetic line. Because of this, we often find the games are naturally non-zero-sum games: when a starving individual and a healthy individual contest over some food, the potential fitness gains to the starving individual are probably much higher than to the healthy one because he may risk death (a heavy price to pay) if no food is eaten. In abstract models, fitness payoffs can be arbitrarily allocated as the consequences of particular game outcomes. In the real world, however, fitness (more specifically, the relative change in fitness) is much more difficult to quantify. This is a difficult obstacle for biologists who would like to verify game theory predictions by observation. Nevertheless the predictions can provide useful insight and merit study on their own.

A basic game consists of two interacting individuals who (usually) have conflicting interests in the outcome of some situation. A particular game is described by a payoff matrix of the form

$$\begin{matrix} & \begin{matrix} S_1 & \cdots & S_j & \cdots & S_n \end{matrix} \\ \begin{matrix} S_1 \\ \vdots \\ S_i \\ \vdots \\ S_n \end{matrix} & \begin{pmatrix} A_{11} & \cdots & A_{1j} & \cdots & A_{1n} \\ \vdots & & \vdots & & \vdots \\ A_{i1} & \cdots & A_{ij} & \cdots & A_{in} \\ \vdots & & \vdots & & \vdots \\ A_{n1} & \cdots & A_{nj} & \cdots & A_{nn} \end{pmatrix} \end{matrix}$$

which gives the payoff  $A_{ij}$  received by an individual who plays the game with strategy  $S_i$  against an individual who plays strategy  $S_j$  (who himself receives  $A_{ji}$ ). Each payoff  $A_{ij}$  can be positive or negative. It is assumed there is a set  $\{S_1, S_2, \dots, S_n\}$  of possible strategies to choose from that must be determined as part of the game (This can sometimes be a weakness of the approach if a plausible and exclusive set of strategies cannot be imagined. Some games are naturally expressed only in terms of a continuum of possible strategies; the war of attrition is a good example (Maynard Smith, 1974): A strategy is described by the persistence time of how long an individual is prepared to pursue a confrontation. The winning individual, who receives a reward, is the one with the longer persistence time but both players must pay a cost proportional to the actual length of the contest, which is the shorter time.) Using just one matrix represents a symmetric game in which both contestants are indistinguishable. An added complication is to consider asymmetric games with two associated matrices, each describing the payoff to one of the participants when they find themselves in different roles, *e.g.* as current owner and threatening challenger in a contest over possession of a territory.

Game theory was developed as a static (*i.e.* non dynamic) system. Its fundamental assumption is that each participant behaves rationally, in the sense of aiming to maximise its own payoff, selfishly so if this is to the detriment of the other player. Given a payoff matrix, one can apply game theory results to help decide which strategy from the strategy set is optimal (if any). This may be a pure strategy *i.e.* one played every time, or a mixed strategy in which various different pure strategies are played with certain probabilities (depending on the matrix  $A_{ij}$ ). In the context of animal games, a

rational player does not necessarily have to be a conscious or calculating player. Instinct can guide a player to an optimal strategy. Indeed, the evolution of genetically determined behavioural strategies is the motivation for work on Evolutionarily Stable Strategies (ESS) which are the uninvadable strategies important to evolutionary biology (Maynard Smith, 1982).

To study evolution, one must first study the dynamics. Static game interactions can be used to determine population dynamics by explicitly relating the game payoffs to reproductive success. Suppose a fraction  $x_i$  of the individuals in a population play the game using pure strategy  $S_i$  (we do not consider mixed strategies directly, but any particular mixed strategy can be added to the set of possible strategies and treated as a pure strategy). The expected payoff to an individual playing strategy  $S_i$ , given that he plays the game with a randomly chosen opponent is

$$W_i = \sum_{j=1}^n A_{ij} x_j$$

The corresponding rate of increase of strategy  $i$  players in the population is then naturally given by the replicator equations (Hofbauer and Sigmund, 1987) in which strategies reproduce in proportion to their frequency (like begets like) and their relative fitness:

$$\frac{dx_i}{dt} = x_i (W_i - \overline{W}) \quad (1.10)$$

where

$$\overline{W} = \sum_{j=0}^n x_j W_j$$

is the average payoff received in the population. Subtracting  $\overline{W}$  for each  $i$  in equation (1.10) ensures that the sum of the frequencies  $x_i$  remains constant (equal to one) as required. Note that the absolute size of the population is not considered. Like the SIR equations, only the relative proportions are important. It is possible to write down alternatives to the replicator equations (*e.g.* ones which affect the absolute population size) but none captures the essential features as simply. Taylor and Jonker (1978) and Zeeman (1981) are just two enlightening papers from the vast literature on the subject of relating game payoffs to dynamics.

In the simplest cases, the payoff matrix  $A = (A_{ij})$  is constant, but it could also be a function of the composition of the population,  $A(x)$ , which complicates matters further. Analysis of equations (1.10) for all  $i = 1, \dots, n$  species reveals the course of evolution of the population composition. Many authors have studied these equations and a lot is known about the behaviour of the population frequencies they model. Cressman (1990) gives stability results for symmetric matrices, and Hofbauer (1996) is a recent analysis of the (more complicated) corresponding equations for the case of a bimatrix (asymmetric) game.

The simplest games to consider are symmetric  $2 \times 2$  games (two participants with just two strategies to choose from). Different types of game then arise depending upon the relative ordering of the

four payoffs in the payoff matrix. Names have been allocated to these different games, relating to every-day experiences of the problems they portray. The game of volunteer, for example, has the two strategies of volunteer and don't volunteer. If either of the two participants volunteers, at great personal cost, to perform a necessary but undesirable task, the other will be spared the need to. This is the favoured outcome for the non-volunteer. If neither volunteers, both will suffer badly, but the worst possible outcome is if both players wastefully volunteer together. Another example is chicken, named after the very serious game of nerve in which two cars drive head on towards each other. If one swerves (the chicken), the other is the brave winner. In game theory the choices, made at the beginning of the game, are swerve or don't swerve; the worst possible case of course being if neither swerves, followed by you swerving and your opponent not, then both swerving. The winning result for you is when your opponent swerves but you choose not to.

Two other games with natural biological interpretations, used as examples in the thesis, are now described:

### 1.5.1 Hawks and Doves

Consider competition between two behavioural strategies, labelled hawks (h) and doves (d) (Maynard Smith, 1982). Hawks are aggressive by nature, doves are not (the names hawk and dove are not intended to suggest different species, but merely different strategies among a single population). A game arises out of pairwise contests occurring over possession of a resource (food, for example). It is assumed that the resource confers a relative fitness value of  $v$  to whomever secures it. If both contestants are doves (*i.e.* play the dove strategy), the resource is shared and each receives a reward of  $v/2$ . If a dove meets a hawk, the aggressive hawk takes all the resource and the dove goes away empty handed. If two hawks meet, a fight occurs. A winning hawk gets the reward  $v \geq 0$ , but the losing hawk suffers injury and receives a penalty  $c \geq 0$ . On average, because all hawks are assumed identical, a hawk will score  $(v - c)/2$  in such a contest. The payoff matrix for the game is therefore

$$\begin{array}{c} d \\ h \end{array} \begin{pmatrix} d & h \\ v/2 & 0 \\ v & (v - c)/2 \end{pmatrix}$$

The interesting case is  $v < c$  when no strategy dominates (if  $v > c$  it is always better to play hawk). Analysis of equation (1.10) quickly shows there is only one equilibrium value, corresponding to a fraction  $1 - v/c$  of doves in the population. All non-trivial initial conditions (*i.e.* those where both doves and hawks are present) converge monotonically to this equilibrium. Therefore a population of doves is unstable to the invasion of a few hawks, and a population of hawks is similarly unstable to invasion by a few doves.

### 1.5.2 The Prisoner's Dilemma

The prisoner's dilemma is another interesting and much studied game with just two possible strategies to choose from. The name originates from an accompanying descriptive anecdote, first attributed to the mathematician Albert Tucker (Poundstone, 1992); a modern version is:

Two suspects are questioned about a major crime, but the police do not have quite enough evidence to convict them. If neither implicates the other as being responsible, they will both be charged and convicted of a minor offence; one year in jail each. If one testifies that the other was responsible, he will be released whilst the other will receive a hefty prison sentence; three years. If both suspects implicate each other they will both receive two years in jail.

Given neither suspect knows the other's intentions, choosing to betray your partner is the rational choice, because it reduces your prison sentence whatever your partner decides to do (from one year to none if he keeps quiet, or from three years to two if he also talks). As a result, both suspects talk, and both receive two years in jail. The dilemma is that both would have done better (only one year in jail) if they had both kept quiet.

The two strategies are traditionally termed cooperate (C) and defect (D), for keeping quiet and talking respectively, and the payoff matrix (in the general case) becomes

$$\begin{array}{c} C \\ D \end{array} \begin{pmatrix} C & D \\ R & S \\ T & P \end{pmatrix}$$

where  $R$  is the reward for cooperating,  $P$  the punishment for defecting, and  $S$  and  $T$  the sucker and temptation payoffs when one player cooperates and the other defects. The prisoner's dilemma occurs when we have  $T > R > P > S$ .

The prisoner's dilemma is of particular relevance to many biologists who are interested in the evolution of cooperative behaviour (Nowak, May and Sigmund, 1995), widely seen in the animal kingdom but difficult to reconcile with the apparent gains to be made by individual cheats. (Cooperation can no longer be treated as an adaptive trait in a group selection process, which is now considered by most to be naive). One possible explanation is through reciprocal altruism (Axelrod and Hamilton, 1981) - benefiting others by performing good deeds, at some cost to yourself, in the expectation that similar deeds will be returned to you such that the net benefit to everyone is higher than it would have been without any cooperation. Axelrod and Dion (1988) describe substantial experimental support for this concept in many diverse populations, including bats, monkeys and sessile invertebrates. Such systems, however, are clearly vulnerable to exploitation by defecting individuals who take but

do not give. Although it is at best only a crude analogy, the prisoner's dilemma does represent the same kind of problem, and much attention has been focused on studying mechanisms that promote cooperative behaviour within the game. In particular, more complex studies where many rounds of the game are played against the same opponents, the so called Iterated Prisoner's Dilemma (IPD), have produced very interesting results (May, 1987). Chapter 5 discusses the IPD in more detail.

## 1.6 Ecological Models

Many other models fall into a category that can broadly be described as ecological models, The most famous example is the simple two-species predator-prey model of Lotka and Volterra (Lotka (1925) and Volterra (1926), see also Roughgarden (1979), Murray (1990)):

$$\begin{aligned}\frac{dV}{dt} &= V(b_V - d_V P) \\ \frac{dP}{dt} &= P(b_P V - d_P)\end{aligned}\tag{1.11}$$

Here  $V$  is the prey (victim) population size,  $P$  the predator population size, and the total population size  $V + P$  is not fixed. Without predator-prey interactions (which are again assumed to occur at a rate proportional to  $V \times P$  using the mass-action principle) the prey, feeding on an unlimited resource, grow exponentially at their birthrate  $b_V$ , and the predators die from starvation at rate  $d_P$ . Prey numbers are directly checked by predation with deaths occurring at rate  $d_V V P$ , and new prey are born at a similar rate  $b_V V P$  more indirectly due to the increased food supply for the predators. Equations (1.11) famously exhibit cycles (figure (1.4)) in which the number of predators endlessly chase the number of prey. The equations are neutrally stable and no matter what initial conditions, provided  $P$  and  $V$  are non-zero, the populations will both keep returning to their starting values simultaneously. (The function  $H$ , defined by

$$H = b_P V + d_V P - d_P \log\left(\frac{b_P}{d_P} V\right) - b_V \log\left(\frac{d_V}{b_V} P\right)$$

is found to be constant in time.) There is one internal equilibrium at  $V = b_V/d_V$  and  $P = d_P/b_P$  which is also neutrally stable.

More generally, Lotka-Volterra type interactions can be extended to an arbitrary number of species,  $n$ , by considering the equations

$$\frac{dx_i}{dt} = x_i \left( r_i + \sum_{j=0}^n A_{ij} x_j \right)\tag{1.12}$$

where  $x_i$  is the number of species  $i$  and  $r_i$  and  $A_{ij}$  are constants. The intrinsic rates of increase  $r_i$  can be either positive for birth rates (as for the prey above) or negative for death rates (as for the predators); the interaction constants  $A_{ij}$  represent in a non-mechanistic way the effect of species  $j$  on species  $i$  and are again assumed to relate to homogeneously mixed contact rates. Negative values

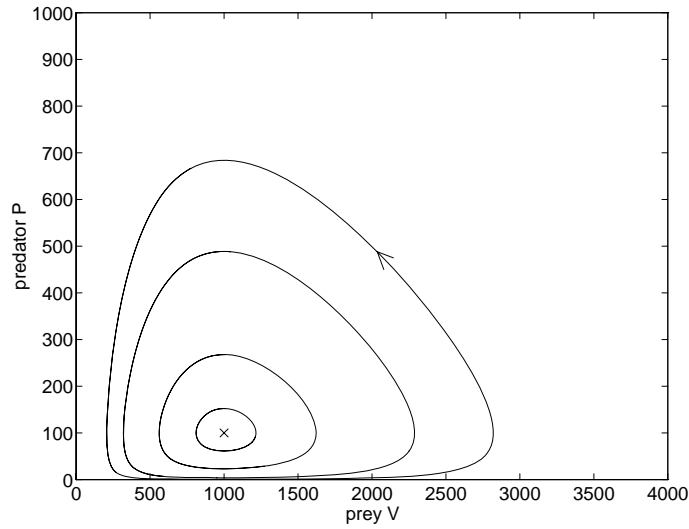


Figure 1.4: Examples of the cycles in phase space produced by the Lotka-Volterra predator prey model. Four different initial conditions are shown, leading to four different closed orbits which flow anti-clockwise. The internal equilibrium is marked with a cross. The parameters are  $b_V = 1.0, b_P = 0.005, d_V = 0.01$  and  $d_P = 5.0$ .

represent harmful effects (*e.g.* parasitism, predation, competition for resources) and positive ones are beneficial (catching food, symbiosis), so these equations can be formulated to describe a wide range of species interactions and interdependencies, albeit non-mechanistically.

One should note the similarity between the game theory equations (1.10) and equations (1.12). Both determine species abundances by a payoff or influence matrix; the first in terms of frequency, the second by actual population size.

Such models are clearly just about as simple as it is possible to get when considering interacting species, but it is possible to add further realism. Density-dependent growth is one way, *e.g.* by replacing a birth rate  $rx$  with logistic growth  $rx(N - x)$ . If this is done for the predator-prey model, all the non-generic limit cycles collapse to one globally attracting (in the positive quadrant) fixed point of coexistence, providing  $N$  is sufficiently large (greater than  $d_P/b_P$ ). If  $N$  is too small, the predators cannot coexist with the prey and are eliminated altogether. A further natural modification is predator satiation, where the mass-action assumption  $VP$  is modified to take account of the fact that a fixed number of predators can't kill prey at arbitrarily high rates. The linear dependence on  $V$  in  $VP$  is replaced by a term that is also increasing, but is bounded above, for example  $c(1 - e^{-kV})$  with  $c$  and  $k$  constants. Including this with prey density-dependence gives a system of equations which either collapse to an internal equilibrium or undergo a Hopf bifurcation and exhibit a unique attracting limit cycle towards which all trajectories tend. Time delays are another possible addi-

tion, perhaps most naturally expressed in the predator-prey system through predator birth being dependent on prey availability some time in the past,  $b_P V(t - T)P(t)$ , instead of at current levels,  $b_P V(t)P(t)$  thus complicating any analysis considerably. Nevertheless, useful analytical results are available in some cases. Lyapunov functions, for example, are a valuable technique for proving the global asymptotic stability of equilibria, as in Ardito and Ricciardi (1995) who study a wide class of predator-prey systems.

In this manner, more and more improvements to the basic model can be made, generally in a non-mechanistic way and generally at the expense of introducing more and more parameters. The details of increasingly specific systems can be ever more closely emulated, although this is not altogether surprising as the number of parameters available for fine tuning the model increases. Whether or not more understanding is gained by such phenomenological processes is an open question, but a comprehensive study of different models can be enlightening.

Models have been developed which focus on many particular aspects of the dynamics and evolution of interacting populations which do not even feature in the basic systems. A good example is the question of sexual reproduction. The models discussed so far have implicitly assumed asexual reproduction (*i.e.* all individuals are able to reproduce independently), but many organisms (and most higher animals) reproduce sexually. At first sight, sexual reproduction, which is an ancient behaviour, appears to be an extremely wasteful process: With half the population comprising ‘useless’ males, ‘rival’ asexual individuals should have a two-fold reproductive advantage. In evolutionary terms, this is a huge advantage, and one would expect the sexual species to be doomed. Models which explicitly represent sexual populations have suggested a possible solution to this problem: sex is a mechanism for escaping excessive parasite burdens (Hamilton, Axelrod and Tanese, 1990). Parasitism is a ubiquitous life-style, and virtually all organisms suffer it to some extent. If susceptibility to a parasite is in any way, or in any part, genetically determined (as is possible), then genetically identical asexual populations could be much more vulnerable than the variable individuals in a sexual population. We can also ask why there are only two sexes, or what are the benefits of being hermaphrodite. A key feature of this explanation is the presence of genetic variability within the population, which sex can mix and recombine. At a more fundamental level, models with explicit genetic structure are widely studied to understand the consequences of dynamics at the level of the gene.

## 1.7 Interactions, Events and the Spatial Environment

Real biological systems of the kind discussed above consist of interacting individuals (belonging to one or more species), and undergo change mainly through a series of discrete events. Common ex-



amples of these events include birth, death, infection, predation and change in behavioural strategy, such as choosing to fight or to retreat. Typically they occur instantaneously on time-scales relevant to the dynamics of the system as a whole. Even with more draw-out affairs, it is often possible to define a particular moment as the instant at which the event occurs - we are not usually interested in the protracted process of labour, merely that an individual has given birth. (Of course, not all biological systems can be described in this framework. The best exceptions are the more continuous effects such as vegetative growth or migration where change takes place but not in a recognisable sequence of discrete events).

Many of these events, often including those of dynamic importance, are directly connected with the interactions between individuals; and whether explicitly or implicitly, successful models must incorporate these interactions. Consider, for example, the logistic growth of a population (equation (1.3)). At first sight, this does not appear to have much to do with individual interactions. As an abstract model it provides a useful, though basic description of likely population growth in a very non-mechanistic, phenomenological way. All details of the relevant fundamental biological processes in any real system have been obscured. However, more often than not, these processes will in reality be dependent on discrete interactions; the density dependent death in a single species population (*i.e.* increased per capita mortality in larger populations) is, at a deeper level, almost certainly due to a biological process such as lack of food, increased incidence of disease or lower chance of survival for offspring. At this level, the importance of interactions between individuals (inter or intra-specific) is evident: the less prey food available, the fewer predator-prey interactions per predator; more susceptible individuals, more disease transmitted through susceptible-infected interactions; higher density of individuals, more behavioural interactions leading to fighting, injury and death.

Of course, some models are explicitly directly based on the important interactions in their system. In either case, whether explicitly present or not, the challenge is to quantify these interactions and this is not always an easy task.

### 1.7.1 The Spatial Environment

No aspect of spatial structure figured in the range of models discussed in section (1.3) beyond the basic mass-action principle. However, in any real system the frequency of a particular interaction is likely to be extremely dependent on how the population(s) is distributed through, or how it moves around, its spatial environment: A host-parasite system where the host is a forest of trees will behave quite differently from one where it is a flock of birds. Ignoring spatial structure can therefore be a very large assumption to justify, despite its tremendous gains in reduced complexity. All models must make assumptions on the nature of the spatial environment, whether explicit or not. There

are many possible alternative assumptions and many possible approaches.

The traditional approach to space has been to ignore it, which is understandable when it was a distracting complication to more fundamental interactions that needed to be understood (the cycling of predator-prey systems, or threshold transmissibilities for endemic infections for example). Increasingly, however, many authors have regarded space as an interesting and profitable area of study (see reviews by Bascompte and Solé, 1995; May, 1994; Nowak and May, 1992). Incorporating spatial structure has the potential benefits not only of refining predictions made by non-spatial models to more accurately reflect the real world, but occasionally also of revealing quite different behaviour. There are several contrasting approaches available as alternatives to the mass-action assumption (also variously referred to as a well-mixed or homogeneous population, or mean-field model) of non-spatial models. The suitability of any particular one must be addressed in the context of the system under study.

### 1.7.2 Metapopulations and Patch Models

An obvious method of incorporating non-trivial spatial structure is through the use of metapopulations. The idea is simple: instead of one single interacting, well-mixed population, several are considered, each occupying its own separate patch. (A population is just a group of individuals belonging to one or more species.) Independently for each population, *i.e.* within each patch, the same appropriate mean-field equations are used. For example each patch might contain its own predator-prey system, governed by equations (1.11). Of course the patches need to be linked in some way for the system to be interesting. This is done by allowing a (usually) small amount of migration of all species between the different patches. Assuming continuous time evolution, this is achieved by adding diffusion terms to the original equations. For a simple two-patch predator-prey example, the equations would become

$$\begin{aligned}
 \frac{dV_1}{dt} &= V_1(b_V - d_V P_1) + \varepsilon(V_2 - V_1) \\
 \frac{dP_1}{dt} &= P_1(b_P V_1 - d_P) + \varepsilon(P_2 - P_1) \\
 \text{and} & \\
 \frac{dV_2}{dt} &= V_2(b_V - d_V P_2) + \varepsilon(V_1 - V_2) \\
 \frac{dP_2}{dt} &= P_2(b_P V_2 - d_P) + \varepsilon(P_1 - P_2)
 \end{aligned} \tag{1.13}$$

where  $\varepsilon$  controls the amount of migration, and  $V_1$  denotes the prey population in patch number 1, *etc.* In the equations above, as is typically the case, the flow out of a patch is proportional to the size of the population within it and there is no net loss or gain of individuals to the system due to migration, but other assumptions are possible. With more than two patches, migration is often chosen to be equally to all patches from all other patches.

With these assumptions, all the patches are indistinguishable. There is no extra, large scale, spatial structure imposed; no two patches are closer to each other, in any sense, than to a third patch, and no patch is in any way bigger than any other. Furthermore there is no local spatial structure either, because each patch is thoroughly mixed. Nevertheless, meta-population models can provide new dynamics. One question to ask is whether the different patches become entrained and evolve in phase with each other (by symmetry this will always be the case in a completely deterministic system when the initial conditions in each patch are identical) resulting in the dynamics of the original non-spatial equations, or whether they remain out of phase in which case the total population of each species (summed over all patches) may have very different dynamics. This usually depends upon the level of diffusion, where too much will often lead to the original in-phase dynamics.

Metapopulation models can be made much more complicated. The symmetry between patches can be destroyed, with different diffusion rates used to indicate (roughly) the remoteness of particular patches. In infection models, for example, this could be a large city with several smaller satellite towns (Lloyd and May, 1996). Different diffusion rates could also be used for each different species, and each patch could also have its own parameter values to represent actual spatial heterogeneities. (Indeed, as mentioned previously, alternative migration rules can also be considered and this could extend to using discrete time mappings where seasonal migration is important. Such models, though, are less common in the literature).

In short, many different models can be entertained with all these possibilities, representing many conceivable variations on the nature of the patches. The following recently studied systems, which are fundamentally metapopulation models, are described to give an indication of the variety of such systems in the literature: Glendinning (1994) considers an island chain model in which there is a global structure imposed on the patches. Migration is between neighbouring islands along a one dimensional line of islands. Weisser and Hassell (1996) studied a host-parasitoid metapopulation which incorporated the effect of a delay for individuals migrating between patches by using a dispersing pool category. This delay was found to have a stabilising effect on the dynamics of the whole system. Finally, Tilman (1994) modelled sessile but dispersive grasses, using a metapopulation-like spatial structure but without explicit metapopulation model equations. Instead, he used as variables the proportion of spatial sites (patches) that each species occupied at any one time. His results suggested that many more species should be able to coexist than non-spatial models predict. The inclusion of space gives the opportunity for highly dispersive but less competitive species to exploit parts of the spatial area not currently occupied by other dominant grasses.

Metapopulation models provide an interesting extension of non-spatial models, but they do not address directly the role of spatial structure at the level of the individual. Other spatial models seek to answer this criticism.

### 1.7.3 Explicit Spatial Models

Most other spatial modelling techniques involve a much more explicit structure for the underlying spatial environment than is the case for patch models. In these models, discrete individuals or local populations occupy a specific position (site) within some spatial domain which has a specific relation to all other positions (contrast with the metapopulation approach where there is no such explicit positioning of the patches). A two dimensional domain is a common and obvious choice, reflecting the fact that many species live on the surface of the Earth, but others can be considered; one dimensional domains (simple line of sites), for example, are often easier to study. For non-spatial models there is a choice between discrete and continuous time evolution (difference equations or ODEs respectively). A similar choice also exists for explicit spatial models, not just for time, but also for space and the population state too. Essentially, the spatial sites can be discretised or form a continuum, and the population(s) at each site can also be represented by either a continuous or a discrete variable. The former employs the continuity assumption and implicitly models a relatively large local population; the latter is more suited to small local populations where the number of individuals is important. Taken to the extreme, this can be as small as just one (or none) individual per site.

Further questions such as the size and shape of the spatial domain, its boundary conditions and its internal structure (in the discrete space case) also arise. Because of the increased complexity of a spatial model, most authors consider simple solutions here, such as regular lattices of discrete spatial sites, commonly arranged in a square grid (like squares on a chess board) or occasionally alternatives such as a tessellation of hexagonal sites. If space is not infinite in extent it is often restricted to a square domain (in two dimensions) and the two pairs of opposite edges joined up to form a torus, thus eliminating awkward boundaries. Figure (1.5) illustrates these common arrangements. In principle, however, much more exotic spatial structure could be employed, and for particular systems it could be tailored to match a known spatial environment.

#### 1.7.3.1 Cellular Automata

A Cellular Automaton (CA) is a discrete space, discrete population state, discrete time spatial model. CA were first considered by von Neumann (Poundstone, 1992), and they have found applications in many areas, including physics, chemistry and more recently in biology and population dynamics.

Given the state of the system (*i.e.* the value of every site) at time  $t$ , a set of rules exists to determine the state of the system at the next time step  $t + 1$ . Usually these rules are applied simultaneously to all the spatial sites, called synchronous updating, but asynchronous updating, when the sites are updated one at a time, is another alternative. In most cases the updating rules are identical for all

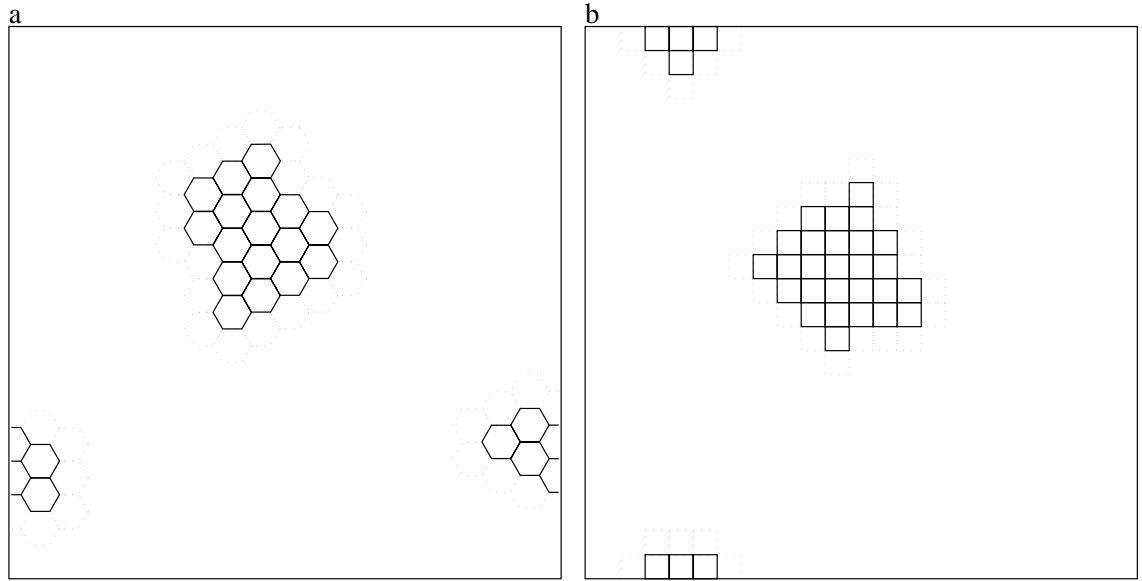


Figure 1.5: Typical arrangements for discretised spatial structure within a two dimensional square domain: a) hexagonal tessellation, where every site directly neighbours six others and b) square tessellation, with four neighbours per site. Each diagram shows a sample patch of the sites which actually cover the whole domain. If toroidal boundary conditions are employed the top and bottom of each diagram are identified, as are the left and right, wrapping the space onto a torus. In this case the two small patches at the bottom of the hexagonal domain (one to the left and one to the right) form one connected patch of seven sites, as do the two small patches in the square domain.

spatial sites, and they usually depend upon the state of other sites in a local spatial environment, as well as the site itself. This environment typically (but not necessarily) consists of a few neighbouring sites around the site to be updated, a popular choice on a square grid being the four nearest sites above, below, to the left and to the right (called a von Neumann neighbourhood). The philosophy is that only the state of near by sites can influence the time evolution of any other site. (Clearly there is no point in expressing an explicit spatial structure if it is not relevant to the dynamics.) Both deterministic and stochastic (probabilistic) rules are possible.

For many applications the discrete set of possible states a site could be in is both finite and small. Each possible value then corresponds to the presence of a particular species (biological, chemical, *etc.*) at the site, so each site represents just one individual. (What constitutes a ‘species’ is interpreted loosely, for example a predator, an infected host, a particular molecule or an empty space are all possibilities.) In such cases, the updating rules are often very naturally stated in terms of the possible events that the system can undergo, and stochastic rules can reflect the role of chance in nature. In a spatial infection model, for example, a susceptible individual at one site might become an infected individual at the next time step with a certain probability that depends upon the number of infected individuals amongst its neighbours. Infected individuals might die (become an empty site) with another probability, and other individuals similarly give birth to offspring into neighbouring empty sites. One can arrive at a model for a biological system in which every individual is explicitly tracked (in some spatial domain) in a way which the traditional non-spatial models avoided.

Another possibility is for each site to represent a small (hence discrete) well mixed population of one or more species. It is then important to have an interpretation of the individual CA sites and global CA structure appropriate to the system. If each site represents just one tree, for example, then a square grid seems very suitable for modelling a forest plantation. If every site is one (mobile) animal, then the square grid may seem quite rigid and restrictive (but possibly not if there are rules governing migration, or the animals are particularly territorial). On the other hand, if each site represents a small population, it must be small in the sense that complete mixing is reasonable within the site, and neighbourly contact is reasonable between the sites (given the global CA structure and CA rules).

In any event, CA can result in very large dimensional systems that are often useful for gaining intuition about the importance of spatial structure in a system, but which are also extremely difficult to understand analytically. The increased use of computer simulation has been very important to their recent popularity and has been instrumental in studying their behaviour, especially through the use of computer graphics. It is often found that despite the isometry and homogeneity of such spatial domains as a regular square lattice, the mere presence of a spatial environment combines with local rules to allow self-emergent spatial structure and pattern to grow over much larger scales than those of direct local influence. This can, and does, affect the combined spatial population dynamics (*i.e.*

the total population over the whole space) in interesting ways.

Finally, if each CA site can be identified as an individual belonging to a component species in an ecological system, and the CA rules reflect only physically possible behaviour of these individuals (*e.g.* eating, moving, mating) towards each other, then the system is sometimes referred to as an Artificial Ecology (AE). CA and AE are sometimes collectively described as Interacting Particle Systems (IPS). Durrett and Levin (1994b) provide a comprehensive guide to stochastic IPS in ecology; a typically detailed study of an IPS based on Prisoner's Dilemma interactions is given by Herz (1994).

#### **1.7.3.2 Coupled Map Lattices**

Coupled Map Lattices (CMLs) are very similar to CA in many respects - they use discretised space and discrete time - but the population state at each site is a continuous variable, representing one or more (large) local population. As with CA, CMLs are usually updated synchronously by means of difference equations (*i.e.* maps) applied to each site that depend not only on the current state of the site, but also on the state of some neighbouring sites. Typically, this incorporates a diffusive component similar to that used in metapopulation models. Indeed, a CML is essentially an explicit domain of metapopulation patches that are linked in a local fashion and updated in discrete time. Because space is explicitly mapped this can result in the large-scale pattern formation often seen with CA, but impossible for patch models.

Despite the difficulties, some success has been obtained with analytical study of CA. Usually only the simplest cases are considered, *e.g.* just two species (called spin systems) and simplifying assumptions such as an infinitely extended space. Then the dynamics of mean species densities or other simple functions of the state space may be predictable to a degree (*e.g.* Granovsky and Rozov, 1994). On the other hand, understanding the mass of numerical data produced by CA and CML is a problem in itself, requiring the development and use of new techniques (Rand and Wilson, 1995; Rand, 1994).

#### **1.7.3.3 Reaction Diffusion Equations**

Reaction Diffusion Equations (RDEs) are classical continuous space models. Time and population state are also continuous variables. RDEs have a vast range of applications to biological phenomena, not only in population dynamics but also to embryonic development, pattern formation and wound healing to mention just some areas (see Murray, 1990). Part of the reason for their successful application is the prevalence of wave-like phenomena (from travelling chemical concentrations to invading insect populations) and spatial pattern formations (*e.g.* animal coat markings) observed in nature that are readily reproduced by the equations.

Because time evolution is continuous, it is easiest to describe RDEs in relation to non-spatial ODEs. In the latter, the species density  $\mathbf{u}$  is a function of time and the dynamics are governed by an ODE:

$$\frac{d\mathbf{u}}{dt} = \mathbf{f}(\mathbf{u}, t)$$

If more than one species is present,  $\mathbf{u}$  has a dimension greater than one ( $\mathbf{u} \in \mathbb{R}^n$ ); it expresses the total population over an unspecified but thoroughly mixed spatial domain. In an RDE system,  $\mathbf{u} = \mathbf{u}(\mathbf{x}, t)$  is a function of time and a function of space,  $\mathbf{x}$  (usually in one or two dimensions), and the time evolution of species density at a point in space has two components. One (the reaction) is derived from the ODE equation and describes the interaction with other individuals at the same spatial location, the other is diffusion which represents migration or spread of individuals over space to nearby locations. Combining the two gives a set of partial differential equations (PDEs):

$$\frac{\partial \mathbf{u}}{\partial t} = \mathbf{f}(\mathbf{u}, t) + D \nabla^2 \mathbf{u} \quad (1.14)$$

The diffusion matrix  $D$  gives the diffusion rates for the different species, and need not necessarily be constant. It is usually diagonal for biological systems, prohibiting cross-diffusion between species. The role of space in such RDE systems is best interpreted as representing uncountably many self contained populations, each of which is linked to neighbouring populations by migration. In this sense individuals in a population do not directly interact with others in a neighbouring population as they do in a CA.

As an example, consider a single species governed by logistic growth, in just one spatial dimension with constant diffusion (see Murray, 1990). After scaling time and space, equation (1.14) reduces to

$$\frac{\partial u}{\partial t} = u(1 - u) + \frac{\partial^2 u}{\partial x^2} \quad (1.15)$$

This equation, known as Fisher's equation since its proposal as a model for gene spread by Fisher in 1937, admits travelling wave solutions in the population density that can sweep across space. More complicated multi-species systems can exhibit even more interesting behaviour, including large-scale pattern formation through the mechanism of Turing instabilities.

Again, computer simulation is a valuable tool in the analysis of RDE systems because the PDE evolution equations for all but the simplest systems are hard to tackle analytically. Solving them numerically necessarily involves discretising space and time, and in principle this reduces them to the equivalent of a CML, although in practice the diffusion scales are often quite different and CML coupling can be much more general than the equivalent of ordinary diffusion.



## 1.8 Mathematics

### 1.8.1 Event rates

In reality, a specific event, *e.g.* the capture of a particular prey by a particular predator, occurs at a time governed by many factors, not the least of which is chance. In a model, however, we must be much more specific about quantifying this. Only the current state of the system, and chance, can possibly effect the time (or rate) at which future events occur. (The extent to which chance is different from just more environmental interactions (bad weather, being seen, attracting a mate...) is debatable right down to the question of whether or not we live in a deterministic universe. However, most people would agree that, even when all reasonable factors are taken into account, luck still has a part to play. The rabbit slipping on wet ground or choosing to dart left instead of right may be all that stands between life and death in the jaws of a fox.)

Sometimes, time is an important factor and must be included in specifying the state of the system. It may manifest itself as a seasonal variation in some phenomenon (*e.g.* annual reproduction, or excess winter mortality), or through the duration of a lengthy process (*e.g.* pregnancy). But it is often convenient to ignore time and leave it out of the equations. This implies that nothing changes between events and the state of the system must therefore remain constant. This has important consequences for the allowable event rates, which must be independent of the length of time since the last event. We are lead to a uniform rate of occurrence in the sense that in any small interval of time  $\delta t$ , the probability of an event happening is

$$\lambda \delta t + O(\delta t^2) \tag{1.16}$$

Here,  $\lambda$  is the event rate which in general will depend on the current state of the system and the specific event in question, but not on time itself.

The probability  $P_\lambda(t)$  of waiting a time  $t$  until the event first occurs in the next  $\delta t$  can be calculated by writing  $t = n\delta t$  where  $n \in \mathbb{N}$ . It corresponds to  $n$  failures of the event to happen in intervals  $[0, \delta t], [\delta t, 2\delta t], \dots, [(n-1)\delta t, t]$ , and then success in the interval  $[t, t + \delta t]$ :

$$P_\lambda(t) \approx (1 - \lambda \delta t)^n \lambda \delta t + O(\delta t^2)$$

On substituting for  $\delta t$  and using the fact  $(1 + x/n)^n \rightarrow e^x$  as  $n \rightarrow \infty$ , we find

$$P_\lambda(t) = \lambda e^{-\lambda t} \delta t + O(\delta t^2)$$

The waiting time for such an event is therefore exponentially distributed and has a probability density function given by

$$\phi(t) = \begin{cases} \lambda e^{-\lambda t} & \text{if } t \geq 0 \\ 0 & \text{if } t < 0 \end{cases} \tag{1.17}$$

A random variable with this distribution is often called a Sojourn time. It has mean  $1/\lambda$  and variance  $1/\lambda^2$ . A more detailed discussion and derivation is given in Rozanov (1977) where the topic is approached from the viewpoint of a continuous Markov process.

It is important to note that the probability of such an exponentially distributed event happening in an interval is independent of any past length of time during which the event has not happened. The event remembers no history. A useful fact is the following: If  $T_1$  and  $T_2$  are two independent random variables, exponentially distributed with rates (or parameter)  $\lambda_1$  and  $\lambda_2$  then  $T = \min(T_1, T_2)$  is exponentially distributed with parameter  $\lambda_1 + \lambda_2$ . This is easily verified from first principles by noting that the probability of either one of, or both, events in an interval  $\delta t$  is

$$\lambda_1 \delta t (1 - \lambda_2 \delta t) + \lambda_2 \delta t (1 - \lambda_1 \delta t) + \lambda_1 \delta t \lambda_2 \delta t + O(\delta t^2) = (\lambda_1 + \lambda_2) \delta t + O(\delta t^2)$$

In general, the waiting time until the first event for any finite number of such events is similarly exponentially distributed with parameter the sum of the individual rates.

The mathematics is appealing, and for this reason, the case of exponential waiting times is by far the most useful for constructing model systems and in many cases it can be easily justified. Disease transmission through the contact of an infected and susceptible individual, for example, is often a rather opportunistic and random affair, so the assumption of a constant rate for an effective contact taking place seems realistic, or at least as good as any other. But other events are not so naturally exponentially distributed and this is a drawback of the approach. Consider the time for recovery of an infected individual (to an immune class, or perhaps back to being susceptible). For many infections, this time is observed to be much more normally distributed about a certain mean than exponentially distributed, and even when the mean is the same, the difference can be substantial.

However, the effect this assumption will have on the system's behaviour, even when clearly unjustifiable biologically, will generally depend on the system itself. Whilst assuming a human pregnancy lasts an exponentially distributed time may seem bizarre at the individual level, it may not have a significant effect of the dynamics of a whole population compared to the more usual assumption of a nine month average and standard deviation measured in days, especially if reproduction takes place at all times of the year. (But see Keeling and Grenfell (1997) for an example from epidemiology where the exponential distribution is abandoned to important effect).

Models that do explicitly depend upon time are called autonomous. The epidemiology of measles provides an example, where it is thought that school age children are crucial to the continued transmission. Many models incorporate a seasonal effect to model the passage of school terms and holidays, between which contact rates differ. More will be said on this subject in Chapter 6.

Whilst explicitly including time helps to overcome some problems, like those where an interaction rate is seasonally modulated, the question of replacing an unnatural exponential distribution for processes like disease recovery is still not fully answered short of modelling every individual's state (or at least the distribution of their states). It is typically events which do not rely on interactions directly, but embody the result of some undescribed internal process, that are the difficulty.

Nevertheless, there is a partial solution available within the framework of exponentially distributed event times. Instead of modelling a group of infected individuals, for example, by just one class,  $I$ , with exponential decay to a recovered class  $R$ , a sequence of infected classes  $I_1, I_2, \dots, I_n$  can be used. Individuals then move (exponentially) between the classes in order; from class  $I_1$  to  $I_2$ , then  $I_2$  to  $I_3$  *etc.* until finally from  $I_n$  to  $R$ . If the  $n$  transition rates between the classes are identical, then it can be shown that the expected time for an individual to move through all  $n$  infected classes into the recovered class is the same as for just one infected class at an  $n$  times slower rate. The distribution, though, is otherwise different. Figure (1.6) shows this difference as a graph of the proportion of infected individuals (*i.e.* the sum of all those in the infected classes) remaining against time for the case of one, two and seven infection classes. As the number of classes is increased, the initially exponential decay becomes closer to the (backwards) S shaped curve associated with a normal distribution. If members of all the infected classes are treated identically from a dynamical point of view, this technique of increasing the number of classes can alter the effective decay rate assumptions. An unnatural exponential distribution of waiting times can be replaced by a more natural, more normal one with a modest increase in the complexity of the equations.

In view of this possibility, and despite other shortcomings, we should not lose sight of the advantages of not having to model every individual that make uniform rates and the corresponding exponential distributions an obvious starting point in most circumstances.

### 1.8.2 Stability Analysis

Linear stability analysis is a fundamental technique in the analysis of nonlinear differential equations, and it is frequently used in this thesis. The dynamical behaviour of a system of nonlinear coupled ODEs

$$\frac{dx_i}{dt} = f_i(x_1, \dots, x_n, t) \quad (1.18)$$

where  $i = 1, 2, \dots, n$  can be extremely complicated, but equilibrium points (or fixed points) play a crucial role. These are the points in the phase space of the system for which trajectories once at the point will remain there indefinitely. They are easily found (in principle) by solving  $f_i = 0$  for  $i = 1, \dots, n$  simultaneously. Any given fixed point is described as stable (or attracting) if trajectories starting sufficiently close by in phase space (in any direction) approach the point arbitrarily closely as

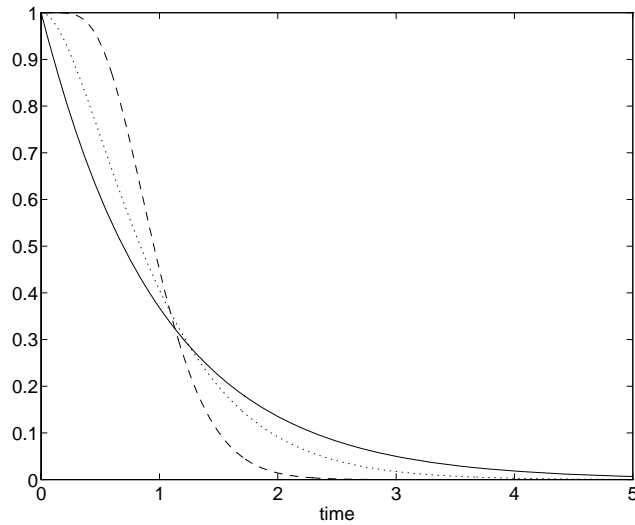


Figure 1.6: Exponential decay for one (solid), two (dotted) and seven (dashed) decay classes. The decay rates are uniform from class to class and are scaled such that the expected time in each case for an individual to decay through all the classes is the same (see text).

$t \rightarrow \infty$ . If this is not true, even in just one direction, the point is unstable or repelling. Ascertaining the stability of fixed points is a relatively simple process which involves calculating the eigenvalues of the corresponding Jacobian matrix of partial derivatives, evaluated at the fixed point. The entries of this matrix are simply

$$\frac{\partial f_i}{\partial x_j}$$

and the fixed point is stable if and only if all the eigenvalues have negative real part. For a detailed exposition, see Guckenheimer and Holmes (1983).

One of the reasons fixed point stability is important is that this local attraction is often reflected as global attraction for trajectories starting in large areas of the phase space. Another is because of the qualitative changes that can occur in the system's dynamical structure when the stability (or existence) of fixed points changes as system parameters are varied. Such points are called bifurcation points and they can provide useful reference points by which to relate the behaviour of the system. A common example is the Hopf bifurcation which occurs when a fixed point loses stability (in the supercritical case) to a limit cycle (periodic orbit) which is born around the fixed point. Such periodic orbits, which appear as maintained oscillations in time for the system variables, can have important biological interpretations.

## 1.9 Summary

‘Probably the most significant and the most questionable assumption involved in the (SIR equations) and their friends and relatives is that of homogeneous mixing.’

Anderson and May’s quote above (1992, page 65) is both illuminating and appropriate to the wider range of model systems introduced in this chapter. Other researchers have also recognised this point and, as discussed, considerable effort has been directed into developing models that have a spatial component. Because of the detailed assumptions and choices involved, spatial models can be more difficult to derive and study. There is certainly no ‘best’ method of representing space; different approaches bring with them different benefits, shortcomings and characteristics.

The aim of the rest of this thesis is to develop another approach to spatial modelling which is substantially different from all those described in this chapter. The hope is that by increasing the library of available techniques, judicious application of this new method will, in conjunction with other spatial models, increase understanding of the importance of spatial structure.

**2**

## **Using Pair Models to Represent Space**

## 2.1 Pair Approximations in the Literature

In a series of recent papers, several authors have studied stochastic CA models with explicit spatial structure in the form of a regular lattice in one or two dimensions. The range of applications has covered vegetative propagation and seed dispersal in plant populations (Harada and Iwasa, 1994), host-pathogen interactions (Satō, Matsuda and Sasaki, 1994), forest gap dynamics (Kubo, Iwasa and Furumoto, 1996) and more general systems of one or two interacting species experiencing birth, death and migration events (Matsuda, Ogita, Sasaki and Satō, 1992; Harada, Ezoe, Iwasa, Matsuda and Satō, 1995; Satō and Konno, 1995). In each case the authors have derived low order systems of ODEs in an attempt to understand or approximate the behaviour of the full stochastic system, without resorting to computationally expensive (and often intuition-lacking) simulations. Crucially, and unlike the mass-action derived systems in Chapter 1, the equations do not completely ignore spatial structure. Instead, these systems measure the abundance of small spatial clusters of individuals, from which information about global densities and spatial correlations can be derived. ODEs are obtained as a truncation of an infinite cascade of equations. There are different ways of truncating such equations, using suitable approximations, and the choice determines the level of spatial structure the equations ‘see’. Indeed, the first natural approximation, often called the mean-field, recovers the mass-action law. It resolves no spatial structure whatsoever and is equivalent to assuming that the population is thoroughly mixed, or that a site’s neighbours are independent of its occupant. Slightly more sophisticated approximations, variously called the pair approximation or doublet decoupling approximation, are the first to involve non-trivial structure.

In all the above cases, it was found that pair approximations compared favourably with the mean-field in quantitative predictions for the behaviour of the CA. Sometimes they even correctly predicted qualitatively different results that the mean-field equations missed. Despite the fact that the dynamical behaviour of both the ODEs and the original CA was invariably simple (species densities converging to equilibrium values), these studies clearly show the value of this new technique. A few other papers have also investigated similar pair approximations in different circumstances.

In Tomé and Drugowich de Felício (1996) an abstracted model of the immune system was considered using a three state probabilistic cellular automaton representing naive T-helper cells and two kinds of antigen-presented T-helper cells. In contrast to the above, their automaton was updated synchronously (*i.e.* all sites simultaneously), but a pair approximation was still successfully used to understand the model, aided by a system symmetry which enabled various results to be obtained without any approximation. Pair approximation techniques have a still longer history in the physics literature, for example in the study of phase transitions in surface-based chemical reactions (Dickman, 1986), and this approach is more typical of Physicists’ interest in bifurcations and symmetry breaking.

The above papers consider only regular lattices (one-dimensional lines or two-dimensional square grids) as spatial environments for the interacting species; the merits and drawbacks of which will be explored later. However, a significantly different pair analysis technique was used by Altmann (1995) in an extension of the study of SIR epidemic models. The unique and appealing difference of this approach is in formulating a model exactly in terms of pair correlations rather than using them to simulate other (lattice) systems, which are themselves of course idealisations of biological realities and not necessarily particularly good ones in the case of disease transmission. Pairwise social contacts, through which infection is transmitted, were directly modelled alongside other non-contacting pairs of individuals, and controlled the dynamics of the epidemic. Contact making and breaking rates also gradually stirred up the population, with no consideration of any large-scale spatial structure. This model too is not dynamically very interesting, because immunity to the disease is never lost so ultimately the infection has to die out. However, expressions for  $R_0$ , the reproductive number, the growth rate of the infectious population, and the final epidemic size provide interesting comparison with the traditional mean-field SIR results with regard to the effect of number of partnerships and contact duration.

Levin and Durrett (1996) and Keeling and Rand (1996); see also Keeling (1995); also study infection systems. The former is based on the contact process, a simplified two-state infection model, and discusses general interacting particle systems on two dimensional lattices. Their moment closure techniques are the equivalent of other authors' mean-field and pair approximations. The latter is an interesting pair-model simulation of measles epidemics with no unnatural underlying lattice assumption. Incorporating age structure with the SEIR equations leads to a large number of pair correlation equations, which are integrated numerically with encouraging results.

In summary, several authors have recently experimented with a novel modelling technique loosely described here as the pair approximation. However, each analysis has been based on a particular example system and there is little discussion of the assumptions and approximations that are directly involved. Such a discussion is the aim of this thesis. This chapter starts the process by taking as an example a two-player game, set in a spatial context and analysed using similar mean-field and pair approximation techniques to those described above.

## 2.2 Spatial Games

The first step is to extend a basic system to a spatial setting. We wish to consider the effect of spatial distribution of the individuals on the dynamics of a population whose interactions are governed by the rules of the simple two-player game of section (1.5). Recall that in the non-spatial case, the dynamics are most easily related to the payoff matrix by the replicator equations. Here we seek the



analog of these equations, appropriate for a range individual based spatial models that are described below.

In spatial models we are forced to consider the individual members of the population more carefully. We assume that individuals play the game not against the whole population but against some local neighbourhood; a specified subset of the population. Given such a neighbourhood, and the payoff matrix for the game, it is natural to define the fitness of an individual as the average score achieved when the game is played with each member of the neighbourhood. The idea common to all the following models is in connecting the game fitness so defined with reproductive success of the individuals: The fitness of an individual at a particular site is interpreted as the rate at which it invades neighbouring sites. Invasion can be thought of as either the death of the neighbour and replacement with an offspring of the invader's type, or alternatively as the neighbour choosing to change strategy to the one displayed by the invader. This is a particularly simple way of relating game fitness to reproductive success in a necessarily individual context, and it assumes the total population stays at a fixed size. More complicated, real-world, processes such as birth, death and contesting are subsumed here into the single process of invasion. Of course, to make sense as a rate, we must ensure the fitness is always non-negative and therefore impose the constraint that the payoff matrix must also be non-negative. It is assumed that the rate of invasion is a constant rate; so given a rate, an actual invasion time is randomly determined from the corresponding exponential distribution as described in section (1.8.1). This makes all three models described below stochastic.

### 2.2.1 Lattice Model

Of the three, this is the model (actually a CA) which most directly accounts for the spatial distribution of the players. Space is explicitly represented as a two dimensional square grid of sites, with the edges joined to give a torus (eliminating boundaries). Each site is occupied by exactly one individual, so the total population remains constant. Any site on the grid has four closest neighbouring sites: North, South, East and West; the Von Neumann neighbourhood of Chapter 1. These constitute the local neighbourhood of the site and affect the dynamics in two ways: Firstly, the fitness of an individual, at any time, is the average score achieved when the game is played against each member of this neighbourhood. (Note that the central site is not included in the neighbourhood, so an individual does not play the game against itself). Secondly, a site can be invaded only by individuals in its local neighbourhood. Invasion is the sole dynamical force on the system, as described above, and can be thought of as the combined effect of death of weak individuals and reproduction of strong ones. At any instant, then, the rate of invasion of an individual site is determined by all individuals up to two sites distant from it, *i.e.* its neighbours and their neighbours; see figure (2.1). Because all individuals of the same type or species are identical, only inter-specific invasions, where a site changes state, are interesting. Invasion events occur stochastically at a rate determined by

each potentially invading individual. The rate is precisely the invader's fitness, as described above. Higher fitness individuals will tend to invade their neighbours at a faster rate.

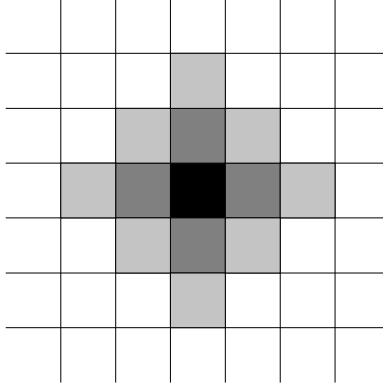


Figure 2.1: The four neighbours (dark grey) of a central site, with the neighbours' neighbours also shown (light grey), on a square grid. Each of the four direct neighbours can potentially invade the central site, and do so at a rate equal to their fitness (which is directly dependent on their neighbours too). Conversely, the central site can also invade each of its neighbours. Which happens first in a particular instance is down to chance.

The state space of the system is  $\{0, 1, \dots, (n - 1)\}^N$  where  $N$  is the total number of individuals (grid sites); typically large, and  $n$  is the number of different species. Here we take  $n = 2$  but the extension to larger  $n$  is easy in principle. As with other CA, rigorous analysis is difficult on such a high dimensional system but the model is easily simulated on a computer with this algorithm: Using the payoff matrix, calculate each individual's fitness. Then for each site in the grid, evaluate the time of invasion of that site as being the shortest invasion time of any of its four neighbours that are of a different type. (Recall these times are picked randomly from the appropriate exponential distribution of each neighbour and there is no need to consider neighbours of the same species). The invasion of the site with the smallest invasion time is then implemented (*i.e.* the invaded site changes state) and the process is repeated.

### 2.2.2 Mean-field Model

This model eliminates as many spatial effects as possible, consistent with using the same approach to the game's dynamics as with the lattice model. It models a fixed total population size ( $N$  indi-

viduals), where fitness and invasion are again determined by interaction with a neighbourhood of four individuals, but where these individuals are selected at random from the total population after each invasion event instead of being explicitly represented in a grid.

The state of this system is therefore uniquely described by just the number of each of the  $n = 2$  species present, and so it is a one-dimensional system because the total population is constant. Computer simulation is achieved in the following way: The probability of picking any individual at random from the population is known. We can further calculate the probability that it finds itself in contact with any particular local neighbourhood, comprising of four neighbours, given the assumption that they are selected at random from the remaining population, (without replacement, in probabilistic terms). There is no distinction made about any relative positioning of the four neighbours, and this is taken into account when the probabilities are calculated. For example, there are six ways the four neighbouring sites could be divided amongst two species A and two species B individuals (namely species A in neighbourhood sites 1&2, 1&3, 1&4, 2&3, 2&4 or 3&4) so the probability of finding such a neighbourhood is six times what it would be if we were interested in particular relative positions (say A to the North and South, B to the East and West). In this fashion, the probability of selecting, at random from the population, any configuration of central site and local neighbourhood can be derived. This gives a frequency distribution of these possible neighbourhood types, over which  $N$  neighbourhoods are distributed; every individual being at the centre of just one. Two species therefore produce ten neighbourhood types: five with species A at the centre (0,1,2,3 or 4 species A neighbours) and five with species B at the centre. As with the lattice model, the rate at which the central site is invaded depends upon its neighbours' fitnesses which in turn depend upon their own neighbours. So to calculate the fitness of the neighbours in a given neighbourhood, we also randomly allocate to each three more neighbours from the remaining population (the fourth, of course, is the central site of the given neighbourhood).

Given these probabilities it is then possible to calculate the next invasion event. For each neighbourhood type, an evaluation of the invasion time of its central site is calculated as the shortest invasion time of any of its neighbours (that are of different type); each of these times is drawn from the exponential distribution with its fitness as parameter but weighted by the relative frequency of the central neighbourhood. This ensures that the probability of a particular neighbourhood being invaded is proportional to its relative frequency as well as its vulnerability, in exactly the same way it would be if all  $N$  individual neighbourhoods were separately formed. (This is possible because of the assumed exponential distribution of invasion times). The invasion of the central site of the neighbourhood type with the smallest invasion time is then carried out by appropriate adjustments of the species totals. The process is then repeated. Effectively, the mean-field model behaves exactly as the lattice model would do if, between each event, all the individuals in the grid were randomly shuffled, so destroying any emerging spatial correlations.

### 2.2.3 Pair Model

The pair model lies somewhere between the lattice and mean-field models; space is neither mapped directly, nor effectively ignored. The intermediate path chosen is to model directly the connections between neighbouring individuals, but nothing else. It is best described by comparison with the mean-field model. Instead of each single species' total population size, the state variables used are the numbers of pairs of direct neighbours. With  $n = 2$  species this gives  $n^2 = 4$  pair types; writing  $P_{AB}$  (respectively  $P_{BA}, P_{AA}, P_{BB}$ ) for the number of A-B (respectively B-A, A-A, B-B) pairs. Further supposing that every individual has, in common with the lattice model, exactly four nearest neighbours implies that the sum of the numbers of pairs is constant, equal to four times the population size if each connection is counted twice; once in each direction. (An A connected to a B therefore counts as an A-B pair and a B-A pair and we have  $P_{AB} = P_{BA}$  because of the symmetry of neighbours. It is convenient to retain both  $P_{AB}$  and  $P_{BA}$  as variables.) The number of individuals of each species,  $S_A$  and  $S_B$ , are then determined by the pair variables because we know every individual has exactly four neighbours. In summary, for the case of just  $n = 2$  species, A and B, we have

$$\begin{aligned} S_A &= \frac{1}{4}(P_{AA} + P_{AB}) \\ S_B &= \frac{1}{4}(P_{BA} + P_{BB}) \end{aligned}$$

and of course

$$\begin{aligned} N &= S_A + S_B \\ P_{AB} &= P_{BA} \\ 4N &= P_{AA} + P_{AB} + P_{BA} + P_{BB} \end{aligned}$$

(Similar equations hold when  $n > 2$  and so a general system is of dimension  $\frac{1}{2}n(n+1) - 1$ ). When  $n=2$  this gives a second order system compared with the first order mean-field model.

Computer simulation of this model is carried out in a similar way to the mean-field model - by considering each of the possible neighbourhood types in turn. The difference is in the calculation of the relative frequencies of the different neighbourhood types, using the pair variables  $P_{AB}$  instead of the single variables  $S_A$ . Given an individual of type A (of which there are a total number  $S_A$ ), then a given neighbour is assumed to be of type B with probability

$$\frac{P_{AB}}{P_{AA} + P_{AB}}$$

*i.e.* the number of A-B pairs divided by the total number of A- pairs. By considering all four neighbours independently in this manner, the relative frequencies of the neighbourhood types can be calculated (again, without replacement in the finite population). Furthermore, fitness is attributed

to each of the neighbours by assuming they themselves are the centre of such a pair-wise randomly chosen neighbourhood, but with one of the four neighbours forced to be the occupant of the original central site. As in the mean-field model, invasion events are implemented in the neighbourhood with shortest invasion time. Pair totals of the four connections broken and the four new connections made are altered as the central site changes.

#### 2.2.4 Model Extensions

For the mean-field and pair models it was assumed that each individual had four neighbours. For comparison to the lattice model this is an obvious choice, but it would be just as easy to consider any other general (but fixed) number of neighbours,  $m$ , per individual. This will be developed in the analysis of section (2.4); all simulations in the next section are in the original case of  $m=4$ .

### 2.3 The Hawk-Dove Game

We take as an example the hawk-dove game of section (1.5.1). Unfortunately, the payoff matrix in its original form is not non-negative for the interesting case when  $v < c$ . This can be remedied so it is applicable here by adding a constant to the matrix, chosen to bring the lowest score, hawk against hawk, up to zero. If we then scale the matrix, which only effects the time scale and not the dynamics, it can be written as

$$\begin{matrix} & \begin{matrix} d & h \end{matrix} \\ \begin{matrix} d \\ h \end{matrix} & \begin{pmatrix} 1 & 1-s \\ 1+s & 0 \end{pmatrix} \end{matrix} \quad (2.1)$$

where  $s = v/c$ , so  $0 \leq s \leq 1$ . For convenience, label the strategies  $d$  for dove and  $h$  for hawk, instead of A and B.

All three models of the last section (mean-field, pair and lattice) were simulated on a computer using payoff matrix (2.1) for various population sizes, initial conditions and values of the game parameter,  $s$ . It is interesting to compare the three models, which produce increasing detail of output. The mean-field gives the single species population totals  $S_d$  and  $S_h$  as a function of time; the pair model also gives the numbers of neighbouring pairs ( $P_{dh}$ , *etc.*), and the lattice model provides a wealth of detail on spatial correlations as well as the single and pair totals. Preliminary investigations involving just the totals  $S_d$  and  $S_h$  therefore allow a degree of comparison between the models.

The main observation was that every run converged to an equilibrium proportion of doves and hawks in the total (fixed) population, notwithstanding stochastic fluctuations. (Although different in one or two minor details from the original hawk-dove example, the models are similar in spirit and this

behaviour was no surprise.) This proportion was found to be very robust to various non-trivial initial conditions, which included random mixes at various proportions, indicating a global basin of attraction. Figure (2.2) show typical output of the three models. Of course by chance either species can (and did) go extinct occasionally when there appeared to be a stable equilibrium of coexistence, but this was rare if the equilibrium, and initial condition, was not very close to either all doves or all hawks.

With the lattice spatial model, the choice of grid size was addressed. Figure (2.3) shows an attempt to determine an appropriate population size for which to collect data. Too small, and stochastic effects will dominate. Too large, and computation time becomes excessive. (For this system, with its equilibrium dynamics, there does not appear to exist a spatial scale above which information is lost by spatial averaging as can happen with other systems (Keeling, 1995)). A grid size of  $50 \times 50$  was established as optimum and used for further simulations, and the same population size, 2500, used for the mean-field and pair models too. Similarly, Convergence times to equilibrium were measured for a range of parameter values and long time simulations were run way in excess of these times to be sure of reaching (stochastic) equilibrium.

Figure (2.4) shows three moments in the evolution of the lattice model pictorially. Even to the eye, there is a clearly discernible spatial pattern present; the clumping of individuals of the same type caused by the local nature of the invasion process. This spatial detail can only be partly captured (to differing degrees) by the mean-field and pair models, so if they are viewed as approximations to the lattice model, their success will be determined by just how important it is to the dynamics of the lattice model. Even though the model may have reached equilibrium proportions of doves and hawks, it is far from being static. The spatial pattern of hawks and doves constantly changes and evolves, so a patch of doves at one time may disappear without trace some time later, while other hawks give way to doves.

The equilibrium proportion of doves in the population as  $s$  varies is shown in figure (2.5). Notice the pair model is a good approximation of the lattice model in this respect; the mean-field less so. Also shown is the non-spatial equilibrium  $1 - v/c$  for the fraction of doves as given by equation (1.10) of section (1.5). This is the population proportion at which the expected fitness of a dove (playing one randomly selected opponent) equals that of a hawk. In comparison to this, the mean-field model predicts the doves always do worse, (*i.e.* are present in lower numbers), whereas the others exaggerate the equilibrium: if doves are favoured in the non-spatial model, they are favoured even more so in the spatial case (and similarly for hawks).

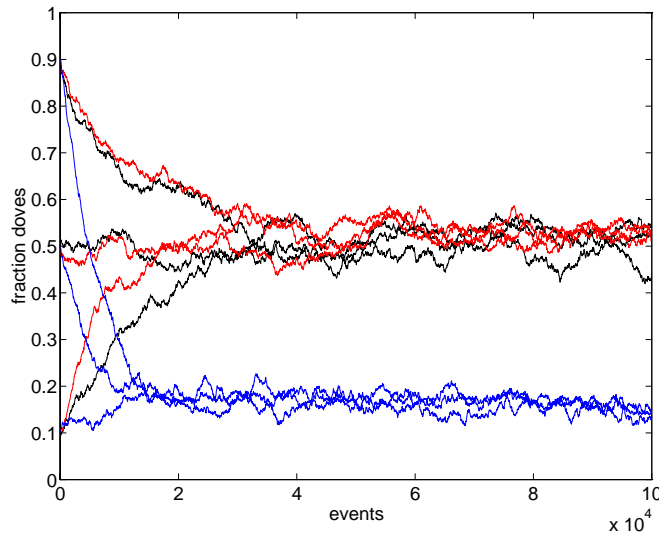


Figure 2.2: Three runs each of the lattice (black), pair (red) and mean-field (blue) models at initial conditions of 10%, 50% and 90% doves (mixed randomly).  $s = 0.5$  in each case, and the grid size is  $50 \times 50$ . The plots indicate the global basin of attraction of the equilibrium and give an idea of both the size of the stochastic perturbations to it and the time of convergence (approximately 30000 events here).

## 2.4 Analysis

In order to understand these results we now aim to analyse their dependence on the system's specification and parameters, particularly  $s$  and the size of the local neighbourhood,  $m$ . Stochastic simulations themselves are of very little use in obtaining any insight, so we mirror the approach taken by others (section (2.1)) and derive a deterministic limit.

As an illustrative example, assume in a population of size  $N$  each individual undergoes some kind of transformation event (removing it from the population) at a uniform rate  $\lambda$ , so  $\lambda\delta t + O(\delta t^2)$  is the probability of the event happening in any interval  $\delta t$ . Summing over all individuals, the size of the population at a later time  $t + \delta t$  can be expressed as

$$\begin{aligned}
 N(t + \delta t) &= N(t) - \sum_{i=1}^{N(t)} [\lambda\delta t + O(\delta t^2)] \\
 &= N(t) - N(t)\lambda\delta t + O(\delta t^2) \\
 \Rightarrow \quad \frac{dN}{dt} &= -\lambda N
 \end{aligned}$$

in the limit  $\delta t \rightarrow 0$ , providing we allow  $N$  to vary as a real variable - the continuity assumption. For large populations this assumption is justifiable as an individual makes up only a small fraction of the total; essentially we are ignoring stochastic fluctuations when their magnitude is small compared to the population size.

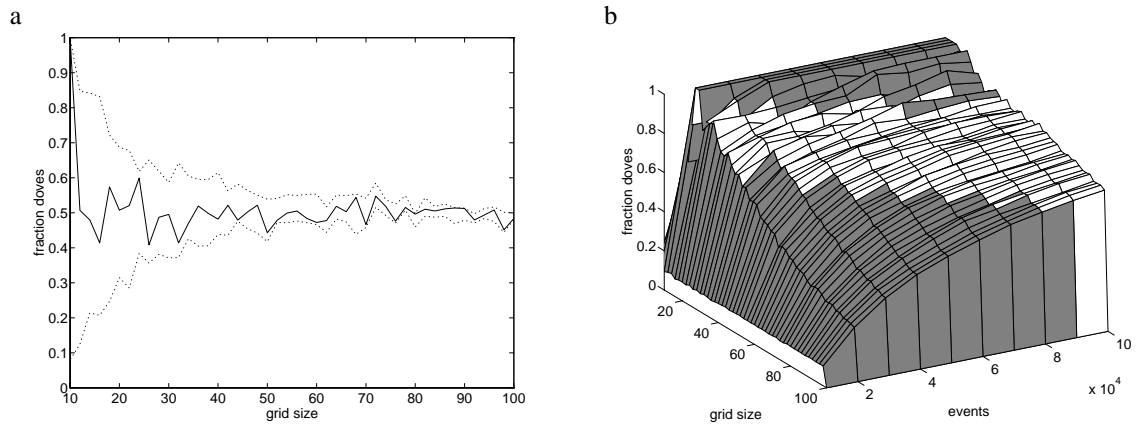


Figure 2.3: Varying the size of the grid for the lattice model from  $10 \times 10$  to  $100 \times 100$ . (a)  $s=0.5$  with 50% doves initially (approximately at equilibrium). The model was run for 50000 events to reach equilibrium then continued for a further 50000 over which the maximum, minimum (dotted) and final (solid) number of doves was recorded. The range of variability decreases with grid size and is within  $\pm 10\%$  for grids of size  $50 \times 50$  and over. (b)  $s=0.4$  with 10% doves initially (far from the expected equilibrium of approximately 80%). For each grid size, the graph shows an average of 5 runs each up to 100000 events. The graph is coloured white when the fraction of doves is between 70% and 90%. Convergence times to equilibrium can be seen to increase with grid size and are in excess of 40000 events for size  $60 \times 60$  and over.

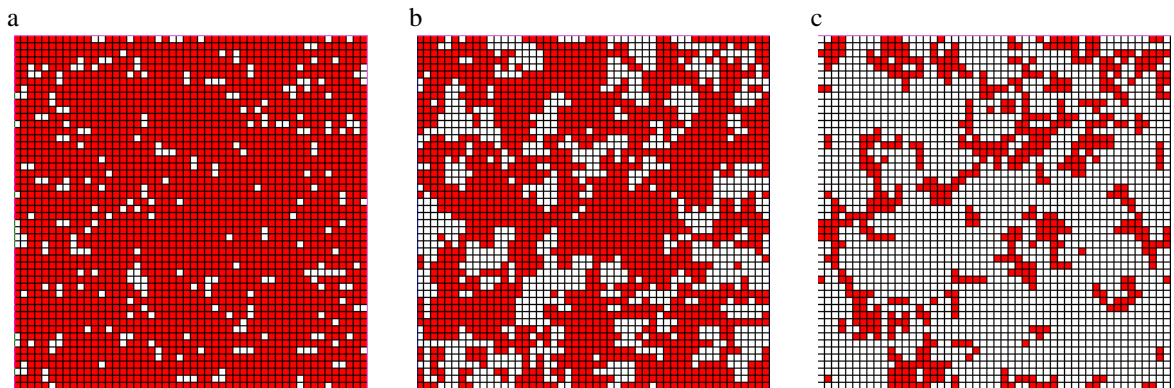


Figure 2.4: Snapshots of the lattice model for  $s = 0.4$  after 0, 3990 and 25890 events on a  $50 \times 50$  grid. Doves (white) and hawks (red) are initially randomly distributed in the ratio 10:90. The patches become more pronounced as the doves increase in number, and by 25890 events the equilibrium proportion of approximately 80% doves is reached (although the spatial pattern constantly changes).



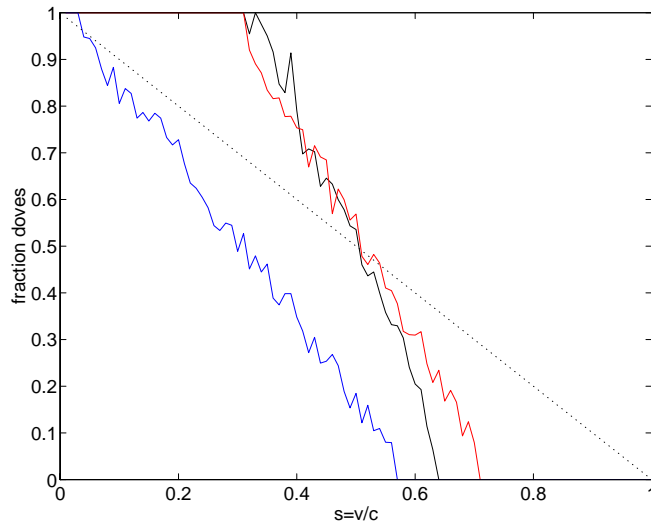


Figure 2.5: Equilibrium composition of the population against  $s$  for the three models: lattice (black), pair (red) and mean-field (blue). The dotted line is the non-spatial theoretical proportion. The explicit model was run on a  $50 \times 50$  grid for 30000 events, the other two models were on a 2500 population over 100000 events.

This method of conversion from stochastic rate to deterministic flow was applied to the mean-field and pair model equations and is detailed below. Standard nonlinear techniques (*e.g.* stability analysis) were then used to study the resulting ODEs.

### 2.4.1 Analysis of Mean-field Dynamics

As discussed previously, it will be useful to perform the analysis of the original model by allowing each individual to interact with a general number,  $m$  (fixed for the whole population) of neighbours instead of fixing this at four.

Define  $r = S_d/N$  to be the fraction on the population who are doves, or equivalently the probability of a randomly selected individual being a dove (recall  $N = S_d + S_h$  where  $S_d$  and  $S_h$  are the dove and hawk populations respectively). There are two types of event to consider: hawks invading doves and doves invading hawks; start with the first. A neighbouring hawk replaces a dove by invasion at a rate equal to the hawk's fitness, so let  $F_h$  be the expected fitness of a hawk given that it is neighbouring (at least) one dove and its other neighbours are selected at random. Recall fitness here

is the average score when playing against its  $m$  opponents, so matrix (2.1) implies

$$\left. \begin{aligned} F_h &= (1+s) \left( \frac{1+(m-1)r}{m} \right) \\ F_d &= (1-s) \left( \frac{1+(m-1)(1-r)}{m} \right) + \frac{(m-1)r}{m} \end{aligned} \right\} \quad (2.2)$$

where  $F_d$  is similarly the expected fitness of a dove given at least one neighbouring hawk.

The rate of invasion of any particular dove actually depends upon its neighbourhood and in particular how many hawks it neighbours. The probability  $\mathbb{P}(d, i)$  of a dove centred neighbourhood, with  $i \in \{0, 1, \dots, m\}$  dove neighbours, being formed from the population, given the rules of the mean-field model, is

$$\mathbb{P}(d, i) = \frac{S_d}{N} \begin{bmatrix} m \\ i \end{bmatrix} r^i (1-r)^{m-i}$$

using the binomial coefficient

$$\begin{bmatrix} m \\ i \end{bmatrix} = \frac{m!}{i!(m-i)!}$$

and we therefore expect to find  $N\mathbb{P}(d, i)$  such doves in total. Each of these is invaded by its  $m-i$  neighbouring hawks at rate  $F_h$ , equivalent to a first invasion rate of  $(m-i)F_h$ . So the overall rate  $\lambda_h$  of invasion of doves by hawks in the population is given by

$$\begin{aligned} \lambda_h &= \sum_{i=0}^m (m-i)F_h \times N\mathbb{P}(d, i) \\ &= \frac{m}{N} S_d S_h F_h \end{aligned}$$

using the standard binomial results of Appendix (A) to substitute for the sum. The reverse argument for invasion of hawks by doves gives, by symmetry,  $\lambda_d = \frac{m}{N} S_d S_h F_d$  and putting these two together finally gives the ODE for  $S_d$  (dot indicates derivative with respect to time)

$$\begin{aligned} \dot{S}_d &= \frac{m S_d S_h (F_d - F_h)}{N} \\ \Rightarrow \dot{r} &= r(1-r)(F_d - F_h) \\ &= \frac{r(1-r)}{m} ((m-1)(1-r) - (m+1)s) \end{aligned} \quad (2.3)$$

Equation (2.3) has three roots. Two are rather trivial:  $r=0$  (all hawks) and  $r=1$  (all doves); the third

$$r = 1 - \frac{(m+1)}{(m-1)} s$$

represents coexistence of hawks and doves, provided it is physically meaningful *i.e.*  $0 \leq r \leq 1$ ; this is provided  $0 \leq s \leq (m-1)/(m+1)$ . Linear stability analysis confirms that this root is stable in this range, and when  $(m-1)/(m+1) \leq s \leq 1$  the  $r=0$  equilibrium is stable.

### 2.4.2 Analysis of Pair Model Dynamics

A similar procedure works for the pair analysis. Again, extend the model to a size  $m$  neighbourhood and calculate the expected fitnesses  $F_h$  and  $F_d$  of a hawk neighbouring a dove and a dove neighbouring a hawk. In the mean-field case, the probability of a given neighbour of a dove site also being a dove was simply  $r$ , here it is replaced by the conditional probability

$$\frac{P_{dd}}{P_{dd} + P_{dh}}$$

which is a function of the pair variables. Using similar formulae the pair model's analogy of equation (2.2) becomes

$$\left. \begin{aligned} F_h &= (1+s) \left( \frac{1}{m} + \frac{(m-1)}{m} \frac{P_{hd}}{(P_{hd} + P_{hh})} \right) \\ F_d &= (1-s) \left( \frac{1}{m} + \frac{(m-1)}{m} \frac{P_{hd}}{(P_{hd} + P_{dd})} \right) + \frac{(m-1)}{m} \frac{P_{dd}}{(P_{hd} + P_{dd})} \end{aligned} \right\} \quad (2.4)$$

The system is second order and can be uniquely described by the number of dove-dove ( $d-d$ ) and hawk-hawk ( $h-h$ ) pairs,  $P_{dd}$  and  $P_{hh}$ . We can write down differential equations for these in the form

$$\left. \begin{aligned} \dot{P}_{dd} &= 2\lambda_{dd}^{hd} - 2\lambda_{hd}^{dd} \\ \dot{P}_{hh} &= 2\lambda_{hh}^{hd} - 2\lambda_{hd}^{hh} \end{aligned} \right\} \quad (2.5)$$

where

$$\lambda_{x'y'}^{xy}$$

is defined as the rate of change of  $x$ - $y$  contacts to  $x'$ - $y'$  contacts. (Changes between  $d-d$  and  $h-h$  only occur through a  $d-h$  intermediary as any one event only changes one individual.) The factor two in equations (2.5) enters because each contact (pair) is counted in both directions, so for example when a  $d-d$  contact changes to a  $d-h$ ,  $P_{dd}$  decreases by two and  $P_{hd}$  and  $P_{dh}$  both increase by one.

Consider first the change of  $d-d$  contacts into  $h-d$  contacts. This happens when a dove is invaded by a hawk and the rate depends upon the neighbourhood, so consider the  $m+1$  dove centred neighbourhoods with  $i$  dove neighbours, where  $i$  ranges from 0 to  $m$ . As in the mean-field case, the rate of invasion of the central dove is proportional to both the number of hawk neighbours,  $m-i$ , and their expected fitness,  $F_h$ . However, the probability  $\mathbb{P}(d,i)$  of a randomly selected neighbourhood being of this type (dove centred with  $i$  dove neighbours) is now

$$\mathbb{P}(d,i) = \frac{S_d}{N} \left[ \begin{matrix} m \\ i \end{matrix} \right] \frac{P_{hd}^{m-i} P_{dd}^i}{(P_{hd} + P_{dd})^m}$$

because of the pair correlations between the central dove and each of its neighbours. Furthermore, in this neighbourhood an invasion of the central dove will change  $i$   $d-d$  pairs into  $h-d$  pairs (and also  $m-i$   $h-d$  pairs into  $h-h$  pairs). So,

$$\begin{aligned}
\lambda_{hd}^{dd} &= \sum_{\text{doves}} \text{rate of invasion of the dove} \times \text{number of dd to hd pair changes} \\
&= \sum_{i=0}^m \text{rate of invasion} \times \text{pair changes} \times \text{number of type } (d, i) \text{ nhds} \\
&= \sum_{i=0}^m (m-i)F_h \times i \times N\mathbb{P}(d, i) \\
&= \frac{F_h S_d}{(P_{hd} + P_{dd})^m} \sum_{i=0}^m (mi - i^2) \begin{bmatrix} m \\ i \end{bmatrix} P_{hd}^{m-i} P_{dd}^i \\
&= \frac{F_h S_d}{(P_{hd} + P_{dd})^m} (m^2 P_{dd} (P_{hd} + P_{dd})^{m-1} - m P_{dd} (m P_{dd} + P_{hd}) (P_{hd} + P_{dd})^{m-2}) \\
&= \frac{(m-1)P_{hd}P_{dd}F_h}{(P_{hd} + P_{dd})}
\end{aligned}$$

where use has again been made of the binomial theorem results in Appendix (A). The other three rates can similarly be calculated; in summary giving

$$\begin{aligned}
\lambda_{hd}^{dd} &= \frac{(m-1)P_{hd}P_{dd}F_h}{(P_{hd} + P_{dd})} \\
\lambda_{dd}^{hd} &= F_d P_{hd} \left( m - \frac{(m-1)P_{hh}}{P_{hd} + P_{hh}} \right) \\
\lambda_{hd}^{hh} &= \frac{(m-1)P_{hd}P_{hh}F_d}{(P_{hd} + P_{hh})} \\
\lambda_{hh}^{hd} &= F_h P_{hd} \left( m - \frac{(m-1)P_{dd}}{P_{hd} + P_{dd}} \right)
\end{aligned} \tag{2.6}$$

Notice the common factor of  $P_{hd}$ . Substituting for each  $\lambda$  into the ODEs (2.5) immediately reveals an equilibrium when  $P_{hd}=0$ . In fact, this corresponds to a whole set of equilibria where  $P_{dd}+P_{hh}=mN$ , the total (and fixed) number of pairs. This represents a static, segregated population where doves and hawks don't mix at all. There can be any ratio of doves to hawks, including all doves ( $P_{dd}=mN$ ) and all hawks ( $P_{hh}=mN$ ). We can also look for a non-trivial coexistence fixed point where  $P_{hd}$ , hence  $S_d$  and  $S_h$ , are non-zero. Equation (2.5) at equilibrium becomes

$$F_d P_{hd} \left( m - \frac{(m-1)P_{hh}}{P_{hd} + P_{hh}} \right) = \frac{(m-1)P_{hd}P_{dd}F_h}{(P_{hd} + P_{dd})} \tag{2.7}$$

$$F_h P_{hd} \left( m - \frac{(m-1)P_{dd}}{P_{hd} + P_{dd}} \right) = \frac{(m-1)P_{hd}P_{hh}F_d}{(P_{hd} + P_{hh})} \tag{2.8}$$

multiplying each by  $(P_{hd} + P_{hh})(P_{hd} + P_{dd})$ , dividing by  $P_{hd} \neq 0$  and a little algebra implies

$$F_d(P_{hd} + P_{dd})(mP_{hd} + P_{hh}) = F_h(m-1)P_{dd}(P_{hd} + P_{hh}) \tag{2.9}$$

$$F_h(P_{hd} + P_{hh})(mP_{hd} + P_{dd}) = F_d(m-1)P_{hh}(P_{hd} + P_{dd}) \tag{2.10}$$

eliminating  $F_d$  and  $F_h$  from these two gives

$$(mP_{hd} + P_{hh})(mP_{hd} + P_{dd}) = (m-1)^2 P_{hh} P_{dd} \tag{2.11}$$

Furthermore, substituting from (2.4) for  $F_d$  and  $F_h$  into (2.9), dividing through by  $(mP_{hd} + P_{hh})$  and more algebra produces  $P_{hd}$  in terms of  $P_{dd}$ :

$$P_{hd} = \frac{ms - 1}{m(1 - s)} P_{dd} \quad (2.12)$$

Using (2.12) and  $P_{dd} + 2P_{hd} + P_{hh} = mN$  gives  $P_{hh}$  in terms of  $P_{dd}$ :

$$P_{hh} = mN - \frac{m + ms - 2}{m(1 - s)} P_{dd} \quad (2.13)$$

Finally, putting everything back into (2.11) we can find the non-trivial equilibrium solution:

$$\begin{aligned} P_{dd} &= \frac{m^2 N (1 - s)(m - ms - 1)}{(m - 2)(m - 1)} \\ P_{hh} &= \frac{m^2 N s(ms - 1)}{(m - 2)(m - 1)} \\ P_{hd} &= \frac{mN(m - ms - 1)(ms - 1)}{(m - 2)(m - 1)} \\ \text{so} \quad S_d &= \frac{N(m - ms - 1)}{m - 2} \\ \text{and} \quad S_h &= \frac{N(ms - 1)}{m - 2} \end{aligned} \quad (2.14)$$

Of course, the population size  $N$  is assumed to be large, and as in the mean-field case it is easier to work not with the number, but with the resulting fraction of doves,  $r = (m - ms - 1)/(m - 2)$ . To be meaningful again we must ensure that  $0 \leq P_{dd}, P_{hd}, P_{hh} \leq 4N$  and  $0 \leq S_d, S_h \leq N$ . This is the case whenever  $s \in [1/m, (m - 1)/m]$ , and numerical investigations indicate that this equilibrium is stable and attracting whenever  $P_{hd}$  is initially non-zero. The local stability is confirmed here analytically by calculating the eigenvalues of the Jacobian (the matrix of partial derivatives) of equation (2.5). Using the MAPLE (Appendix B) mathematical software the eigenvalues were found to be  $U \pm \sqrt{V}$  where

$$\begin{aligned} U &= \frac{1}{2} \frac{(m - 2)(3s^2 m - ms - 2m + 2)}{(m - 1)} \\ V &= U^2 + 2 \frac{(m - 2)(1 - s)(1 + s)(ms - m + 1)(ms - 1)}{(m - 1)} \end{aligned}$$

Assume  $m > 2$ , so in particular  $m > 0$ . The condition  $s \in (1/m, (m - 1)/m)$  then implies

$$(ms - m + 1)(ms - 1) < 0$$

Therefore  $V < U^2$  and we have either two real roots of the same sign or two complex roots. In either case the stability is determined by the sign of  $U$ , which since  $m > 2$  is the sign of  $(3s^2 m - ms - 2m + 2)$ . It is readily checked that this is negative for  $s$  in the required interval and so the equilibrium solution (2.14) is stable. We similarly find for  $s \in [0, 1/m)$ ,  $S_d = 1$  is stable and for  $s \in ((m - 1)/m, 1]$ ,  $S_d = 0$  is stable.

## 2.5 Discussion

Figure (2.6) compares the theoretical equilibria derived from the mean-field (equation (2.3)) and pair (equation (2.14)) ODE analysis with the stochastic simulation data for these two models at  $m = 4$ . With a population of only 2500 individuals there is clearly good agreement between the simulations and ODE systems, and with this hindsight the continuity assumptions can be justified.

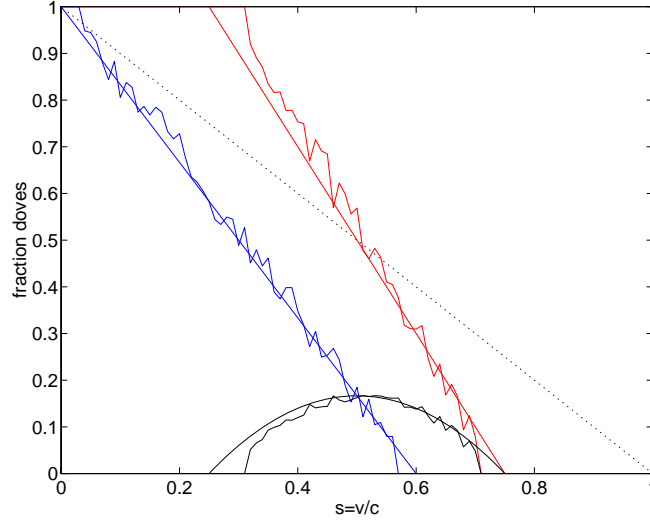


Figure 2.6: Comparison of pair (red) and mean-field (blue) simulation data (irregular lines - from figure (2.5)) with the corresponding theoretical equilibria (straight lines). Also shown for the pair model is the fraction of hawk-dove pairs in the total number of pairs (black) for the simulation and theory and the non-spatial theoretical equilibrium (dotted).

Not surprisingly, the largest discrepancy between the ODE and simulations occurs when both predict a small proportion of hawks or a small proportion of doves. The tendency is for a small population to become extinct much more readily in the stochastic models, as was observed in the simulations, whereas deterministic ODE equilibria do not suffer this fate. For predicting the general trend of the simulations this causes no problem, but it cannot be ignored in the prediction of a particular outcome when a small population is expected. For example, in the pair model at  $s = 0.3$  the ODE predicts an equilibrium population of 10% hawks but the stochastic simulation, run over an intermediate time-scale may well eliminate hawks all together. Of course in a larger population (larger  $N$ ), one expects, and finds, this disagreement is reduced. Small fractions are then represented by larger numbers of individuals and the expected time to extinction is much greater. (However it is worth noting that in any such finite stochastic system an absorbing state of extinction for one species will ultimately always be reached, though possibly over irrelevantly large times-scales). Whilst keeping

in mind these concerns of demographic stochasticity, we should not lose sight of the fact that the qualitative agreement is clearly close enough to merit continued study of the ODE systems.

It is interesting to note the dependency of the mean-field and pair ODE equilibria on  $m$ , the neighbourhood size. The equations for both the straight lines in figure (2.6) imply that both ‘swing round’ to approach the line  $r = 1 - s$  (and each other) as  $m \rightarrow \infty$ ; the mean-field line pivots at  $s = 0, r = 1$  and the pair line pivots in the middle at  $s = 0.5, r = 0.5$ . As individuals interact with larger and larger neighbourhoods, they see a larger and statistically less variable proportion of the total population. In the limit, everyone interacts with everyone and we arrive at the non-spatial case. Both mean-field and pair models therefore capture one interesting aspect of the nature of the spatial game - the importance of the small size of the interaction neighbourhood. The mean-field model in particular shows how important this can be in comparison to the usual assumption of complete mixing of the population (*c.f.* the original hawk-dove game). It is also clear that the pair model is able to incorporate other spatial effects, connected with correlations between neighbours, that the mean-field does not and these too have significant effect on the model behaviour.

In this example, the pair model appears to faithfully reproduce most of the essential behaviour of the interactions seen in the lattice model - at least as far as discernible using the pair variables - although the importance of any further secondary structure to the dynamics is unclear. The question of whether the lattice model itself is a useful or naive model remains unanswered; it is certainly very restrictive in its treatment of spatial relations and alternatives will be discussed in later chapters. It may be argued that pair models alone provide a better framework for a spatial model in some biological systems. But for the moment their use is confined to tools for understanding more explicit systems like the lattice model; as models of models.

## 2.6 General $2 \times 2$ Games

It is possible to extend the Pair model analysis of section (2.4.2) to consider a general payoff matrix for an identical two player, two strategy game. Label the strategies  $x$  and  $y$  and write the payoff matrix as

$$\begin{array}{l} \text{species } x \\ \text{species } y \end{array} \begin{pmatrix} x & y \\ a & b \\ c & d \end{pmatrix} \quad (2.15)$$

Again, the only restrictions on the entries are that all must be non-negative. Proceeding as before, the expected fitnesses  $F_x$  and  $F_y$ , respectively of an  $x$  individual neighbouring at least one  $y$  and a

$y$  neighbouring at least one  $x$  are now

$$\begin{aligned}
F_x &= a \frac{(m-1)}{m} \frac{P_{xx}}{P_{xy} + P_{xx}} + b \left( \frac{1}{m} + \frac{(m-1)}{m} \frac{P_{xy}}{(P_{xy} + P_{xx})} \right) \\
&= \frac{1}{m(P_{xy} + P_{xx})} (a(m-1)P_{xx} + b(mP_{xy} + P_{xx})) \\
F_y &= c \left( \frac{1}{m} + \frac{(m-1)}{m} \frac{P_{xy}}{(P_{xy} + P_{yy})} \right) + d \frac{(m-1)}{m} \frac{P_{yy}}{P_{xy} + P_{yy}} \\
&= \frac{1}{m(P_{xy} + P_{yy})} (d(m-1)P_{yy} + c(mP_{xy} + P_{yy}))
\end{aligned} \tag{2.16}$$

The rates  $\lambda$  are identical to equations (2.6). The algebra involved in solving for the equilibrium in this case is predictably longer and the final forms given below were derived using MAPLE (Appendix B). For convenience,  $N$  was scaled to one. In addition to the segregated equilibria at  $P_{xy}=0$ ,  $P_{xx}+P_{yy}=m$ , the following non-trivial fixed points were found.

**solution 1**

$$\begin{aligned}
P_{xx} &= \frac{m^2(d-b)((d-b)(m-1) - (a-c))}{(m-1)(m-2)(a-c+d-b)^2} \\
P_{yy} &= \frac{m^2(a-c)((a-c)(m-1) - (d-b))}{(m-1)(m-2)(a-c+d-b)^2} \\
P_{xy} &= \frac{m((a-c)(m-1) - (d-b))((d-b)(m-1) - (a-c))}{(m-1)(m-2)(a-c+d-b)^2} \\
x &= \frac{(d-b)(m-1) - (a-c)}{(m-2)(a-c+d-b)} \\
y &= \frac{(a-c)(m-1) - (d-b)}{(m-2)(a-c+d-b)}
\end{aligned} \tag{2.17}$$

**solution 2**

$$\begin{aligned}
P_{xx} &= \frac{bm^2(d(m-1) + c)}{(m-1)(m(ac+bd-2ad) - 2(a-b)(c-d))} \\
P_{yy} &= \frac{cm^2(a(m-1) + b)}{(m-1)(m(ac+bd-2ad) - 2(a-b)(c-d))} \\
P_{xy} &= \frac{-m(a(m-1) + b)(d(m-1) + c)}{(m-1)(m(ac+bd-2ad) - 2(a-b)(c-d))} \\
x &= \frac{(b-a)(d(m-1) + c)}{m(ac+bd-2ad) - 2(a-b)(c-d)} \\
y &= \frac{(c-d)(a(m-1) + b)}{m(ac+bd-2ad) - 2(a-b)(c-d)}
\end{aligned} \tag{2.18}$$

Solution 2 can be effectively discounted as it is unphysical ( $0 \leq P_{xx}, P_{xy}, P_{yy} \leq m$  and  $0 \leq x, y \leq 1$  do not hold) in almost all cases:

*Lemma*

There exists only one non-trivial physically meaningful solution of form (2.18) for payoff matrices of type (2.15), which is given by  $P_{xx} = P_{yy} = 0$ ,  $P_{xy} = m/2$  in the case  $b = c = 0$ .



*Proof*

Suppose there is such a solution with  $a, b, c, d \geq 0$  and  $m > 1$ . We have

$$(m-1)d + c \geq 0$$

$$(m-1)a + b \geq 0$$

Let  $D = (m-1)(m(ac + bd - 2ad) - 2(a-b)(c-d))$  be the denominator of  $P_{xx}, P_{xy}$  and  $P_{yy}$  in equation (2.18).

If  $P_{xx} > 0$ , (2.18)  $\Rightarrow D > 0 \Rightarrow P_{xy} < 0$ , a contradiction so  $P_{xx} = 0$ .

If  $P_{yy} > 0$ , (2.18)  $\Rightarrow D > 0 \Rightarrow P_{xy} < 0$ , a contradiction so  $P_{yy} = 0$ .

This leaves the unique solution  $P_{xx} = P_{yy} = 0, P_{xy} = m/2$  obtained when  $b = c = 0$ .  $\square$

Furthermore, solution 2 is unstable: Calculating the eigenvalues of the Jacobian matrix of partial derivatives using MAPLE found them to be  $(m-1)a$  and  $(m-1)d$ , both of which are positive for non-trivial payoff matrices.

Solution 1 is more interesting. It depends only on the values  $a - c$  and  $d - b$ , not  $a, b, c$  and  $d$  individually, so substitute  $\alpha = a - c$  and  $\beta = d - b$ . We can then find restrictions on the payoff parameters  $\alpha$  and  $\beta$  which admit meaningful solutions with  $P_{xy} \neq 0$ . Note it is sufficient to further check  $P_{xx}$  and  $P_{yy}$  are non-negative, because then  $0 \leq P_{xx}, P_{xy}, P_{yy} \leq m$  and  $0 < S_x, S_y < 1$  are guaranteed. For its existence, we must assume  $m > 2$  and  $\alpha + \beta \neq 0$  in the remainder of this section. The first assumption is a natural one to make, for the only population with just two neighbours per individual is necessarily strung out along a rather unnatural one-dimensional line. The second assumption eliminates a special but uninteresting case when one species outcompetes the other.

Now suppose  $\alpha > 0$  and we have such a solution. From (2.17),

$$P_{yy} \geq 0 \Leftrightarrow \beta \leq (m-1)\alpha$$

but

$$\beta \leq (m-1)\alpha \quad \text{and} \quad P_{xy} > 0 \quad \Leftrightarrow \quad \beta \geq \frac{1}{(m-1)}\alpha$$

so we must have

$$\frac{1}{(m-1)}\alpha \leq \beta \leq (m-1)\alpha \tag{2.19}$$

and  $P_{xx} \geq 0$  follows. Similarly, if  $\alpha < 0$  we find that

$$(m-1)\alpha \leq \beta \leq \frac{1}{(m-1)}\alpha \tag{2.20}$$

Figure (2.7) shows these restricted regions on the  $\alpha, \beta$  plane.

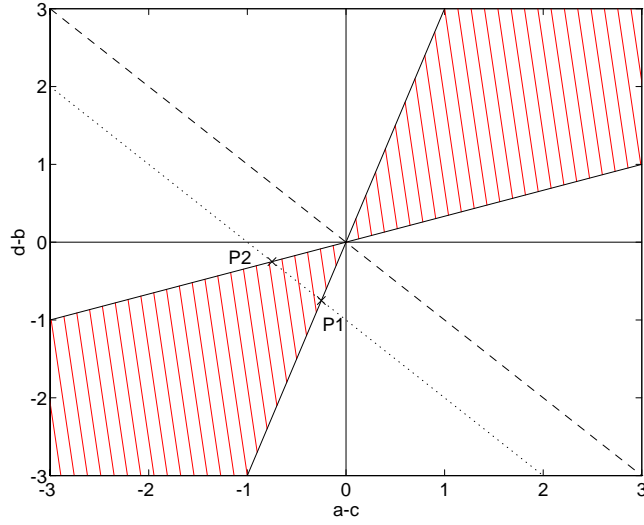


Figure 2.7: A plot of the  $\alpha, \beta$  plane showing the region (shaded) in which solution 1 represents a non-trivial and meaningful equilibrium solution. The dashed line is the singular case  $\alpha + \beta = 0$ . The dotted line is that corresponding to the original hawk-dove game; points  $P_1 = (\frac{1}{m}, \frac{m-1}{m})$  and  $P_2 = (\frac{m-1}{m}, \frac{1}{m})$  are the limits of the solution (*cf.* figure (2.5)).

### 2.6.1 Stability

Calculating the stability of the fixed points is slightly more complicated in the general case, but linearisation about the equilibrium using the Jacobian matrix yields the following result about solution 1:

*Lemma*

When it exists as a meaningful solution, in the sense of figure (2.7), solution 1 is stable for  $\alpha, \beta < 0$  and unstable for  $\alpha, \beta > 0$ .

*Proof*

Using MAPLE the two eigenvalues are found to be  $U \pm \sqrt{V}$  where

$$U = -\frac{1}{2} \frac{(m-2)}{(m-1)} \frac{(m\alpha\beta + 2m(\alpha b + \beta c) - (\alpha + \beta)(b + c))}{(\alpha + \beta)}$$

$$V = U^2 + 2 \frac{(m-2)}{(m-1)} \frac{(\alpha\beta + \alpha b + \beta c)(\alpha(m-1) - \beta)(\beta(m-1) - \alpha)}{(\alpha + \beta)^2}$$

The equation for  $P_{xy}$  implies  $(\alpha(m-1) - \beta)(\beta(m-1) - \alpha)$  is always positive, because  $P_{xy}$  must be positive. Therefore  $V \leq U^2$  if and only if

$$\alpha\beta + \alpha b + \beta c = \alpha b + \beta a \leq 0$$

There are two cases:

- i.  $\alpha, \beta > 0 \Rightarrow V > U^2$  and both eigenvalues are real, but are of opposite sign. The equilibrium is therefore an unstable saddle-point.
- ii.  $\alpha, \beta < 0 \Rightarrow V < U^2$  so either both eigenvalues are real and of the same sign as  $U$ , or they are a complex conjugate pair with real part  $U$ . Both cases are stable if and only if  $U < 0$ , and we show that this must be the case:

The sign of  $U$  is the sign of

$$\begin{aligned}\omega &= m\alpha\beta + 2m(\alpha b + \beta c) - (\alpha + \beta)(b + c) \\ &= b((2m-1)\alpha - \beta) + c((2m-1)\beta - \alpha) + m\alpha\beta\end{aligned}$$

Equation (2.20) implies  $(2m-1)\alpha - \beta < 0$  and recall  $a, b, c, d \geq 0 \Rightarrow \alpha \geq -c \Rightarrow m\alpha\beta \leq -mc\beta$ , so

$$\begin{aligned}\omega &< 0 + c((2m-1)\beta - \alpha) - mc\beta \\ &= c((m-1)\beta - \alpha) \\ &\leq 0 \quad \text{using (2.20) again} \quad \square\end{aligned}$$

By similar analysis, it is possible to show that when the coexistence equilibrium is unstable, both the single species solutions (all  $x$  or all  $y$ ) are themselves locally stable, and the eventual equilibrium position depends on the initial conditions.

## 2.7 Other Ways of Incorporating Space

The regular square grid chosen as a spatial environment for the lattice model (and motivation for the mean-field and pair models) is just one of many possible choices, albeit a very popular choice for models in the literature. However, it is impossible to tell just how important (in a biological sense) this, or any other, particular choice is in determining the overall behaviour of the system without comparing and contrasting other approaches. This point is often overlooked in the literature where it is common practice to choose one spatial context for a model and present results with reference to this alone. This is particularly dangerous when specific biological insight is being sought, but is also a concern even when more abstract models are studied for their own sake. The effect of varying the spatial structure is surely as valid a question to ask as varying any other system parameter.

	discrete individuals	infinitesimal individuals
explicit space	IPS	RDE
well mixed	PATCH	ODE

Table 2.1: Relative representations of spatial structure and the continuity approximation for the different models studied in Durrett and Levin (1994a).

A useful exception, especially relevant here, is the paper by Durrett and Levin (1994a). They considered four different approaches to modelling species interactions, and took as their example system a two player spatial game similar to the one discussed in this chapter. They contrasted :

- i. An Ordinary Differential Equation (ODE) model, where space is ignored (equivalently, the population is well mixed) and the population is assumed to be composed of infinitesimal individuals, so it is represented by a continuous variable.
- ii. Reaction Diffusion Equations (RDE), where space was explicitly represented by Partial Differential Equations (PDEs) but the population is still assumed to be continuous.
- iii. A Patch model that grouped discrete individuals into patches within which there is thorough mixing, and without additional spatial structure between the patches (which were linked by migration).
- iv. An Interacting Particle System (IPS), in which individuals are discrete, and are grouped in small numbers in well-mixed spatial cells. Space is then treated explicitly in the form of a square grid of these cells.

The ODE and RDE systems ignore the discreteness of individuals and are deterministic; the patch model and IPS incorporate discreteness and are necessarily stochastic, their behaviour being determined by simulation. Spatial structure, however, is explicitly represented only in the RDE and IPS models. This is summarised in table (2.1).

The dynamics of these systems are similar in principle to the spatial game considered in this chapter, though more complex in detail. An individual's fitness was determined by playing the game against an appropriate subset of the population (the whole population, the local population density, members of your patch or members of neighbouring sites; depending on the model), and this determined its birth/death rate (negative game scores were allowed and represented death rates, not birth rates). Additionally, density dependent death was included to keep the non-constant population in check,

and migration terms were introduced for appropriate mixing of the population. The authors chose three game matrices and demonstrated that no two of the models agreed in all three cases. They observed that both spatial structure and the discreteness of individuals can substantially effect the outcome.

For example, using the payoff matrix (and following my notation)

$$\begin{array}{c} \text{species } x \\ \text{species } y \end{array} \begin{pmatrix} x & y \\ 0.7 & 0.4 \\ 0.4 & 0.8 \end{pmatrix} \quad (2.21)$$

they noted that either species may dominate (and the other go extinct) with the ODE and PATCH models, depending on initial conditions. Calculating the basins of attraction for the two attracting fixed points of the ODE system (all species  $x$  or all species  $y$ ) easily verifies this. However, both the RDE and IPS predict that species  $y$  will ultimately dominate, from any generic initial condition, and drive species  $x$  extinct. The explanation is dependent on the spatial structure. If a locally large population of species  $y$  builds up, which it almost certainly will somewhere, it will gradually spread through the whole system because of it's slight advantage at a front with species  $x$ .

Another example (less comparable to my earlier model because of the negative payoffs and dynamic population size) indicates the importance of discreteness:

$$\begin{array}{c} \text{species } x \\ \text{species } y \end{array} \begin{pmatrix} x & y \\ -0.6 & 0.9 \\ -0.9 & 0.7 \end{pmatrix} \quad (2.22)$$

In an isolated round of the game, species  $x$  always does better than species  $y$  regardless of the opponent, but a population consisting of purely species  $y$  dies out (because a negative score represents a negative net birth rate). In the discrete systems, PATCH and IPS, coexistence is possible, which is not found in the continuous systems, where species  $x$  drives species  $y$  extinct and then dies itself. The possibility of local extinctions in the discrete models enables species  $y$  to survive in pockets of space, temporarily escaping 'predation' by species  $x$ . Without this source of 'food', species  $x$  could not exist.

This paper concisely demonstrates the crucial effect that the choice of model can have, particularly with regard to spatial structure and the nature of individuals. Preliminary results from the pair approximation derived in this chapter have shown that it is able to capture a component of the behaviour attributable to space and discreteness, but now is the time for a note of caution.

Figure (2.8) shows graphically the behaviour of the general  $2 \times 2$  PA with  $m = 4$  and the payoff matrix (2.21). The phase space is the surface of  $P_{xx} + 2P_{xy} + P_{yy} = \text{constant}$  (scaled to 1) constrained by the requirement that all pair variables are non-negative. It is viewed from above, with

the three apexes representing the extremes of all  $h-h$  pairs, all  $d-h$  pairs and all  $d-d$  pairs. Typical trajectories show that the internal equilibrium is unstable, and phase space is divided into two basins of attraction - one leading to the extinction of species  $x$ , and one leading to the extinction of species  $y$ . The PA therefore behaves in a similar way to the ODE and PATCH models, and fails to show the almost certain dominance of species  $y$ . Unlike with the IPS model, the relevant demographic stochasticity in small discrete populations has been missed by the pair approximation.

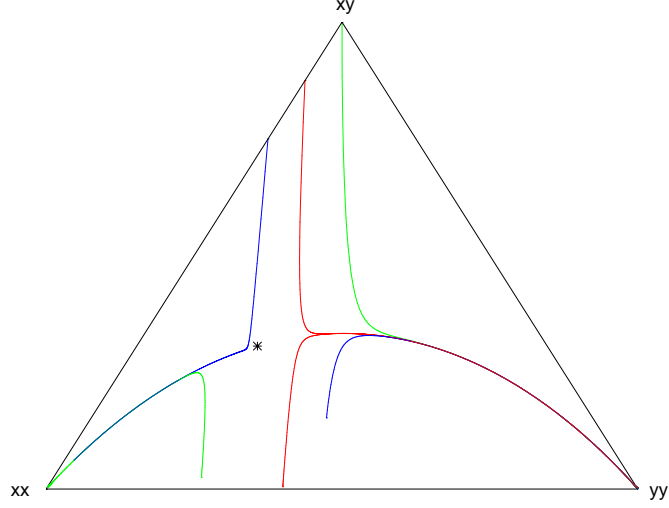


Figure 2.8: Trajectories in the ODE pair approximation spatial game for payoff matrix (2.21) with  $m = 4$ . The equilibrium here is unstable (black cross) and trajectories are attracted to either all species  $x$  or all species  $y$  depending on initial conditions. A representative sample are shown.

It is unlikely that any deterministic models will easily incorporate the stochastic effects (such as local extinctions) produced by small populations. The Durrett and Levin example serves as a reminder that we must be vigilant when these are dynamically important. However, we have seen that one consequence of individuals can be incorporated through considering interactions in small local neighbourhoods. Add to this the analytical convenience, and pair ODEs look like a promising tool, worthy of further investigation.

Figure (2.9) shows the dynamics for the hawk-dove game in phase space at  $s = 0.4$ . In contrast to figure (2.8), the internal coexistence equilibrium is globally attracting (except for the trivial boundary any initial condition on the line from  $dd$  to  $hh$  where  $P_{hd} = 0$  and the model is stationary). Attention will return to simple game theory pair models in Chapter 5.

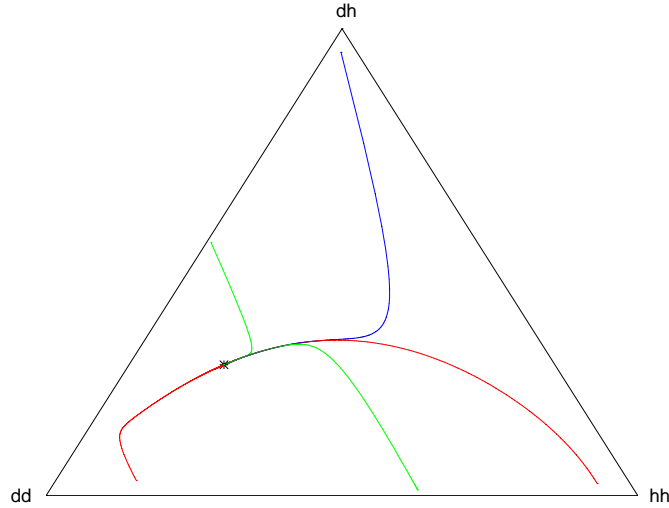


Figure 2.9: Trajectories in the ODE pair approximation hawk-dove spatial game at  $s = 0.4$ . The attracting fixed point is shown as a small cross.

## 2.8 Summary

In this chapter a stochastic pair model was introduced as an alternative description of space for a model between two contesting species. From this model a deterministic system of ODEs was derived which accurately matched its behaviour and therefore reduced the need for numerical simulation. Furthermore, in the dynamically simple case studied, these ODEs were able to predict the behaviour of another high dimensional, spatially explicit lattice model much more accurately than a mean-field approach was able to do. They also compared favourably with different classes of model used in other studies in the analysis of spatial games, in term of analytical tractability and spatial awareness. This is an encouraging start.

Because game theoretic interactions are relatively simple, and they can be adapted to a wide range of applications (and not just in biology), they are a particularly useful system to study in a spatial context. Attempting to understand cooperation, through the IPD, will be their main application in this thesis, but other authors have addressed different questions. One topic closely related to cooperation is the emergence of altruistic behaviour. In a spatial environment, limited mixing may promote altruism (as opposed to egotistical behaviour) by increasing the relatedness of closely neighbouring individuals. The problem is understanding how the altruistic behaviour could be ‘exported’ to more selfish environments (Wilson, Pollock and Dugatkin, 1992). This invasion problem is tackled by van Baalen and Rand (1997) who also apply a pair model analysis developed in parallel to the work in this thesis. A different problem is that of honest signalling in the biological world. Communication systems between individuals, for example to indicate suitability as a mate, are vulnerable to cheating

individuals who give false signals for personal gain. One adaptation against this is the development of costly signals which are too expensive to fake; the peacock's tail is a good example. Krakauer and Pagel (1995), however, use a spatial model to suggest that low cost signals could be stable under certain conditions.

Other authors have addressed the problem of tractably incorporating the effects of spatial structure in related ways. Based on a spatial model for plant population growth, Bolker and Pacala (1996) also derive evolution equations for mean population density and spatial covariance (first and second moment equations) by ignoring all higher moments. Their single-species model is based on a continuous spatial dimension, not individual spatial sites, and their dynamic interactions are therefore diffuse in space. They too report encouraging results in comparison with explicit stochastic simulations. A degree of analysis is also possible with simple local dynamics in one dimensional space.

Despite its success, the derivation of the ODEs was a rather heuristic affair in this example, particularly in respect to assigning an average fitness to invading individuals. Especially if the pair model is to be viewed as an approximation to the lattice model (which it certainly was in motivation), the nature of the approximation assumptions was not made clear. A more formal approach, where assumptions are more readily quantified, is the subject of the next chapter. There are comparable attempts in the literature to formally approximate high dimensional (spatial) systems by successive cascades of smaller systems, *e.g.* Lemaitre, Chaté and Manneville (1995), but these are not specifically directed at the biological problems that are relevant to this thesis. In addition to putting the pair approximation on a rigorous footing, it is hoped a more general approach will enable such pair models to be viewed as model systems in their own right, where the very restrictive structure of a square grid is replaced by a less rigid concept of space which is arguably more realistic in many situations.



**3**

# **Formalisation of the Pair Approximation**

### 3.1 Chapter Aims

This chapter aims to make the process of pair approximation more formal, in a way which makes it clear what the approximation is and exactly what is being thrown away.

We study the following general biological system and start with virtually no restrictive assumptions on the system's spatial structure; only that it is comprised of individuals and neighbourly connections between them, together forming a network. Each individual occupies one site of the network, and every site contains one individual (or occupant). It will invariably be the case that the connections play a fundamental role in the dynamics of the system. The system undergoes change in time through discrete events. An event is any change to the structure or composition of the population. In many models, events will change only an individual's type (*e.g.* from susceptible to infected) but other events may change the individual's connections to its neighbours, remove (deceased) individuals, or introduce new ones. An event type, such as infection, occurring at different sites constitutes different specific events (so typically lots of particular infection events are simultaneously possible). Whilst the network remains in a state  $\sigma$ , we assume that any particular event happens at a uniform rate, so the expected waiting time is exponentially distributed.

Each individual belongs to a certain type or species. The network may be described as regular if any two sites are indistinguishable (*i.e.* have the same pattern of connections with respect to other sites) when the occupying individuals are ignored *e.g.* a square lattice with each site neighbouring its four nearest neighbours and toroidal boundary conditions. A network is irregular if it is not regular. Regularity is a property of the spatial structure alone. A network is fixed if all sites and connections within it remain constant (events only change the occupant of each site) and dynamic if the number of sites changes or connections are made or broken.

Further restrictions and assumptions will be applied to specific models only as is necessary to form dynamic approximations. But one of these is common to all systems: the assumption that the network is composed of a sufficiently large number of individuals and connections that a continuity approximation is valid. Without this, no differential equations could be written and we would be left to consider small populations, stochastic fluctuations and chance. In situations where this is the case, different approaches are required.

### 3.2 Basic Premise and Notation

The state of the system is defined by the state (*i.e.* occupant) of every site in the network and the connections between them. Let  $\sigma = \sigma^t$  represent the state at time  $t$ , and represent the individual currently occupying a site  $x$  in the network by  $\sigma(x)$ . At any one time, any two individuals are either

connected (equivalently interacting, or neighbouring) or not. Assuming each individual belongs to a set of species (or types) labelled  $i, j, k, \dots$ , we can count the following path connections over the whole network:

- $(i)$  = number of sites in state  $i$
- $(ij)$  = number of  $ij$  pairs  
*i.e.* direct connections from an  $i$  site to a  $j$  site
- $(ijk)$  = number of  $ijk$  triples  
*i.e.* occurrences of an  $i$  neighbouring a  $j$  which neighbours a  $k$  (distinct from  $i$ )

In general, we say an  $n$ -path ( $n \geq 2$ ) is any ordered set of  $n$  distinct individuals,  $x_1, \dots, x_n$  such that  $x_i$  neighbours  $x_{i+1}$  for  $i \in \{1, \dots, n-1\}$ . (There may or may not be other connections between the  $x_i$ s). Write  $(i_1 \dots i_n)$  for the number of paths of type  $i_1, \dots, i_n$  *i.e.* paths along individuals of types  $i_1, \dots, i_n$  in a given network. (There is usually no ambiguity over which network the path numbers refer to, so for convenience no  $\sigma$  subscript is used.)

It is convenient to count each path in both directions, so certain symmetries hold *e.g.*  $(ij) = (ji)$  and  $(ijk) = (kji)$ , and other terms, *e.g.*  $(ii)$  and  $(iji)$  are always even. In particular note that triples, which are paths of length three, must be between three distinct individuals, so a connection from an  $i$  to a  $j$  and back again does not count. Different paths can overlap and particular individuals or connections will typically be part of many different paths of various lengths. (In the language of Chapter 2,  $(ij)$  is identical to  $P_{ij}$  and  $(i)$  is identical to  $S_i$ ).

We call any finite set of individuals and subset of the possible connections between them (such that there is a path within the set from any individual to any other) an element. Essentially, elements are just connected subsets of a whole network and are usually thought of as small. The size of any element is the number of individuals it contains, and its diameter,  $D$ , is the smallest number such that any two individuals within the element can be connected by a path of length at most  $D$ . For example, an  $n$ -path itself is an element of size  $n$  and diameter  $n-1$ .

### 3.2.1 Dynamics

Let  $E^\sigma$  be the set of all possible events that can occur in a particular system, given the network is in state  $\sigma$ . The system changes state (write  $\sigma \longrightarrow \sigma_e$ ) when an event  $e \in E^\sigma$  occurs; let  $r^\sigma(e)$  be the rate at which this happens. (Recall that we assume each event has an exponentially distributed occurrence time).

We must consider the effect of combined events. Suppose a system  $\sigma$  is susceptible to two events, 1 and 2, which can occur sequentially in either order. If each event rate is independent of the

other event, then the probability of both occurring in a small time interval  $\delta t$  is the product of the probability of each happening separately (see section (1.8.1)):

$$\mathbb{P}[1, 2 \text{ in } \delta t] = r^\sigma(1)r^\sigma(2)\delta t^2 + O(\delta t^3)$$

The situation is more complicated if the events are not independent, which in general they will not be. The probability of both happening is then dependent on which event happens first, and precisely when; see figure (3.1). However, this probability can be bounded above, because independently event 1 occurs at a rate not greater than  $\max\{r^\sigma(1), r^{\sigma^2}(1)\}$ , and event 2 not greater than  $\max\{r^\sigma(2), r^{\sigma_1}(2)\}$ , giving

$$\mathbb{P}[1, 2 \text{ in } \delta t] \leq \max\{r^\sigma(1), r^{\sigma^2}(1)\} \times \max\{r^\sigma(2), r^{\sigma_1}(2)\} \times \delta t^2 + O(\delta t^3)$$

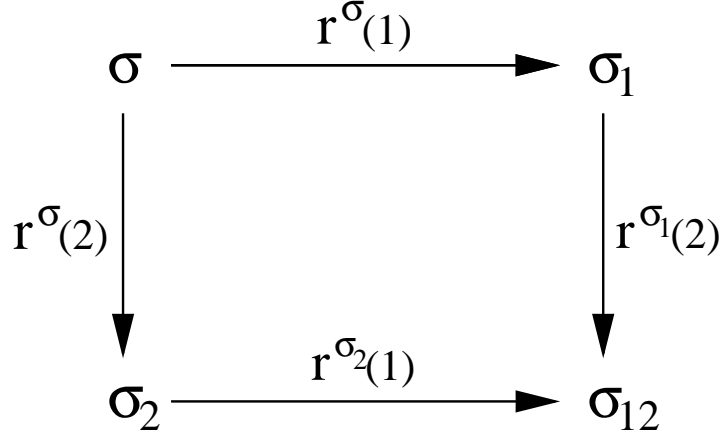


Figure 3.1: Two alternative routes for two events to occur in a network initially in state  $\sigma$ : event 1 then event 2, or event 2 then event 1. Event rates are shown alongside the corresponding paths.

Importantly, this is still a second order term in  $\delta t$ . We will therefore find that in either case, it is not necessary to consider the possibility of closely spaced events as  $\delta t \rightarrow 0$ .

Take  $f(\sigma)$  to be any real-valued function of the network whose value can be reasonably approximated as continuous. In view of the preceding remarks, to first order we need only consider the effect of all possible events individually on the value of  $f$  over a short time  $\delta t$ . Using the individual probabilities, the expectation of the value of  $f$  at time  $t + \delta t$  is

$$\mathbb{E}[f(\sigma^{t+\delta t})] = f(\sigma^t) + \sum_{e \in E^\sigma} (r^\sigma(e)\delta t + O(\delta t^2)) (f(\sigma_e^t) - f(\sigma^t))$$

On taking the limit  $\delta t \rightarrow 0$  and using the assumption that  $\mathbb{E}[f(\sigma)] \approx f(\sigma)$  in this limit, this equation becomes

$$\dot{f} \equiv \frac{df}{dt}(\sigma) = \sum_{e \in E} r^\sigma(e) \delta f_e \quad (3.1)$$

where  $\delta f_e = f(\sigma_e) - f(\sigma)$ , the change in  $f$  caused by event  $e$ .

This is the main building block of the chapter and forms the basis of the dynamics for all such network models, under the given assumptions. Common choices for  $f$  will include  $f = (i)$ , the total number of individuals of type  $i$ , or  $f = (ij)$ , the number of  $i$ - $j$  pairs. An example of a function  $f$  that does not satisfy the assumptions would be the number of type  $i$  neighbours of a particular site  $x$ , because an individual site typically has only a limited number of neighbours and  $f$  could not reasonably be assumed continuous and independent of stochastic fluctuations.

### 3.3 Averages and Errors

The system's dynamics, as controlled by the event rates, will usually be determined by the application of local rules (*i.e.* rules dependent only on the state of the local spatial neighbourhood), and events will typically affect only a small number of sites - possibly just one. In these circumstances, knowing the number of neighbours of each particular type for a particular site  $x$  is enough to calculate the rate  $r^\sigma(e)$  of an event  $e$  occurring at site  $x$ , and possibly also the resultant change  $\delta f_e$ . Unfortunately, knowing these numbers for each site  $x$  amounts to knowing the state of the whole network which is of no help in understanding or modelling the system. However, useful approximations can be made which do help achieve these goals and this is a good place to start.

Define  $Q_x^\sigma(i)$  to be the number of type  $i$  individuals neighbouring site  $x$  when the system is in state  $\sigma$ . If we can't know  $Q_x^\sigma(i)$  for every site, the best approach is to average it over a particular range of sites. For example, let  $\overline{Q}^\sigma(i)$  be the average number of  $i$  neighbours per site over all sites, so

$$\overline{Q}^\sigma(i) = \frac{1}{N} \sum_{x \in \sigma} Q_x^\sigma(i) \quad \text{or equivalently} \quad \sum_{x \in \sigma} \overline{Q}^\sigma(i) = \sum_{x \in \sigma} Q_x^\sigma(i)$$

where  $N$  is the total population size. We can also take the average  $\overline{Q}^\sigma(i|j)$  over all sites in state  $j$ :

$$\overline{Q}^\sigma(i|j) = \frac{1}{(j)} \sum_{(j)} Q_x^\sigma(i) \quad \text{or equivalently} \quad \sum_{(j)} \overline{Q}^\sigma(i|j) = \sum_{(j)} Q_x^\sigma(i)$$

and let  $\overline{Q}^\sigma(i|jk)$  be the average number of  $i$  neighbours of the  $j$  site over all  $j$ - $k$  pairs:

$$\overline{Q}^\sigma(i|jk) = \frac{1}{(jk)} \sum_{(jk)} Q_x^\sigma(i) \quad \text{or equivalently} \quad \sum_{(jk)} \overline{Q}^\sigma(i|jk) = \sum_{(jk)} Q_x^\sigma(i)$$

To explain the summation notation,  $\sum_{(i_1, \dots, i_n)}$  denotes the sum over all paths of type  $i_1, \dots, i_n$  in the network where the  $i_1$  individual occupies site  $x$ . (When it becomes necessary, we will further

say that individual  $i_2$  occupies site  $y$  and individual  $i_3$  occupies site  $z$ ).

Associated with each average is an error term  $\eta_x^\sigma$ , which is the difference between an actual site's neighbourhood and the corresponding average value. We can then write

$$\begin{aligned} Q_x^\sigma(i) &= \overline{Q}^\sigma(i) + \eta_x^\sigma(i) \\ Q_x^\sigma(i) &= \overline{Q}^\sigma(i|j) + \eta_x^\sigma(i|j) \quad \text{when } \sigma(x) = j \\ Q_x^\sigma(i) &= \overline{Q}^\sigma(i|jk) + \eta_x^\sigma(i|jk) \quad \text{when } \sigma(x) = j \text{ and } \sigma(y) = k \text{ with } x \text{ and } y \text{ neighbouring sites.} \end{aligned} \quad (3.2)$$

As a consequence, the following linear  $\eta_x^\sigma$  sums vanish, for all choices of  $i, j$  and  $k$  from the set of species types:

$$\begin{aligned} \sum_{x \in \sigma} \eta_x^\sigma(i) &= 0 \\ \sum_{(j)} \eta_x^\sigma(i|j) &= 0 \\ \sum_{(j,k)} \eta_x^\sigma(i|jk) &= 0 \end{aligned} \quad (3.3)$$

### 3.3.1 Reduction

With a little thought it is possible to express the  $\overline{Q}$  averages in terms of the numbers of paths. For example,

$$\overline{Q}^\sigma(i|j) = \frac{(ij)}{(j)}$$

holds for all  $i$  and  $j$ . Similarly for the triple averages, and providing  $i \neq k$ , we have

$$\overline{Q}^\sigma(i|jk) = \frac{(ijk)}{(jk)}$$

If  $i = k$  we must remember that the  $j$  site in every  $i$ - $j$  pair is a neighbour of the  $i$  site, but that this double connection is not counted as a true triple. The correct expression involves one extra neighbour to give the average as

$$\overline{Q}^\sigma(i|ji) = \frac{(iji)}{(ji)} + 1$$

Consider the triple  $(ijk)$  when  $i \neq k$ . We have

$$\begin{aligned} (ijk) &= \sum_{(j)} Q_x^\sigma(i) Q_x^\sigma(k) \\ &= \sum_{(j)} \left( \overline{Q}^\sigma(i|j) + \eta_x^\sigma(i|j) \right) \left( \overline{Q}^\sigma(k|j) + \eta_x^\sigma(k|j) \right) \\ &= \sum_{(j)} \left( \overline{Q}^\sigma(i|j) \overline{Q}^\sigma(k|j) + \eta_x^\sigma(i|j) \eta_x^\sigma(k|j) \right) \\ &= (j) \overline{Q}^\sigma(i|j) \overline{Q}^\sigma(k|j) + \sum_{(j)} \eta_x^\sigma(i|j) \eta_x^\sigma(k|j) \\ &= \frac{(ij)(jk)}{(j)} + (j) \Gamma^\sigma(i|j|k) \end{aligned} \quad (3.4)$$

where use has been made of equations (3.3) and  $\Gamma^\sigma(i|j|k)$  is defined to be

$$\Gamma^\sigma(i|j|k) = \frac{1}{(j)} \sum_{(j)} \eta_x^\sigma(i|j) \eta_x^\sigma(k|j) \quad (3.5)$$

Similarly for  $i = k$ :

$$\begin{aligned} (iji) &= \sum_{(j)} Q_x^\sigma(i) (Q_x^\sigma(i) - 1) \\ &= \sum_{(j)} \left( \overline{Q}^\sigma(i|j) + \eta_x^\sigma(i|j) \right)^2 - \sum_{(j)} Q_x^\sigma(i) \\ &= (j) \overline{Q}^\sigma(i|j)^2 - (j) \overline{Q}^\sigma(i|j) + \sum_{(j)} \eta_x^\sigma(i|j)^2 \\ &= \frac{(ij)(ji)}{(j)} - (ij) + (j) \Gamma^\sigma(i|j|i) \end{aligned} \quad (3.6)$$

Therefore substituting for  $(ijk)$  from either equation (3.4) or equation (3.6) into the expression for  $\overline{Q}^\sigma(i|jk)$  gives

$$\overline{Q}^\sigma(i|jk) = \overline{Q}^\sigma(i|j) + \frac{1}{\overline{Q}^\sigma(k|j)} \Gamma^\sigma(i|j|k) \quad (3.7)$$

in both the cases  $i = k$  and  $i \neq k$ .

### 3.4 The Aim of the Pair Approximation

The idea behind a pair approximation is to be able to express the system dynamics purely in terms of the number of different pair connections at a given time; in our language, this is in terms of the  $(ij)$  variables, (although we also use the ‘lower order’ singles  $(i)$  too).

Without further approximation, equation (3.7) gives an exact relation between high order average terms  $\overline{Q}^\sigma(i|jk)$  and lower order average terms  $\overline{Q}^\sigma(i|j)$ , together with an error term  $\Gamma^\sigma(i|j|k)$ . Terms like  $\overline{Q}^\sigma(i|jk)$  (and others similar) appear naturally in many systems in the evolution equations for pair variables,  $(ij)$ , formed using equation (3.1). However, we shall see that these systems of equations do not form closed systems and are therefore of little use by themselves. This is because (recall section (3.3.1)) each  $\overline{Q}^\sigma(i|jk)$  is a function of higher order triple (3-path) totals. Writing as equation (3.7) allows us to close the system by sensibly approximating  $\Gamma^\sigma(i|j|k)$ , which turns out to be a particularly natural process.

It is worth noting that at this point we are still independent of any assumptions about the system’s spatial structure or particular dynamics. These enter on a model by model basis in the consideration of each  $\Gamma^\sigma(i|j|k)$ .

### 3.5 Estimating the Error Terms, $\Gamma$

Consider  $\Gamma^\sigma(i|j|k)$  as defined in equation (3.5). Although  $\eta_x^\sigma$  is the difference between an actual number of neighbours and the average number of neighbours of a site  $x$ , it will not necessarily be small compared to this average; any individual site could, for many reasons, have a far from average set of neighbours. In fact, all sites could, with some below the average and some above. There is therefore no justification in simply setting each  $\eta_x^\sigma$ , and hence every  $\Gamma^\sigma$ , to zero. This is also clear from equation (3.7) directly. Approximating  $\Gamma^\sigma(i|j|k) \approx 0$  implies  $\overline{Q}^\sigma(i|jk) \approx \overline{Q}^\sigma(i|j)$  *i.e.* it assumes that knowing a particular  $j$  site has a  $k$  neighbour has no effect on the expected number of  $i$  neighbours it will have. Although this ignores any triple correlation between the  $i$  and  $k$ , this is not an issue when we are considering a pair model. What matters is that it also ignores all effects of the number of neighbours. This can be a very important point. For example, with a regular grid structure, where each individual has exactly  $m$  neighbours knowing a  $j$  site has a  $k$  neighbour means it has only  $m - 1$  other neighbours which could possibly be an  $i$ . We should at the very least expect

$$\overline{Q}^\sigma(i|jk) \leq \overline{Q}^\sigma(i|j)$$

if  $i \neq k$ , and

$$\overline{Q}^\sigma(i|ji) \geq \overline{Q}^\sigma(i|j)$$

otherwise. A more sophisticated approach than to simply set each  $\eta_x^\sigma$ , and hence every  $\Gamma^\sigma$ , to zero is required.

We return to the stochastic spatial hawk-dove lattice model of Chapter 2 to observe  $\Gamma^\sigma(i|j|k)$  experimentally; figure (3.2) shows the results. Each simulation (one at  $s = 0.4$ , one at  $s = 0.5$ ) gave a time series for  $\Gamma^\sigma(i|j|k)$  as the system approached, and remained at, an equilibrium proportion (at  $s = 0.5$  this was approximately 50% doves; at  $s = 0.4$  it was near 80% doves). A total population size of 10000 was used. Of the eight possible  $\Gamma^\sigma(i|j|k)$  if fact only two are independent. Clearly  $\Gamma^\sigma(d|d|h) = \Gamma^\sigma(h|d|d)$  and  $\Gamma^\sigma(d|h|h) = \Gamma^\sigma(h|h|d)$ , and it can be further shown that

$$\eta_x^\sigma(i|j) = -\eta_x^\sigma(j|j)$$

because the population is comprised of just two species and each individual has a constant neighbourhood size, so knowing the number of  $d$  neighbours gives the number of  $h$  neighbours.

It can be seen from the graphs that  $\Gamma^\sigma(i|j|k)$  is, as expected, far from zero. In this equilibrium example at least, each  $\Gamma^\sigma(i|j|k)$  has a clearly defined non-zero mean with relatively small fluctuations around it. It is a good target for approximation, in the first instance by its mean.



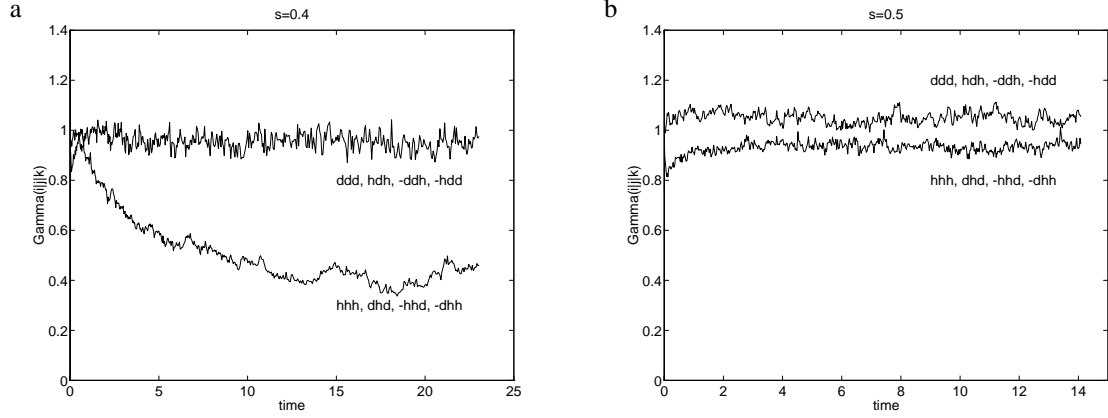


Figure 3.2: Time series of both independent  $\Gamma^\sigma(i|j|k)$  terms for the lattice spatial hawk dove model of section (2.2.3), run at a)  $s = 0.4$  and b)  $s = 0.5$ . The letter groupings (ddd *etc.*) represent the  $ijk$  in  $\Gamma^\sigma(i|j|k)$ .

### 3.5.1 $\Gamma^\sigma(i|j|i)$

A closer inspection of the case when  $i = k$  reveals that  $\Gamma^\sigma(i|j|i)$  is a sum of squares (see equation (3.5)) and so is guaranteed to be non-negative. Substituting for  $\eta_x^\sigma(i|j)$ ,

$$\begin{aligned}\Gamma^\sigma(i|j|i) &= \frac{1}{(j)} \sum_{(j)} \left( Q_x^\sigma(i) - \overline{Q}^\sigma(i|j) \right)^2 \\ &= \mathbb{E}_j \left[ (Q_x^\sigma(i) - \mathbb{E}_j [Q_x^\sigma(i)])^2 \right] \\ &= \text{var}_j [Q_x^\sigma(i)]\end{aligned}$$

where  $\mathbb{E}_j [\cdot]$  is the average value (mean) over all sites  $x$  such that  $\sigma(x) = j$ , and  $\text{var}_j [\cdot]$  the variance. In words then,  $\Gamma^\sigma(i|j|i)$  is the variance, over the network, in the number of  $i$  neighbours of all  $j$  individuals. If the distribution of  $Q_x^\sigma(i)$  is observed to be close to some standard distribution, it may be possible to estimate this variance using well known results.

The question to ask is: what is a justifiable assumption on the distribution of  $Q_x^\sigma(i)$ ? Two common cases, the Poisson and the Binomial distribution, applicable to discrete variables such as  $Q_x^\sigma(i)$ , are discussed below.

**Poisson** This is the easiest case to consider analytically. If  $Q_x^\sigma(i)$  is Poisson distributed over  $j$  sites with parameter  $\lambda$ , then both the mean and variance of  $Q_x^\sigma(i)$  equal  $\lambda$ . But the mean is known to be  $\overline{Q}^\sigma(i|j)$  therefore

$$\Gamma^\sigma(i|j|i) = \overline{Q}^\sigma(i|j)$$

Substituting into equation (3.7), this assumption gives a refined estimate for the expected

number of  $i$  neighbours of the  $j$  over all  $(ji)$  pairs as

$$\overline{Q}^\sigma(i|ji) = \overline{Q}^\sigma(i|j) + 1 + \text{error}$$

**Binomial** The binomial distribution is described by two parameters,  $n$  the number of trials and  $a$  the probability of success; see Appendix (A). The mean number of successes is  $na$  and the variance  $na(1-a)$ . So, the average number of successes  $na = \overline{Q}^\sigma(i|j)$  is known but further information is needed to determine  $n$  and  $a$  individually, and hence calculate the variance. We must specifically decide what is meant by a trial, and what is a success.

The regular grid case is easy. Because each individual has  $m$  neighbours it is natural to take  $n = m$  trials and say a success occurs when a particular neighbour of a given  $j$  site is of type  $i$ . Then,  $a = \overline{Q}^\sigma(i|j)/m$  and we have

$$\Gamma^\sigma(i|j|i) = \overline{Q}^\sigma(i|j) \left( 1 - \frac{\overline{Q}^\sigma(i|j)}{m} \right) \quad (3.8)$$

and substituting into equation (3.7) gives

$$\overline{Q}^\sigma(i|ji) = \frac{(m-1)}{m} \overline{Q}^\sigma(i|j) + 1 + \text{error}$$

If we do not have a regular grid it is less clear how to proceed and the binomial distribution is possibly less relevant. We could view  $n$  as the whole species  $i$  population (assumed large enough to satisfy the continuity approximation) and think of each one as a potential neighbour, with a success representing every actual neighbour. In this case typically  $a \ll 1$ , because an individual usually interacts with only a small fraction of the whole population directly, and the binomial distribution is very closely approximated by the Poisson distribution, as considered above. Alternatively, we could assume a composite distribution for the number of type  $i$  neighbours  $Q_x^\sigma(i)$  of  $j$  sites which involves the binomial distribution. For example, the total number of neighbours of any  $j$  site could be assumed to be Poisson distributed, and within each (differently sized) neighbourhood, the number of type  $i$  neighbours could be further assumed to be binomially distributed. In certain cases, simple overall distributions may be recovered. However, justifying these assumptions in particular cases, along with the associated calculations, may not be easy and the task is left to others.

### 3.5.2 $\Gamma^\sigma(i|j|k)$

The case of  $\Gamma^\sigma(i|j|k)$  when  $i \neq k$  is slightly more complicated.

$$\begin{aligned} \Gamma^\sigma(i|j|k) &= \frac{1}{(j)} \sum_{(j)} \eta_x^\sigma(i|j) \eta_x^\sigma(k|j) \\ &= \frac{1}{(j)} \sum_{(j)} \left( Q_x^\sigma(i) - \overline{Q}^\sigma(i|j) \right) \left( Q_x^\sigma(k) - \overline{Q}^\sigma(k|j) \right) \\ &= \mathbb{E}_j [Q_x^\sigma(i) Q_x^\sigma(k)] - \overline{Q}^\sigma(i|j) \overline{Q}^\sigma(k|j) \end{aligned}$$

and we find that  $\Gamma^\sigma(ijk)$  is actually the covariance of  $Q_x^\sigma(i)$  and  $Q_x^\sigma(k)$ . To make progress now we have to consider the distribution of both  $i$  and  $k$  neighbours in parallel around the same given  $j$  site. The increased complexity arises because these are not necessarily independent, but there are two analogous choices to the  $i = k$  case:

**Poisson** If we assume the number of  $i$  and  $k$  neighbours of a given  $j$  site are separately Poisson distributed, with means  $\overline{Q}^\sigma(i|j)$  and  $\overline{Q}^\sigma(k|j)$  respectively, then the calculation is trivial. The two random variables are independent and their covariance,  $\Gamma^\sigma(i|j|k)$ , must be zero. This gives

$$\overline{Q}^\sigma(i|jk) = \overline{Q}^\sigma(i|j)$$

when substituted into (3.7).

**Trinomial** This is a natural extension of the binomial distribution. It also represents  $n$  independent trials of an experiment, but success or failure to select a type  $i$  neighbour is now replaced by a three-way condition: success at selecting an  $i$  neighbour, success at selecting a  $k$  neighbour, or failure to select either. Appendix (A) gives the theorem, and useful results, derived from two successive applications of the binomial theorem. The average number of  $i$  and  $k$  successes are given respectively by  $na_i$  and  $na_k$  where  $a_i$  ( $a_k$ ) is the probability of choosing an  $i$  ( $k$ ) neighbour. Matching  $na_i$  to  $\overline{Q}^\sigma(i|j)$  and  $na_k$  to  $\overline{Q}^\sigma(k|j)$  gives  $a_i$  and  $a_k$  when  $n$  is known. As with the binomial distribution, this is most natural in the regular network case where  $n = m$  is fixed for all individuals.

This trinomial approach is fully consistent with the binomial distribution in the case  $i = k$  because although  $Q_x(i)$  and  $Q_x(k)$  are not independent variables, each separately has a binomial distribution in the absence of any knowledge about the other. See Appendix (A).

Using equation (A 8) with  $a = a_i$ ,  $b = a_k$ ,  $c = 1 - a - b$  and  $n = m$ , we have

$$\begin{aligned} \Gamma^\sigma(i|j|k) &= \mathbb{E}_j [Q_x^\sigma(i)Q_x^\sigma(k)] - \overline{Q}^\sigma(i|j)\overline{Q}^\sigma(k|j) \\ &= m(m-1)a_ia_k - \overline{Q}^\sigma(i|j)\overline{Q}^\sigma(k|j) \\ &= \frac{m-1}{m}\overline{Q}^\sigma(i|j)\overline{Q}^\sigma(k|j) - \overline{Q}^\sigma(i|j)\overline{Q}^\sigma(k|j) \\ &= -\frac{1}{m}\overline{Q}^\sigma(i|j)\overline{Q}^\sigma(k|j) \end{aligned} \tag{3.9}$$

and substituting into equation (3.7) this time gives

$$\overline{Q}^\sigma(i|jk) = \frac{(m-1)}{m}\overline{Q}^\sigma(i|j)$$

as the closure relation.

The approximations for  $\overline{Q}^\sigma(i|jk)$  in the cases covered above can be summarised as

	Poisson	Multinomial ( $m$ neighbours)
$\overline{Q}^\sigma(i ji)$	$\overline{Q}^\sigma(i j) + 1$	$\frac{(m-1)}{m}\overline{Q}^\sigma(i j) + 1$
$\overline{Q}^\sigma(i jk)$ ( $i \neq k$ )	$\overline{Q}^\sigma(i j)$	$\frac{(m-1)}{m}\overline{Q}^\sigma(i j)$

The next step is to decide which of these assumptions, if any, is the most suitable for a particular system. A first guess might be that the Multinomial is more natural for regular networks and the Poisson for irregular ones, and so we return to the example from Chapter 2 to see how this looks in practice.

### 3.6 Example - Spatial Game Revisited

We now reformulate the two-player spatial game of Chapter 2, in this new notation. Labelling the species  $i$  and  $j$ , equation (3.1) splits into two sums, the first representing invasions of a  $j$  (at site  $y$ ) by an  $i$  (at site  $x$ ), and the second invasions of an  $i$  (at site  $y$ ) by a  $j$  (at site  $x$ ):

$$\dot{f} = \sum_{(ij)} \left[ \frac{aQ_x^\sigma(i) + bQ_x^\sigma(j)}{Q_x^\sigma(i) + Q_x^\sigma(j)} \right] \delta f_{ij} + \sum_{(ji)} \left[ \frac{cQ_x^\sigma(i) + dQ_x^\sigma(j)}{Q_x^\sigma(i) + Q_x^\sigma(j)} \right] \delta f_{ji}$$

where we have used the fact that the rate  $r^\sigma(e)$  is the fitness of the invading individual, equal to its average score against all its neighbours. This is  $[aQ_x^\sigma(i) + bQ_x^\sigma(j)] / [Q_x^\sigma(i) + Q_x^\sigma(j)]$  if it is of type  $i$ , and  $[cQ_x^\sigma(i) + dQ_x^\sigma(j)] / [Q_x^\sigma(i) + Q_x^\sigma(j)]$  if it is of type  $j$ . When  $f = (i)$ , a quantity of fundamental interest,  $\delta f_{ij} = +1$  and  $\delta f_{ji} = -1$  corresponding to gaining or losing one individual from the species  $i$  population, and we have (with dot denoting derivative with respect to time)

$$(\dot{i}) = \sum_{(ij)} \left[ \frac{aQ_x^\sigma(i) + bQ_x^\sigma(j)}{Q_x^\sigma(i) + Q_x^\sigma(j)} \right] - \sum_{(ji)} \left[ \frac{cQ_x^\sigma(i) + dQ_x^\sigma(j)}{Q_x^\sigma(i) + Q_x^\sigma(j)} \right] \quad (3.10)$$

An identical procedure gives the  $(\dot{j})$  equation, and because the total population size is fixed, we find  $(\dot{i}) + (\dot{j}) = 0$ . It is therefore sufficient to consider  $(i)$  alone. We also need the pair equations; consider first  $f = (ii)$ . Now  $\delta f_{ij} = 2Q_y^\sigma(i)$ , the number of  $i$  neighbours of the invaded  $j$  multiplied by two to count each i-i pair in both directions, and similarly  $\delta f_{ji} = -2Q_y^\sigma(i)$ , so the  $(ii)$  equation becomes

$$(\dot{ii}) = 2 \sum_{(ij)} \left[ \frac{aQ_x^\sigma(i) + bQ_x^\sigma(j)}{Q_x^\sigma(i) + Q_x^\sigma(j)} \right] Q_y^\sigma(i) - 2 \sum_{(ji)} \left[ \frac{cQ_x^\sigma(i) + dQ_x^\sigma(j)}{Q_x^\sigma(i) + Q_x^\sigma(j)} \right] Q_y^\sigma(i) \quad (3.11)$$

The equations for  $(jj)$  and  $(ij)$  are similarly found to be

$$(jj) = -2 \sum_{(ij)} \left[ \frac{aQ_x^\sigma(i) + bQ_x^\sigma(j)}{Q_x^\sigma(i) + Q_x^\sigma(j)} \right] Q_y^\sigma(j) + 2 \sum_{(ji)} \left[ \frac{cQ_x^\sigma(i) + dQ_x^\sigma(j)}{Q_x^\sigma(i) + Q_x^\sigma(j)} \right] Q_y^\sigma(j) \quad (3.12)$$

$$(ij) = \sum_{(ij)} \left[ \frac{aQ_x^\sigma(i) + bQ_x^\sigma(j)}{Q_x^\sigma(i) + Q_x^\sigma(j)} \right] (Q_y^\sigma(j) - Q_y^\sigma(i)) \\ + \sum_{(ji)} \left[ \frac{cQ_x^\sigma(i) + dQ_x^\sigma(j)}{Q_x^\sigma(i) + Q_x^\sigma(j)} \right] (Q_y^\sigma(i) - Q_y^\sigma(j)) \quad (3.13)$$

In a fixed network model such as this, where no event makes or breaks any contact, the total number of pair connections must remain constant (as indeed must the number of all size paths) and it is no surprise to find that  $(ii) + 2(ij) + (jj) = 0$ . Attention can therefore be restricted to the equations for  $(ii)$  and  $(jj)$ . We have not yet used any knowledge of the network structure; equations (3.10), (3.11), (3.12) and (3.13) apply equally well to a square lattice as to any other regular or irregular network.

### 3.6.1 Regular Networks

If we assume a regular network, as was the case in Chapter 2, the above equations can be simplified because every individual has the same number of neighbours, so  $Q_x^\sigma(i) + Q_x^\sigma(j) = m$ , constant, for all  $x$ . The  $Q_x^\sigma$  terms now appear only either linearly or quadratically, so substitution for them using (3.2) and (3.3) allows the sum to be transformed, with no further approximation, into a product and error terms:

$$(i) = \frac{(ij)}{m} \left[ a\overline{Q}^\sigma(i|ij) + b\overline{Q}^\sigma(j|ij) - c\overline{Q}^\sigma(i|ji) - d\overline{Q}^\sigma(j|ji) \right] \\ (ii) = \frac{2(ij)}{m} \left[ (a-c)\overline{Q}^\sigma(i|ij)\overline{Q}^\sigma(i|ji) + b\overline{Q}^\sigma(j|ij)\overline{Q}^\sigma(i|ji) - d\overline{Q}^\sigma(j|ji)\overline{Q}^\sigma(i|ij) \right. \\ \left. - (a-c)\Gamma^\sigma(i|ij|i) - b\Gamma^\sigma(j|ij|i) + d\Gamma^\sigma(i|ij|j) \right] \quad (3.14) \\ (jj) = \frac{2(ij)}{m} \left[ (d-b)\overline{Q}^\sigma(j|ji)\overline{Q}^\sigma(j|ij) + c\overline{Q}^\sigma(i|ji)\overline{Q}^\sigma(j|ij) - a\overline{Q}^\sigma(i|ij)\overline{Q}^\sigma(j|ji) \right. \\ \left. - (d-b)\Gamma^\sigma(j|ij|j) - c\Gamma^\sigma(j|ij|i) + a\Gamma^\sigma(i|ij|j) \right]$$

High order averages  $\overline{Q}^\sigma(i|jk)$  abound in the equations, but new error terms  $\Gamma^\sigma(\cdot|ij|\cdot)$  also appear because of the nonlinearity in the  $(ii)$  and  $(jj)$  equations. They are defined in an analogous way to equation (3.5):

$$\Gamma^\sigma(i|jk|l) = \frac{1}{(jk)} \sum_{(jk)} \eta_x^\sigma(i|jk) \eta_y^\sigma(l|kj) \quad (3.15)$$

Note also that in this regular network case, the equation for  $(i)$  in (3.14) is redundant, because  $(i) = [(ii) + (ij)]/m$ . This is readily checked by observing that  $\Gamma^\sigma(\cdot|\cdot|\cdot|i) + \Gamma^\sigma(\cdot|\cdot|\cdot|j) = 0$  when there are only two species and every site has  $m$  neighbours.

The histograms in figures (3.3) to (3.5) show the distribution of  $Q_x^\sigma(i)$  and  $Q_x^\sigma(j)$  over both  $i$  sites and  $j$  sites using data collected from the square grid lattice model of Chapter 2. As would be expected, the random initial conditions closely fit a binomial distribution, but a binomial distribution continues to be a reasonable fit when the system is at statistical equilibrium, at both  $s = 0.4$  and  $s = 0.5$  (where the equilibrium proportions are around 80% and 50% doves respectively). In each case, it is noticeably better than the Poisson distribution (not shown), which is an especially poor fit when the average number of neighbours is close to the maximum of 4 (figure (3.4a)).

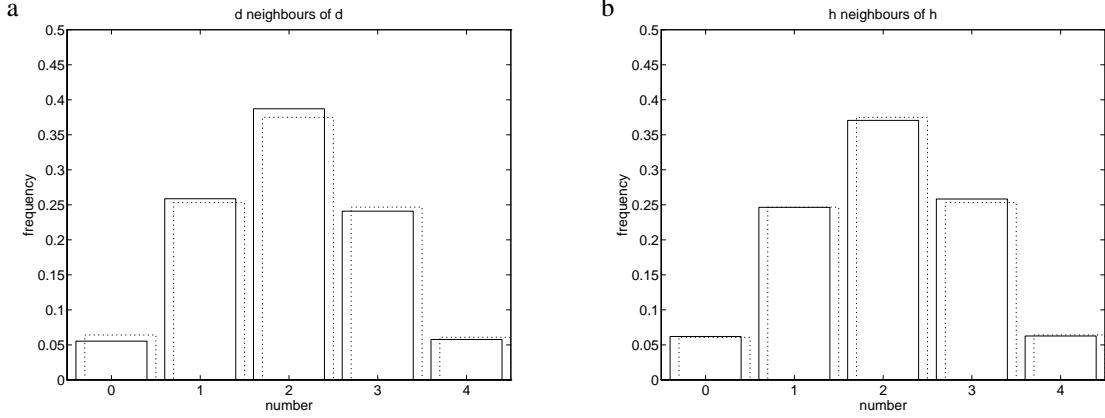


Figure 3.3: Bar charts of the initial distribution of the number of dove neighbours of doves and of hawk neighbours of hawks in the square grid lattice spatial hawk dove model using a total population of 2500. The initial condition is of 50% doves and 50% hawks randomly positioned in the lattice. For any site, the number of dove neighbours plus the number of hawk neighbours sums to four. Also indicated is the corresponding binomial distribution having the same mean and  $n = 4$  trials (dotted line).

If we ignore (for now) the  $\Gamma^\sigma(i|jk|l)$  error terms, and assume a binomial distribution for each  $Q_x^\sigma(i)$ , the evolution equations (3.14) can be closed using the results of the previous section.

$$\begin{aligned}
(ii) &= \frac{2(ij)}{m} \left[ (a-c) \frac{(m-1)}{m} \frac{(ii)}{(i)} \left( \frac{(m-1)}{m} \frac{(ij)}{(j)} + 1 \right) \right. \\
&\quad \left. + b \left( \frac{(m-1)}{m} \frac{(ij)}{(i)} + 1 \right) \left( \frac{(m-1)}{m} \frac{(ij)}{(j)} + 1 \right) - d \frac{(m-1)^2}{m^2} \frac{(ii)}{(i)} \frac{(jj)}{(j)} \right] \\
(jj) &= \frac{2(ij)}{m} \left[ (d-b) \frac{(m-1)}{m} \frac{(jj)}{(j)} \left( \frac{(m-1)}{m} \frac{(ij)}{(i)} + 1 \right) \right. \\
&\quad \left. + c \left( \frac{(m-1)}{m} \frac{(ij)}{(i)} + 1 \right) \left( \frac{(m-1)}{m} \frac{(ij)}{(j)} + 1 \right) - a \frac{(m-1)^2}{m^2} \frac{(ii)}{(i)} \frac{(jj)}{(j)} \right]
\end{aligned} \tag{3.16}$$

Recalling  $m(i) = (ii) + (ij)$  and  $m(j) = (jj) + (ij)$  we find these are identical equations to the heuristically derived equations (2.5) of the analysis in Chapter 2, so the original assumptions now become clear, namely: a binomial distribution of neighbours around individuals and ignoring second order correlation error terms  $\Gamma^\sigma(i|jk|l)$ . Of course we could also consider these error terms in the

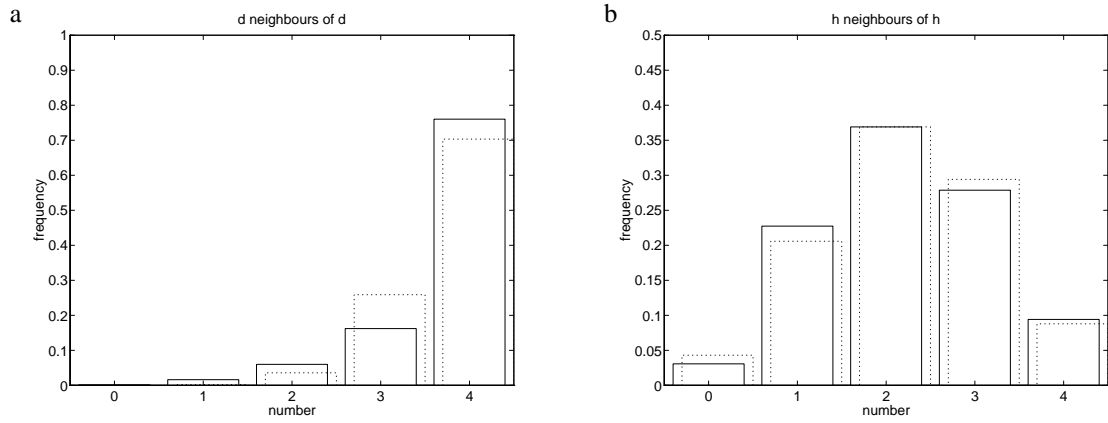


Figure 3.4: The distributions at equilibrium (500000 events) when  $s = 0.4$  in the lattice hawk-dove model. Bar charts of the number of dove neighbours of doves and of hawk neighbours of hawks are shown together with the corresponding binomial distributions having the same mean and  $n = 4$  trials (dotted line).

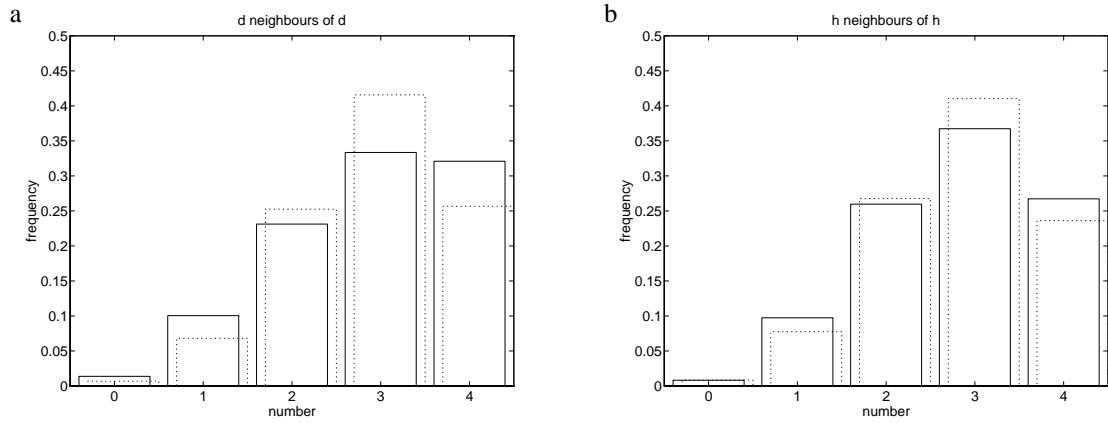


Figure 3.5: The distributions at equilibrium (500000 events) when  $s = 0.5$  in the lattice hawk-dove model. Bar charts of the number of dove neighbours of doves and of hawk neighbours of hawks are shown together with the corresponding binomial distributions having the same mean and  $n = 4$  trials (dotted line).

same way as  $\Gamma^\sigma(i|j|k)$ . Again,  $\Gamma^\sigma(i|jk|l)$  is a covariance, between the number of  $i$  neighbours of a  $j$  site and the number of  $l$  neighbours of a  $k$  site (neighbouring the  $j$ ). On a square lattice there are no common neighbours of both members of a given pair and so no direct overlap between the sets of neighbours. Therefore assuming the two are independent seems reasonable, and leads to a zero covariance, for any values of  $i, j, k$  and  $l$ .

Thinking more deeply, we may not expect  $\Gamma^\sigma(i|jk|l)$  to always vanish in practice because of the indirect influence of any site on the lattice on any other, through all the connecting paths between them. Even at a pair level it is possible that this influence could be felt because it is possible that a neighbour of one member of a pair is directly connected to a neighbour of the other member (when they form a square). If there are triangular connections, for example on a regular hexagonal grid, the situation is more serious because an individual can neighbour two neighbours. This more subtle issue will be addressed in the next chapter. In the real world, one should expect that higher than nearest neighbour correlations will persist, at the triple level and beyond, which do effect the dynamics, and hence the assumptions surrounding the  $\Gamma$  error terms. This can be seen in figure (3.2) as the imperfection in the binomial approximation. In some cases it may only be possible to acquire greater accuracy in a model by moving up to a triple approximation.

### 3.6.2 Irregular Networks

The importance of spatial structure can be clearly seen if we contrast this regular square grid lattice embedding of the spatial hawk-dove game with other, irregular spatial networks. Even in the dynamically simple case of an attracting equilibrium of species abundances, which all the systems below display, there can still be significantly different results. Consider the following models which are also based on the same spatial game. One is a fixed network, the other two are dynamic:

- i. Instead of a square grid, the individuals are placed randomly at any real (continuously valued) position in a square area, of side length one unit, and remain fixed forever. Any given individual interacts with all others that are within a radius  $\rho$  of its own position (using a conventional Euclidean distance measure), so the number of neighbours will vary from individual to individual. To eliminate any boundary effects, the two pairs of edges of the unit square are identified in the same manner as the square grid to transform the space into a torus. The game dynamics are identical to the square lattice case, with the fitness being the average score achieved against all a site's neighbours. Isolated individuals with no neighbours have zero fitness and do not change.
- ii. This model has identical spatial structure to (i) above initially, *i.e.* random position on a torus, but it is not fixed and evolves dynamically. The sole difference is during an invasion event which is now best thought of as a combined birth and death process. The invaded individual is



killed (removed from the network) and a new individual (offspring of the invader, of identical type) is introduced to the network at a random position within the radius of interaction of the invader (or parent). For convenience, this is chosen to be at a uniformly random angle, a uniformly random distance (up to  $\rho$ ) from the parent. Connections are made or broken in the obvious way, depending on the distance separating two individuals, so as to maintain the radius  $\rho$  rule. For direct comparison with the other systems, only inter-specific invasion, not intra-specific, is considered. In this model not only is the number of connections variable from individual to individual, it also varies with time. The total population, of course, remains constant, and any individual remains in a fixed position for its whole lifetime.

- iii. Finally, a simple variation on model (ii) is to change the birth rule slightly. Instead of offspring being born into a random position within the neighbourhood of their parent, they are positioned at a place chosen uniformly randomly over the whole space. For reference, we call this the global birth model as opposed to the local birth model in (ii).

Sample output from simulations of each model is shown as the equilibrium proportion of doves against  $s$ ; figures (3.6) and (3.7), *c.f.* figure (2.5). Each model was run from an equal mix initial random scatter with a population size of 2500 and a value of  $\rho = 0.04$  which gives an initial expected number of contacts as approximately 12.6 per individual, and an expected mere 0.008 of an individual in an isolated site (so any two sites in the network are almost certainly connected by some path). In the dynamic models (ii) and (iii), these quantities are likely to change because contacts are made and broken as the system evolves. The reason  $\rho \approx 0.023$  was not chosen, giving an expected 4 neighbours per individual as in the square lattice model, was to keep the number of isolated individuals low and keep the network reasonably connected. (We would expect around 46 isolated individuals in this case). For comparison, the equilibrium proportion for the pair approximation to the square grid lattice but calculated at  $m = 12.6$  is also shown in figures (3.6) and (3.7).

Despite the uncomplicated dynamics of these new simulations, it is clear that the alternative spatial structures have had a dramatic effect on their behaviour. The dynamic network models in particular show an interesting sensitivity to the change in the spatial aspect of the birth rule, with dove-like behaviour being much more common with the local birth model.

Figure (3.8) shows typical snapshots of the full spatial structure present in the three irregular models. Some spatial aggregation (clumping of hawks and doves) is visible in the fixed network model, more obviously than in the global birth model. Although the global positioning of offspring mixes the population quite thoroughly, space still has a role to play as individuals in the most suitable environments will be the most successful. We may therefore still expect (and find) spatial correlations to exist. The most interesting structure is in the local birth model. Very tight clusters are formed which eventually lead, over large areas of the available space, to many isolated patches of just one species (hawks or doves). With time, the only dynamics is to be found on relatively small boundaries where doves and hawks meet. There are many reasons, biologically speaking, why such

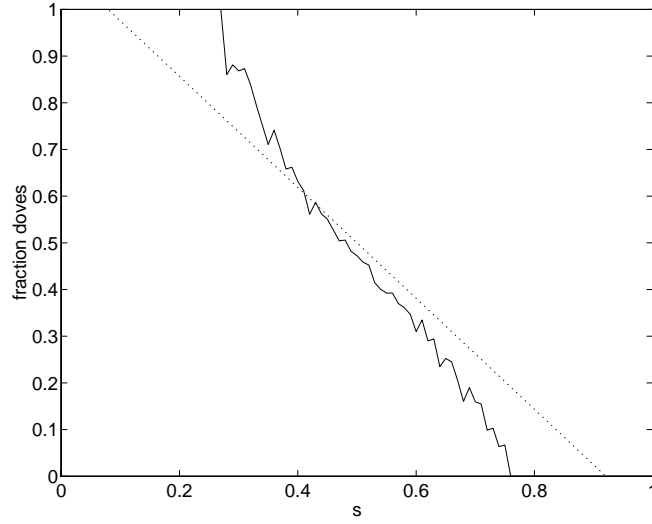


Figure 3.6: Equilibrium composition of the population against  $s$  for the fixed network random position model (i) run with 2500 individuals over 100000 events. Also shown for comparison (dotted) is the square grid pair approximation result of Chapter 2 for  $m = 12.6$ .

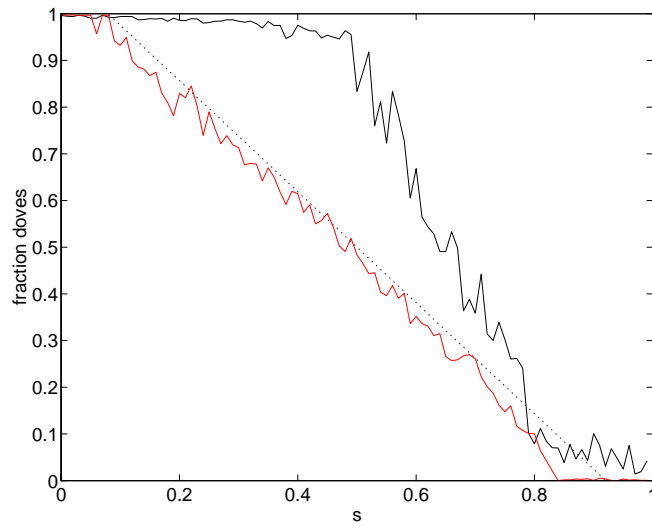


Figure 3.7: Equilibrium composition of the population against  $s$  for the dynamic network random position models (ii) and (iii); each run with  $\rho = 0.04$ , 2500 individuals and over 100000 events. The local birth model (ii) is in black, the global birth model (iii) in red. Also shown for comparison (dotted) is the square grid pair approximation result of Chapter 2 for  $m = 12.6$ .

a model may be an unrealistic one for describing the interaction of cooperating and aggressive individuals (an obvious criticism being that isolated patches of doves or hawks do not interact at all). But as abstract models they nevertheless show that the spatial dimension is clearly an interesting and important aspect.

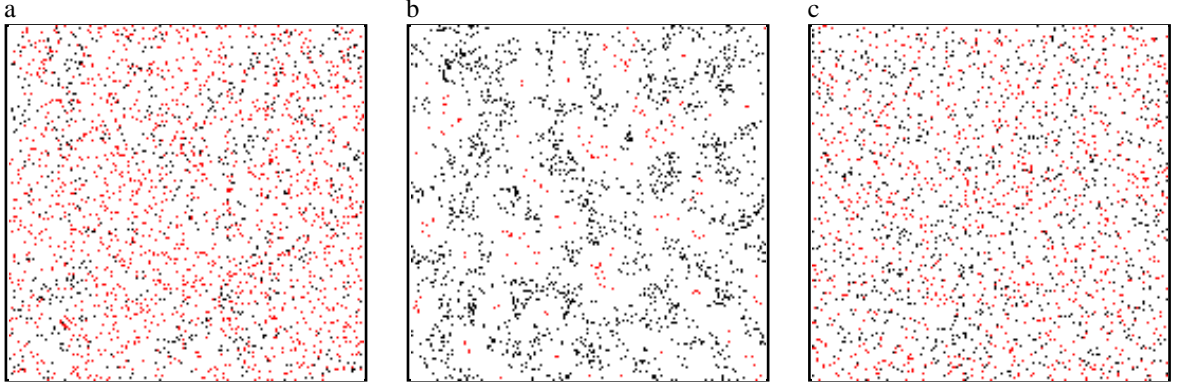


Figure 3.8: Snapshots of the spatial structure in each of the three irregular network hawk-dove models after transient behaviour when statistical equilibrium is reached. In all three cases the population size was 2500 and  $\rho = 0.04$ ; the doves are shown in black, hawks in red. a) fixed network at  $s = 0.6$  with an equilibrium proportion of approximately 30% doves. b) dynamic network with local birth rule at  $s = 0.5$ , leading to approximately 90% doves. c) dynamic network with global birth rule also at  $s = 0.5$ , approximately 50% doves at equilibrium.

There is no reason to expect that the dotted line in figures (3.6) and (3.7) should be relevant to the irregular simulations in any way, because it was specifically derived as the pair approximation to a regular network model. In practice, with  $m = 12.6$  it shows equilibrium behaviour quite similar to the original non-spatial hawk-dove model, which is certainly not the case with the local birth or fixed network models. The global birth model, by contrast, is close to the dotted line. This would seem to indicate that the birth rule mixes the population sufficiently to destroy most pair correlations (an observation also born out by figure (3.8)), and also that the pair approximation is not a bad approximation for this irregular network too.

We can also look at the observed distribution in the number of neighbours of both hawk and dove sites as we did in the lattice case. Figure (3.9) shows the initial distributions for all three models, and the corresponding binomial distribution that is expected to fit well (and does) because of the random initial placement of individuals. (For a given site, view each of the remaining 2499 individuals as a neighbour independently with probability  $\pi\rho^2 \ll 1$ . The Poisson distribution is almost indistinguishable from a binomial here because the probability is so small.). More interest-

ingly, we see the Poisson distribution itself can also be a good fit when the model dynamics have altered the spatial structure; figures (3.10), (3.11) and (3.12). Each figure shows the equilibrium distribution of dove and hawk neighbours (and both combined) for both dove sites and hawk sites, again run at  $\rho = 0.04$  and  $N = 2500$ . The chosen value of  $s = 0.6$  gives equilibrium proportions of approximately 30%, 60% and 35% doves for the fixed, local and global models respectively. The fixed network model and the global birth model are particularly encouraging in this respect, at least for these parameter values (and many others - not shown). The local birth model is not so good, with the spread in the number of dove neighbours of doves being underestimated, and the number of hawk neighbours overestimated, it would be much harder to justify a Poisson assumption in this case.

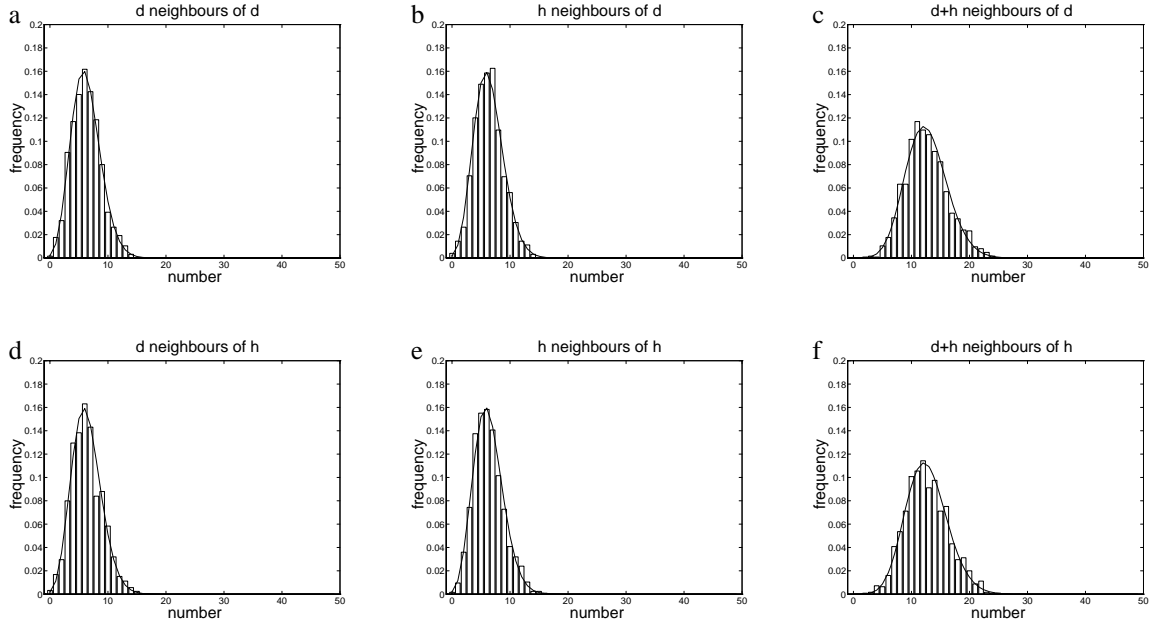


Figure 3.9: Bar charts showing a typical initial distributions of neighbours for the irregular network random position spatial hawk-dove models (i), (ii) and (iii) at  $\rho = 0.04$  with 2500 individuals. Each solid line represents the corresponding theoretical binomial distribution and is almost indistinguishable from its Poisson approximation.

### 3.6.3 Alternative Pair Approximations

Given the irregular network models described above, and the observed distribution of neighbours found in simulation, can reasonable alternative pair approximations be formed which capture the essential behaviour (in particular, perhaps, to predict the results of figures (3.6) and (3.7)) in any of these new situations? We certainly have less grounds to be optimistic than for the original case - substantial difficulties are presented because of the increased nonlinearity in event rates, and in the dynamic cases because events now do not just change individuals, they also change connections.

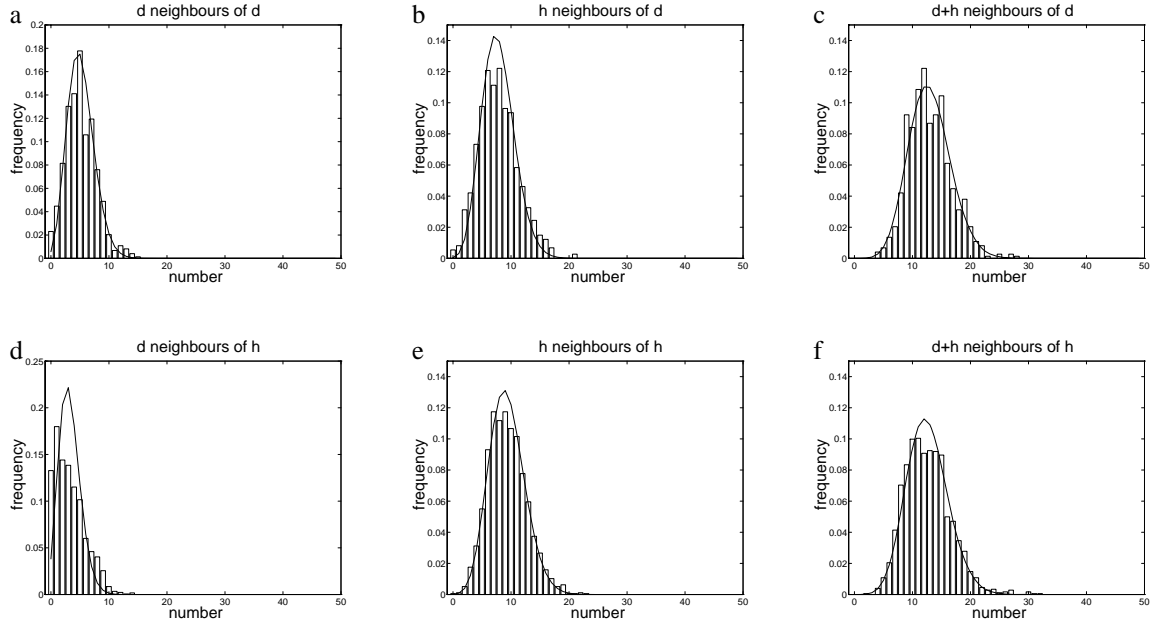


Figure 3.10: Bar charts showing typical equilibrium distributions of neighbours for the random position fixed spatial hawk-dove model (i) at  $s = 0.6$  with  $\rho = 0.04$  and 2500 individuals. This value of  $s$  corresponds to approximately 30% doves at equilibrium.

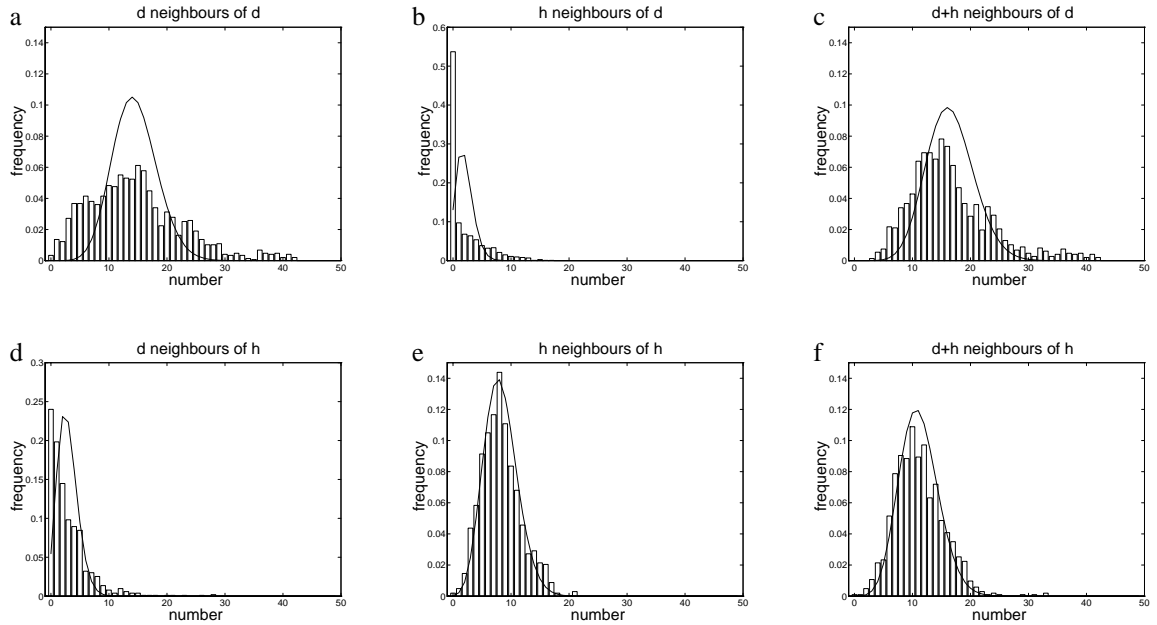


Figure 3.11: Bar charts showing typical equilibrium distributions of neighbours for the random position dynamic spatial hawk-dove model with local birth rule (ii) at  $s = 0.6$  with  $\rho = 0.04$  and 2500 individuals. This value of  $s$  corresponds to approximately 60% doves at equilibrium.

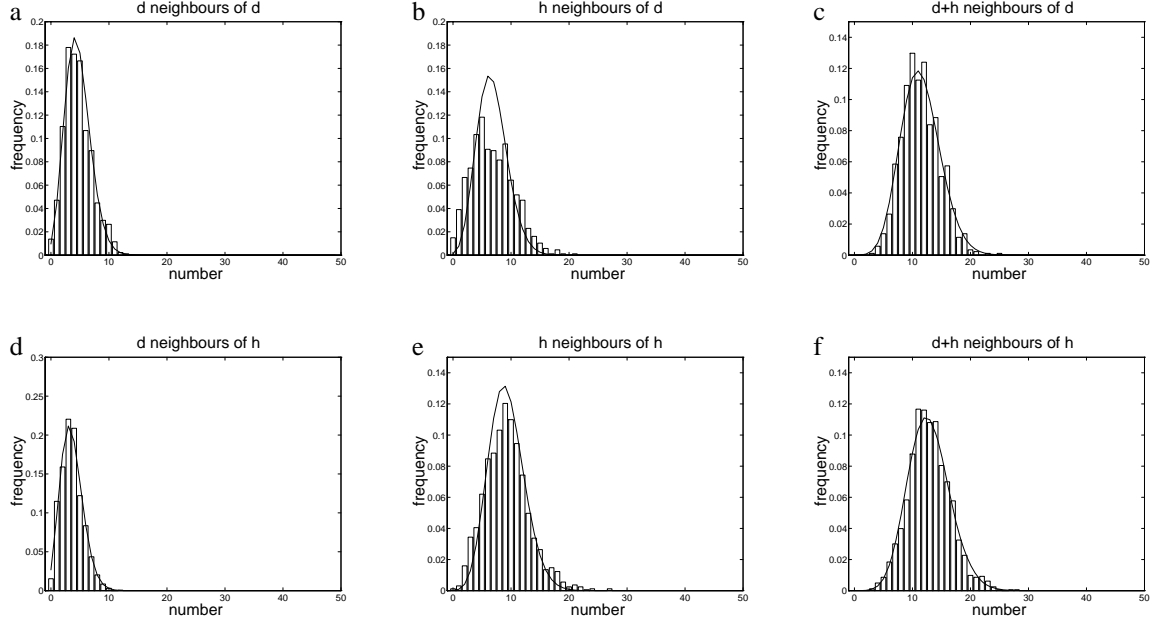


Figure 3.12: Bar charts showing typical equilibrium distributions of neighbours for the random position dynamic spatial hawk-dove model with global birth rule (iii) at  $s = 0.6$  with  $\rho = 0.04$  and 2500 individuals. This value of  $s$  corresponds to approximately 35% doves at equilibrium.

However, we can perhaps justify a Poisson distribution (at least in some cases) for the individual neighbourhood distributions which might help a bit.

Equations (3.11) to (3.13) are still valid for the fixed network with random placement, but we can no longer assume  $Q_x^\sigma(i) + Q_x^\sigma(j)$  is constant, and must also use equation (3.10) for the evolution of  $(i)$  which can now no longer be derived from  $(ii)$  and  $(jj)$ . For the two dynamic networks, an even bigger rethink is required. When a site is invaded the number of connections broken is, as in the fixed case, just proportional to the number of particular neighbours of the invaded individual. However, the number of connections made is much less tractable. In either the local or global birth case it depends on both chance (the random placement of ‘offspring’) and the detailed structure of the network; information which is simply not available through the pair totals alone. We are forced to consider a simplifying assumption which circumvents this lack of detail, for example that the offspring neighbours all (or a fraction) of its parent’s neighbours, or the neighbours of a randomly chosen individual. This kind of assumption is unfortunately an example of the kind of unsatisfactory approximation we aimed to avoid in setting out the more formal approach to deriving pair approximations, but there seems no way round it in certain circumstances.

In all three cases there are still significant problems posed by the now very nonlinear (*i.e.* not just quadratic) event rates. In many respects this is a rather untypical and complex example, but it

serves very well to illustrate potential problems. The real difficulty is caused by the reciprocal of the number of neighbours of a site entering in the expression for the average score achieved against all neighbours (nonlinear polynomials in the numerator are not such a problem and can be treated in the same manner as the regular network case).

Biologically, this assumption may be slightly odd, but it poses a problem nonetheless. The problem is more clearly illustrated by a slightly simpler example. Consider an event where a species  $i$  individual invades a neighbouring species  $j$  individual at a rate equal to the reciprocal of the number of  $i$  neighbours of the  $j$  site (which is therefore guaranteed to be at least one). Then the dynamical equations will consist of expressions like

$$\sum_{(ji)} \frac{1}{Q_x^\sigma(i)} = \sum_{(ji)} \frac{1}{\overline{Q}^\sigma(i|ji) + \eta_x^\sigma(i|ji)}$$

Because  $\eta_x^\sigma(i|ji)$  is not necessarily small compared to  $\overline{Q}^\sigma(i|ji)$  it is not possible to expand  $1/Q_x^\sigma(i)$  as a convergent (or even asymptotic) series expansion in  $\eta_x^\sigma(i|ji)/\overline{Q}^\sigma(i|ji)$  that can be truncated to give an accurate approximation. Furthermore, and unfortunately, no progress can be made by writing

$$\frac{1}{Q_x^\sigma(i)} = \mathbb{E}_{(ji)} \left[ \frac{1}{Q_x^\sigma(i)} \right] + \xi_x^\sigma(i|ji)$$

as an analogy to equation (3.2) - so linear  $\xi_x^\sigma(i|ji)$  sums vanish - because it is not possible to write the expectation of  $1/Q_x^\sigma(i)$  in terms of the path totals  $(i)$ ,  $(ij)$ ,  $(ijk)$ , *etc.*, as it is with  $\overline{Q}^\sigma(i|ji)$ .

We may be able to estimate  $\mathbb{E}_{(ji)} [1/Q_x^\sigma(i)]$  using analysis similar to that in section (3.5) if a close match is found for  $Q_x^\sigma(i)$  at  $j$ - $i$  pairs to a standard distribution. Unfortunately, the calculation is not likely to be easy:

Consider the simplest of the three cases - model i, the irregular but fixed network - and assume that the number of each type of neighbour is Poisson distributed in an individual's neighbourhood (the simplest distribution justified by figure (3.10)). The Poisson parameters are given by the averages  $\overline{Q}^\sigma(i|j)$  *etc.*. We need to estimate  $[Q_x^\sigma(i) + Q_x^\sigma(j)]^{-1}$  at sites,  $x$ , which have at least one neighbour (recall our rules insist that isolated sites are dormant). Because the sum of two Poisson variables is also Poisson distributed, this reduces the calculation to evaluation of the sum

$$\Omega(\lambda) = \frac{1}{e^\lambda - 1} \sum_{n=1}^{\infty} \frac{1}{n} \frac{\lambda^n}{n!} e^{-\lambda} \quad (3.17)$$

where  $\lambda$  is the known Poisson parameter. Unfortunately, further investigation of this sum is not productive.

In this case, the only approach left may be to set all error terms  $\eta_x^g(i|ji) = 0$  and estimate  $1/Q_x^g(i)$  simply by  $1/\overline{Q}^g(i|ji)$ . But this is a drastic measure because ignoring the error terms is an unconsidered assumption that also contradicts the original assumption of Poisson distribution of neighbours. We are left to reflect on the fact that constructing pair approximations to model systems is not always a natural or easy task.

### 3.7 Discussion

This chapter set out to produce a methodical framework for the modelling of spatially distributed, interacting populations. Using the variations of hawk-dove spatial game as an example, some of the choices and difficulties present in developing sensible pair approximations are more clearly seen with this approach than with the heuristic analysis of Chapter 2. Choices often reflect the nature of the spatial structure in the underlying system. And because in any real biological (or complex mathematical) system this is typically far too intricate to capture precisely, simplifying assumptions must be made.

A lot depends on the interpretation of the resulting pair models. On the one hand, they can be viewed as approximations of their parent models (such as the explicit lattice mathematical models in the hawk-dove game). On the other hand, they are alternative spatial models for the underlying biological systems of interest; not ‘models of models’ and no less valid than any other model. Even when considering abstract systems which are not seen directly in the real world, such as the hawk-dove game, this second interpretation is possible; this may be so in this case if we are interested in the spatial game interactions themselves, and not the fact that a regular lattice is imposed on the players. Indeed, because the large scale structure imposed on an explicit model is often artificial and rigid (a square grid, for example), interpreting pair models as alternative descriptions of space in their own right can be more appealing.

We have demonstrated that under appropriate assumptions, the formal pair model derivation in this chapter reproduced the probabilistically derived results of Chapter 2. The equivalence of these approaches is reassuring and convenient. (On occasions, as familiarity with pair models increases, it can be quicker to derive pair equations using the original conditional probability approach. However, because of its extended spatial support (requiring neighbours of neighbours), the spatial game is not such a good example). Crucially, both approaches ultimately lead to the same central problem, which is how to close the cascading system of equations that naturally arise. The binomial assumption (or conditional probability approach) was natural when attempting to approximate the regular lattice spatial game. But where spatial structure is more of an unknown (often the case biologically), more than one pair model may reasonably represent a particular system, and we can



not then speak of ‘the’ pair model for a system without further clarification.

It may not always be possible to derive useful pair models for all systems that possess spatial structure. Two of the reasons why this may be the case were illustrated by the three irregular network variations of the hawk-dove game.

Firstly, event rates may depend crucially not just on the number and type of neighbours individually, but on the whole set of neighbours of a given site together. (In our case, this was the nonlinearity resulting from fitness being measured as the average payoff to each individual in networks with variations in the size of local neighbourhoods). Pair variables represent information on the number of neighbours and the correlations between pairs of neighbours, but not on complete neighbourhoods themselves. Whether or not this is a problem depends on the system. Infection systems (Chapter 6), for example, do not pose much of a problem because the important aspect of spatial structure is the number of susceptible-infectious contacts directly, and not the whole neighbourhood of a site.

Secondly, spatial structure on medium and large scales (*i.e.* not just local scales) may be important to the dynamics. Clearly, pair models can not hope to reflect this structure. (That is not to say, however, that no correlations on larger scales are implicit in a pair model; only that they necessarily result from combined pair-wise correlations). The dynamic network hawk-dove game with local birth rule was such an example, with successful isolated patches of doves having a profound effect: Dynamically, there is a big difference between all doves experiencing the average dove neighbourhood, and the case where there is variation (some with fewer dove neighbours, some with more). It is difficult for pair models to capture this variation. Even if this is a problem for a particular mathematical system, it may not be a problem biologically (where the rules are less clearly defined). This is another situation where treating pair models as alternative spatial models, not approximations of other models, is a valuable approach.

With experience, it becomes easier to identify the cases when a pair model approach will work and when it will not. For practical purposes, we have found that the assumption of regularity, where network sites are indistinguishable, is particularly useful and more likely to lead to interesting and accurate pair models. There are also some tricks which can help render a difficult system amenable to pair analysis. One which is particularly helpful for dynamic networks is to introduce ‘empty sites’ as an extra species. Variable size populations, variable size neighbourhoods and migration can then be emulated with appropriate events. An predator-prey example with empty sites is discussed in Chapter 5.

4

# Extensions and General Pair Models

## 4.1 Introduction

The previous chapter introduced some notation and techniques for formulating pair models. Given the success that the resulting pair model approximations have demonstrated in improving on mean-field systems, one obvious question to ask is ‘what next?’. Can higher order approximations (triple models) do still better?

In this chapter the work is taken a stage further by considering extensions of previously successful pair models, and the implications of spatial geometries different from the square lattice. In pursuing these topics, which turn out to be tightly interlinked, we find that more awkward questions frequently arise and the complexity of models rapidly increases. It quickly becomes clear why the literature is almost entirely empty of spatial correlation models more complicated than the simplest pair approximations. Nevertheless, progress can be made, even though on occasion we are forced into the realms of conjecture and the proposition of models which are not deduced entirely from first principles. Thinking back to Chapter 1, it is worth reminding ourselves, of course, that this is not without precedent in mathematical biology. Many useful and interesting models have heuristic or phenomenological origins. The examples studied in Chapters 5 and 6 assess the validity of the resulting models.

## 4.2 More Terminology

A necessary first step before advancing the work of the previous chapter is to expand the notation it introduced. Recall that this was based on such average quantities as  $\overline{Q}^\sigma(i|j)$  and  $\overline{Q}^\sigma(i|jk)$  - defined in terms of  $(i)$ ,  $(ij)$  and  $(ijk)$  - with corresponding error terms  $\eta_x^\sigma$ . Together, these were used to represent the neighbours of a particular site,  $Q_x^\sigma(i)$ . Furthermore, useful models were only obtained after the fundamental dynamical equations were closed at the pair level. This was achieved by writing each  $(ijk)$  as a function of the lower order  $(i)$  and  $(ij)$  and error terms  $\Gamma(i|j|k)$  whose value was estimated using closure assumptions (such as the binomial distribution of neighbours).

For higher order analysis (*i.e.* that where spatial correlations beyond the pair level are taken into account), however, it is no longer sufficient to consider just the direct neighbours of a site. If we want to know the evolution equations for triples  $(ijk)$ , for example, we will require knowledge of the neighbours’ neighbours too, because an event at one particular site will be reflected in the triples composed of all individuals up to a radius of two connections away.

Recall that a path is a set of  $n$  distinct individuals that are sequentially connected: *i.e.* individual  $i_1$  neighbours  $i_2$ ,  $i_2$  neighbours  $i_3$  *etc.* up to  $i_{n-1}$  neighbours  $i_n$ . Now define  $Q_x^\sigma(ij)$  to be the number of  $\sigma(x)$ - $i$ - $j$  paths starting at site  $x$  in the network  $\sigma$  (see figure (4.1) for a graphical example).  $Q_x^\sigma(ij)$

terms appear as naturally in higher analysis as  $Q_x^\sigma(i)$  do in pair analysis. In exactly the same manner as section (3.3), averages and errors with respect to  $Q_x^\sigma(ij)$  can be defined. Let

$$\overline{Q}^\sigma(ij|kl) = \frac{1}{(kl)} \sum_{(kl)} Q_x^\sigma(ji)$$

be the number of k-j-i paths starting at site  $x$ , averaged over all k-l pairs with k occupying site  $x$ . (Note the reversal in the order of  $i$  and  $j$  between the  $\overline{Q}$  and  $Q$  terms so the letters appear in the correct, neighbourly, order). Writing  $\eta_x^\sigma(ij|kl) = Q_x^\sigma(ji) - \overline{Q}^\sigma(ij|kl)$  also implies

$$\sum_{(kl)} \eta_x^\sigma(ij|kl) = 0$$

in an analogous way to the previous chapter. In principle definitions of this type can be extended to arbitrary length paths  $Q_x^\sigma(i_1 \cdots i_n)$ , averages  $\overline{Q}^\sigma(i_n \cdots i_1|j_1 \cdots j_m)$  and errors  $\eta_x^\sigma(i_n \cdots i_1|j_1 \cdots j_m)$ .

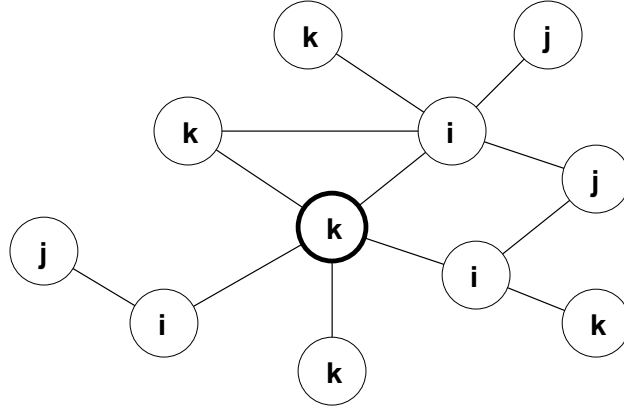


Figure 4.1: An example of a neighbourhood in an irregular network. Each site is represented by a circle, and the straight lines denote connections. If site  $x$  is the bold central circle containing the k individual, then  $Q_x^\sigma(ij) = 4$ ,  $Q_x^\sigma(ik) = 3$  and  $Q_x^\sigma(ki) = 1$ . All other  $Q_x^\sigma(\cdot \cdot)$  are zero

In fact these ‘straight path’ quantities are not the only ones that will be needed. We shall see that two other average  $\overline{Q}^\sigma$  quantities also appear in the extended analysis of the spatial game, essentially because invasion rates depend upon the fitness of neighbours, which in turn depend upon their neighbours. For convenience we also define these here. They are best described by example, although the principle is exactly the same as for the case above: Loosely speaking, we say  $\overline{Q}^\sigma(Xi|jY)$  is the number of distinct  $X$ - $i$ - $j$  structures neighbouring a  $j$ - $Y$  (through a common  $j$ ), averaged over all  $j$ - $Y$  neighbourhoods.  $X$  and  $Y$  represent any specific local connected network structures

(or neighbourhoods) and  $X-i-j$  and  $j-Y$  are both sets of distinct individuals, though there may be overlap between  $X-i$  and  $Y$ . The two examples required are

$$\begin{aligned}\overline{Q}^{\sigma}(i|j<_l^k) &= \text{average number of } i \text{ neighbours of the } j \text{ per } k\text{-}j\text{-}l \text{ path.} \\ \overline{Q}^{\sigma}(i|j<_{lm}^k) &= \text{average number of } i \text{ neighbours of the } j \text{ per } k\text{-}j\text{-}l\text{-}m \text{ path.}\end{aligned}$$

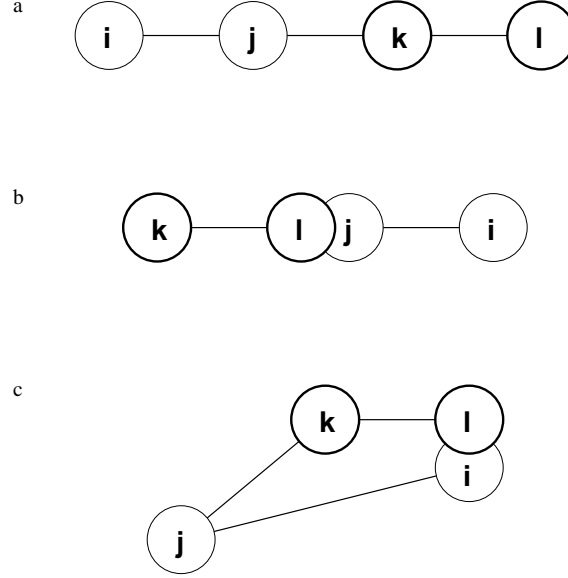


Figure 4.2: Local neighbourhood configurations which effect  $\overline{Q}^{\sigma}(ij|kl)$ , the expected number of j-i neighbours per k-l pair. Overlapping circles represent the same individual. a) four distinct individuals. b) three individuals connected in a line when  $l = j$ . c) three individuals connected in a triangle when  $l = i$ . The value of  $\overline{Q}^{\sigma}(ij|kl)$  can therefore depend on  $(ijkl)$ ,  $(ijk)$  and  $\langle jkl \rangle$ . See text.

#### 4.2.1 Expressions for $\overline{Q}^{\sigma}$

We need an expression for each  $\overline{Q}^{\sigma}$  in terms of the system variables, which is valid (at least for now) for any regular or irregular network. In most cases, however, this is not as easily done as was the case with  $\overline{Q}^{\sigma}(i|jk)$  and  $\overline{Q}^{\sigma}(i|j)$ . As an example, consider  $\overline{Q}^{\sigma}(ij|kl)$ ; the potential pitfall is illustrated by figure (4.2): Care must be taken to allow for overlap of the two paths i-j-k and k-l. Although each is separately composed of distinct individuals, the two paths may intersect each other.

We need to count all possible i-j-k-l connections (including self-intersections) subject to  $i, j, k$  and  $k, l$  being two sets of distinct individuals. There are three possibilities: individual i and individual l are identical (identical here means occupy the same site as a unique individual, not just belong to the same species), individual j and individual l are identical, or all four are distinct. Each of these

three may or may not be relevant to a particular  $\overline{Q}^\sigma(ij|kl)$  calculation, depending on the values of  $i, j, k$  and  $l$ : clearly two individuals cannot be identical if they are of different types. Linear paths along  $i$ - $j$ - $k$ - $l$  (figure (4.2a)) always contribute to  $\overline{Q}^\sigma(ij|kl)$  regardless of the values of  $i, j, k$  and  $l$ . If  $l = j$  (figure (4.2b)) then  $i$ - $j$ - $k$  paths also contribute because the  $k$  individual is at the beginning of both a  $k$ - $j$  path and a  $k$ - $j$ - $i$  path. If  $l = i$  (figure (4.2c)) then  $j$ - $k$ - $l$  paths can contribute providing that the  $j$  neighbours the  $l$ . *i.e.* only closed  $j, k, l$  triangles contribute (the  $k$  individual is then also at the beginning of both a  $k$ - $i$  path and a  $k$ - $j$ - $i$  path). In every case, dividing by the number of  $k$ - $l$  pairs gives the average. Writing  $\langle ijk \rangle$  for the number of triangles ( $i$ - $j$ - $k$  paths of length three with the ends,  $i$  and  $k$ , connected) in the network between type  $i, j$  and  $k$  individuals leads to the following exact relation.

$$\overline{Q}^\sigma(ij|kl) = \begin{cases} \frac{(ijkl)}{(kl)} & \text{if } l \neq i, l \neq j \\ \frac{(ljk)}{(kl)} + \frac{\langle jkl \rangle}{(kl)} & \text{if } l = i, l \neq j \\ \frac{(ilk)}{(kl)} + \frac{(ilk)}{(kl)} & \text{if } l \neq i, l = j \\ \frac{(llk)}{(kl)} + \frac{\langle lkl \rangle}{(kl)} + \frac{(llk)}{(kl)} & \text{if } l = i = j \end{cases}$$

Using the  $\delta$  function notation

$$\delta_{ij} = \begin{cases} 1 & \text{if } i = j \\ 0 & \text{if } i \neq j \end{cases}$$

this can more succinctly be written as

$$\overline{Q}^\sigma(ij|kl) = \frac{(ijkl)}{(kl)} + \frac{\langle jkl \rangle}{(kl)} \delta_{il} + \frac{(ijk)}{(kl)} \delta_{jl}$$

Note that, as with linear paths, triangles are to be counted in both directions (clockwise and anticlockwise), and also necessarily from each starting point, so any three mutually neighbouring individuals count as six such triangles. Symmetry implies  $\langle ijk \rangle = \langle jki \rangle = \langle kji \rangle$  and  $\langle ijk \rangle = \langle ikj \rangle$ . Further, if three individuals are connected in a triangle they are also connected in a line, so  $\langle ijk \rangle \leq (ijk)$  for all  $i, j$  and  $k$ .

For the first time here, we see that it is not sufficient to consider just linear  $n$ -paths. It will be shown that this has important consequences not just for deriving spatial correlation models at higher levels than the pair approximation, but also when considering other (non square lattice) geometries in the underlying spatial structure.

By considering every possible overlap between individuals, similar expressions can be derived for other  $\overline{Q}^\sigma$ , like those previously discussed. (Again, no simplifying assumptions about the structure of the network  $\sigma$  are made here). Table (4.1) gives a usefully representative sample of these expressions. As with triangles for  $\overline{Q}^\sigma(ij|kl)$ , we are forced to consider other connected shapes (elements) in the network. Table (4.2) gives the notation used to do this.

Average quantity	Equivalent expression
$\overline{Q}^\sigma(i j)$	$\frac{(ij)}{(j)}$
$\overline{Q}^\sigma(i jk)$	$\frac{(ijk)}{(jk)} + \delta_{ik}$
$\overline{Q}^\sigma(i jkl)$	$\frac{(ijkl)}{(jkl)} + \delta_{ik} + \frac{\langle jkl \rangle}{(jkl)} \delta_{il}$
$\overline{Q}^\sigma(i jklm)$	$\frac{(ijklm)}{(jklm)} + \delta_{ik} + \frac{(m-\langle lkj \rangle)}{(jklm)} \delta_{il} + \frac{[jklm]}{(jklm)} \delta_{im}$
$\overline{Q}^\sigma(ij kl)$	$\frac{(ijkl)}{(kl)} + \frac{\langle jkl \rangle}{(kl)} \delta_{il} + \frac{(kli)}{(kl)} \delta_{jl}$
$\overline{Q}^\sigma(ij klm)$	$\frac{(ijklm)}{(klm)} + \frac{(m-\langle lkj \rangle)}{(klm)} \delta_{il} + \frac{[jklm]}{(klm)} \delta_{im} +$ $\frac{(il-\langle km \rangle)}{(klm)} \delta_{jl} + \frac{(i-\langle mlk \rangle)}{(klm)} \delta_{jm} + \frac{\langle klm \rangle}{(klm)} \delta_{il} \delta_{jm} + \delta_{im} \delta_{jl}$
$\overline{Q}^\sigma(i j\langle k \rangle_l)$	$\frac{(ij\langle k \rangle_l)}{(kj\langle l \rangle)} + \delta_{ik} + \delta_{il}$
$\overline{Q}^\sigma(i j\langle k \rangle_{lm})$	$\frac{(mlj\langle k \rangle_{lm})}{(kj\langle l \rangle m)} + \delta_{ik} + \delta_{il} + \frac{(k-\langle jlm \rangle)}{(kj\langle l \rangle m)} \delta_{im}$

Table 4.1: Exact expressions for the  $\overline{Q}^\sigma$  average quantities in any general network  $\sigma$ .




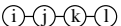

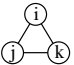
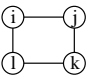
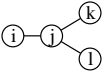
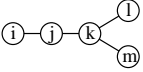
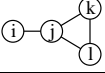
Physical Shape	Notation	Symmetries
	$(i)$	1
	$(ij)$	2
	$(ijk)$	2
	$(ijkl)$	2
	$(ijklm)$	2
	$\langle ijk \rangle$	6
	$[ijkl]$	8
	$(ij\langle^k_l\rangle)$	6
	$(ijk\langle^l_m\rangle)$	2
	$(i\langle jkl \rangle)$	2

Table 4.2: A complete list of the notation for the numbers of various neighbourhood elements as used in the text. The symmetries column indicates the number of ways a physical neighbourhood can (and should) be counted. For example, an  $i$ - $j$  neighbourhood must be counted as both an  $(ij)$  and a  $(ji)$  pair, and a triangle composed of  $i, i$  and  $j$  must be counted six times:  $\langle iij \rangle = 2$ ,  $\langle iji \rangle = 2$  and  $\langle jii \rangle = 2$ .



### 4.3 An Alternative Perspective

Recall that the pair approximation to the square grid hawk-dove model in Chapter 3 was closed by approximating values for the error terms  $\Gamma^\sigma(i|j|k)$  - equations (3.8) and (3.9) - which were justified by assumptions on the distribution of neighbours, based on theory and observation. Using these assumptions, we can return directly to equations (3.4) and (3.6) and derive estimates  $E_{(ijk)}^P$  for the absolute number of triples  $(ijk)$  in the network, which hold for all  $i, j$  and  $k$ , as a function of the pair and single variables when each site has  $m = 4$  neighbours:

$$(ijk) \approx E_{(ijk)}^P = \frac{(m-1)}{m} \frac{(ij)(jk)}{(j)} \quad (4.1)$$

This formula has three natural and desirable properties for such an estimate:

- i. It is proportional to the abundance of each constituent pair,  $(i-j$  and  $j-k)$ , and is therefore zero if any of these are absent from the network.
- ii. The total number of triples in the whole network is correctly predicted when each site in the network is occupied by a single species: we expect  $12N$  triples overall (each of the  $4N$  pairs can be extended to a triple by the connection to one of the other three neighbours), which equals  $3/4 \times (4N)^2/N$ , from equation (4.1).
- iii. If the pair correlations vanish, so  $(ij) = 4(i)(j)/N$ , the expected number of  $i-j$  contacts if everybody has 4 neighbours, then the estimate  $E_{(ijk)}^P$  reduces to

$$12N \frac{(i)}{N} \frac{(j)}{N} \frac{(k)}{N}$$

which is the expected number of  $i-j-k$  triples if all sites are independent of their neighbours; the mean-field estimate.

(Note that property ii. is really a special case of property iii. because pairwise correlations are trivial when there is only one species present. It will, however, prove useful to consider ii. directly later.) A natural question to ask next is what can be said about other elemental totals? Consider the following identity for 4-paths:

$$\begin{aligned} (ijkl) &= \sum_{(jk)} \left[ Q_x^\sigma(i) - \delta_{ik} \right] \left[ Q_y^\sigma(l) - \delta_{lj} \right] - \langle ijk \rangle \delta_{il} \\ &= \sum_{(jk)} \left[ \overline{Q}^\sigma(i|jk) - \delta_{ik} + \eta_x^\sigma(i|jk) \right] \left[ \overline{Q}^\sigma(l|kj) - \delta_{lj} + \eta_y^\sigma(l|kj) \right] - \langle ijk \rangle \delta_{il} \\ &= (jk)(\overline{Q}^\sigma(i|jk) - \delta_{ik})(\overline{Q}^\sigma(l|kj) - \delta_{lj}) + (jk)\Gamma^\sigma(i|jk|l) - \langle ijk \rangle \delta_{il} \\ &= \frac{(ijk)(jkl)}{(jk)} + (jk)\Gamma^\sigma(i|jk|l) - \langle ijk \rangle \delta_{il} \end{aligned} \quad (4.2)$$

The first sum counts all  $i-j-k-l$  paths by counting all  $j-k$  paths multiplied by the number of distinct  $i$  neighbours of the  $j$  site and the number of  $l$  neighbours of the  $k$  site. However, this also counts triangles in which the  $i$  and  $l$  are the same site, and these must be subtracted to give just  $(ijkl)$ .

Use has also been made of equation (3.3) and table (4.1). Because  $\langle ijk \rangle = 0$  on a square grid, the pair approximation estimates for  $(ijk)$  in equation (4.1) combine to give

$$(ijkl) \approx \frac{(m-1)^2}{m^2} \frac{(ij)(jk)(kl)}{(j)(k)} \quad (4.3)$$

providing we also justify the original assumption of  $\Gamma^\sigma(i|jk|l) \approx 0$  from Chapter 3. This looks like a natural extension of equation (4.1); however, there is a complication. On a square grid with  $N$  individuals, there are  $4 \times 3 \times 3 \times N = 36N$  4-paths in total, but  $8N$  of these also form closed squares, where the two ends neighbour each other. There is no particular reason, except convenience, why this extra connection between  $i$  and  $l$  should be ignored in this latter case, as it effectively is when setting  $\Gamma^\sigma(i|jk|l) = 0$  to give equation (4.3). In fact, a similar problem arises with triangles in the estimation of 3-path totals when they exist in a network, for example on a regular hexagonal grid where each individual interacts with its closest six neighbours. Under such circumstances the multinomial assumption of Chapter 3 would be hard to justify as two neighbours of a site, being neighbours themselves in two-fifths of all cases, could not reasonably be assumed to be independent in a pair approximation.

Focusing on the 4-path  $\Gamma^\sigma(i|jk|l)$ , we attempt to tackle this problem. Because, as discussed in chapter 3, it is difficult to provide an estimate for  $\Gamma^\sigma(i|jk|l)$  directly we must consider an alternative. One choice is to attempt to estimate  $(ijkl)$  by splitting it into the contribution of open 4-paths, where the  $i$  and  $l$  are not neighbours, and closed 4-paths, or squares, where they are. The squares are the most difficult, and we start with these.

We need to estimate  $[ijkl]$ . Any amount of formal analysis along the lines considered so far in this thesis seems to quickly fall flat on its face. Instead, consider a heuristic approach based on the estimate for  $E_{(ijk)}^P$  found above, which aims to have the same three properties. For any constant  $c$ ,

$$c \frac{(ij)(jk)(kl)(li)}{(i)(j)(k)(l)}$$

satisfies the first property. We can choose  $c$  so that the second property also holds by solving  $c(4N)^4 N^{-4} = 8N$  (there are  $8N$  countable squares in total), which gives an estimate that also satisfies property three:

$$E_{[ijkl]}^P = \frac{N}{32} \frac{(ij)(jk)(kl)(li)}{(i)(j)(k)(l)} \quad (4.4)$$

If we follow the same heuristic procedure to get an estimate for just the number of open 4-paths (where the  $i$  and  $l$  are not neighbours), of which we expect  $28N$  in total, we obtain

$$\frac{7}{16} \frac{(ij)(jk)(kl)}{(j)(k)}$$

which is just  $28/36$  of equation (4.3). Note the difference between this and the square estimate  $E_{[ijkl]}^P$  is, up to proportionality, just a factor  $(il)/(i)(l)$  which alone is just the probability that from the network, a randomly chosen  $i$  site and a randomly chosen  $l$  site are neighbouring. (There are

$(i) \times (l)$  possible  $i$ - $l$  pairs, but only  $(il)$  realised  $i$ - $l$  pairs). Combining the open and closed 4-path estimates, we have:

$$E_{(ijkl)}^P = \frac{(ij)(jk)(kl)}{(j)(k)} \left[ \frac{7}{16} + \frac{N}{32} \frac{(li)}{(i)(l)} \right] \quad (4.5)$$

Figure (4.3) shows typical predictions of the estimate for  $E_{[ijkl]}^P$  when compared to the mean-field estimate  $8N^{-3}(i)(j)(k)(l)$  and the observed values of  $[ijkl]$  from a square grid simulation. The pair estimate is clearly much better than the mean-field, and this was true in all cases for simulations at many different parameter values.

Unfortunately it is difficult to tell whether or not  $E_{[ijkl]}^P$  is the best possible pair estimate (in general) because of its heuristic derivation. It is certainly very natural (by comparison to  $E_{(ijk)}^P$ ), and it also does better than many other guesses, such as

$$\frac{1}{2N} \sqrt{(ij)(jk)(kl)(li)} \quad (4.6)$$

which is another feasible pair approximation to  $[ijkl]$  that satisfies the three criteria - see also figure (4.3). (Actually, this estimate is it not directly proportional to each constituent pair frequency, because of the square root. But, importantly, it does vanish if any constituent pair is not present. In fact, we do not have proportionality in the strict sense in equation (4.1) either, because the set of all pair  $(ij)$  and single  $(i)$  variables is not independent).

The extra nonlinearities introduced into the  $E_{[ijkl]}^P$  equation, in comparison to that for  $E_{(ijk)}^P$ , have interesting consequences: Whereas the sum of the estimates  $E_{(ijk)}^P$  for all possible  $i, j$  and  $k$  is easily shown to be a constant  $12N$ , the sum of the estimates  $E_{[ijkl]}^P$  is not constant; *e.g.* at  $(ii) = 2N$ ,  $(ij) = N$ ,  $(jj) = 0$  the sum is  $656N/81 \approx 8.1N$ , compared to the ideal  $8N$ . At  $(ii) = (jj) = 2N$ ,  $(ij) = 0$ , the sum is  $16N$ . One should note, however, that this last distribution of strongly correlated pairs is highly artificial. No real square lattice could attain such values.

When both estimates (4.3) and (4.5) for  $(ijkl)$  are compared graphically (not shown), there appears to be very little to choose between them. For some parameter values and some  $(ijkl)$  the estimate incorporating closed squares is closer to the observed value than the  $\Gamma^\sigma(i|jk|l) = 0$  estimate; for others it is worse. Put another way, it appears that  $\Gamma^\sigma(i|jk|l)$  is equally well approximated by zero as by

$$\frac{(ij)(kl)}{(j)(k)} \left[ \frac{N}{32} \frac{(li)}{(l)(i)} - \frac{1}{8} \right] \quad (4.7)$$

which is the expression derived by combining equation (4.2) with the estimates in (4.1) and (4.5). This is small when  $i$ - $l$  correlations are close to neutral:  $(il) = 4(i)(l)/N$ . There could be many reasons for this observation: The contribution from closed squares may be too insignificant compared to those omitted higher order correlations (triples, *etc.*), or perhaps there is a better square approximation than  $E_{[ijkl]}^P$  that has been missed.

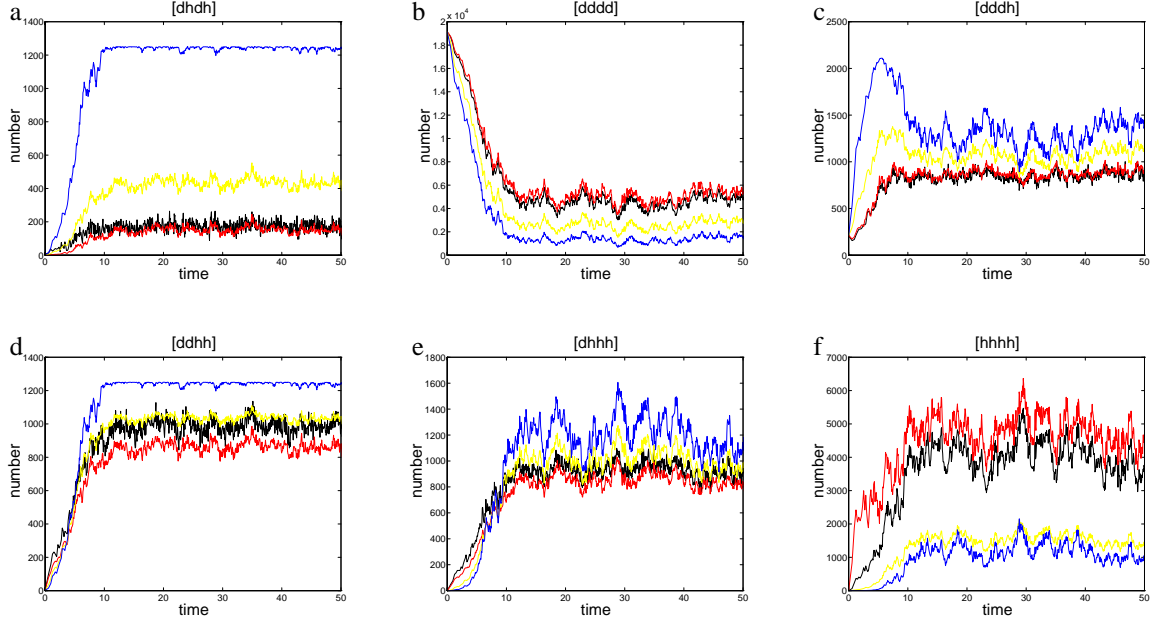


Figure 4.3: Comparison between estimates for  $[ijkl]$  (black) as observed in the lattice hawk-dove simulation: the mean-field (blue), pair estimate  $E^P_{[ijkl]}$  (red) and alternative pair estimate - equation (4.6) (yellow). The simulation was run at  $s = 0.5$  and  $N = 2500$  from a random initial comprising 99% doves.

In deriving equation (4.5), we have attempted to use our knowledge of the actual spatial structure (in this case an abstract square grid) to incorporate the effect of a number of known neighbourly contacts which were originally ignored - namely the closed square contacts for 4 paths. In principle, however, there is no reason to stop with direct neighbours. Even for a pair approximation, the influence of more indirect connections can be considered: The estimate  $E^P_{(ijk)}$  for triples on a square grid, for example, could be modified to incorporate the effect of a possible common neighbour of the  $i$  and  $k$ , in the case when  $i, j, k$  and a fourth individual form a closed square. One would separately consider the contribution from the ‘straight line’  $i-j-k$  triples and from the ‘bent’ triples contained within  $[ijkl]$  squares for every possible species  $l$  in the system. The next step would be to consider twice removed common neighbours, then three times removed neighbours, and so on.

Undoubtedly, the difficulty in deriving the equations each time would rapidly increase as more remote common connections were considered. We may also expect a diminishing payoff in terms of the returned extra accuracy of each successive estimate. After all, such a chain of models are still based only on pair correlations (nothing higher) and there is no reason why they should asymptotically approach the behaviour of an explicit space parent system. More and more information about the spatial structure of the network is required with each successive model, and probably sooner rather than later it would be more productive to consider higher order models based on higher correlations than pairs alone.

## 4.4 Extending the Pair Analysis

A natural question to ask, in view of the successful pair approximation for the two-player spatial game, is what can be gained from a higher order analysis? There is certainly good reason to believe that spatial correlations do persist in many systems beyond the pair level. Figure (4.4) gives an example from the familiar lattice hawk-dove game, comparing the observed triple totals ( $ijk$ ), as measured from a square lattice model, with the pair model estimate  $E_{(ijk)}^P$  of the previous section. With  $m = 4$  for a square grid, we see that the estimate  $E_{(ijk)}^P$  is often good but occasionally quite bad.

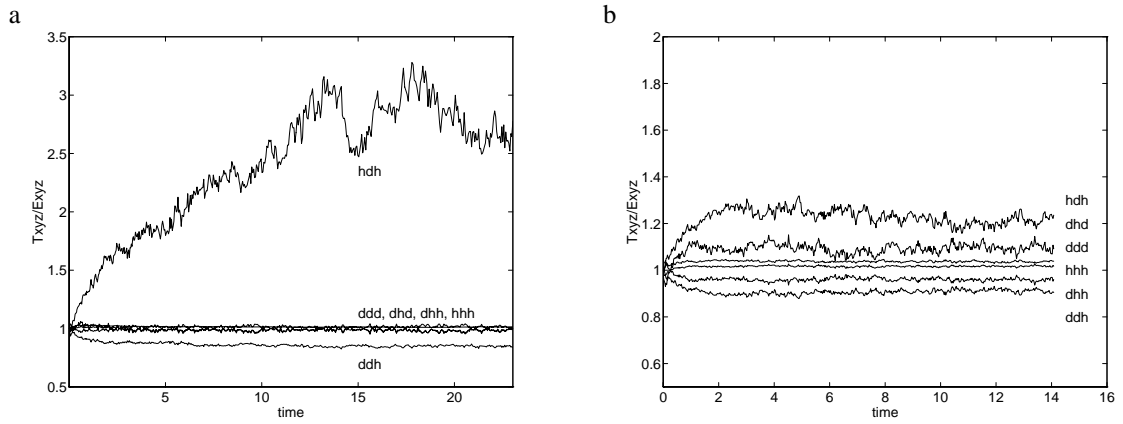


Figure 4.4: Time series of  $(ijk)/E_{(ijk)}^P$  for the six distinct values of  $(ijk)$  in the hawk-dove spatial game. (a) is for  $s = 0.4$  and (b) is for  $s = 0.5$ . Simulations were in each case over 500000 events for the lattice model with 2500 individuals from a random initial condition.

When  $s = 0.4$  (equilibrium population approximately 80% doves) although the overall density of  $h-d-h$  triples is very low (in fact the lowest of the six), they are present in equilibrium at almost three times the density expected from the pair approximation estimate. Similarly,  $d-d-h$  triples are significantly less represented in the explicit model than would be expected if neighbouring pairs were independent. For the case  $s = 0.5$  (equilibrium population approximately 50% doves) the estimates fare better but there is still up to 20% deviation from unity for the ratio observed/estimated consistently displayed. Interestingly,  $h-d-h$  and  $d-d-h$  are again the furthest away.

Analysis leaving closure to a higher level is possibly the only real solution if we are not satisfied with approximation errors like these, and we attempt this now. The approximation methods of section (4.3) will be of fundamental importance in the even more nonlinear world of triple approximations.

#### 4.4.1 Triple Approximation in the Two-Player Spatial Game

The easiest way to illustrate the theory is with a practical example; choosing our original spatial game also enables direct comparison with earlier results, and easier measurements of the potential benefits. Because the triple equations are much more complicated than pair equations, and because of the success of the pair approximation in this case, we consider only the case of a fixed, regular network in the form of a square lattice with connections to the four nearest neighbours.

Ultimately the aim is to write closed dynamical equations in terms of nothing higher than the triple totals  $(ijk)$  in the same way that the pair approximation considered nothing higher than pairs  $(ij)$ . In fact, we only need to consider triples  $(ijk)$  themselves because the regularity of the grid ensures that every individual is the first member of 4 (physical) pairs and each of these the start of 3 distinct triples. This gives (with the two contesting species labelled  $i$  and  $j$ ):

$$\begin{aligned} 4(i) &= (ii) + (ij) \\ 4(j) &= (jj) + (ij) \\ 3(ii) &= (iii) + (iij) \\ 3(ij) &= (iji) + (ijj) \\ 3(jj) &= (jji) + (jjj) \end{aligned}$$

and of course  $(i) + (j) = N$ , the constant population size. The regular network also reduces the number of independent variables by symmetry. Clearly  $(iij) = (jii)$  and  $(ijj) = (jji)$ , and another is lost because the total number of triples is a constant  $12N$ . Finally, on a square grid, the number of triples starting with i-j must equal the number ending with i-j, so  $(iji) + (ijj) = (iij) + (jji)$ . Therefore the  $8 = 2^3$  triple variables can be reduced to just 4 independent ones, and it is sufficient to consider  $(iii)$ ,  $(iij)$ ,  $(iji)$  and  $(ijj)$ .

The evolution equations for these variables, using equation (3.1), are

$$\begin{aligned} (iii) &= \frac{1}{4} \sum_{(ij)} [aQ_x^\sigma(i) + bQ_x^\sigma(j)] [2Q_y^\sigma(ii) + Q_y^\sigma(i) (Q_y^\sigma(i) - 1)] \\ &\quad + \frac{1}{4} \sum_{(ji)} [cQ_x^\sigma(i) + dQ_x^\sigma(j)] [-2Q_y^\sigma(ii) - Q_y^\sigma(i) (Q_y^\sigma(i) - 1)] \\ (iij) &= \frac{1}{4} \sum_{(ij)} [aQ_x^\sigma(i) + bQ_x^\sigma(j)] [Q_y^\sigma(ij) + Q_y^\sigma(i)Q_y^\sigma(j) - Q_y^\sigma(ii)] \\ &\quad + \frac{1}{4} \sum_{(ji)} [cQ_x^\sigma(i) + dQ_x^\sigma(j)] [Q_y^\sigma(ii) - Q_y^\sigma(i)Q_y^\sigma(j) - Q_y^\sigma(ij)] \\ (iji) &= \frac{1}{4} \sum_{(ij)} [aQ_x^\sigma(i) + bQ_x^\sigma(j)] [2Q_y^\sigma(ji) - Q_y^\sigma(i) (Q_y^\sigma(i) - 1)] \\ &\quad + \frac{1}{4} \sum_{(ji)} [cQ_x^\sigma(i) + dQ_x^\sigma(j)] [Q_y^\sigma(i) (Q_y^\sigma(i) - 1) - 2Q_y^\sigma(ji)] \end{aligned} \tag{4.8}$$

$$\begin{aligned}
(i\dot{j}j) &= \frac{1}{4} \sum_{(ij)} [aQ_x^\sigma(i) + bQ_x^\sigma(j)] [Q_y^\sigma(jj) - Q_y^\sigma(i)Q_y^\sigma(j) - Q_y^\sigma(ji)] \\
&\quad + \frac{1}{4} \sum_{(ji)} [cQ_x^\sigma(i) + dQ_x^\sigma(j)] [Q_y^\sigma(ji) + Q_y^\sigma(i)Q_y^\sigma(j) - Q_y^\sigma(jj)]
\end{aligned}$$

In each sum the first factor is the invasion event rate (average fitness of the site  $x$  individual; the factor  $\frac{1}{4}$  appears because each has  $m = 4$  neighbours), exactly as in previous analysis, and the second factor is the associated change  $\delta f$ . For example, when an  $i$  invades a  $j$  (at site  $y$ ), the number of  $i$ - $i$ - $i$  triples is increased by  $2Q_y(ii)$  for triples starting or ending at site  $y$ , and by  $Q_y(i)(Q_y(i) - 1)$  for triples with  $y$  the middle site. The other equations follow similarly, taking particular care to count every triple in both directions.

#### 4.4.2 Closure

Substituting into equations (4.8) directly for each  $Q_x^\sigma$  as a suitable average  $\overline{Q}^\sigma$  plus an error  $\eta_x^\sigma$  results in a daunting array of new compound error  $\Gamma$  terms, defined as

$$\begin{aligned}
\Gamma(i|jk|l) &= \frac{1}{(jk)} \sum_{(jk)} \eta_x(i|jk) \eta_y(l|kj) \\
\Gamma(i, l|jk|\cdot) &= \frac{1}{(jk)} \sum_{(jk)} \eta_x(i|jk) \eta_x(l|jk) \\
\Gamma(l|jk|hi) &= \frac{1}{(jk)} \sum_{(jk)} \eta_x(l|jk) \eta_y(ih|kj) \\
\Gamma(l|jk|h, i) &= \frac{1}{(jk)} \sum_{(jk)} \eta_x(l|jk) \eta_y(h|kj) \eta_y(i|kj)
\end{aligned}$$

As was the case with pair analysis in Chapter 3, some of these error terms will be small, and justifiably approximated by zero, whilst others will not. Approximating these non-trivially is an even more complicated task, taking triple correlations into account, than that which defeated rigorous analysis in the pair approximation (*e.g.* for  $\Gamma(i|jk|l)$ ). One option is to ignore all the error terms, which results in equations of the form

$$\begin{aligned}
(iii) &= 2(ij) [mb + (a - b)\overline{Q}(i|ij)] [\overline{Q}(ii|ji) + \overline{Q}(i|ji) (\overline{Q}(i|ji) - 1)] \\
&\quad - 2(ij) [md + (c - d)\overline{Q}(i|ji)] [\overline{Q}(ii|ij) + \overline{Q}(i|ij) (\overline{Q}(i|ij) - 1)] \\
&\quad + \text{error terms}
\end{aligned}$$

but this is unnecessarily crude. Instead, we follow the alternative perspective ideas of the previous section and use direct heuristic approximations for the network elements appearing in table (4.2). But before this can be done, the equations (4.8) must first be expanded in terms of these network element totals.

Observe that, for any function  $f(x)$  of the network site  $x$ , the following relations hold:

$$\sum_{(i)} Q_x(i) f(x) = \sum_{(ii)} f(y) \quad (4.9)$$

$$\sum_{(ij)} Q_x(i) f(x) = \sum_{(iij)} f(y) \quad (4.10)$$

Each relation simply corresponds to writing out the multiplication by  $Q_x(i)$  as a sum over larger network neighbourhoods. If, for example,  $f(x) = Q_x(j)$  then using tables (4.1) and (4.2) we have

$$\sum_{(ij)} Q_x(i) Q_x(j) = \sum_{(iij)} Q_y(j) = (iij) \overline{Q}(j|i <_j^i) = (ji <_j^i) + (iij)$$

Slightly more complex cases arise, such as

$$\sum_{(ij)} Q_x(j) f(x) = \sum_{(jij)} f(y) + \sum_{(ij)} f(x)$$

because there is already one  $j$  neighbour of the  $x$  site in the original  $i$ - $j$  pair, but the principle is always the same. By repeatedly applying this and similar rules, the sum of arbitrary products of  $Q_x$  can be reduced to linear terms, whereupon the sum then disappears and leaves a multiple of an associated average  $\overline{Q}$  term. Using table (4.1) these can be expanded in terms of the elemental neighbourhood variables themselves. It is important to note that no further approximation has been involved during this stage, and the equations so formed are identical to the equations with  $\Gamma$  error terms included. In many ways, the logic is like that used to deduce table (4.1) applied in reverse (and exact expressions for each  $\Gamma$  error term can therefore be derived in terms of these element expressions, approximation of which then indirectly gives an approximation of each  $\Gamma$ ). The resulting equations (see below) must be closed by direct approximation of the elements larger than triples.

On the regular square grid, each individual has  $m = 4$  neighbours, and all terms involving triangles (*i.e.*  $<ijk>$  and  $(i-<jkl>)$ ) are necessarily zero (and are ignored). Expanding equations (4.8) for  $(iii)$ ,  $(iij)$ ,  $(iji)$  and  $(ijj)$  as described above results in the following equations:

$$\begin{aligned} (iii) &= a \left[ 2(iij) + 2(ii ji) + 2(iij ii) + 2[iii j] + 2(ji <_i^i) + (iij <_i^i) \right] \\ &+ b \left[ 2(iij) + 2(iji) + 2(ii ji) + 2(iji j) + 2(ii ji j) + 2(ii <_j^j) + (ij <_i^i) + (ji j <_i^i) \right] \\ &+ c \left[ -2(iii j) - 2(iii ji) - 2[iii j] - (ji <_i^i) - (iji <_i^i) \right] \\ &+ d \left[ -2(iii j j) - (jji <_i^i) \right] \\ \\ (iij) &= a \left[ -(iij) + (iij j) - (iij ii) + (iij ij) - [iii j] + (ii <_j^j) - (ji <_i^i) + (iij <_j^i) \right] \\ &+ b \left[ 2(jij) + (ijj) - (iij) + (iji j) + (ji j j) - (iij i) + (ji j ij) - (iij ij) + [ij ij] \right. \\ &\quad \left. + (ji <_j^j) + (jj <_i^i) - (ii <_j^j) + (ji j <_j^i) \right] \\ &+ c \left[ -(iij) + (iii j) - (iij i) - (jii j) + (iii ji) - (ij iij) + [iij j] - (ii <_j^j) - (iji <_j^i) \right] \end{aligned}$$



$$+d \left[ - (iijj) + (iiij) - (jiiij) - [iijj] - (jji <_j^i) \right] \quad (4.11)$$

$$\begin{aligned} (iji) &= a \left[ - 2(iiji) + 2(iijji) + 2[iijj] - (iij <_i^i) \right] \\ &+ b \left[ - 2(iji) + 2(ijji) - 2(ijij) + 2(ijjij) - (ij <_i^i) - (jj <_i^i) \right] \\ &+ c \left[ - 4(iji) - 2(ijij) - 2(ijiji) - 2[iijj] + (ji <_i^i) - 2(ij <_i^i) + (iji <_i^i) \right] \\ &+ d \left[ - 2(ijijj) - 2(jj <_i^i) + (jji <_i^i) \right] \\ \\ (ijj) &= a \left[ - (iijj) + (iijjj) - (iijji) - [iijj] - (iij <_i^i) \right] \\ &+ b \left[ - (ijj) + (ijjj) - (jjij) - (ijji) + (jjjj) - (ijjjj) + [iijj] - (jj <_i^i) - (jj <_j^i) \right] \\ &+ c \left[ 2(iji) + (iij) - (ijj) + (ijij) + (iiji) - (jjjj) + (ijiji) - (ijijj) + [ijij] \right. \\ &\quad \left. + (ij <_i^i) + (ii <_j^i) - (jj <_i^i) + (iji <_j^i) \right] \\ &+ d \left[ - (ijj) + (iijj) + (ijijj) - (jjijj) - [iijj] + (jj <_i^i) - (ij <_j^i) + (jji <_j^i) \right] \end{aligned}$$

Each of the variables on the right hand side in equations (4.11) has to be expressed in terms of triple variables. We therefore seek triple estimates  $E^T$  corresponding to the pair estimates  $E^P$  of section (4.3), and the previous approach is extended by analogy. For a given triple approximation ( $E^T$ ) to any particular element, it should be the case that:

- i. It is proportional to the abundance of each constituent triple and is therefore zero if any of these are absent from the network.
- ii. The number of the particular element in the whole network is correctly predicted when all individuals belong to the same species.
- iii. If the triple correlations vanish, in the sense of  $(ijk) = E_{(ijk)}^P$ , the pair estimate for  $(ijk)$ , then the estimate reduces to the corresponding pair approximation estimate.

As an example, consider a triple approximation  $E_{[ijkl]}^T$  for  $[ijkl]$ . There are four triples involved in any such square, so we take  $E_{[ijkl]}^T$  to be proportional to

$$(ijk)(jkl)(kli)(lij)$$

In this expression, each of the four physical pairs in the square is then accounted for in two distinct triples, so dividing by each one once will ensure the correct dependency when triple correlations disappear. (Each individual  $((i), (j), (k)$  and  $(l))$ , being a component of three triples but also two pairs is then accounted for just once, and no correction is needed). Finally scaling in the case of a monospecific population (property ii.) gives

$$E_{[ijkl]}^T = \frac{8N}{81} \frac{(ijk)(jkl)(kli)(lij)}{(ij)(jk)(kl)(li)} \quad (4.12)$$

As required by iii. this estimate reduced to  $E_{[ijk]l}^P$  (equation (4.4)) if  $(ijk) = E_{(ijk)}^P$  (equation (4.1)).

This procedure (starting with triples, and correcting for pairs and singles as necessary) also works well for the range of other estimates needed to close equations (4.11), but not always in as straightforward a fashion: For most other element shapes, the geometry of a square grid complicates matters further by providing several alternative spatial layouts for one particular element. (The same complication was encountered in the pair approximation estimate  $E_{(ijkl)}^P$  for which open paths ( $i$  not neighbouring  $l$ ) and closed paths ( $i$  neighbouring  $l$ ) considered separately produced equation (4.5)). Each specific layout is likely to be composed of different triples. For example, a 5-path could be composed of only three triples if it is drawn out into a straight line or only moderately bent, but it contains six triples if it is bent tightly to cover a square in the grid - see figure (4.5). Taking this, and similar, considerations into account, table (4.3) gives the resulting triple approximation  $E_{(ijklm)}^T$ , along with four other approximations that are necessary for the analysis of the spatial hawk-dove game on a regular square lattice.

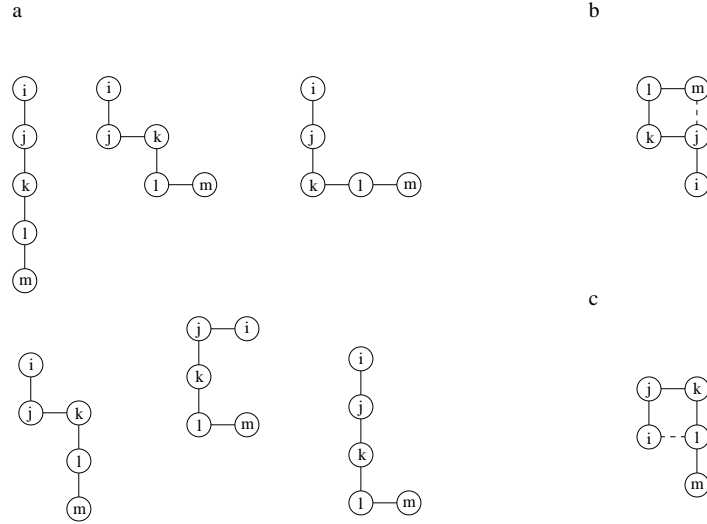


Figure 4.5: Possible orientations of a 5-path on a square grid. For the six arrangements in a) only  $i-j-k$ ,  $j-k-l$  and  $k-l-m$  triples are present. However, due to the known connections on a square grid (dashed line), the configuration in b) also includes the triples  $i-j-m$ ,  $m-j-k$  and  $l-m-j$  and the configuration in c) includes  $i-l-k$ ,  $i-l-m$  and  $l-i-j$ . Of the  $116N$  5-paths on a square grid composed of  $N$  individuals, there are  $84N$  of type a),  $16N$  of type b) and  $16N$  of type c). The contribution from each of these three classes is clearly seen in the estimate  $E_{(ijklm)}^T$  in table (4.3).

Element	Triple Approximation, $E^T$
$[ijkl]$	$\frac{8N}{81} \frac{(ijk)(jkl)(kli)(lij)}{(ij)(jk)(kl)(li)}$
$(ijkl)$	$\frac{(ijk)(jkl)}{(jk)} \left[ \frac{7}{9} + \frac{8N}{81} \frac{(kli)(lij)}{(ij)(kl)(li)} \right]$
$(ji<_l^k)$	$\frac{8}{9} \frac{(jik)(jil)(kil)(i)}{(ij)(ik)(il)}$
$(ijklm)$	$\frac{(ijk)(jkl)(klm)}{(jk)(kl)} \left[ \frac{7}{9} + \frac{64N}{729} \frac{(ilk)(ilm)(lij)(l)}{(kl)(lm)(ij)(il)^2} + \frac{64N}{729} \frac{(ijm)(mjk)(lmj)(j)}{(ij)(jk)(lm)(jm)^2} \right]$
$(ijk<_m^l)$	$\frac{(ijk)(jkl)(jkm)(lkm)(k)}{(kl)(km)(jk)^2} \left[ \frac{40}{81} + \frac{64N}{729} \frac{(jil)(ilk)}{(il)(ij)(kl)} + \frac{64N}{729} \frac{(jim)(imk)}{(im)(ij)(km)} \right]$

Table 4.3: Triple approximations for elements in an N-individual regular square lattice network with 4 neighbours per site.

#### 4.4.3 Results

We can now finally give a triple approximation for the square lattice hawk-dove game by closing equations (4.11) with the estimates in table (4.3). The resulting fourth order ODE system behaves in a qualitatively identical way to the pair approximation, with all trajectories attracted to an equilibrium proportion of doves and hawks. Figure (4.6) shows this equilibrium composition, against  $s$ , in comparison to the original pair approximation and full square lattice simulation of Chapter 2. As hoped, the triple model approximates the lattice simulation even more closely than the pair model, which itself was impressive. No analytical value for the equilibrium as a function of  $s$  was obtained, but like the pair model, numerical solution suggested a linear, or very close to linear function.

### 4.5 General Pair Models

We now return to pair approximations, but consider alternatives to a regular square lattice. Suppose instead the spatial domain is a regular hexagonal lattice with each site connected to its nearest six neighbours. It is not sufficient to simply replace  $m = 4$  with  $m = 6$  in the square grid analysis because there are now triangles  $<ijk>$  to consider (on an  $N$  individual grid of  $30N$  triples,  $12N$  are closed triangles and  $18N$  open triples, where the  $i$  and  $k$  are not direct neighbours). Using the techniques of section (4.3) the open  $i$ - $j$ - $k$  paths can be estimated by

$$\frac{18}{36} \frac{(ij)(jk)}{(j)}$$

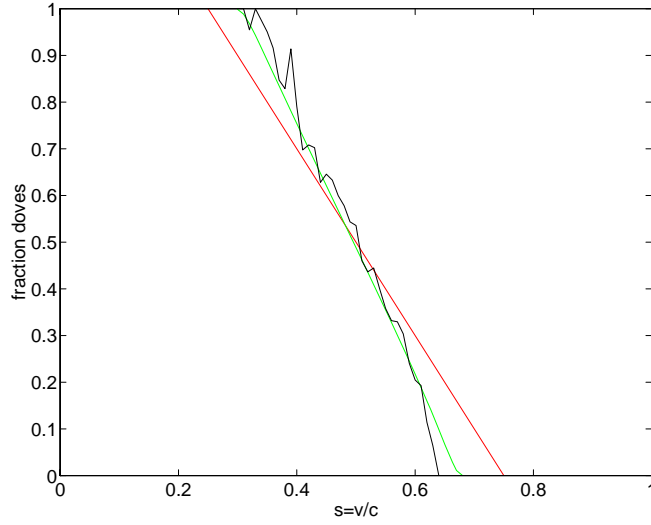


Figure 4.6: Plots of fraction doves in the population at equilibrium against  $s$  for a CA simulation (black) and the pair (red) and triple (green) approximations.

and the closed triangles  $\langle ijk \rangle$  by

$$\frac{12N}{216} \frac{(ij)(jk)(ki)}{(i)(j)(k)}$$

so the hexagonal lattice estimate for all  $(ijk)$  triples, in contrast to the square lattice estimate (equation (4.1)), is

$$E_{(ijk)}^P = \frac{(ij)(jk)}{(j)} \left[ \frac{1}{2} + \frac{N}{18} \frac{(ik)}{(i)(k)} \right] \quad (4.13)$$

Other regular networks might have different proportions of closed triangles than the square or hexagonal grids. Suppose a network has  $m$  neighbours per individual and a proportion of these neighbours also interact with each other. Over the whole population, let  $\phi$  be the fraction of all pairs of neighbours of every individual that are neighbours themselves. Equivalently,  $\phi$  is the ratio of the total number of triangles to the total number of triples:

$$\phi = \frac{\sum_{i,j,k} \langle ijk \rangle}{\sum_{i,j,k} (ijk)}$$

For a square grid we have  $m = 4$  and  $\phi = 0$ ; the regular hexagonal lattice would correspond to  $m = 6$  and  $\phi = 2/5$ . Essentially, there are now two parameters,  $m$  and  $\phi$ , with which to describe the spatial structure of an individual's neighbourhood, whilst maintaining the useful modelling constraint of regularity (all individuals experience the same spatial structure). Returning to the triple estimate, we expect  $m(m-1)N$  triples in total; a fraction  $\phi$  of which are triangles, and  $1 - \phi$  of which are open. In this general case, the estimate for  $(ijk)$  is

$$(ijk) \approx E_{(ijk)}^P = \frac{(m-1)}{m} \frac{(ij)(jk)}{(j)} \left[ 1 - \phi + \frac{\phi N}{m} \frac{(ik)}{(i)(k)} \right] \quad (4.14)$$

of which equations (4.1) and (4.13) are special cases.

A useful yardstick is obtained by calculating  $\phi$  for the case where individuals occupy a random position in 2D space and interact with all others within a radius  $\rho$ . (Compare the irregular models of section (3.6.2). Although an explicit network of this kind will not have exactly  $m$  neighbours per individual, the value of  $\phi$  is still useful.)

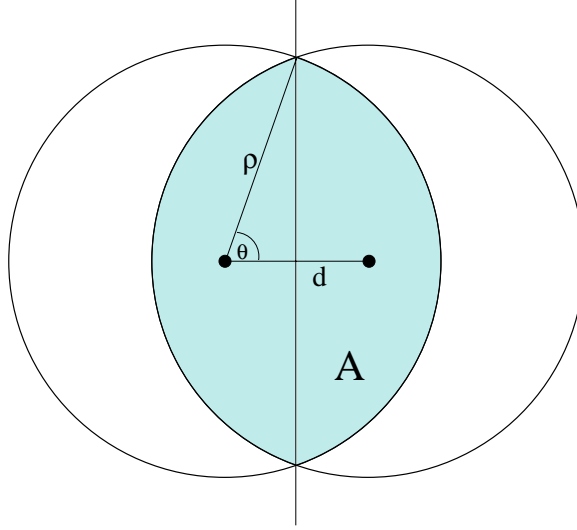


Figure 4.7: Two neighbouring individuals a distance  $d$  apart, each with a radius of interaction  $\rho > d$

Figure (4.7) shows two neighbouring individuals a distance  $d \leq \rho$  apart. The shaded area,  $A$ , represents the area within which a third individual would neighbour the other two. If individuals are distributed uniformly randomly over the whole area, one would expect a randomly chosen neighbour of one of the individuals to neighbour the other with probability  $\phi(d) = A/\pi\rho^2$ . Writing  $y = \rho \sin\theta$  and  $x = \rho \cos\theta$ , we can calculate  $A$  as a function of  $d$  and  $\rho$ ,

$$\begin{aligned} A &= 4 \int_0^{\sqrt{\rho^2 - d^2/4}} \left( \sqrt{\rho^2 - y^2} - \frac{d}{2} \right) dy \\ &= 2\rho^2 \cos^{-1}\left(\frac{d}{2\rho}\right) - \frac{d}{2} \sqrt{4\rho^2 - d^2} \end{aligned}$$

For any pair of connected individuals, the separation distance  $d$  has a distribution given by the density function  $2d/\rho^2$  for  $d \in [0, \rho]$ . So

$$\begin{aligned}
\phi &= \mathbb{E}[\phi(d)] \\
&= \int_0^\rho \frac{2d}{\rho^2} \phi(d) dd \\
&= \frac{16}{\pi} \int_{\frac{\pi}{2}}^{\frac{\pi}{3}} \cos^2 \gamma \sin^2 \gamma - \gamma \sin \gamma \cos \gamma d\gamma \quad \text{using } d = 2\rho \cos \gamma \\
&= 1 - \frac{3\sqrt{3}}{4\pi} \approx 0.586
\end{aligned}$$

#### 4.5.1 No explicit Network

If  $m$  and  $\phi$  are known for any particular regular spatial network then equation (4.14) can be used to close appropriate pair equations, whenever they can be written for a given system, and provide a pair model approximation. Pair models so found then capture aspects of the dynamics seen in the full network simulation, hopefully at least as accurately as a mean-field approximation does (*e.g.* the hawk dove game in Chapter 2). With this interpretation, however, the available choices for  $m$  and  $\phi$  are limited to those for which a corresponding regular spatial network can be imagined. Because the choice of any particular network as a suitable spatial environment for a given biological system is itself often arbitrary and not necessarily realistic, this seems an unnecessary restriction. Instead, we can broaden our interpretation and allow  $m$  and  $\phi$  to take any feasible values and ignore consideration of a possible explicit spatial network. Clearly we expect  $0 \leq \phi \leq 1$  and  $m$  to be positive but the need to insist that  $m$  is integer valued can also be relaxed. In pair model ODEs, individuals are not identified so this presents no mathematical problem. Biologically, a non-integer  $m$  can be interpreted as the average number of neighbours per individual. Strictly speaking, this would imply that some individuals have more neighbours than others which is not the case in a regular spatial network. However, because there is no longer any assumed underlying network this is not a problem if we are content for equation (4.14) to be the underlying approximation.

Taking this a stage further, we are naturally led to consider the second interpretation of pair models: Despite the original motivation as a lattice model approximation, we can view pair models not as approximations to any other particular explicit spatial model, but as alternative descriptions of the spatial environment in their own right. An original assumption, for example, of the form ‘space is a regular hexagonal lattice’ with the further approximation of no spatial correlations at the triple level (or higher) is then replaced by the assumption ‘triple connections in space are described by equation (4.14)’ with an appropriate choice of  $m$  and  $\phi$ . Particularly with regard to population mixing and migration events, which are often omitted or poorly catered for in basic models, abandoning rigid explicit networks as a modelling goal is a sensible idea.

For illustration, figure (4.8) shows the effect of variations in  $\phi$  on an example triple estimate  $(ijj) = E_{(ijk)}^P$  as given by equation (4.14) for a two species system with  $m = 4$  neighbours per individual.

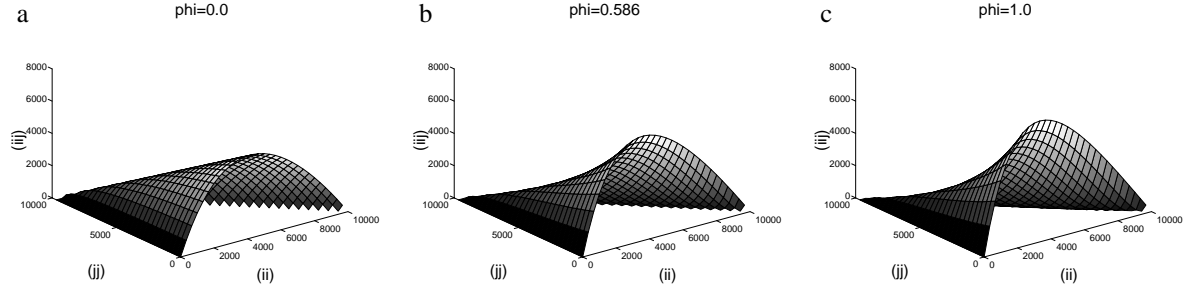


Figure 4.8: The pair approximation for  $(ijj)$  from equation (4.14) illustrated at three values of  $\phi$  for a two species system with  $m = 4$  and  $N = 2500$ .

#### 4.5.2 Clumping

High values of  $\phi$  can have potentially interesting effects. As an extreme example consider the case  $\phi = 1$ . This implies that all  $m$  neighbours of any individual are all connected to each other. If we were to take a global view of space in this case (which is, admittedly, not always a sensible question to ask for a pair model - especially when viewed as an alternative descriptions of space) then the only possible interpretation is of many isolated patches (assuming  $m \ll N$ ), each composed of  $m + 1$  individuals entirely intra-connected, but with no connections between any of the patches. This is clearly a very different spatial structure from the case  $\phi = 0$  (think of the regular square grid for example). This suggests an interpretation for  $\phi$ : Given a fixed value of  $m$  - which fixes the total number of contacts in the population as a whole - increasing  $\phi$  corresponds to increasing the clumping of individuals within the spatial environment (equivalently, think of increasing the degree of spatial heterogeneity in the overall population density, *i.e.* the density of individuals only, without respect to their type or species). Low  $\phi$  is a relatively uniform distribution in space, high  $\phi$  is highly aggregated.

In a truly clumped real population, one would expect to find some individuals in the centre of clumps with more than the average number of connections, and others towards the edges with fewer. Of course, this is not possible for a regular grid interpretation in which every individual has an average spatial environment with precisely  $m$  neighbours a fraction  $\phi$  of which are also connected pairwise. But it is possible for the alternative interpretation. By its nature, a pair model does not explicitly differentiate between individuals in this way because it does not specifically identify individuals at all. The inclusion of  $\phi$  as an extra parameter, in addition to  $m$ , provides another mechanism with which to adjust the spatial structure, and hopefully a method by which the effect of clumping can

be emulated. Examples in the next two chapters will examine how much of this effect is captured in pair models, and its influence on the dynamics.

## 4.6 Discussion

This chapter's attempts to extend the work on correlation models beyond the basic pair approximation quickly revealed some hidden difficulties. The crucial process in deriving any such correlation model is closure of the equations, which is achieved through a suitable approximation. Although this can be couched in various ways (*e.g.* estimating  $\Gamma$  error terms, or approximating large element totals like  $(ijk) = E_{(ijk)}^P$ ), it ultimately reduces to the problem of constructing (approximating) local spatial neighbourhoods which are consistent with a range of known correlation densities. In the simplest cases, like those of the previous chapter, each requirement can be satisfied independently with a clearly stated assumption (*e.g.* the multinomial assumption). But where larger correlations (*e.g.* triples) must be considered, or when the spatial structure incorporates sufficient close connections (*e.g.* triangular connections even in a pair model), a similar approach does not seem possible. Instead, a heuristic solution was presented (the alternative perspective direct approximation of elements) which mirrored, as far as possible, the simple case solutions.

Having to resort to such heuristic methods is, in some ways, a disappointment given that a stated aim of this thesis was to set the subject on a more solid foundation. Nevertheless some success can be claimed, and there may indeed be no alternative (see chapter 7); no better solution was found in the literature. (The only reference to a triple approximation was found in Matsuda, Ogita, Sasaki, and Satō (1992) where the simple case of one dimensional space was considered. As with the square grid pair approximation, individuals connected along a line fall into the simple category for triple approximation, because an individual at the end of the line is only affected by one correlation condition; namely that determined by itself, its neighbour and its neighbour's neighbour).

Deriving the triple approximation equations for the square grid spatial game was a lengthy and detailed procedure, and the improved results for the hawk-dove game predictions were correspondingly satisfying. However, the spatial game is a particularly simple system (and was chosen so deliberately), and triple equation models for more complex systems quickly become very unwieldy. For example, in just moving from a two species system to a three species system, the number of equations jumps from 8 to 27 (before symmetries). This may not be a difficulty for numerical integration on today's computers, but we very quickly go beyond the practical range of analytical study.

There is no doubt that triple equations will in general perform better than pair equations in approximating the behaviour of larger explicit spatial models, but how much better is not clear. Fur-



thermore, when viewing correlation models as stand-alone spatial models, the advantages of triple equations are less apparent: They may simply be capturing more closely the particular spatial characteristics of an arbitrary, abstract and ultimately unrealistic spatial structure (*e.g.* the square grid).

In view of this (and because there is little point in trying to run before you can walk), the neat and flexible  $(m, \phi)$  formulation of the pair equations offers an attractive way forward. Examples based on this are presented in the next two chapters, where the emphasis will be biased towards interpreting the pair models as proper, free-standing, spatial models.

**5**

## **Examples**

## 5.1 The Iterated Prisoner's Dilemma.

The Iterated Prisoner's Dilemma (IPD) plays an important role as a metaphor for understanding cooperation between individuals in biology. It has been extensively studied by many authors who have covered many aspects and variations of the game.

The IPD is a contest between two players, based on playing rounds of the prisoner's dilemma in succession with the same opponent (see section (1.5.2)). The number of rounds in a game can be variously determined, for example by engaging in each subsequent round with a certain probability, or even considering IPD matches with arbitrarily many rounds (where the long term behaviour is of interest). Crucially, when more than one round is played, more complicated strategies (*i.e.* rules for determining when to cooperate and when to defect on a particular round) are available: A player can now use strategies which depend on knowledge of the outcome of previous rounds of the game. The fact that the same opponent is met repeatedly therefore gives the opportunity to establish an 'understanding' between the players, in the sense that a strategy may be able to respond to its opponent's strategy, as displayed in previous behaviour. For example, a selfish (frequently defecting) player may be punished with defection instead of rewarded with cooperation by an opposing strategy which reacts to the previous defections. 'Defect in every round' (referred to as Always Defect), unlike 'Defect' for the one round dilemma, is therefore not necessarily a rational strategy in the IPD. Players score points in the IPD by accumulating the points scored in each round (which are given by the original payoff matrix).

There are many possible strategies in the IPD: As each round is played, the game history available on which to base strategies increases and the number of possible strategies rapidly increase too. A convenient way to limit the scope of strategies under consideration is to restrict attention to those with a memory for only the most recent few rounds. Nevertheless, considering only strategies that can 'remember' either just the opponent's previous move, or possibly both the opponent's and its own previous move, is surprisingly instructive. One such strategy is Tit-for-Tat (TFT). In the history of IPD analysis, TFT was an early successful strategy, and the winner of Axelrod's famous computer tournament (see Hofstadter, 1983). TFT simply cooperates with an opponent on the first round of a game, and thereafter copies its opponent's previous move in all subsequent rounds. TFT is a nice and forgiving strategy which encourages a certain amount of cooperation with suitably minded opponents, but which also punishes defection. Always Defect (AllD) and Always Cooperate (AllC) are two more basic (and self-explanatory) strategies that don't even need any memory of previous game rounds. A strategy that depends upon both players' previous moves is Win-Stay, Lose-Shift (WSLS). This strategy repeats its last move if it received the temptation (T) or reward (R) payoff in the previous round (*i.e.* a winning round), and swaps strategy (between Cooperating and Defecting) if it received the sucker (S) or punishment (P) payoff last round (a losing round). WSLS can out-perform TFT (Nowak and Sigmund, 1993). In general, one would of course expect

strategies with longer memories to do at least as well as those with shorter ones if no costs are associated with the longer memory.

Dynamics can be introduced to a population of IPD players just as for any other game (see Chapter 1): Fitness is determined by the player's IPD score, and those strategies which score highly increase their representation in the population. Typically, the population is assumed to be well mixed (non-spatial or mean-field) so players play opponents selected at random. An important result for the non-spatial IPD is that no pure strategy can be evolutionarily stable (Boyd and Lorberbaum, 1987; extensions in Farrell and Ware, 1989; Lorberbaum, 1994). The proof shows that it is always possible to find a group of invading strategies (perhaps just two) that together can displace any single dominant strategy. This clearly has implications for the evolution of the non-spatial IPD, but there is no known corresponding result for a spatial IPD (*i.e.* an IPD game in which players do not meet each other at random, but play neighbours within some spatial structure). However, restricting attention to a fixed strategy set (*e.g.* strategies which react to only the opponent's previous move) can remove access to these invading strategies. It is then possible to ask which strategies are the most successful, either through calculating expected payoffs or by simulating populations of IPD players where the game payoffs are interpreted as fitness. Both ideas have been pursued in the literature.

There are many other modifications to the IPD that have been investigated in addition to those set in a spatial environment that are the focus in this chapter. Optional games (Batali and Kitcher, 1995) allow contestants the choice of whether or not to participate in each round of the game. It is often found that this promotes more cooperative behaviour by providing a mechanism for escaping from costly periods of mutual defection. In asynchronous (alternating) games, on the other hand, contestants do not choose strategies for each round simultaneously, but in a staggered fashion (Freen, 1994; Nowak and Sigmund, 1994). Interestingly, results from this version of the IPD also suggest that more (guardedly) generous behaviour is profitable, and the continued exploitation of suckers is not.

The variety of IPD-based models in the literature and their different behaviours must serve as a caution against over-confident predictions. Even if the IPD could be a realistic model for the cooperation displayed by a particular species, different implementations of it may easily provide different answers. Furthermore, the IPD is not the only analogy for the evolution and dynamics of cooperative behaviour; other mechanisms are reviewed in Connor (1995).

Nevertheless, important questions can be asked of IPD models. One of which, the focus of this chapter, is the extension to a spatial environment. First, however, we consider stochastic strategies.

### 5.1.1 Stochastic Strategies

A particularly relevant paper (Nowak, 1990) considers stochastic strategies *i.e.* those in which an individual in a round of the IPD plays either C or D not with certainty, but with a certain probability, dependent (in this case) only on the opponent's previous move. The game can then be viewed as a Markov Chain on the state space of possible outcomes of each round (C-C, C-D, D-C, D-D). Very useful results are obtained under the assumptions that

- i. The individuals play an infinite number of rounds of the game with each other (equivalent to the limit  $w \rightarrow 1$  if  $w$  is the probability of each subsequent round occurring).
- ii. There is a small amount of noise involved in playing the game and it is impossible to play either C or D with probability 1. Suppose the closest allowable probability is  $1 - \varepsilon$  where  $0 < \varepsilon \ll 1$ .

Assumption (i) is rather arbitrary, and a biological justification must depend upon the details of a particular system. For the abstract IPD, however, it is as reasonable as any other assumption. It is worth noting, as does Nowak, that this assumption is optimal for the evolution of cooperative behaviour based on reciprocity (the mechanism represented by the IPD). Assumption (ii), however, is very easily justified. In virtually any contest in biology, environmental noise will make the processes of observation and action less than 100% reliable; mistakes will occasionally happen. We can consider both mistakes which are the incorrect perception of a behaviour and those which are the display of an unintended behaviour - different types of mistake from the players' points of view - to be covered by insisting that probabilities must be no closer than  $\varepsilon$  away from certain (*i.e.* they must lie between  $\varepsilon$  and  $1 - \varepsilon$ ). This assumption guarantees that the Markov matrix is mixing and that the probability distribution of rounds of the game over the four states tends to a stationary distribution (given by the largest eigenvector of the matrix). Taken together, (i) and (ii) imply that the payoff received by each player over the whole game, defined as the average score per round of the game, is independent of their initial move and is solely determined by the stationary distribution.

This provides a direct method of obtaining from the one-round PD payoffs of  $R, S, T$  and  $P$  a two-player game payoff matrix, given that the protagonists employ any stochastic strategy dependent (at most) only on the opponent's previous move. Furthermore, given suitable assumptions, this game can now be analysed in a spatial as well as a non-spatial environment using the techniques developed in the preceding chapters.

### 5.1.2 Analysis

Using Nowak's notation, a strategy is defined by  $(p, q)$  where  $p$  is the probability of the player choosing to play C next time, given his opponent played C last time, and  $q$  is the probability of playing C if his opponent previously played D. Hence, recalling assumption (ii),  $(1 - \varepsilon, 1 - \varepsilon)$  is as

	AllC	AllD	TFT	$\gamma$ TFT
AllC	$R$	$S$	$R$	$R$
AllD	$T$	$P$	$P$	$\gamma T + (1 - \gamma)P$
TFT	$R$	$P$	$\frac{1}{4}(R + S + T + P)$	$R$
$\delta$ TFT	$R$	$\delta S + (1 - \delta)P$	$R$	$R$

Table 5.1: Payoff table for the IPD in the limit of infinitely many rounds of the game where the limit  $\varepsilon \rightarrow 0$  has been taken.

close to AllC as it is possible to get;  $(\varepsilon, \varepsilon)$  is AllD,  $(1 - \varepsilon, \varepsilon)$  is TFT, and  $(1 - \varepsilon, \gamma)$  is  $\gamma$ TFT, a more generous Tit-For-Tat that forgives a defection with probability  $\gamma \in (\varepsilon, 1 - \varepsilon)$ . The game payoff to strategy  $E = (p, q)$  when playing  $E' = (p', q')$  is then (Nowak's equation (3)):

$$A(E, E') = Rss' + Ss(1 - s') + T(1 - s)s' + P(1 - s)(1 - s')$$

where  $s$  is the limit ( $n \rightarrow \infty$ ) of the probability of strategy  $E$  playing C in  $n$ th round against  $E'$ , given by

$$s = s(E, E') = \frac{q'(p - q) + q}{1 - (p - q)(p' - q')}$$

and  $s'$  similarly by

$$s' = s'(E', E) = \frac{q(p' - q') + q'}{1 - (p - q)(p' - q')}$$

Table (5.1) shows the application of these formulae when the four strategies listed above meet each other. The limit  $\varepsilon \rightarrow 0$  has been taken after the calculation of  $A$  for each pair, so the case of minimal noise or error is considered. Table (5.2) is the same matrix, but with payoffs given to first order in  $\varepsilon$  (*i.e.* without the limit  $\varepsilon \rightarrow 0$ ) and evaluated in the commonly studied case of  $T = 5, R = 3, P = 1$  and  $S = 0$ . Stochastic strategies - or a little noise - can have a dramatic effect on the long term outcome: Notice that TFT, the winning strategy in Axelrod's original computer tournament, loses much of it's attraction here as it's effectiveness is reduced to that of a random player when playing against itself. By calculating expected payoffs, Molander (1985) discovered that a level of unconditional generosity is preferred for TFT-like strategies in such a noisy environment to avoid becoming trapped in ruts of perpetual recrimination. For  $T = 5, R = 3, P = 1, S = 0$ , the expected payoff is maximised by forgiving a defection with probability  $1/3$  (the strategy  $\frac{1}{3}$ -TFT). Nowak and Sigmund (1992) found the same result from simulations of a non-spatial IPD population.

	AllC	AllD	TFT	$\gamma$ TFT
AllC	$3 - \varepsilon$	$4\varepsilon$	$3 - 4\varepsilon$	$3 + (3\gamma - 4)\varepsilon$
AllD	$5 - 6\varepsilon$	$1 + 3\varepsilon$	$1 + 7\varepsilon$	$1 + 4\gamma + (3 - 5\gamma)\varepsilon$
TFT	$3 + \varepsilon$	$1 + 2\varepsilon$	$\frac{9}{4}$	$3 + \frac{3\gamma - 2}{\gamma}\varepsilon$
$\delta$ TFT	$3 + (1 - 2\delta)\varepsilon$	$(1 - \delta) + 3\varepsilon$	$3 - \frac{2 + 2\delta}{\delta}\varepsilon$	$3 + \frac{2 - 3\gamma + 2\delta}{\gamma\delta - \gamma - \delta}\varepsilon$

Table 5.2: Payoff table for the IPD in the case of many rounds of the game, to order  $O(\varepsilon^2)$  in the case  $T = 5, R = 3, P = 1$  and  $S = 0$ . For convenience, only  $\delta$ TFT is listed vertically, and only  $\gamma$ TFT horizontally. Note that the payoff of  $\gamma$ TFT against itself simplifies to  $3 - \varepsilon/\delta$ .

### 5.1.3 A Spatial Environment

Our interest in the IPD is in the effect of embedding the players in a non-trivial spatial environment. Other authors have also studied this problem. Grim (1995) used precisely Nowak's calculations in a study of the IPD on a square lattice, where each individual plays the game against its four neighbours and sites on the grid are invaded by the neighbouring site with the highest score (if this is greater than the central site's score). This scheme is a close parallel of the explicit lattice spatial game of Chapter 2, differing only in its synchronous updating rule (all sites together) and deterministic nature (higher fitness sites always invade, as opposed to having a higher potential invasion rate). Grim simulated the system on a computer by allowing a subset of 121 distinct strategies to interact (occasionally randomly introducing new strategies to replace extinct ones) and observing the long-term winners. He effectively chose a value of  $\varepsilon = 0.01$  and considered the strategies  $(p, q)$  with  $p, q \in \{0.01, 0.1, 0.2, \dots, 0.9, 0.99\}$ . The payoffs were the commonly used ones of  $T = 5, R = 3, P = 1$  and  $S = 0$ . He found that generous TFT strategies were invariably the most successful in the long-run, with  $(0.99, 0.4), (0.99, 0.5)$  and  $(0.99, 0.6)$  the most common victors and that the results were insensitive to the value of  $\varepsilon$ . These are clearly more generous strategies than Molander's  $\frac{1}{3}$ -TFT, and the explanation put forward is that in a spatial environment, invasion by a single mutant individual is not as important a criterion; the behaviour in a local cluster is. In this sense, spatial structure promotes generosity.

Hsu, Hsu, Mortimer, Panju and Schroeder (1995) also simulated a spatial IPD contest on a square grid with  $T = 5, R = 3, P = 1$  and  $S = 0$ . However, they chose to explicitly calculate ten rounds of the PD per game, in the presence of stochastic errors. Also using a discrete set of opponent-reactive strategies, they observed the coexistence of several different strategies in patchy spatial domains.

Because, unlike Grim's, their work investigates only short and noisy IPD games, it does not relate to the payoff matrices in tables (5.1) and (5.2). But it does provide another reminder that there are many model variations for the IPD which can display different behaviour. Any conclusions must therefore be cautiously interpreted.

#### 5.1.4 IPD Pair Model

What results will a pair model realisation of the IPD predict for the level of generosity? The IPD payoff matrices in tables (5.1) and (5.2) were analysed using the spatial game pair model developed in Chapter 2. To recap, the whole IPD contest has been effectively reduced to another simple game itself, under the assumptions of a little noise and infinitely many rounds. If we assume a spatial structure like that in Chapter 2 *i.e.* a square grid with four neighbours per site, then the original pair approximation can be applied without modification, and we can compare results closely with the Grim model. (Equivalently, in the language of Chapter 4, we assume a spatial structure characterised by  $m = 4$  and  $\phi = 0$ , and we do not have to view the resulting model as an approximation of any other spatial model).

The original spatial game pair model was developed for contests between just two strategies. However, it is easy in principle (and not too difficult in practice) to write down similar sets of equations for contests between  $n$  different strategies. This was done for values of  $n$  up to  $n = 5$ . (The IPD is still played between pairs of players, but players can be drawn from  $n$  different types). In practice, the number of equations grows quickly, as  $(n - 1)(n + 2)/2$ , and the equations themselves become quite long. The case  $n = 3$ , for example, gives the following equations for  $(ii)$  and  $(ij)$  (compare with equation (3.16)) with similar ones for  $(ik)$ ,  $(jj)$ ,  $(jk)$  and  $(kk)$ . The payoff matrix is denoted by  $A = (A_{\alpha\beta})$  where  $\alpha, \beta \in \{i, j, k\}$  and  $A_{ij}$  is the payoff to species  $i$  when playing species  $j$ . The system is closed using the multinomial assumption for  $\overline{Q}^\sigma$  described in Chapter 3.

$$\begin{aligned}
(ii) = & 2(ij) \left[ A_{ii}\overline{Q}^\sigma(i|ij) + A_{ij}\overline{Q}^\sigma(j|ij) + A_{ik}\overline{Q}^\sigma(k|ij) \right] \overline{Q}^\sigma(i|ji) \\
& - 2(ij) \left[ A_{ji}\overline{Q}^\sigma(i|ji) + A_{jj}\overline{Q}^\sigma(j|ji) + A_{jk}\overline{Q}^\sigma(k|ji) \right] \overline{Q}^\sigma(i|ij) \\
& + 2(ik) \left[ A_{ii}\overline{Q}^\sigma(i|ik) + A_{ij}\overline{Q}^\sigma(j|ik) + A_{ik}\overline{Q}^\sigma(k|ik) \right] \overline{Q}^\sigma(i|ki) \\
& - 2(ik) \left[ A_{ki}\overline{Q}^\sigma(i|ki) + A_{kj}\overline{Q}^\sigma(j|ki) + A_{kk}\overline{Q}^\sigma(k|ki) \right] \overline{Q}^\sigma(i|ik)
\end{aligned} \tag{5.1}$$

$$\begin{aligned}
(ij) = & (ij) \left[ A_{ii}\overline{Q}^\sigma(i|ij) + A_{ij}\overline{Q}^\sigma(j|ij) + A_{ik}\overline{Q}^\sigma(k|ij) \right] \left[ \overline{Q}^\sigma(j|ji) - \overline{Q}^\sigma(i|ji) \right] \\
& + (ij) \left[ A_{ji}\overline{Q}^\sigma(i|ji) + A_{jj}\overline{Q}^\sigma(j|ji) + A_{jk}\overline{Q}^\sigma(k|ji) \right] \left[ \overline{Q}^\sigma(i|ij) - \overline{Q}^\sigma(j|ji) \right] \\
& + (ik) \left[ A_{ii}\overline{Q}^\sigma(i|ik) + A_{ij}\overline{Q}^\sigma(j|ik) + A_{ik}\overline{Q}^\sigma(k|ik) \right] \overline{Q}^\sigma(j|ki) \\
& - (ik) \left[ A_{ki}\overline{Q}^\sigma(i|ki) + A_{kj}\overline{Q}^\sigma(j|ki) + A_{kk}\overline{Q}^\sigma(k|ki) \right] \overline{Q}^\sigma(j|ik)
\end{aligned}$$



$$\begin{aligned}
& +(jk) \left[ A_{ji} \overline{Q}^\sigma(i|jk) + A_{jj} \overline{Q}^\sigma(j|jk) + A_{jk} \overline{Q}^\sigma(k|jk) \right] \overline{Q}^\sigma(i|kj) \\
& -(jk) \left[ A_{ki} \overline{Q}^\sigma(i|kj) + A_{kj} \overline{Q}^\sigma(j|kj) + A_{kk} \overline{Q}^\sigma(k|kj) \right] \overline{Q}^\sigma(i|jk)
\end{aligned}$$

The origin of each term can be attributed to particular invasions. For example, the first line of the (ii) equation results from invasion of  $j$  sites by  $i$  neighbours, the second line is invasions of an  $i$  by a  $j$ , the third is invasions of a  $k$  by an  $i$ , and the fourth is invasions of an  $i$  by a  $k$ . There is no term associated with the invasions of a  $j$  by a  $k$ , or vice versa, because neither changes the number of  $i$ - $i$  pairs.

Various combinations of 2, 3, 4 and 5 species IPD contests were simulated using the IPD pair equations. Attention was focused on the set of stochastic strategies incorporating AllC, AllD, TFT and  $\gamma$ TFT (with a range of values for  $\gamma$ ). For simplicity, and ease of comparison, again only the case  $T = 5, R = 3, P = 1, S = 0$  was considered (payoff matrix table (5.2)) with small values chosen for  $\varepsilon$ .

#### 5.1.4.1 Two Species IPD Contests

For the case  $n = 2$  the equilibrium stability results of Chapter 2 are available and we can investigate the games analytically. Within our chosen strategy set, there are seven essentially distinct pairs of strategies to consider, and the fate of each pair in isolation can be calculated using the  $\alpha$  and  $\beta$  of Chapter 2 (note that  $\alpha = A_{11} - A_{12}$  and  $\beta = A_{22} - A_{21}$  in the current notation).

Recall figure (2.7) and section (2.6.1) from Chapter 2. We need to know which region of the  $(\alpha, \beta)$  plane our particular contest falls into. Broadly, each of the four quadrants displays a different behaviour, although the positive ( $\alpha > 0, \beta > 0$ ) and negative ( $\alpha < 0, \beta < 0$ ) quadrants are further divided as a function of the number of neighbours,  $m$ , by equations (2.19) and (2.20). As far as the dynamics are concerned, these divisions can be thought of as effectively tilting the  $\alpha$  and  $\beta$  axes, so the dynamical regions represented by the positive and negative quadrants are reduced in size, and those of the other two quadrants are enlarged. If we assume sufficiently small values of  $\varepsilon$ , and ignore at first the complications imposed by equations (2.19) and (2.20) (so we concentrate only on the four phase space quadrants) the following results are expected:

- i. **AllC vs AllD** - AllD eliminates AllC.
- ii. **AllC vs TFT** - stable coexistence of both strategies.
- iii. **AllC vs  $\gamma$ TFT** -  $\gamma$ TFT eliminates AllC when  $\gamma > 1/3$ ; stable coexistence when  $\gamma < 1/3$ .
- iv. **AllD vs TFT** - unstable coexistence of both strategies.
- v. **AllD vs  $\gamma$ TFT** - AllD eliminates  $\gamma$ TFT if  $\gamma > 1/2$ ; unstable coexistence when  $\gamma < 1/2$ .
- vi. **TFT vs  $\gamma$ TFT** -  $\gamma$ TFT eliminates TFT if  $\gamma < 1/3$ ; stable coexistence when  $\gamma > 1/3$ .

- vii.  $\gamma$ **TFT** vs  $\delta$ **TFT** - stable coexistence if  $\gamma < 1/3$  and  $\delta > 1/3$ , or  $\gamma > 1/3$  and  $\delta < 1/3$ ; otherwise, the strategy with parameter ( $\gamma$  or  $\delta$ ) closer to  $1/3$  eliminates the other.

When the effect of equations (2.19) and (2.20) are incorporated, the regions of coexistence (either stable or unstable) are made smaller, so some of the strategy pairs listed as coexisting will find themselves in a region where one excludes the other. The larger the value of  $m$ , the larger are the domains of coexistence, and the above results will be approached exactly as  $m \rightarrow \infty$ . As an example, consider AllC and TFT which, from equation (2.20), only coexist whenever

$$-2(m-1)\varepsilon \leq -\frac{3}{4} \leq -\frac{2\varepsilon}{(m-1)}$$

therefore unless  $m \geq 1 + 3/(8\varepsilon)$ , one strategy (AllC) will eliminate the other. In practice, with a low noise level ( $\varepsilon$ ), this puts as a significant constraint the minimum value of  $m$  which will allow TFT and AllC to coexist. Put another way, we can say that AllC is likely to eliminate TFT in a spatial environment with a limited number of neighbourly interactions.

For the cases when the coexistence of two species is unstable, almost all initial conditions result in the elimination of one species by the other. Which player dominates is determined by the initial conditions and by the game parameters. If equation (2.19) holds then monocultures of both species are stable, and phase space is split into two basins of attraction. Otherwise, one species will dominate from all initial conditions. With the contest between AllD and TFT, for example, equation (2.19) shows that TFT dominates for  $\varepsilon < \varepsilon_l$ . When  $\varepsilon_l < \varepsilon < \varepsilon_u$ , either TFT or AllD dominates, and for  $\varepsilon > \varepsilon_u$ , AllD always dominates. Both  $\varepsilon_l$  and  $\varepsilon_u$  are functions of  $m$ , and are approximately 0.13 and 0.17 respectively when  $m = 4$ . Increasing  $m$  decreases  $\varepsilon_l$  and increases  $\varepsilon_u$ , therefore enlarging the region where both monocultures are stable.

#### 5.1.4.2 More than Two Species IPD Contests

Many three species contests were also investigated numerically (equations (5.1)). Not surprisingly, these typically displayed more interesting dynamics than two species contests (the resulting ODE system has dimension 5 compared to dimension 2) although none was found to have quasiperiodic or chaotic dynamics. Unfortunately, stability analysis of the kind performed in the two species system was not successfully obtained. However, it often appeared that characteristics of the constituent two species contests could be seen in the three species system behaviour. Two particular three strategy combinations are described below.

**TFT, AllD and AllC.** These three strategies together display oscillations, with repetitions of AllD invading AllC, TFT invading AllD and AllC invading TFT (the last invasion owes much to the presence of noise and TFT's reduced payoff against itself in this case). For low noise, (*e.g.*  $\varepsilon = 0.01$ ), the oscillations continually grow, until the populations swing to such small numbers that, because of the

continuity assumption, the pair model becomes unreasonable. For larger noise, (*e.g.*  $\varepsilon = 0.1$ ), the oscillations are damped and all three species eventually coexist in equilibrium. (A value of  $m = 4$  was chosen throughout).

**AllD, TFT and  $\gamma$ TFT.** Providing  $\gamma > \gamma^* \approx 0.45$  these strategies also oscillate (at the chosen values of  $m = 4$  and  $\varepsilon = 0.01$ ) and the oscillations again grow more violent with time. If  $\gamma < \gamma^*$ , then  $\gamma$ TFT dominates and the other two are eliminated. A heuristic explanation of this behaviour can be derived by considering the behaviour of the constituent two species systems. Consider the unstable coexistence in the AllD vs  $\gamma$ TFT contest. Lower and upper bounds ( $\gamma_l$  and  $\gamma_u$ ) on the value of  $\gamma$  for which both AllD and  $\gamma$ TFT can coexist are obtained by evaluating equation (2.19) at  $m = 4$  and  $\varepsilon = 0.01$ . To first order in  $\varepsilon$ , these are  $\gamma_l \approx 0.29$  and  $\gamma_u \approx 0.46$ . AllD eliminates  $\gamma$ TFT in the two species contest when  $\gamma > \gamma_u$ . Notice that  $\gamma^* \approx \gamma_u$  and therefore whenever AllD eliminates  $\gamma$ TFT in the two species contest, oscillations exist in the three species contest. A possible explanation for the three species contest could be that when  $\gamma > \gamma^*$ , AllD all but eliminates  $\gamma$ TFT, leaving itself open to invasion by TFT ( $\varepsilon = 0.01 < \varepsilon_l$  above) which is then itself joined or defeated by  $\gamma$ TFT, and the cycle repeats. However, when conditions in the two species contest allow AllD and  $\gamma$ TFT to naturally coexist, the three species contest includes TFT which can invade the AllD strategists. TFT then gets invaded by  $\gamma$ TFT, and the dynamics then stop because AllD can no longer eliminate  $\gamma$ TFT. Figure (5.1) shows these two cases graphically.

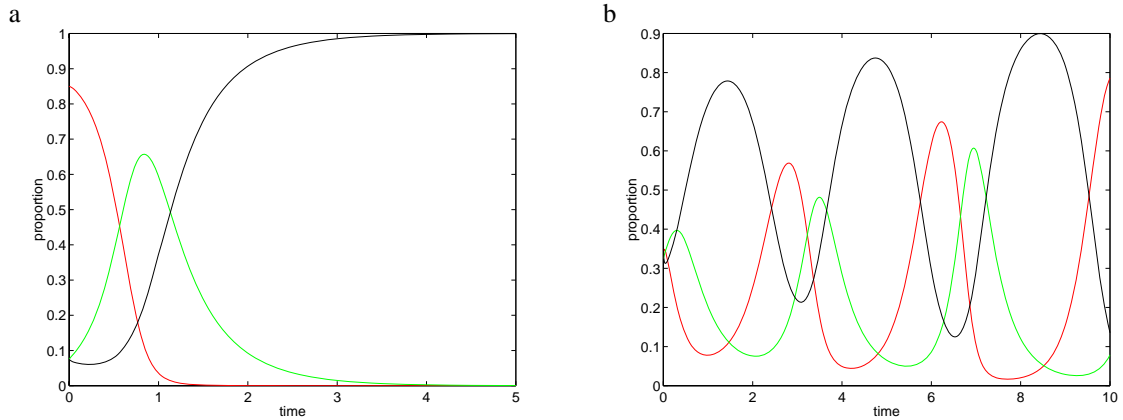


Figure 5.1: IPD pair model for AllD (red), TFT (green) and  $\gamma$ TFT (black). a) is  $\gamma = 0.4 < \gamma^*$  where  $\gamma$ TFT dominates. b) shows the build up of oscillations at  $\gamma = 0.5 > \gamma^*$ : AllD invades  $\gamma$ TFT, TFT invades AllD, and  $\gamma$ TFT invades TFT. Both graphs use  $m = 4$  and  $\varepsilon = 0.01$ .

Several four and five species contests were also numerically studied, and none behaved in a way which appeared inconsistent with their constituent two species sub-systems. As with the three species equations, there were no complex (chaotic or quasiperiodic) dynamics. For comparison with

the other IPD pair models, and the explicit space model studied by Grim (1995), a value of  $m = 4$  was kept throughout, but a range of  $\varepsilon$  was investigated. The results were qualitatively insensitive to sufficiently small values of  $\varepsilon$ , and a value of  $\varepsilon = 0.01$  was typically chosen.

Intensive investigations were focused on trying to identify strategies that were successful, in the long run, against a variety of opponents. In particular, a range of different  $\gamma$ TFT strategies were included for  $\gamma \in (\varepsilon, 1 - \varepsilon)$ , in competition with other  $\gamma$ TFT strategies and others (AllD, AllC, TFT) too. Figure (5.2) shows the evolution of population densities for one of the five species IPD pair models studied.

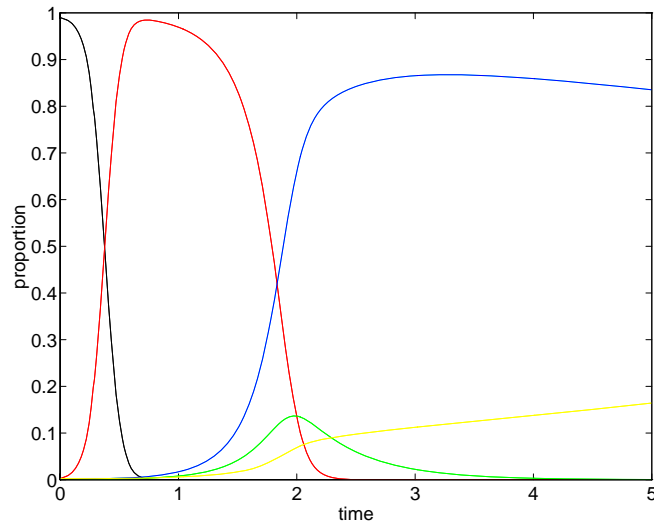


Figure 5.2: IPD pair model for AllC (black), AllD (red), TFT (green), 0.1-TFT (blue) and 0.2-TFT (yellow). The initial condition is 99% AllC and 0.25% of the other four strategies, each isolated with connections only to AllC players. AllD is initially successful at displacing AllC but is then itself displaced by the more cooperative strategies. In the long term (not shown), 0.2-TFT finally dominates all other strategies. This result is qualitatively unchanged by reducing the error rate to  $\varepsilon = 0.001$ .

Because of the large number of potential combinations of strategies, and the unavailability of analytical results, it was not possible to study in detail all possible configurations; findings are therefore only suggestive, not conclusive. Nevertheless, on the whole, the most successful strategies found (against a range of opponents) were those  $\gamma$ TFT strategies with levels of generosity close to  $\gamma = \frac{1}{3}$ .

This result is in contrast to Grim's findings - that more generous strategies performed better - and as such is a little disappointing if the aim was to capture any spatial structure responsible for his

conclusions. However, the result is in general agreement with the list of two player behaviours given previously. Furthermore, it is also in agreement with other non-spatial analysis: The generosity level of  $1/3$  can be derived (Molander, 1985) by optimising fitness using only the IPD game payoff matrix without any reference to dynamical equations, and hence without any reference to the spatial structure of the environment.

The success of more generous  $\gamma$ TFT strategies in Grim's (1995) model, compared to  $\frac{1}{3}$ TFT in non-spatial models and the above pair model IPD requires explanation. It could be attributed to the effect of large scale spatial correlations, but a more likely reason is to be found in the details of the invasion rule, because the pair model was previously found to be a good approximation to the explicit spatial game CA (Chapter 2). Recall that Grim's contestants only invade neighbouring sites if they have a higher fitness. In the pair model, the rule is that the invasion rate is proportional to fitness, so lower scoring individuals can invade, albeit at a lower rate. This difference will be important in the initial stages of invasion when one species is present only in very small densities. Take for example TFT and AllD. An isolated TFT player will have a lower fitness than every other player in a sea of AllD. Under Grim's rule, it would quickly be invaded and a TFT invasion could not take place. In the pair model, however, the equations capture the fact that isolated TFT players will invade their neighbouring AllD opponents, but at a lower rate than they are themselves invaded. Nevertheless, once some TFT have won local battles, small clusters of TFT will result. These clustered TFT players will (with suitable parameters) have higher fitness than the neighbouring AllD because of the benefit derived from their neighbouring conspecifics. TFT patches can then eliminate AllD. (A similar argument holds for non-spatial models that do not identify individuals, but for slightly different reasons. Even when TFT is present in low density, a TFT playing against the average population will play against some other TFT players (there is no concept of an isolated TFT player in non-spatial models). Parameters depending, this may also give TFT the advantage over a sea of AllD).

## 5.2 Other Spatial Games

Further three, four and five species spatial games were also studied using the pair model equations of the previous section. However, instead of IPD derived payoff matrices, a range of arbitrarily chosen matrices was explored in order to investigate (at least superficially) the potential range of behaviours that such models could exhibit. In practice, no substantially different behaviour was found in comparison to the studied IPD matrices. Although we cannot say that more exotic behaviour (quasiperiodic or chaotic) will never be found in these models, the indication is that it is at best rare.

Figure (5.3) shows a representative sample of the behaviour displayed for a general three species

game. The payoff matrices used here were

$$\begin{array}{llll} \text{a.} & \begin{pmatrix} 0 & 1 & 0 \\ 0 & 0 & 1 \\ 1 & 0 & 0 \end{pmatrix} & \text{b.} & \begin{pmatrix} 0 & 5 & 5 \\ 0 & 6 & 0 \\ 0 & 0 & 6 \end{pmatrix} & \text{c.} & \begin{pmatrix} 0 & 4 & 0 \\ 1 & 1 & 1 \\ 0 & 0 & 0.8 \end{pmatrix} & \text{d.} & \begin{pmatrix} 0 & 5 & 0 \\ 1 & 1 & 1 \\ 0 & 0 & 0.8 \end{pmatrix} \end{array}$$

### 5.3 Predator-Prey Systems

Predator-Prey systems, ubiquitous in biology, are an important class of systems which we now consider. In comparison to the pair models covered so far, predator-prey systems are particularly interesting because we can no longer realistically assume a constant population size. This complicates matters considerably and introduces a number of choices. Pair models will be developed by extending the very general, but non-spatial, Lotka-Volterra equations of section (1.6).

With a two species predator-prey system there are four basic events which can occur: birth of a predator, birth of prey, death of predator and death of prey. There are many potential factors which could bring about the death of a prey individual in addition to predation (starvation, disease or old age, for example). From this modelling perspective, however, it will be assumed that all prey death is due to predation, as is implicitly the case in the Lotka-Volterra equations. Similarly, all predator death not attributable to starvation or ‘natural causes’ will be ignored. Furthermore, all birth is assumed to be asexual. Predators are denoted by the letter  $P$ , and prey (victims) by  $V$ .

The spatially important events are those associated with predation, for which the close contact of predator and prey (*i.e.* the  $V$ - $P$  connections) is essential. (For a broad discussion on the interpretation of what constitutes a  $V$ - $P$  connection, see Chapter 7. For now, we assume that a predator and prey being neighbours is synonymous with the prey being within striking distance of the prey). At the very abstract level, the same kind of interaction also plays a fundamental role in host-parasite systems and infectious disease systems (which are considered in Chapter 6): Predators correspond to parasitised or infectious individuals, and prey are the uninfected, susceptible hosts. In basic models, host-parasite systems are essentially a special case of predator-prey systems for which there is a one to one conversion rate from prey (healthy host) to predator (parasitised host). This is rarely the case in a true predator-prey system because one meal does not usually equate to one offspring. Of course many modifications, reflecting particular details of a system, can be introduced to differentiate between these broad classes of models.

As with previous pair analysis, the nature of the spatial structure represented by a pair model requires careful consideration. In this respect, pair models here will not be treated as approximations to other explicitly spatial models, but as alternative representations of space, in the sense of Chapter 4. Two very different approaches to the pair modelling of a general predator-prey system can be

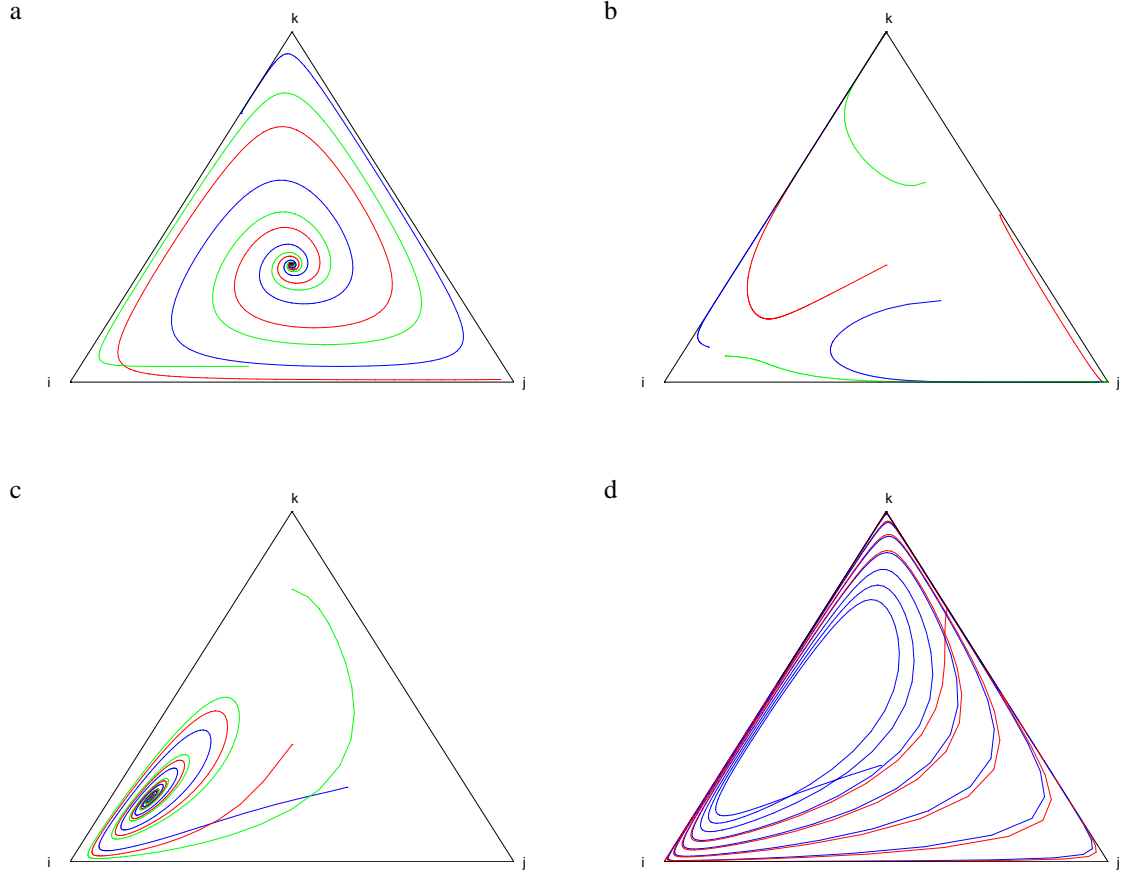


Figure 5.3: Pair model trajectories for various three species games. The five dimensional ODE trajectories have been transformed onto the surface  $(i) + (j) + (k) = N$  (viewed from above). Trajectories close to the  $i$  vertex therefore represent populations composed mainly of species  $i$ , and similarly for the  $j$  and  $k$  vertices. Because this is a projection of phase space, trajectories can appear to cross each other. a) and c) show spiraling attraction to an equilibrium, b) shows multiple domains of attraction, with some trajectories falling into the all  $j$  population and others into all  $k$ . Finally, d) is ever-growing oscillations which spiral out towards the boundaries. Eventually, very small numbers will inevitably arise and the validity of the model (and continuity assumption) must be questioned. For payoff matrices, see text.

distinguished and are detailed below.

### 5.3.1 Variable Population Pair Model

This approach treats just the two species (predators and prey) directly. All events are assumed to occur at uniform rates (section (1.8.1)) with times picked from an exponential distribution. The four basic events, with corresponding rates and their effect on spatial connections are then described as follows.

**Prey Birth** Each prey individual produces an offspring at a rate  $b_V$ , independent of its local spatial environment. The offspring immediately forms connections to a subset of the whole predator and prey population. This subset typically depends on the local spatial structure.

**Prey Death** Predators kill neighbouring prey individuals at a rate  $d_V$  per  $V$ - $P$  contact. On death, all connections to neighbouring individuals are broken.

**Predator Birth** Predators give birth to more predators, simultaneously killing a neighbouring prey, at a rate  $b_P$  per  $V$ - $P$  contact. As with prey birth, new individuals neighbour a subset of the rest of the population. The prey connections are removed.

**Predator Death** Predators die at a rate  $d_P$  and all neighbouring connections are broken accordingly.

Note the similarity between a prey death event and a predator birth event. Essentially, the latter is just a predation event that is accompanied by the birth of a new predator. The motivation for this, as with the original Lotka-Volterra equations, is that predators need food to survive and reproduce. If  $d_V = 0$ , then one new predator is born for every prey killed (*c.f.* the host-parasite analogy). If  $d_V > 0$ , then only some prey kills are accompanied by the birth of a new predator. Of course alternative hypotheses are available, but this one is used because of its similarity to the original non-spatial assumptions.

Apart from the closure considerations, all that remains to be done before the equations can be written down is to specify the subset of the population to which the newborn predators and prey connect. There are many realistic possibilities for this. For example, connection could be made just to the parent individual, or to the parent's neighbours, or to a random sample of the whole population, or even to a combination of these. The choice will largely depend on the interpretation of the spatial environment, and this in turn will reflect the nature of the predator-prey system itself. Of course, for an abstract system (such as this) we are free to use any particular rule. If we denote by  $f_x(i)$  the number of species  $i$  individuals an offspring (either predator or prey) born to a parent at location  $x$  neighbours, then the pair equations become



$$\begin{aligned}
(\dot{V}) &= \sum_{(V)} b_V - \sum_{(VP)} (d_V + b_P) \\
(\dot{P}) &= \sum_{(VP)} b_P - \sum_{(P)} d_P \\
(\dot{VV}) &= \sum_{(V)} 2b_V f_x(V) - \sum_{(VP)} 2(d_V + b_P)Q_x(V) \\
(\dot{PP}) &= \sum_{(PV)} 2b_P f_x(P) - \sum_{(P)} 2d_P Q_x(P) \\
(\dot{VP}) &= \sum_{(V)} b_V f_x(P) - \sum_{(P)} d_P Q_x(V) + \sum_{(VP)} b_P f_y(V) - b_P Q_x(P) - d_V Q_x(P)
\end{aligned} \tag{5.2}$$

Notice that we must now explicitly include the equations for  $(V)$  and  $(P)$  because there is no direct relation between the number of individuals and the number of connections. Numerical investigations were performed with the following form for  $f$ . It assumes each offspring (predator or prey) neighbours its parent, a fraction  $\phi$  of its parent's neighbours (predators and prey), and a fraction  $\xi$  of the rest of the population (also predators and prey, picked at random). Recalling that  $\sigma(x)$  is the species at site  $x$ , we can write

$$f_x(i) = \begin{cases} 1 + \phi Q_x(i) + \xi(i) & \text{if } \sigma(x) = i \\ \phi Q_x(i) + \xi(i) & \text{if } \sigma(x) \neq i \end{cases} \tag{5.3}$$

Combining equations (5.2) and (5.3) leads to the following system:

$$\begin{aligned}
(\dot{V}) &= b_V(V) - (d_V + b_P)(VP) \\
(\dot{P}) &= b_P(VP) - d_P(P) \\
(\dot{VV}) &= 2b_V[\phi(VV) + (V)] - 2(d_V + b_P)(VVP) + 2b_V\xi(V)^2 \\
(\dot{PP}) &= 2b_P[\phi(VPP) + (VP)] - 2d_P(PP) + 2b_P\xi(P)(VP) \\
(\dot{VP}) &= [\phi(b_V + b_P) - d_V - b_P - d_P](VP) + \phi b_P(VPV) - (d_V + b_P)(PVP) \\
&\quad + b_V\xi(V)(P) + b_P\xi(V)(VP)
\end{aligned} \tag{5.4}$$

We can close these equations using equation (4.14), leaving the two parameters  $\phi$  and  $m$  with which to describe the nature of space. Note that  $\phi$  has already been introduced in  $f_x(i)$  as the fraction of contacts an offspring has with its parent's neighbours. This is consistent with the closure assumption that  $\phi$  is the relative proportion of triangles to triples. Furthermore,  $m$ , the average number of neighbours per individual, can now be deduced because the total number of individuals  $(V) + (P)$  and the total number of connections  $(VV) + 2(VP) + (PP)$  are both known. So

$$m = \frac{(V) + (P)}{(VV) + 2(VP) + (PP)}$$

is therefore a dynamic variable, and no longer a constant parameter. In this model there are therefore six parameters to consider ( $b_V, b_P, d_V, d_P, \xi$  and  $\phi$ ) and a whole space of initial conditions.

Preliminary numerical investigations scratched the surface of this vast range of possibilities and revealed some reassuring behaviour. In general, it is easy to find both limit cycles and spiral sinks (in both cases where predators ‘chase’ prey) of a kind similar to those displayed by the non-spatial Lotka-Volterra equations and their close relatives. Figure (5.4) shows typical behaviour in a transect of phase space trajectories for the two parameter regimes listed in table (5.3). Note that the system is five dimensional, since each of the five variables in equations (5.4) is independent of the others.

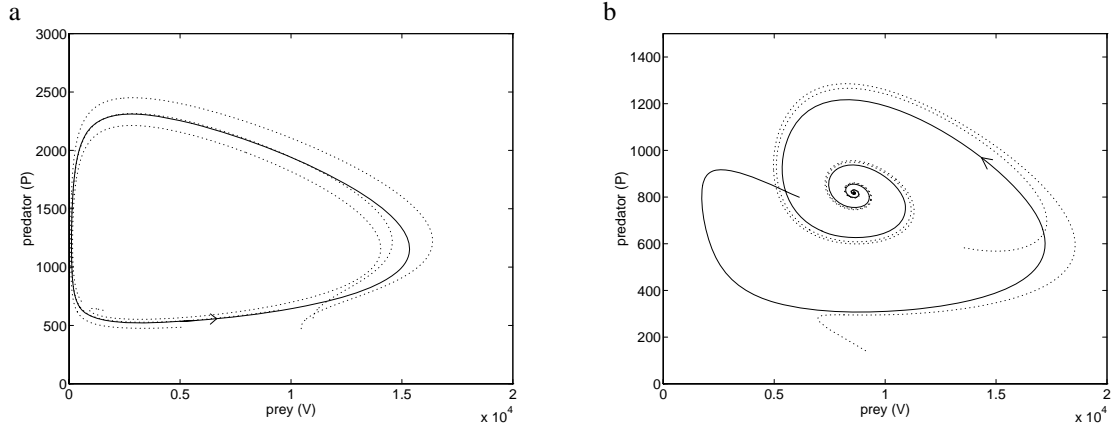


Figure 5.4: Phase space trajectories for the first two parameter regimes given in table (5.3). Several different initial conditions are illustrated (dotted lines) in each case. Note that phase space is five dimensional, so in a two dimensional projection onto the  $\{V, P\}$  plane, trajectories can cross. a) is a limit cycle and b) a spiral sink equilibrium point.

But this is not only possible behaviour. Simulating the model with  $\xi$  sufficiently close to zero quickly results in predator and prey populations isolated from each other (*i.e.*  $(VP) = 0$ ). Predators are then driven extinct, and the prey are left to grow (or die) without limit (system parameters depending - see table (5.3)).

It is easy to see how this can happen. The  $\xi$  terms control the degree of ‘mixing’ within the total population (at least insofar as newborn individuals are concerned). When little or none is allowed, the dynamically essential  $V$ - $P$  contacts are quickly used up through predation events, and because of the like-connects-to-like positive feedback created by offspring neighbouring their parent and their parent’s neighbours, they are not replenished fast enough. The resulting relative abundance of  $V$ - $V$  and  $P$ - $P$  contacts represents certain starvation for the predators. In a real spatial system, the equivalent scenario is of isolated pockets of prey which the predators are unable to find.

As with the non-spatial Lotka-Volterra equations, there are many possible modifications which could help to ‘fix’ this situation. For example, we could introduce a global density dependence to dampen

$b_P$	$b_V$	$d_P$	$d_V$	$\phi$	$\xi$	dynamics
Without Density Dependence						
0.05	0.85	0.1	1.0	0.38	0.001	limit cycle
0.05	0.2	0.1	1.0	0.2	0.001	coexistence equilibrium
0.01	0.01	0.1	1.0	0.2	0.0001	predator extinction
With Density Dependence						
0.05	1.6	0.05	1.0	0.49	0.001	limit cycle
0.05	2.0	0.1	0.5	0.3	0.001	coexistence equilibrium
0.05	2.0	0.5	0.5	0.1	0.001	predator extinction

Table 5.3: Example parameter values used in the variable population Lotka-Volterra pair model with the resulting long term dynamical behaviour. The first three sets use equations (5.4) directly (no density dependence) and the last three are for the density dependent prey growth modification (equation (5.5)) with a carrying capacity value of  $K = 10000$ . Dynamics are either a limit cycle, a fixed point with predator and prey coexisting, or extinction of the predators. In this latter case, the prey population grows (exponentially) indefinitely when there is no density dependent growth, but is bounded above by  $K$  when a density dependent birth rate is used.

the prey birth rate (see table (5.3)):

$$b_V \rightarrow b_V \left(1 - \frac{(V)}{K}\right) \quad (5.5)$$

Alternatively, we could insist that each new born predator acquires contacts with the neighbours of a (nearby) prey individual instead of those of its parent. Whether or not an option is plausible depends crucially on the real predator-prey system being studied, and there are many kinds to chose from. It is beyond the scope of this thesis to study any particular real system. Nevertheless, numerical investigations of these (and other) variants of equation (5.4) in practice did not reveal any qualitatively different behaviour from that in the cases already described (*i.e.* limit cycles, stable coexistence and extinctions).

The intrinsically variable nature of  $m$  in this model is an area of concern. Physically, we require that  $0 \leq m \leq N^2 - 1$  where  $N = (V) + (P)$  is the total population. This represents the extreme of a totally disconnected population right through to a thoroughly mixed one. There is no reason why  $m$ , being the average number of neighbours per individual, should not fall to a value below one. However, this presents a problem for equation (4.14) which was derived from the assumption of a constant number of neighbours per individual: The triple estimate becomes unphysical (negative). For the trajectories in figure (5.4),  $m$  was observed to be greater than one at all times, but no guarantee was found that this would always be the case. This is a potentially serious problem for the variable population pair model, and one which the alternative approach that follows does not suffer from.

### 5.3.2 Empty Site Pair Model

The empty site model is a neat method of formulating and interpreting a pair model that represents the variable population predator-prey interactions. It naturally incorporates a local birth rule for both species (eliminating the need to postulate a version of equation (5.3)) which is a density-dependent rule in the case of the prey population.

The trick is to consider three species - predators ( $p$ ), prey ( $v$ ), and empty sites ( $x$ ) - as a virtual population of a constant size  $N = (p) + (v) + (x)$  instead of two species with a variable total population. Dynamically, we still consider the same four events (prey birth, prey death, predator birth and predator death) as seen in the variable population pair model. These events occur at the same rates as previously, with the exception of prey birth which is complicated by the density dependence requirement of finding a neighbouring empty site ( $x$ ) to the parent into which a prey offspring must be placed: Prey birth into an empty site is therefore at a rate proportional to the number of potential parent prey that neighbour it, and the constant of proportionality is  $b_v$ . This assumption fits predator-prey systems in which offspring stay in close contact with their parents. The event set is summarised in figure (5.5).

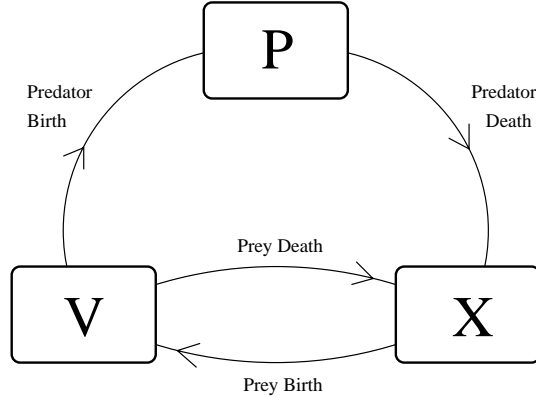


Figure 5.5: Schematic diagram for the empty-site predator prey pair model. Individuals are moved between the three classes of predator (P), prey (V) and empty sites (X) according to the four events shown. The total population size is conserved but the physical population (predators plus prey) is free to vary.

In anticipation of the importance of some migration or mixing of the predator and prey populations, additional to that induced by their dynamic interactions, we introduce one further event. Assume both predators and prey drift randomly into neighbouring empty sites at a constant migration rate  $\xi$  per  $v$ - $x$  or  $p$ - $x$  contact. This form of migration, as desired, will only directly effect the density of pair correlations, and not the singles densities.

As for the variable population approach, this introduces one more parameter - the migration rate  $\xi$ , in addition to  $m$  and  $\phi$  from usual the closure assumption (equation (4.14)) - with which to adjust or describe the pair model's implicit spatial environment. We can think of  $\xi$  as either a property of the species or a property of the space itself. For simplicity, the same  $\xi$  is used for both predators and prey, but this clearly need not be the case.

Combining these five events produces the dynamical equations. Because we have reverted to the fixed population assumption ( $(v) + (p) + (x) = N$ , constant), we can, as with the spatial game examples, deduce single population densities  $(v)$ ,  $(p)$  and  $(x)$  from the pair totals:  $m(z) = (vz) + (pz) + (xz)$  for any  $z$ . The result is another five dimensional system to contrast with equations (5.4):

$$\begin{aligned}
(vv) &= 2b_v[(v xv) + (vx)] - 2d_v(vvp) - 2b_p(vvp) \\
&\quad + 2\xi[(v xv) + (vx) - (vvx)] \\
(vp) &= b_v(vxp) - d_v[(pvp) + (vp)] + b_p[(vvp) - (pvp) - (vp)] - d_p(vp) \\
&\quad + \xi[2(vxp) - (pvx) - (vpv)] \\
(vx) &= b_v[(vxx) - (v xv) - (vx)] + d_v[(vvp) - (pvx)] - b_p(pvx) + d_p(vp) \\
&\quad + \xi[(vxx) + (vvx) - (v xv) - (xvx) - 2(vx) + (vpv) - (vxp)] \\
(pp) &= 2b_p[(pvp) + (vp)] - 2d_p(pp) \\
&\quad + 2\xi[(pvp) + (vp) - (ppv)] \\
(px) &= -b_v(vxp) + d_v[(pvp) + (vp)] + b_p(pvx) + d_p[(pp) - (px)] \\
&\quad + \xi[(pvp) + (ppv) - (pvp) - (xpv) - 2(px) + (pvx) - (vxp)]
\end{aligned} \tag{5.6}$$

Numerical investigation of equations (5.6) was undertaken with ( $\xi > 0$ ) and without ( $\xi = 0$ ) migration. Space was described by equation (4.14) and initial parameter values of  $m = 10$  and  $\phi = 0$ . The relatively high value of  $m$  (in comparison to a square grid approximation) was chosen because of the expected influence of potentially ubiquitous empty sites and because  $m$  should be interpreted as the maximum number of real (*i.e.* non-empty site) neighbours any individual may possess. The minimal value for  $\phi$  represents minimal clumping within the population in the sense of Chapter 4.

In the case of  $\xi = 0$  the behaviour was found to be qualitatively similar to the mean-field Lotka-Volterra equations (1.11) when modified by a density-dependent prey birth rate, *e.g.*  $b_V \rightarrow b_V(N - V)$ : Trajectories typically either fell into a stable coexistence equilibrium or else predators were eliminated and the prey grew to the maximum possible size  $N$ . Increasing  $b_V$  or decreasing  $d_V$ , which increases the number of predators at equilibrium in the non-spatial model did the same in the pair model. Unlike the non-spatial case, however, the prey equilibrium was also decreased instead of remaining unaffected. (It is not surprising that the consequences of altering a parameter are more widespread in the more complex pair model). Increasing  $d_P$  or decreasing  $b_P$  similarly also increased the prey, and decreased the predator, equilibrium populations. Extinction of the predators was found with sufficiently large or small values here respectively. In all cases studied, the results were apparently unaffected by a range of different parameter sets and generic initial conditions, suggesting that this behaviour is robust and stable.

Increasing  $\phi$  upwards from zero always tended to reduce the number of predators and increase the prey in the simulations studied. Sufficiently large  $\phi$  had the effect of eliminating predators in a similar way to changing parameter values (*e.g.* decreasing  $b_V$ ) directly. This is consistent with the interpretation of  $\phi$  as a measure of the degree of spatial clumping within the population (Chapter 4) because predators need contact with prey to survive and reproduce, but prey can exist with or

without any contacts. Therefore in a clumped population, predators might quickly exhaust any local food supply (prey) and then experience difficulty finding more prey outside of their local cluster. By the same argument, increasing  $m$  alone should increase predator numbers by providing more contactable prey, and this was generally found to be the case.

By contrast, increasing the migration rate  $\xi$  away from zero appeared to have very little effect on the system's behaviour, either dynamically or on the final position of the equilibrium. This is not altogether surprising because we expect increased mixing to destroy pair correlations and force the model to behave more like its mean-field cousin. But since the pair model already displays mean-field like behaviour, little change is seen. Figure (5.6) shows typical results of varying  $\xi$  and  $\phi$  away from zero on the approach to and position of the equilibrium for the predator-prey pair model equations (5.6).

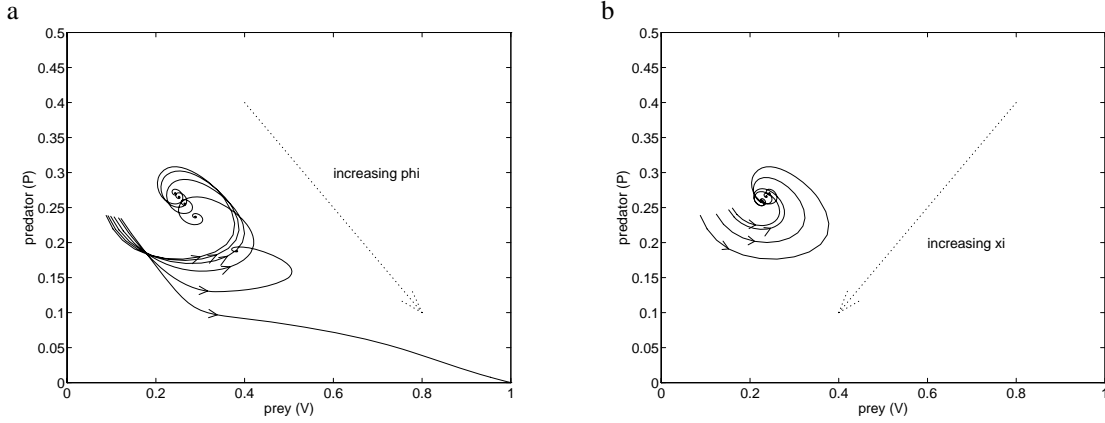


Figure 5.6: The typical effect of increasing the spatial clumping parameter  $\phi$  and the migration rate  $\xi$  on the equilibrium behaviour of the predator-prey-empty site pair model. Both figures were integrated numerically at parameter values  $b_P = 1.0, b_V = 1.0, d_V = 1.0, d_P = 2.0, m = 10$  and  $N = 1$  (which only effects the overall scaling) from identical initial conditions (a thoroughly mixed population with all pairs equally represented). Only the latter portion of each trajectory, approaching the equilibrium, is shown. a) represents increasing  $\phi$  over 0.0, 0.2, 0.4, 0.6, 0.8 and 0.9 for  $\xi = 0$ . The predator population gradually decreases until it can no longer be sustained by the prey, and it eventually becomes extinct (between  $\phi = 0.8$  and  $\phi = 0.9$ ). b) shows increasing  $\xi$  over 0, 1, 10 and 100 for  $\phi = 0$ . Different levels of migration have only a minimal effect on the system.

Although only a relatively small sample of parameter space could be explored, no exceptions were found to the general scheme outlined above when generic initial conditions were used. The only case discovered to have slightly different dynamics resulted from a highly unusual initial condition where

$(vp) = (vx) = (px) = 0$ . Simulations then predicted predator extinction and a prey equilibrium, but where the equilibrium prey density  $(v) < N$  *i.e.* space is not saturated with prey, even in the absence of predators. This result is best attributed to implicit ‘inaccessible’ empty space (the non-zero  $(xx)$ ) into which no offspring can be born (zero  $(xv)$ ) and which therefore must remain empty. Not even an increase in the migration rate  $\xi$  can help because migrants too find the space inaccessible. Interestingly, this spatial segregation effect was only observed for the initial condition  $(vp) = (vx) = (px) = 0$  and not for any other tested alternatives.

## 5.4 Discussion

In some respects, the IPD and predator-prey pair models described in this chapter have been disappointing because their behaviour has been rather similar to that of their non-spatial cousins. However, even negative results require interpretation, and the interpretation may be that space, as represented in these pair models, is not dynamically very important.

In the case of the IPD, the pair model studied did not predict the higher levels of generosity that have been suggested by some other spatial studies. Reasons why this may be the case were discussed. It is important to emphasize that this does not mean that pair analysis has failed, only that this particular implementation was not able to capture the essential requirements for more generous strategies to flourish. There are many other possible formulations of the IPD game rules and spatial structure assumptions from which alternative pair models could be generated, and such models may give different predictions. On the other hand, inability to promote generosity across a range of pair models would positively suggest that larger scale spatial structure is an important factor.

The predator-prey systems highlighted difficulties associated with migration and mortality events from the point of view of pair model analysis. These difficulties are not insurmountable (working models were derived), but the events do raise questions that do not exist in non-spatial analysis because they explicitly involve alterations to the underlying spatial structure. Again, in practice, this means that many alternative pair models, each associated with different assumptions, can readily be derived. Only the simplest cases were considered here. Both types of event are likely to be important in many other systems and Chapter 7 discusses the problem in more detail.

In summary, all the pair models examined did produce sensible output, which could be analysed at length to establish quantitatively the behavioural dependencies on the range of model parameters. Furthermore, there are more of these dependencies than in non-spatial models because of the extra parameters associated with spatial structure.



**6**

## **Infection Systems**

## 6.1 Introduction

This chapter constructs pair models which are based on a range of simple infection systems. As with the previous chapter's examples, the pair models so formed are derived using the general local spatial environment assumptions of Chapter 4, and they are therefore free-standing systems which are not linked to any other spatial models.

## 6.2 The Contact Process

The best place to start is with the contact process, the simplest, most abstracted infection system available (see section (1.4.1)). A fixed size population ( $N$ ) is composed of just two species, susceptible,  $S$ , and infected,  $I$ , and undergoes just two types of event:

**Infection** Infectious individuals infect neighbouring susceptibles at a uniform rate  $\beta$  per contact.

**Recovery** Infectious individuals recover from infection, and become susceptible again, at a uniform rate  $\nu$

As usual, the dynamical equations are derived by considering the effect of all possible events using equation (3.1). This familiar procedure is detailed once more here for clarity. For a suitable function,  $f$ , we have

$$\dot{f} = \sum_{(SI)} \beta \delta f(\text{infection}) + \sum_{(I)} \nu \delta f(\text{recovery})$$

Taking  $f = (S)$ , the number of susceptibles, and  $(I)$ , the number of infecteds, yields

$$\begin{aligned} (\dot{S}) &= \sum_{(SI)} \beta \times (-1) + \sum_{(I)} \nu \times (+1) \\ (\dot{I}) &= \sum_{(SI)} \beta \times (+1) + \sum_{(I)} \nu \times (-1) \end{aligned}$$

and similarly for the pairs  $(SS)$ ,  $(SI)$  and  $(II)$

$$\begin{aligned} (\dot{SS}) &= -2 \sum_{(SI)} \beta Q_x(S) + 2 \sum_{(I)} \nu Q_x(S) \\ (\dot{SI}) &= \sum_{(SI)} \beta [Q_x(S) - Q_x(I)] + \sum_{(I)} \nu [Q_x(I) - Q_x(S)] \\ (\dot{II}) &= 2 \sum_{(SI)} \beta Q_x(I) - 2 \sum_{(I)} \nu Q_x(I) \end{aligned}$$

Because we have assumed there are no contact making or breaking events, or any other form of mixing, we observe that the total number of pair connections remains constant, just as for previous spatial game examples. This implies a redundancy in the above five equations, and  $(I)$  and  $(II)$  can be eliminated using the relations

$$\begin{aligned} (S) + (I) &= N \\ (SS) + 2(SI) + (II) &= M \end{aligned}$$

where  $N$  is the total population size, and  $M$  the total number of connections. Using table (4.1) the equations for  $(S)$ ,  $(SS)$  and  $(SI)$  then simplify to

$$\begin{aligned}(\dot{S}) &= -\beta(SI) + \nu(I) \\(\dot{SS}) &= -2\beta(SSI) + 2\nu(SI) \\(\dot{SI}) &= \beta[(SSI) - (ISI) - (SI)] + \nu[(II) - (SI)]\end{aligned}\tag{6.1}$$

### 6.2.1 Spatial Structure

The interpretation and closure of equations (6.1) depends upon the approximation for triples  $(ijk)$ , which in turn depends upon assumptions about the spatial structure. Even though the contact process is a very simple model, we would like it to be as realistic as possible and certainly capable of extension to more detailed models for more realistic systems. Ultimately, one of the most important applications of such infection models (for us, at least) is to the epidemiology of infectious diseases affecting humans. Infections like measles, mumps and rubella are good examples of diseases whose transmission is governed by a network of social contacts, in contrast to those transmitted by other routes, (*e.g.* water borne cholera or mosquito carried malaria). Sexually Transmitted Diseases too are another good example of network transmission, although this time through a network of sexual partners, instead of social contacts.

Network based infection transmission in general, and social contact networks in particular are the focus of this chapter. In this case, however, a spatial arrangement like the square grid of earlier chapters is often really not a very realistic assumption. It is simply too restrictive and inflexible to be justified in many situations because social contacts rarely, if ever, resemble the structure of a regular square grid, even locally in the neighbourhood of an individual. It would be nice if the spatial assumptions of the pair model could do better.

The important point here, as far as a pair model is concerned, is the fact that for all individuals to have just four contacts, no two of which have a direct contact themselves, is an unlikely scenario. But the pair model closure approximation (equation (4.14)) can easily circumvent this by describing the local spatial environment with the parameters  $m$  and  $\phi$ , and we will use this here. Objections to the inherent regular global structure and static nature of a square lattice (no mixing) are not in themselves problematic for a deterministic pair model. This is because individuals are not explicitly represented in the latter, and neither are global structures addressed directly.

We can therefore introduce a flexibility through  $m$  describing the overall density of connections, and  $\phi$  being a measure of the local degree of connectedness or clumping (in the sense of Chapter 4). As with previous examples, the equation for  $(S)$  becomes redundant because each individual is now assumed to have  $m$  neighbours ( $m(S) = (SS) + (SI)$ ). Recalling  $(I) = N - (S)$  and

$(II) = mN - (SS) - 2(SI)$ , and writing out in full the closure approximation for triples  $(ijk)$ , the resulting second order system is

$$\begin{aligned}(\dot{SS}) &= -2\beta \frac{(m-1)}{m} \frac{(SS)(SI)}{(S)} \left[ 1 - \phi + \frac{\phi N}{m} \frac{(SI)}{(S)(I)} \right] + 2\nu(SI) \\(\dot{SI}) &= \beta \frac{(m-1)}{m} \frac{(SI)}{(S)} \left[ (1 - \phi) [(SS) - (SI)] + \frac{\phi N}{m} \frac{(SI)}{(I)} \left[ \frac{(SS)}{(S)} - \frac{(II)}{(I)} \right] \right] \\ &\quad - \beta(SI) + \nu [(II) - (SI)]\end{aligned}\tag{6.2}$$

### 6.2.2 No Recovery from Infection

First consider the case  $\nu = 0$ , so there is no recovery once infected. Dynamically, such a system is not very interesting: In a completely connected network of susceptibles, we would then expect any infection eventually to spread to every individual. From equations (6.1) and (6.2) we see that both  $(S)$  and  $(SS)$  are decreasing functions of time,  $(I)$  and  $(II)$  are increasing, and the system reaches equilibrium if and only if  $(SI) = 0$ . This equilibrium, however, is degenerate;  $(SS)$  and  $(II)$  can take any non-negative values, providing  $(SS) + (II) = mN$ .

How does the composition of the final equilibrium depend on the initial conditions and model parameters? We can partially answer this question by using linear stability analysis. The Jacobian matrix of partial derivatives for equations (6.2), evaluated for any fixed point  $(SI) = 0, (SS) + (II) = mN$  is

$$\left. \frac{\partial [(\dot{SS}), (\dot{SI})]}{\partial [(SS), (SI)]} \right|_{\text{fixed point}} = \begin{pmatrix} 0 & -2\beta(m-1)(1-\phi) \\ 0 & -\beta[(m-1)\phi - (m-2)] \end{pmatrix}\tag{6.3}$$

which has eigenvalues of 0 and  $-\beta[(m-1)\phi - (m-2)]$ , with eigenvectors that point along the  $(SS)$  axis and  $(SI)$  axis respectively. The zero eigenvalue is no surprise because of the degenerate line of fixed points, but the other is interesting. We define

$$\phi^* = \frac{(m-2)}{(m-1)}\tag{6.4}$$

If  $\phi < \phi^*$  then the second eigenvalue is positive. Consider the phase space  $\{(SS), (SI)\}$ . Linear analysis tells us that trajectories sufficiently close to (but not on) the line of fixed points along  $(SI) = 0$  will be initially repelled almost perpendicularly away, parallel to the  $(SI)$  axis (figure (6.1a)). Once away from the axis, under the influence of the equations' nonlinearity, the trajectories will necessarily move in the direction of decreasing  $(SS)$  because  $(\dot{SS})$  is then strictly negative. The trajectories will inevitably end up approaching the point  $(SS) = (SI) = 0$ , where  $(II) = mN$ , because they can never reach anywhere else on the  $(SS)$  axis and there is nowhere else for them to go. Conversely, if  $\phi > \phi^*$ , the second eigenvalue is negative (figure (6.1b)) and trajectories anywhere close to the  $(SS)$  axis will be attracted towards it, whereupon  $(SI)$  approaches zero and the system comes to rest, but this time not necessarily at the origin  $(SS) = (SI) = 0$ .

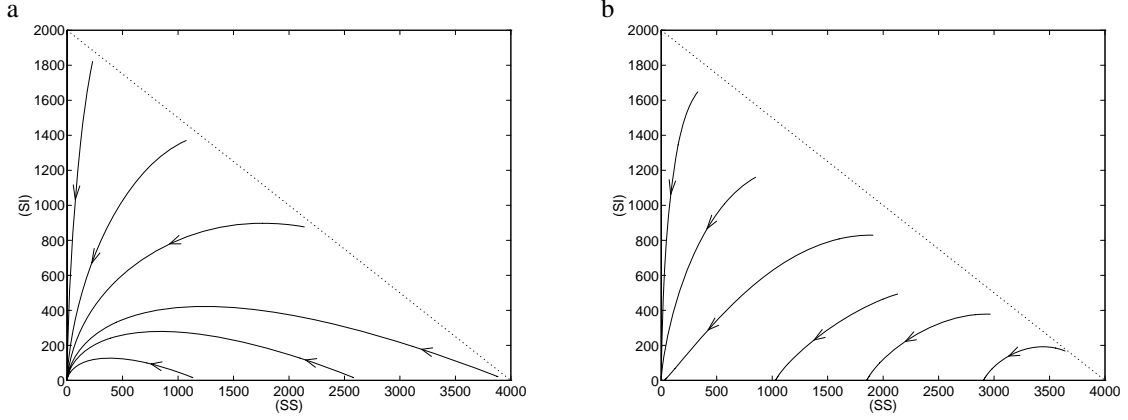


Figure 6.1: Typical trajectories in  $\{(SS), (SI)\}$  phase space for the cases a)  $\phi = 0.3 < \phi^*$  and b)  $\phi = 0.9 > \phi^*$  for the contact process pair model with no recovery,  $\nu = 0$ . Parameters are  $\beta = 1$ ,  $N = 1000$  and  $m = 4$  which gives  $\phi^* = \frac{2}{3}$ .

The consequences of this for the spread of an infection are illustrated in figure (6.2). Equations (6.2) were numerically integrated for  $m = 4$ , where  $\phi^* = 2/3$  and the divide between simulations with higher and lower values of  $\phi$  is striking. (Qualitatively identical behaviour, in agreement with the linear analysis, was observed at all other investigated parameter values). Essentially, if  $\phi$  is sufficiently high, the infection does not spread to the whole population (unless there is a large enough initial infection; this is not shown in figure (6.2), but is visible in figure (6.1b) in the two left-most trajectories). Otherwise, the entire population eventually becomes infected. Furthermore, increasing  $\phi$  from any value appears always to reduce the speed of the spread of infection.

These findings are intuitively in agreement with the previous interpretation of  $\phi$  as representing the degree of spatial clumping (section (4.5)), because a disease will find it more difficult to spread between different clumps where there are fewer connections. As the degree of clumping increases (whilst maintaining the total number of connections constant), we may expect some parts of the population to become isolated and therefore ‘out of reach’ of the infection. We see the effect of this fragmentation whenever  $\phi > \phi^*$ .

The value of  $\phi^*$  also fits naturally with the following interpretation. Consider a neighbouring pair of sites,  $A$  and  $B$  (figure (6.3)). Site  $A$ , having an assumed total of  $m$  neighbours, has  $(m - 1)$  neighbours excluding  $B$ . Of these, we expect a fraction  $\phi$  to also be neighbours of  $B$ . So if  $B$  is to have any connections ‘outwards’ to other individuals,  $C$ , in the network, it must have at least one spare connection, from its total of  $m$ , that is not already linking to  $A$  or any of  $A$ ’s neighbours. Hence we require

$$1 + \phi(m - 1) < m - 1$$

or in other words,  $\phi < \phi^*$ .

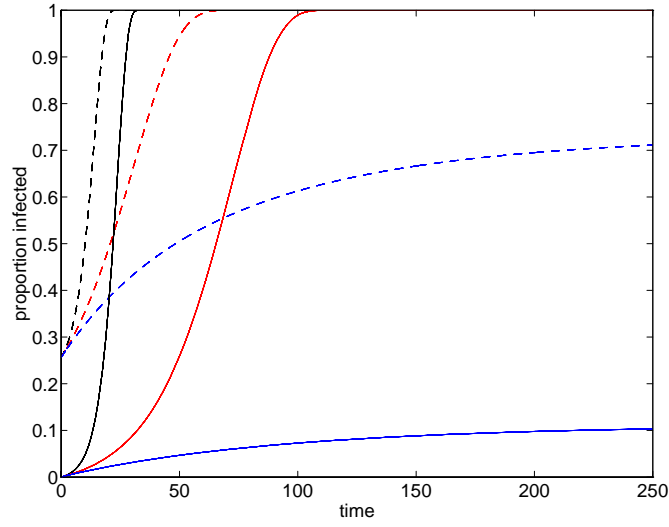


Figure 6.2: Numerical output from the contact process pair equations with no recovery from infection,  $\nu = 0$ . The infection rate is scaled to  $\beta = 1$  and the number of neighbours per individual,  $m = 4$ . Two sets of initial conditions are illustrated, representing a small initial infection and a much more widespread one:  $(SS) = 3998, (SI) = 1, (II) = 0$  (solid lines) and  $(SS) = 2960, (SI) = 15, (II) = 1010$  (dashed lines). The value of  $\phi$  is variously chosen to be  $\phi = 0.6$  (black),  $\phi = 0.65$  (red) and  $\phi = 0.67$  (blue), showing typical behaviour on either side of the critical value of  $\phi^*$ , which equals  $2/3$  in the case  $m = 4$ .

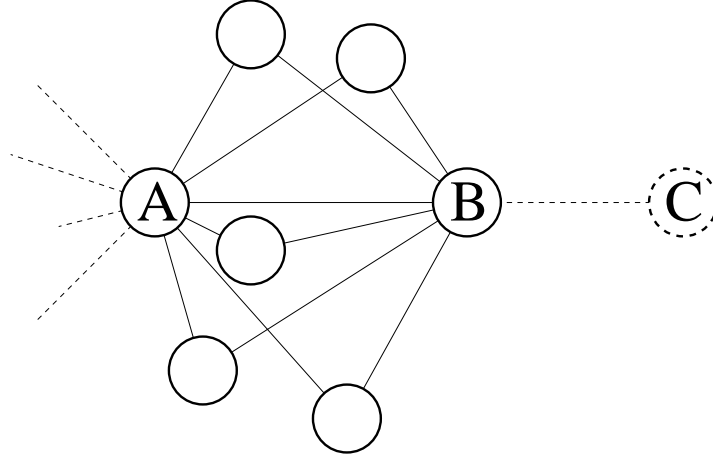


Figure 6.3: Schematic diagram of sites connected with an  $(m, \phi)$  spatial structure. For interpretation, see the text.

### 6.3 Susceptible-Infectious-Recovered

The contact process is extended to an SIR model by allowing infected individuals to enter a recovered (and immune) class instead of reverting to susceptible again on losing their infection. To keep the dynamics interesting we must also introduce mortality and reproduction to provide a fresh stock of susceptible individuals. Mortality is chosen to exactly balance reproduction so as to keep the total population constant. As usual for a spatial pair model, we must also describe the change in neighbourly connections occurring at these events. The simplest assumption to implement is that new offspring inherit the same spatial environment that deceased individuals lose. An alternative interpretation of the birth and death process is to view ‘death’ merely as subsequent loss of immunity of previously immune individuals. These individuals naturally return to the susceptible class and remain in their established spatial neighbourhood. No actual birth or death events need to be considered at all; contrast with section (1.4.2). To summarise, the events and corresponding rates are now

**Infection** Infectious individuals infect neighbouring susceptibles at a rate  $\beta$  per contact.

**Recovery** Infectious individuals recover and enter the removed (immune) class, R, at rate  $\nu$

**Birth and Death** Individuals die, and susceptibles are born (in the same spatial neighbourhood), at rate  $\mu$ .

From these, the evolution equations are obtained in the usual manner. For the single totals, we have

$$\begin{aligned}(\dot{S}) &= \mu N - \mu(S) - \beta(SI) \\(\dot{I}) &= -\mu(I) + \beta(SI) - \nu(I) \\(\dot{R}) &= -\mu(R) + \nu(I)\end{aligned}\tag{6.5}$$

and for the pairs,

$$\begin{aligned}(\dot{SI}) &= \mu[(II) + (IR) - (SI)] + \beta[(SSI) - (ISI) - (SI)] - \nu(SI) \\(\dot{SR}) &= \mu[(IR) + (RR) - (SR)] - \beta(RSI) + \nu(SI) \\(\dot{IR}) &= -2\mu(IR) + \beta(RSI) + \nu[(II) - (IR)] \\(\dot{SS}) &= 2\mu[(SI) + (SR)] - 2\beta(SSI) \\(\dot{II}) &= -2\mu(II) + 2\beta[(ISI) + (SI)] - 2\nu(II) \\(\dot{RR}) &= -2\mu(RR) + 2\nu(IR)\end{aligned}\tag{6.6}$$

Reassuringly, equations (6.5) are recognisable as the non-spatial SIR equations where the mass-action assumption for  $S$ - $I$  contacts,  $(S)(I)$ , has been replaced by the true number,  $(SI)$ . Again we observe the usual result that the total number of singles and the total number of pairs are both constant because there are no contact making or breaking events, just as for the contact process.

$$(S) + (I) + (R) = N, \text{ constant}$$

and

$$(SS) + (II) + (RR) + 2(SI) + 2(SR) + 2(IR) = M, \text{ constant}$$

Closing the equations with the usual  $(m, \phi)$  neighbourhood description implies  $M = mN$  and leaves the fifth order system given by the first five lines of equations (6.6) in which singles totals  $(X)$  are given by  $m(X) = (SX) + (IX) + (RX)$ .

### 6.3.1 Behaviour

The behaviour of this SIR pair model was explored numerically for different values of the parameters  $\beta, \mu, \nu, m$  and  $\phi$ . In comparison to the non-spatial SIR equations, which always tend to equilibrium, the dynamics are much more interesting. The major difference is that the pair equations can produce limit cycle behaviour. Figure (6.4) shows the effect of varying  $\phi$  whilst keeping other parameters fixed at  $\beta = 100, \mu = 0.02, \nu = 1$  and  $m = 4$ . These are not intended to be realistic values for any particular infection, but they are certainly plausible, with the expected lifetime of the host animal fifty times the expected duration of the infection. For low  $\phi$  values the result is an equilibrium, but as  $\phi$  increases past a critical value, limit cycles (periodic orbits) are born in a super-critical Hopf bifurcation. Further increasing  $\phi$  increases the size of the orbits, but no further bifurcations were observed for  $\phi$  between 0 and 1. This Hopf bifurcation structure appeared very stable to change



in the other parameters, with increasing  $\phi$  often producing limit cycles. Some parameter regimes oscillated for all  $\phi \in (0, 1)$ , and others did not cycle for any value of  $\phi$ . (When limit cycles become too large, the troughs correspond to very small densities and because of the continuity assumption we must treat the model cautiously. Real life stochastic perturbations in such circumstances will be important, but these, of course, are not present in the pair model. Nevertheless, many limit cycles exist away from the axes where this is not a problem.)

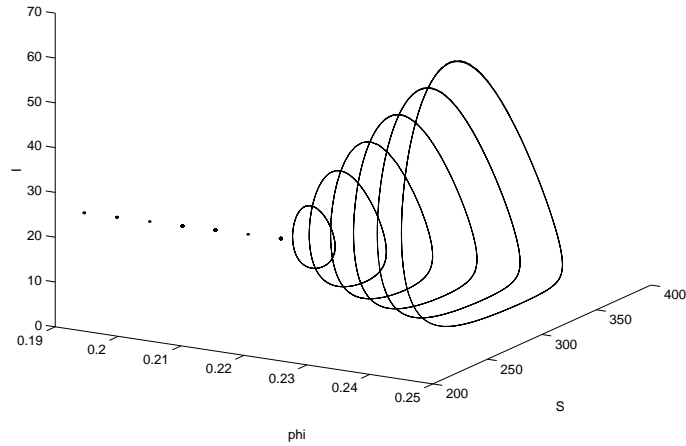


Figure 6.4: The SIR pair model showing a super-critical Hopf bifurcation as  $\phi$  is increased. Parameter values are  $\beta = 100, \mu = 0.02, \nu = 1, m = 4, N = 1000$ . The bifurcation is numerically observed to occur at  $\phi \approx 0.21$ , when the equilibrium position is approximately  $(S) \approx 290$  and  $(I) \approx 14$ .

### 6.3.2 Stochastic Simulation

The temptation to compare this behaviour with that produced by an explicit space stochastic simulation is hard to resist. Despite the fact that the pair model is best viewed as a model in its own right, its spatial structure can reflect that of appropriately configured lattice models in a similar way to the hawk dove game example of Chapter 2. Consider an even more transmissible and long lived infection specified by  $\beta = 500, \mu = 0.02, \nu = 0.3$ , released on a population of size  $N = 10000$  which is arranged in a regular hexagonal lattice of  $100 \times 100$  individuals. Each site neighbours its six nearest neighbours (using toroidal boundary conditions at the edges) and hence the spatial structure is equivalent to  $m = 6$  and  $\phi = 2/5$ . Stochastic simulation of this system was performed using an initial condition consisting of a random scatter of individuals in the proportions 10% susceptible, 5% infected and 85% recovered. Figure (6.5) shows the results graphically as snapshots of the spatial structure, and figure (6.6) shows the corresponding time series for the total susceptible, infected

and recovered populations. The pattern is one of repeated rapid epidemics, each followed by a more gradual replenishment of susceptibles. Each epidemic typically covers the whole spatial domain, and despite some stochastic noise (most easily seen in the time series of the less abundant infecteds) the result obtained in the majority of simulations (as shown) is surprisingly regular oscillations with a period of the order of 40 time units.

Establishing the oscillations from the random initial condition was not a certain process; on about half of the attempts the infection did not ‘take hold’ and died off. However, it did appear that an infection established for the period of one cycle was usually followed by several more oscillations, indicating that the spatial structure had to be correctly formatted, in some sense, to avoid the infection burning out. Of course the system is always vulnerable to stochastic fade-out, especially in the infection troughs where the number of infected individuals falls very low, in which case remaining recovered individuals decay exponentially back into susceptibles (not shown in figure (6.6)). Simulations on a smaller  $50 \times 50$  lattice suffered fade-outs much more frequently, and maintained oscillations were harder to support.

Figure (6.7) shows the time series output of the pair model SIR equations for the same parameter values as used in the stochastic simulation of figures (6.5) and (6.6) using equivalent initial conditions and displayed on identical axes. Also shown is the original non-spatial SIR equation output, again using the same initial conditions and parameter values, with the exception of the transmissibility rate,  $\beta$ . Recall from section (1.4.2) that in the mean-field model,  $\beta = \beta^M$  was really a composite rate of the density of  $S$ - $I$  contacts (relative to the product  $SI$ ) multiplied by the probability of effective disease transmission. In both the pair model and lattice simulation, however, the contacts are explicitly known and  $\beta = \beta^P$  is purely the effective transmission rate per contact. To compensate for this, we arrange for the net transmission rates to be identical when there are no spatial correlations: there are (almost)  $N^2$  contacts in a model where everyone interacts with everyone (implied by the mass-action principle), but only  $mN$  in the pair and lattice models. With identical species densities and no spatial correlations, the fraction of these that are  $S$ - $I$  contacts in the different models will be in the same ratio so we expect the relation between mean-field  $\beta^M$  and pair model  $\beta^P$  transmission rates to be

$$\beta^M N^2 = \beta^P mN$$

This gives  $\beta^M = 0.3$  as the proper value to correspond with  $\beta^P = 500$ , and this value is used in figure (6.7).

On comparing figures (6.6) and (6.7), the first impression is very favourable for the pair model. It produces cycling similar to that observed in the lattice simulation, whereas the mean-field equations, as they must do, only approach an equilibrium. A closer inspection reveals that the match between the two oscillating models is not perfect: the pair model has more rapid cycling than the stochastic

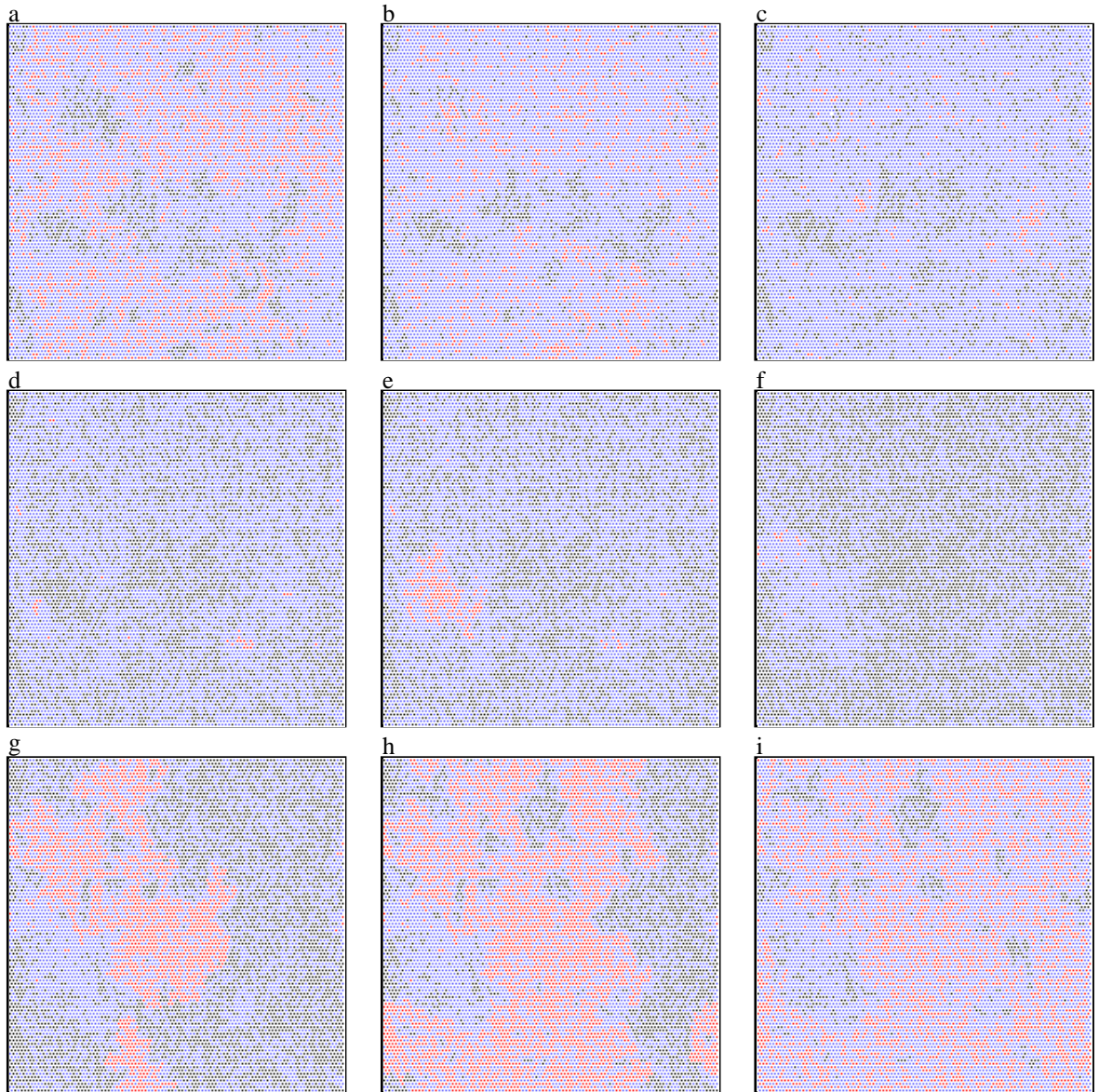


Figure 6.5: Snapshots of the spatial structure shown by the hexagonal grid SIR model at  $\beta = 500$ ,  $\mu = 0.02$ ,  $\nu = 0.3$ ,  $N = 10000$  and  $\phi = 0.4$ . Black represents susceptible individuals, red is infected individuals and the recovered are blue. Viewing from top left to bottom right, the system can first be seen recovering from a large epidemic (a,b,c). Eventually a large body of susceptibles builds up, but (e) some of the few remaining infected individuals begin another large epidemic which rapidly sweeps through the population again. Typically, this cycle repeats over and over again, giving successive epidemics, until the infection is eliminated by chance, usually in one of its troughs.

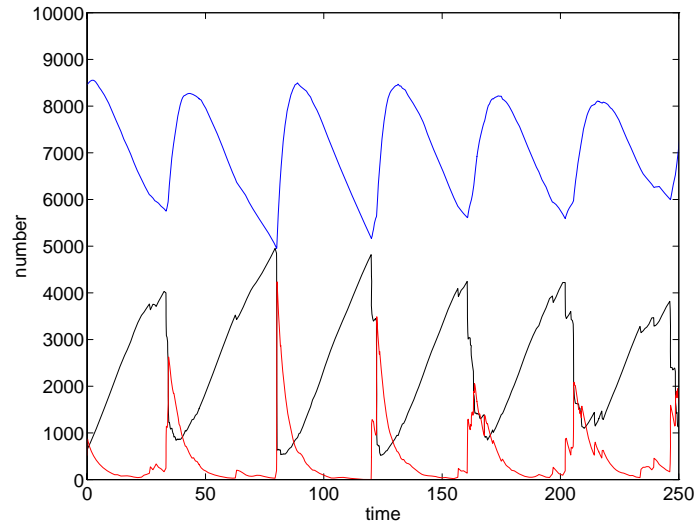


Figure 6.6: Time series corresponding to figure (6.5) for the hexagonal lattice simulation, showing several subsequent epidemic outbursts. Susceptibles, infecteds and recoveredds are respectively black, red and blue and were initially present in a random mixture in the proportions 10%,5%,85%. The parameters are  $\beta = 500$ ,  $\mu = 0.02$ ,  $\nu = 0.3$ ,  $N = 10000$  and  $\phi = 0.4$ .

simulation, with a period of approximately 28 time units, and the amplitude of each cycle is smaller than the lattice model. On the other hand, the mean values of the number of susceptible, infected and recovered individuals are broadly correct (unlike the mean-field equations which predict only a tiny fraction of the observed number of susceptibles, and correspondingly too many recoveredds). Of course, the cycles are perfectly regular in the deterministic pair model and it shows none of the stochasticity that will eventually inevitably disrupt the dynamics of the lattice simulation.

There are undoubtedly many factors involved in producing oscillations in the lattice simulation. Spatial structure is clearly important based on the visual evidence of figure (6.5) alone, but just how much of this is the result of local pair correlations and how much is dependent upon larger spatial structures or indeed the size of the grid is unknown. No thorough attempt was made to investigate the effect of grid size beyond the  $100 \times 100$  and  $50 \times 50$  lattice simulations, but it is likely that on significantly larger grids (too large to simulate with comparable computing power) the neat oscillations seen here will disappear as spatial structure is averaged away over widely separated and out of phase areas. One might also expect to see travelling waves of infection spreading rapidly through space, leaving areas of recoveredds and then new susceptibles in their wake. (Such behaviour is occasionally seen on truly large scales in the real world, for example with human influenza epidemics sweeping through continents). The choice of population size ( $N = 10000$ ) and high transmissibility ( $\beta = 500$ ) studied here probably made it easier for the pair model to reproduce similar dynamics to the lattice

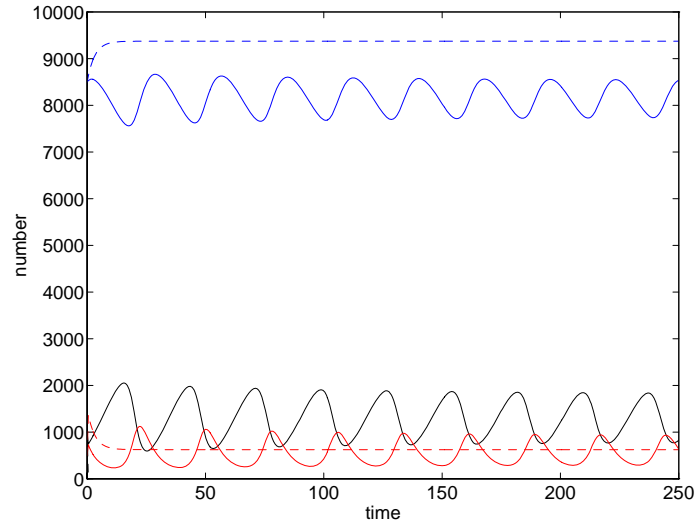


Figure 6.7: Time series (solid) for the pair model SIR equations for  $\beta = 500$ ,  $\mu = 0.02$ ,  $\nu = 0.3$ ,  $N = 10000$ ,  $\phi = 0.4$  and  $m = 6$ . The numerical integration starts from an initially random distribution (*i.e.* no pair correlations) of 10% S, 5% I and 85% R which is close to the stable limit cycle to which it is quickly attracted. Susceptibles are black, infected red and recovered blue. The dashed lines are output from the non-spatial SIR equations (Chapter 1) with the same parameters except for  $\beta = 0.3$  - see the text for an explanation. In this case, the susceptibles are present only in extremely small numbers and are hardly visible on the graph).

simulation because they correspond to epidemics that are able to infect virtually all areas of the spatial domain almost simultaneously. This reduces the amount of important large scale spatial structure. It is more difficult to imagine how pair models could accommodate parameter regimes for which very large scale spatial heterogeneities are present.

Nevertheless, the achievement of the SIR pair model is substantial in accommodating oscillations at all, and all the more interesting because of the undoubted importance and frequency with which such oscillations appear in the real world. It is interesting to note that the pair model numerically solved for identical parameters to those of figure (6.7) except for the simpler case of  $\phi = 0$  predicts only an equilibrium solution, so the contribution of closed triangular connections is important to the model predictions. Because we are interested in the pair equations as a stand alone model, discrepancies with lattice model simulations (which are of course inadequate in many ways themselves, for example by not incorporating any migration in an otherwise very rigid spatial structure) are less significant. The key point is that many real systems are likely to exist in a spatial environment that is more similar to the lattice model than to the mean-field equations, so the behaviour of the pair equations is a step in the right direction.

### 6.3.3 Seasonal Forcing

A common modification to the basic SIR equations is to add a degree of seasonal forcing (*i.e.* seasonal variation in the model parameters), in recognition of the fact that conditions effecting the spread of an infection do not necessarily remain constant all year round. The reasons can be varied, ranging from biological to sociological. For example, transmission rates could rise in cold winter months because of relatively weak host immune defenses, or perhaps during summer because more favourable conditions for a particular pathogen (bacteria, virus) survival exist then. Alternatively, for example, people spending more time indoors during winter could substantially effect social mixing patterns, as could the presence or absence of children at school during term time and holidays. (This latter point is thought to be particularly important for measles - see section (6.4)).

Of the three variables  $\mu, \nu$  and  $\beta$  in the non-spatial SIR equations,  $\beta$  has most often been the one selected to be seasonally forced because it is easier to justify seasonal changes in transmissibility than in the expected infection period or host life time. However, directly adjusting the transmission rate is not always a satisfactory answer either. With the pair model we have the advantage of two more parameters,  $m$  and  $\phi$ , which specifically reflect the spatial structure. Forcing either (or both) of these is an obvious way of incorporating the changes in social behaviour (*e.g.* school terms) that have nothing to do with the biological detail of the infection (transmissibility, recovery rate *etc...*).

As a purely hypothetical example, consider the pair SIR model (equations (6.6)) appropriately closed

by equation (4.14)) in which  $\phi$  alone is seasonally forced sinusoidally, representing an annual cycle of a relatively more and less clumped population:

$$\phi = \frac{\phi_{\max} + \phi_{\min}}{2} + \frac{\phi_{\max} - \phi_{\min}}{2} \sin(2\pi t) \quad (6.7)$$

So time,  $t$ , is measured in years. Numerical investigations of this system revealed a rich spectrum of possible behaviours as the model parameters were varied. Annual cycles were common, sometimes with just a simple peak, sometimes with a double peak each year. Quasi-periodic orbits were also found with one or more dominant frequencies ranging from more than once every eight months to below once every thirty months. Two typical examples are shown in figure (6.8). The forcing frequency 1.0 is clearly dominant in figure (6.8b) but a frequency of approximately 1.4 prevails in figure (6.8a). A degree of seasonal forcing is clearly able to excite the equations and produce more complicated behaviour than either equilibria or limit cycles. It was not necessary to have large changes in  $\phi$  to do this, nor was it necessary to repeatedly vary  $\phi$  above and below the critical clumping value  $\phi^*$  found for the contact process equations. The range of behaviour described above is actually quite similar to that possible with non-spatial forced SIR equations.

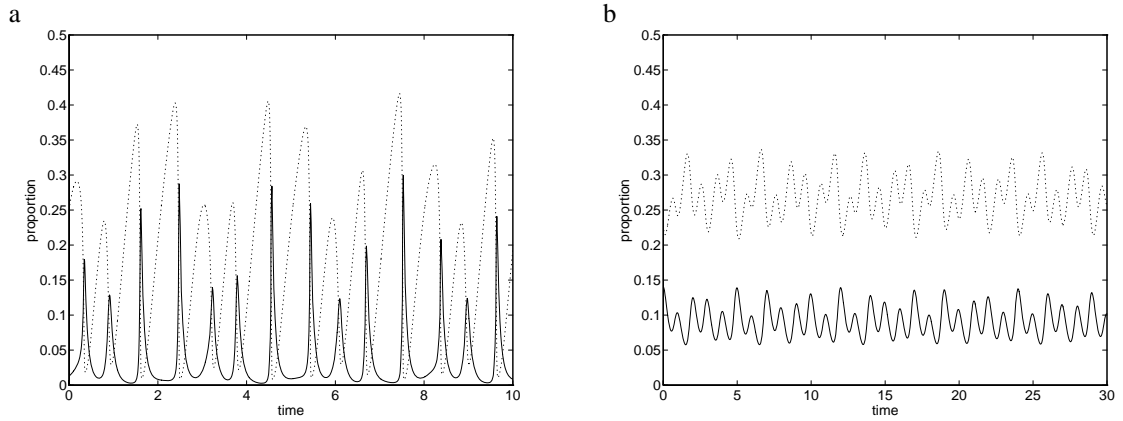


Figure 6.8: Two examples of different parameter regimes in the seasonally forced SIR pair model showing typical irregular quasi-periodic behaviour. a)  $\mu = 1, \beta = 100, \nu = 20, m = 10, N = 1000$  and  $\phi$  sinusoidally varied between 0.6 and 0.8 with a period of one time unit. b)  $\mu = 0.628, \beta = 62.8, \nu = 4.4, m = 4, N = 1000$  with  $\phi$  similarly varied between 0.4 and 0.65. In each figure the solid line is the proportion of infected individuals and the dotted line is the susceptibles.

Given the interesting behaviour displayed by these hypothetical infection models, attention is now focused on predictions for an important real world disease.

## 6.4 Measles

Measles is one of the most infectious communicable diseases. It also poses a serious health problem. Measles is fatal in young and malnourished children in between 5% and 10% of cases, and it causes many deaths in the developing world. The potential benefits to be gained by successful eradication or control of the disease are obvious, and many of the methods which can help to achieve this, for example appropriate vaccination programmes, must be based on a sound understanding of the underlying epidemiology.

Figure (6.9) shows the weekly reported cases of measles in England and Wales for a twenty year span from 1948 to 1968 before mass vaccination was introduced. This data is unusually good for any area of ecology or epidemiology, and coupled with its importance in human terms it is easy to understand why measles has become one of the most studied and analysed of all diseases.

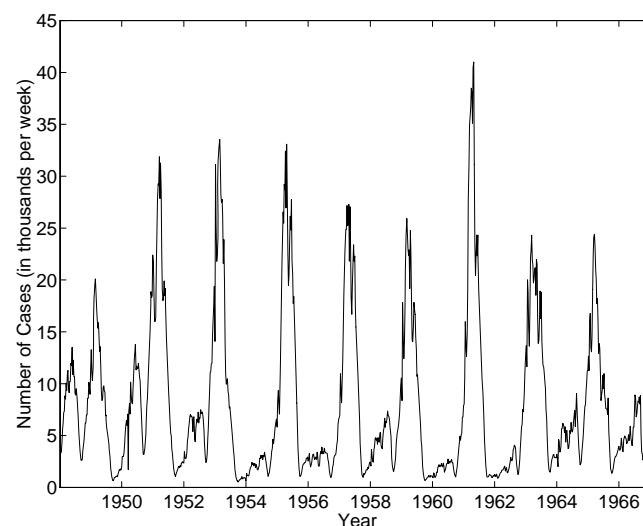


Figure 6.9: Weekly notifications of measles in England and Wales for the period 1948 to 1968, before mass vaccination was introduced. Data from Grenfell, B.T. via Keeling, M.J.

Much work has been done on trying to understand and replicate, through modelling, the characteristic structure of the measles time series. Most notably this is the fairly regular 2 to 3 yearly epidemic cycles, but also crucial is the threshold population size for persistence: For effectively isolated populations (possibly large cities, for example) it is observed that a critical population size of approximately half a million is required for the infection to regularly persist through the troughs (Bolker and Grenfell, 1995, and references therein). Smaller populations frequently suffer fade-outs and the infection is only reintroduced at a later time by the immigration of other infected individu-



als. Other data sets from New York and Copenhagen have proved useful in this respect.

### 6.4.1 Modelling

Most measles models are based around the SEIR equations (see section (1.4.3)) because the life-history of a measles infection in an individual is well classified by an exposed (but not infectious) stage followed by the fully infectious stage and then life-long recovery. Typical durations are measured in a few days for each, and the remainder of this chapter will use the values given by Olsen and Schaffer (1990) of 10.2 days for the average length of the exposed stage and 3.65 days for the infectious period. With time measured in years these correspond to  $\gamma = 35.78$  and  $\nu = 100$ . Life expectancy for humans has naturally varied from time to time, and from place to place through history, but an average value of 50 years ( $\mu = 0.02$ ) is a reasonable estimate. Estimating the transmission rate  $\beta$  is more difficult, as previously mentioned because it represents the combined effect of rate of contact formation (assuming the mass-action principle) with effective disease transmission.

On their own, with either the parameter values given here or indeed with any others, the SEIR equations like the SIR equations display only long-term equilibrium dynamics, sometimes through damped oscillations. The basic equations therefore dramatically fail to capture the epidemic behaviour observed in reality, but there are some modifications have helped to rectify this discrepancy. These are now discussed.

#### 6.4.1.1 Seasonal Forcing

Measles is predominantly a childhood disease with over 90% of a pre-vaccination era population typically having been infected before the age of twenty (Keeling, 1995). Because of the importance of schooling and its consequences for social mixing in this age group, many authors have considered seasonally forcing the basic SEIR model to simulate the changes in population contact rates between school term times and holidays. The simplest approach, and a crude first step, is to vary  $\beta$  sinusoidally over a period of one year, with low  $\beta$  during the summer (holiday) and high  $\beta$  during the winter term time (Olsen and Schaffer, 1990; Rand and Wilson, 1991; Bolker and Grenfell, 1993).

With appropriately chosen parameters, previous studies of the forced SEIR equations have shown that they can display much more dynamic (occasionally chaotic) trajectories than the unforced versions (see, for example, Rand and Wilson, 1991). In this respect the behaviour is closer to that observed in the measles data. For realistic parameters, the time series of the number of infected individuals also displays occasional epidemic outbursts (spikes) but there is an accompanying problem in that the troughs in between are typically very low indeed. The deterministic equations can recover from these to produce another epidemic, but in a stochastic model (and certainly in the real world)

the infection would be in great danger of disappearing. In a simulated population of around half a million, the troughs commonly represent the equivalent of way less than one infected individual, and an accurate prediction of the population size for persistence is therefore not available. Another consequence of the very low troughs (through which the orbits are ‘stretched’ by the attractor) is that the spacing between subsequent spikes is very irregular - anything from one to five years is common - in contrast to the much more regular peaks observed in England and Wales (figure (6.9)) and other data sets.

#### 6.4.1.2 Age Structure

Because measles primarily affects children, age-structure is an important consideration. Rather than assuming all individuals in a population are indistinguishable, some models split up the population according to the individuals’ age distribution. The presence of schools means that individuals of different ages will typically have different mixing rates both with other individuals of a similar age and with individuals of other ages (they will also have potentially different mortality rates and recovery rates *etc.* too). Tailoring the (increased number of) model parameters to fit more specifically observed age-related data gives opportunity of refining the model to more accurately reflect real events.

One approach is to convert the SEIR ODEs into a system of PDEs (see Anderson and May, 1992 for general techniques) that gives age-specific parameter responses to a continuum of ages from zero up to the maximum required age. Such a system then models not only the size but also the complete age distribution of all individuals in each class (S,E,I or R) of the model. A further advantage is that the questionable assumption of exponentially distributed expected life times can then be replaced with age-dependent mortality. The cost, of course, is a resulting PDE system which is very difficult to analyse and relatively difficult to investigate numerically due to the vastly increased set of parameters (each single parameter in the ODE corresponds to an arbitrary distribution with respect to age in the PDE). For reasons of clarity and manageability, many authors prefer to consider a second approach, where the population is divided into a few distinct age categories. A popular choice is the four class system consisting of pre-school children (aged 0 to 5 years), primary school children (aged 6 to 10), secondary school children (aged 11 to 15) and adults (aged 16+).

This latter classification is used by the Realistic Age Structure (RAS) model of measles dynamics (Bolker and Grenfell, 1993, 1995). This is another SEIR-based model that also incorporates school-year motivated seasonal forcing. Each of the four age categories is split into the four disease categories resulting in a  $16 - 1 = 15$  dimensional model (the population has a fixed total size). To date, the RAS model is one of the most successful measles models in terms of replicating the observed dynamics. It significantly improves on the behaviour of the basic forced SEIR model, most noticeably by reducing the persistence population size to around two million. This is a step in the

right direction if not yet quite perfect.

One consequence of increasing the number of population categories in models like the RAS model is the difficulties associated with the corresponding increase in the number of model parameters. A single transmission parameter,  $\beta$ , for example, is replaced by an entire age-structured ‘who acquires infection from whom’ (WAIFW) matrix (Anderson and May 1992). Furthermore, this matrix is given even more flexibility with the introduction of seasonal variation. The first difficulty this presents is how to measure realistic values for each of these parameters in the field. Edmunds, O’Callaghan and Nokes (1997) have taken an experimental first step and measured the age-structured contact rates (based on the incidence of conversations) amongst a sample of adults that may be important in the transmission of infectious disease. Information of this kind, combined with possible age-dependent physiological factors, is essential for estimating the model parameters. The second difficulty is that numerical analysis of the equations becomes a much more laborious task, with vast parameter spaces to search. Given a judicious choice of enough parameters, there is also the increased likelihood of being able to reproduce a whole spectrum of different behaviour with a single model. This can lead to the problem of justifying why any one behaviour is more important or relevant than any other.

#### 6.4.1.3 Spatial Structure

Perhaps because of the many possibilities presented by seasonal and age-related modifications, and also because of the absence of an obvious practical approach, spatial structure has received comparatively little attention in measles modelling (but see Grenfell, Bolker and Kleczkowski, 1995 for a metapopulation discussion). This is despite the significant contributions it has made to other ecological model systems, and the clear prospect of space being an important factor in explaining measles dynamics. A pair model analysis provides a possible solution to tractably incorporating spatial effects and this is now explored. The pair induced limit cycling found in the SIR pair equations is particularly exciting now because of the observed oscillations in the measles data.

#### 6.4.2 Measles Pair Model

Following the now standard procedure, the conventional SEIR system can be reformulated as a pair model. The standard closure assumption is used, where triple densities are described by equation (4.14) and the spatial environment by  $(m, \phi)$ . Singles totals are, as usual, determined by the pairs:  $m(X) = (SX) + (EX) + (IX) + (RX)$ . After symmetry, and making use of the fixed total population, a nine dimensional ODE system is left:

$$\begin{aligned}
(\dot{S}) &= 2\mu[(SE) + (SI) + (SR)] - 2\beta(SSI) \\
(\dot{S}E) &= \mu[(EE) + (EI) + (ER) - (SE)] + \beta[(SSI) - (ESI)] - \gamma(SE) \\
(\dot{S}I) &= \mu[(IE) + (II) + (IR) - (SI)] - \beta[(ISI) + (SI)] + \gamma(SE) - \nu(SI) \\
(\dot{S}R) &= \mu[(ER) + (IR) + (RR) - (SR)] - \beta(RSI) + \nu(SI) \\
(\dot{E}E) &= -2\mu(EE) + 2\beta(ESI) - 2\gamma(EE) \\
(\dot{E}I) &= -2\mu(EI) + \beta[(ISI) + (SI)] + \gamma[(EE) - (EI)] - \nu(EI) \\
(\dot{E}R) &= -2\mu(ER) + \beta(RSI) - \gamma(ER) + \nu(EI) \\
(\dot{I}I) &= -2\mu(II) + 2\gamma(EI) - 2\nu(II) \\
(\dot{I}R) &= -2\mu(IR) + \gamma(ER) + \nu[(II) - (IR)]
\end{aligned} \tag{6.8}$$

To investigate the system numerically, the seven parameters  $\beta, \gamma, \nu, \mu, m, \phi$  and  $N$  must be considered. Choosing  $\nu = 100$ ,  $\mu u = 0.02$  and  $\gamma = 35.78$  as before keeps the model realistic for measles and a typical large city population size for  $N$  of one million is considered throughout, although the model behaviour, being deterministic, is not affected by this choice, and the results can be scaled to represent any population size. (This raises an important point regarding inference of critical community size for persistence. In a deterministic model, judgement must be made on the likelihood of an infectious population successfully negotiating a trough in its numbers, because no stochastic forces exist to force extinction. The depth and duration of the trough are both important, as is the intrinsic variability in the population numbers expected in the real (stochastic) system). This leaves  $m, \phi$  and  $\beta$ , which govern aspects of the spatial structure and contact formation rates, to vary as free parameters.

Equations (6.8) as they stand behave in a very similar way to the pair SIR equations, with some orbits attracted to equilibrium and other parameter values leading to limit cycles after a Hopf bifurcation. Table (6.1) shows the basic response of the system to relative increases in the three free parameters when the dynamics are in the oscillatory regime (decreases produced the opposite response). Extensive investigation revealed no real exceptions to these trends, notwithstanding the fact that some parameter changes reduced the limit cycle behaviour, through a Hopf bifurcation, to fixed point behaviour. The system appeared insensitive to choice of initial conditions in phase space, so long as all four species were initially present (and not disconnected). Essentially, any small parameter change appears to either increase the strength of the oscillations (through both higher peaks and lower troughs) or decrease them. Independently, it will also either increase or decrease the period of oscillation. As intuitively expected, increasing the transmission rate  $\beta$  speeds up the epidemic spread and results in a shorter period with larger numbers infected (relatively fewer susceptible-infectious contacts are wasted through recovery). The two spatial parameters  $m$  and  $\phi$  behave in a similar manner with increases in  $\phi$  having the same qualitative effect as decreases in  $m$ . Both increase the period of oscillation as might be expected for a more sparse, more clumped

	effect on cycle peaks	effect on cycle troughs	effect on cycle period
increasing $\beta$	↑	↓	↓
increasing $m$	↓	↑	↓
increasing $\phi$	↑	↓	↑

Table 6.1: The numerically observed effect of relative increases in each of the free parameters  $\beta, m$  and  $\phi$  on a) the height of the peaks, b) the height of the troughs and c) the period of oscillation of the number of infectious individuals through time in the unforced measles pair model. ↑ represents an increase, ↓ represents a decrease.

spatial network of contacts. Interestingly, the same changes also result in an increased strength of oscillation (*i.e.* more violent epidemics).

The obvious next step, because of its crucial role in non-spatial measles modelling, is to introduce seasonal forcing to compensate for the presumed changes in spatial contact structure during school terms. We choose only to force  $m$  and  $\phi$ ; the transmission rate  $\beta$  (and all other parameters) will be seasonally constant. Instead of a sinusoidal variation in the forced parameters, a discontinuous forcing process more recognisable as changes between the two states of holiday and term-time was used. Based on an idealisation of the usual practice in England and Wales, each school year, starting in September and lasting 52 weeks, is assumed to comprise three equal length terms (14 weeks each). The first and second terms are separated by a two week Christmas holiday, the second and third by a two week Easter holiday, and one year to the next by a six week summer holiday. Each parameter ( $m$  and  $\phi$ ) correspondingly varies discretely between a term-time value ( $m_T, \phi_T$ ) and a holiday value ( $m_H, \phi_H$ ), changing instantly whenever the current time moves from a holiday period to a term period, or vice versa. Forcing  $\phi$  is a straight forward process, but forcing  $m$  is slightly more complicated because a different value of  $m$  corresponds to a different number of pair connections. The total number of pairs  $((SS) + (SE) + \dots + (RR))$  must always equal  $mN$  and there is a decision to be made on changing between holiday and term time about which pair connections are made or broken. Clearly the simplest case, considered here, is to make (or break) new contacts in proportion to their current frequency in the population, so the pair totals  $(XX)$  are simply scaled by the ratio  $m_{\text{new}}/m_{\text{old}}$  whenever  $m$  changes. This assumes the changed circumstances (school or holiday) do not alter the current pair correlations. Other, more complicated, boundary conditions could potentially involve different assumptions such as random (unbiased) contact formation, but none were considered here. Whatever assumption is used, the number of individuals in each category will naturally be continuous over the term-holiday boundaries.

We now have five free parameters ( $m_T, m_H, \phi_T, \phi_H$  and  $\beta$ ) to numerically investigate in the forced equations. Whilst keeping the values reasonably sensible for measles, the parameter space was explored to find the range of expressed dynamical behaviour. It was typically assumed that more mixing took place during school terms than during holidays, so usually  $m_T > m_H$  and  $\phi_T > \phi_H$  to indicate a population clumped into classes or schools. Furthermore, two alternative forcing schemes were also considered. One extended the basic three holiday year to include three more week-long half term holidays in the middle of each school term. The other filled in the Christmas and Easter vacations to leave just one six week holiday and a 46 week school term. Finally, note that although the model is seasonally forced to mimic school terms, it does not include age structure, so school children are not separated from adults. All parameters, therefore, must refer to average or expected values over the whole population.

#### 6.4.2.1 Results

One important finding was the overall high sensitivity of the whole system to changes in any of the free parameters. Another was the frequent presence of very long periods of transient dynamics, so slight changes in the initial conditions, as well as in the parameter values, often produced strikingly different time series. (Most simulations were started from an initial condition corresponding to a population split of 95% R, 4% S 0.5% E and 0.5% I, with no biased pair correlations). For many choices of parameter the trajectory eventually settled down to predictable behaviour on an attracting periodic orbit. The period in such cases was very often a two year cycle, although four year cycles were also observed. Orbits that did not fall onto a periodic attractor may not have been given enough time to do so (very likely), or may have been genuinely chaotic.

In any case, because of the very long transients (anything up to several hundred years was not uncommon before the dynamics recognisably settled down), the final attractor is, epidemiologically speaking, not necessarily very important. This is particularly true given the model assumptions (constant population size, fixed school term forcing, specific spatial structure *etc...*) which historically have not held (and probably will not hold) for human populations over time scales of hundreds of years. It is perfectly possible for time series such as the England and Wales data to be more transient in nature than attractor based. Whilst this is a blow for long term prediction hopes, it is still possible to ask questions about the general structure of the transient time series and its dependency upon system parameters that the models can help to answer.

Figure (6.10) shows various stages of a single typical simulation from the usual initial conditions using free parameter values of  $m_T = 80, m_H = 20, \phi_T = 0.3, \phi_H = 0.1$  and  $\beta = 65$  with a school year consisting of 3 holidays. This choice of parameter values is certainly within the bounds of plausibility (subject to the interpretation of a contact - see Chapter 7). However, similar dynamics was

found in various other regions of parameter space. The numerical integration was performed with a Runge Kutta algorithm and a time step length of one tenth of a day. Integrating over more than 2700 years ( $10^7$  integration steps) was sufficient to remove practically all transient dynamics, after which the system was fixed onto a periodic attractor of period exactly two years (figure (6.10a,b)). At these parameters, the epidemic grows during school terms and decays during the holidays, with every other year being particularly strong. Two twenty year intervals of transient dynamics are also shown (figure (6.10c,d)) for 100 and 430 years after the initial condition. They show contrasting behaviour, firstly with very large epidemic spikes more thinly spaced at a period of approximately 3.3 years, and secondly more irregular dynamics but still maintaining a dominant period of approximately two years with large epidemics every other year.

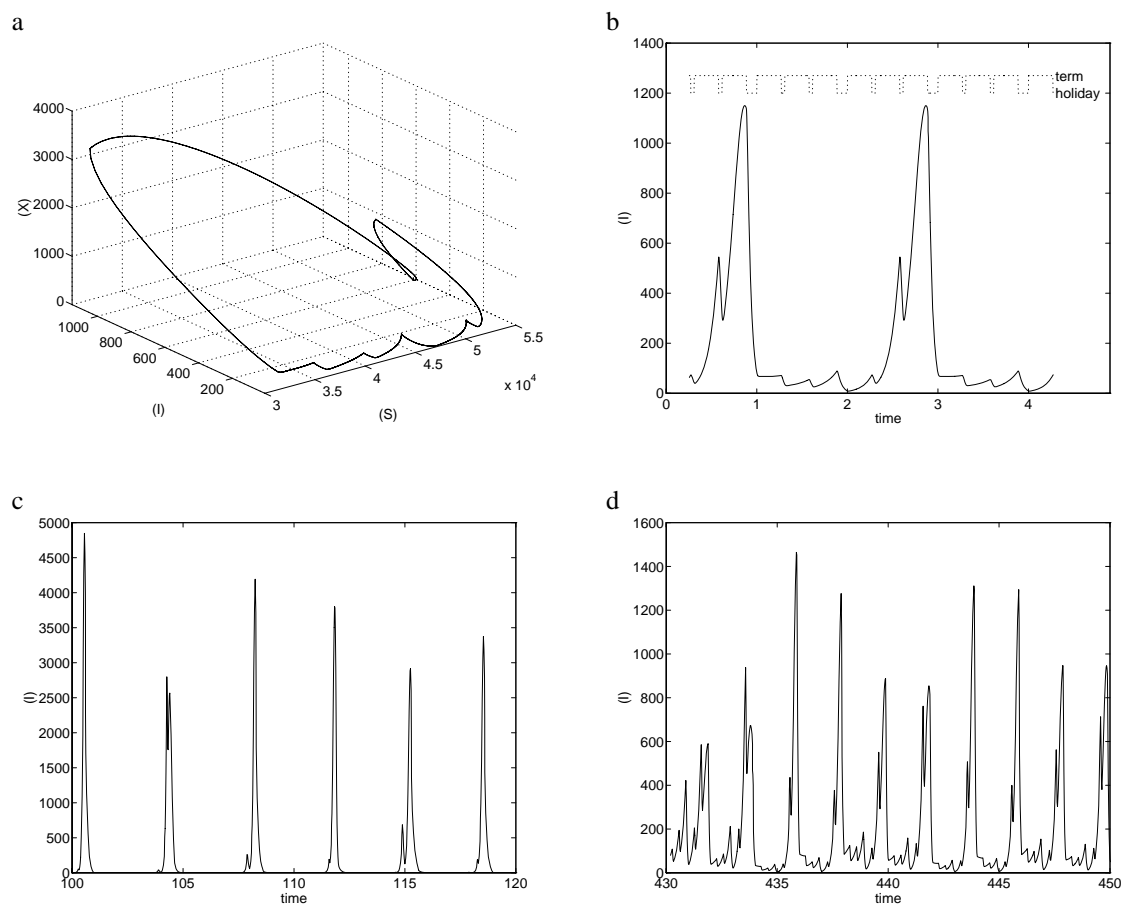


Figure 6.10: Output from the seasonally forced measles SIR model. Trajectory locked into a period two orbit, after transients have been removed. Parameters are as normal. c) and d) show typical transient behaviour at times 100 years and 430 years.

It was typically found that dynamics such as figure (6.10c) were accompanied by very low infectious populations in the troughs, down to the order of  $10^{-2}$  individuals here, and often below, in a pop-

ulation of one million. Obviously this is far below any level which could be reasonably sustained in a real, stochastic, individual model. However, such dynamics are more common early on in the time series, *i.e.* closer to the initial conditions, and this is therefore not quite the serious problem it might appear to be, because the initial conditions, although sensible, were guessed and so are not necessarily close to the model attractor. More extreme behaviour is to be expected in such circumstances, before the pair densities have time to settle down. On the other hand, the dynamics in figure (6.10d) do not have unrealistically low troughs, with the typical minimum being of the order of  $10^1$  infectious individuals in a one million population. As previously mentioned, to speak of persistence of the infection really requires a stochastic individual based model and a statistical interpretation of the results, but the deterministic evidence here is encouraging. A population of size order  $10^5$  would correspond to troughs of the order of  $10^0$  infecteds which is likely to be too small to withstand stochastic extinction for any length of time; similarly a population of  $10^7$ , with troughs of  $10^2$  is much more robust. One may therefore estimate that a population of the order one million is close to the critical persistence size, in reasonable agreement with the observed estimate. Furthermore, the overall dynamics displayed in figure (6.10d) are remarkably similar in appearance to the real data of figure (6.9). Notifications per week in England and Wales (total population of the order 50 million) of 30000 would scale to 600 in a population of one million. Because individuals remain infected for a time of the order of one week, we see the scale of weekly notifications (neglecting any under-reporting errors) and model predictions for the instantaneous number infective are encouragingly comparable.

Dynamics similar to those of figure (6.10d), sometimes with a mixture of the more spiky figure (1.10c) signal, persist for time of the order 100 years before getting locked into the two-year attractor which is their ultimate destiny. One would expect this sensitive measles model to spend most of its time in this transient mode if the other model parameters were subject to even slight perturbation and drift, as would be the case in a changing world, hence transient dynamics are likely to be as important as the attractor.

A similar picture of sensitivity, long and varied transients was displayed with the other seasonal holiday schemes and with other parameter values, although figure (6.10d) was the observed time series most similar to the England and Wales data. Integrations were reasonably insensitive to the choice of step size. The two-year attractor was a common finding, but no three year attractor was discovered. As with all the examples covered in this thesis, a systematic and detailed investigation of the model behaviour in parameter space would be an essential and worthwhile next step in the study of this system.



## 6.5 Discussion

In contrast to previous examples, it is clear that the pair model formulations in this chapter have had a significant effect on the behaviour of their respective systems. Furthermore, this new behaviour is biologically interesting and has opened up the possibility of doing much more useful work with similar model systems. The exposition in this chapter has really only touched the surface.

Some analytical results were obtained for the contact process pair equations, and a useful next step would be to tackle the SIR pair equations analytically. In particular, it may be possible to derive a pair model equivalent of  $R_0$ , the mean-field basic reproductive rate. Comparison of the two may show the importance of the local environment to the initial stages (and the ultimate fate) of a new disease invasion. This has important implications for the design of control programmes. It would also be interesting to know how the SIR pair model's Hopf bifurcation depended on the spatial environment. Because of its complexity, analysis of the measles pair model is likely to be difficult.

The modelling of measles, despite being conceptually accessible, is a very complicated subject. Every single measles model (and there are many) is based on a huge list of assumptions about the epidemiology of the disease and the structure of its host population. This new pair model is no exception. Isolating the important factors from the irrelevant ones is the key task of the modeller, and also one of the hardest. This is typical of the problems faced when models turn from being abstract constructions to representations of a specific real world process.

A superficial study of the measles pair model in this chapter certainly revealed enough promising behaviour to merit further study. But there can be no guarantee that any real breakthrough has been made until extensive further investigations can be done. In theory, the pair model approach should be compared and contrasted with a non-spatial approach in combination with a whole range of different accompanying assumptions, in order to establish that it is spatial correlations that are the key factor. (This range of assumptions might include such areas as different seasonal forcing patterns, the effects of migration, and the incorporation of age-structure). In practice, pair model predictions should be systematically tested against experimentally collected data. As well as being in agreement with the time series for the basic numbers of infecteds and susceptibles *etc.*, predictions should also match the number of pair contacts at any stage in the cycle. Collecting such data, of course, may not be easy.

For all the infection systems in this chapter, there are many possible pair model variants that were not considered but which perhaps deserved to be. Obvious omissions include models incorporating the effects of migration (mixing) within the population, and immigration into the population. It is also likely that the form of any seasonal forcing is very important to the behaviour of the SIR and measles pair models, just as it is for their non-spatial equivalents (recall it is the difference

between equilibrium and complex dynamics). Figure (6.10b) in particular shows how the measles phase space attractor becomes entrained with the pattern of school holidays. Seasonal forcing of  $\phi$  and  $m$ , although natural, raises not only questions regarding timing (one holiday, three holidays, continuous or discrete jumps, *etc.*), but also the need to consider how spatial contacts themselves are to change. There is more work to be done in this area.

Finally, we note that combining pair-wise spatial structure with age structure quickly complicates matters. For example, a pair model formulation of the SEIR model with four age classes has potentially  $(4 \times 4)^2 = 256$  different categories (before symmetry reductions). Without further simplifications, such models are difficult to handle.

**7**

## **Conclusions**

## 7.1 Review

In this thesis we have investigated a relatively new approach to the spatial modelling of simple ecological systems. Instead of explicit spatial models in which populations are distributed over some assumed spatial domain, these derived models take the form of smaller ODE systems which are not much more complicated than comparable mean-field, non-spatial models.

Given a system to be studied, the modelling process begins by identifying the set of possible events which the system can undergo, and which determine the dynamics. For spatially interesting systems, usually one or more of these events will be dependent (for its existence and its rate of occurrence) on the interactions of an individual with its local environment. This environment is comprised of other individuals. Using the symbolic notation developed in this thesis, the dynamical equations governing evolution of the system can be built up with reference to these crucial local interactions.

This procedure is subject to some fundamental modelling assumptions, such as the continuity assumption and the exponential distribution of waiting times for each event, but it is otherwise independent of any assumptions on the structure of space. These enter through the closure assumptions, and there are often choices to be made, leading to different models: One option is to assume the law of mass-action, whereupon all spatial information is lost and mean-field equations are obtained. But other assumptions result in non-trivial correlation models, and the simplest of these is the pair model. (After this, there are triple models, and so on). Furthermore, there is not usually a unique pair model for a given system, because subtly different closure approximations may be possible, each leading to a distinct pair model. Interpreted as approximations, pair models reflect the nature of a parent model's explicit spatial structure. Interpreted as independent models in their own right, pair equations provide an alternative description of space directly.

## 7.2 Discussion

One important question which has not been addressed so far is the question of what constitutes a neighbour or contact. The answer is obvious in explicit lattice models, but this masks a less clear situation in the real world, and also for pair models. The short answer, of course, is that this depends upon the system in question, and different interpretations are possible. Unless migration and mobility events are specifically included in the pair model specification, the structure of a pair model necessarily implies that connections are long term, persistent associations that can only change with each discrete system event. However, this does not mean we must interpret a connection in a pair model as the permanent close physical proximity of two individuals. The interpretation could more loosely be that of an occasional regular social contact, or the expectation of a high degree of contact over a suitable period. As an extreme example, a predator-prey contact may equate to an astute

predator who is successful at finding prey (when it is available) in a way that others are not. Whatever the interpretation, this is an important consideration when using correlation models.

Comparison of the pair approximation process as described in this thesis with other published work listed in Chapter 2 is worthwhile and reassuring. (See Harada and Iwasa, 1994; Satō, Matsuda and Sasaki, 1994; Kubo, Iwasa and Furumoto, 1996; Matsuda, Ogita, Sasaki and Satō, 1992; Harada, Ezoe, Iwasa, Matsuda and Satō, 1995; Satō and Konno, 1995).

Fundamentally, the processes are very similar, and result in equivalent models in most cases. The method of derivation, however, is significantly different. The approach common to all these other papers is to use conditional probabilities. In their common notation, for example,

$$q_{\sigma|\sigma'}$$

is used to represent the probability that a randomly selected neighbour of an individual of type  $\sigma'$  is itself of type  $\sigma$ , and

$$q_{\sigma|\sigma'\sigma''}$$

is the probability that, given a  $\sigma'$  individual which is known to have a  $\sigma''$  neighbour, another randomly chosen neighbour is of type  $\sigma$ . These quantities are easily related to our n-path variable totals  $(i)$ ,  $(ij)$  and  $(ijk)$  (Note the conflicting notation -  $\sigma$  now represents an individual instead of the whole network as is the case in this thesis).

In these papers, the dynamical equations for these probabilities do not appear to be derived from any notational framework, but simply stated directly. With experience, this is not difficult to do for simple systems, but it is not necessarily an easy task in more complicated cases. The basic pair approximation then takes form

$$q_{\sigma|\sigma'\sigma''} \approx q_{\sigma|\sigma'}$$

*i.e.* one neighbour of a site does not affect another. In our language, this turns out to be equivalent to the multinomial assumption of Chapter 3, and it therefore does not incorporate any of the triangular effects discussed in Chapter 4 and present in our main  $(m, \phi)$  closure assumption. (All the models were built as approximations to 4-neighbour square grids or 2-neighbour one-dimensional lines).

Two of these papers (Satō, Matsuda and Sasaki, 1994; Harada, Ezoe, Iwasa, Matsuda and Satō, 1995) did consider a more sophisticated closure assumption, called the ‘Improved Pair Approximation’. This is based on the observation that some species form highly aggregated clumps in the explicit grid models. (In the systems they studied, this was mainly due to local birth rules). For example with + representing infected individuals and 0 susceptibles in a standard infection system, it was

typically the case that

$$q_{+|0+} > q_{+|0} \quad \text{and} \quad q_{+|00} < q_{+|0}$$

Instead of using the basic pair approximation directly, appropriate probabilities were biased with a scaling factor,  $\varepsilon$ , to reflect this observation, *e.g.*

$$q_{+|00} = \varepsilon q_{+|0}$$

where  $\varepsilon < 1$  is constant. An appropriate value for  $\varepsilon$  was estimated by assuming criticality of the host population without the infection. Alternatively, non-constant forms for  $\varepsilon$  were also considered in which  $\varepsilon$  varied as a function of a system parameter (in this case migration rate). In effect, the improved pair model approach biases a standard pair model in a way that reflects *a priori* the existence of higher order (triple) correlations which are known to exist. (see Keeling (1995) for a similar approach).

We have seen that pair models can be successful (spatial game lattice approximations, infection systems), but that this is not always the case. To understand this, we must remember that pair variables,  $(ij)$ , represent the relative correlations likely to be found between neighbouring individuals, but this is essentially all they do. In themselves, they do not say anything about the nature of entire local neighbourhoods. This information has to be implicitly deduced to construct a pair model, and this is one of the roles of the closure approximation. The usual approximations (covering all those in this thesis) effectively assume that each neighbourhood is an average neighbourhood consistent with known correlations. For example, the original hawk-dove spatial game pair approximation behaves as if each dove experiences the average environment for a dove (which depends on  $(dd)$  and  $(dh)$ ), and each hawk similarly sees the average hawk neighbourhood. This is a natural choice to make because any other approximation would require extra information on the distribution of neighbourhoods. This information is not available from the pair variables directly and must therefore be arbitrarily imposed in the model.

Unfortunately for pair models, some systems crucially depend on the structure of the entire local neighbourhood of an individual, and ignoring variability that exists between individuals' neighbourhoods has serious consequences. The best examples of this discussed in the thesis are the dynamic network spatial games (Chapter 3), where individual fitness, being the average score per neighbour, was highly non-linearly dependent on the individual's whole neighbourhood (because the number of neighbours is important). This system does not behave in the same way as would one in which all members of each species experience an average neighbourhood. By contrast, the spatial component of infection systems is only fundamentally concerned with the number of  $S$ - $I$  contacts, and pair models can easily cope with this.

### 7.3 Future Work

A large amount of work remains to be done on the detailed study and analysis of examples of pair models, in order to fully appreciate the range of behaviour, successes and failures that are possible. This applies both to those systems introduced in this thesis and to many more which were not. Thorough investigation should check that the pair models are behaving sensibly and compare the predictions of pair models with equivalent non-spatial systems. For successful models, it will usually be interesting to explore the range of behavioural dependencies that the models have on their parameters, especially spatial parameters (like  $m$  and  $\phi$ ), so that the implications of space can be qualitatively described. Because pair models will usually contain more parameters than their mean-field counterparts, this may be a lengthy task. Furthermore, as discussed, one biological system can easily lead to several pair models which are worthy of consideration, and this increases the work still further.

Systems incorporating individual migration and mobility, areas which were not addressed in detail in this thesis, are an obvious choice for other systems to study. The benefit to be gained from studying higher order correlation models is probably small while there is much to be done with pair models, especially because their complexity increases dramatically.

The  $(m, \phi)$  closure approximation is another area which should be considered in greater detail. Despite appearing to be a very natural way of closing pair equations, it was not derived from particularly clearly stated assumptions. There may or may not be a better way of deriving it, and it would be interesting to discover any alternatives. Furthermore, there may be other useful closure approximations which are worthy of consideration.

Finally, although analytical study of pair equations is not always easy, the differential equations produced by a successful pair model can provide a valuable starting point for further approximation. This is especially the case where the number of equations is considerable (more than two species, leading to more than five equations). One may be able to reduce the number of equations and ‘distill’ down the ODEs to reveal essential or fundamental relationships. For example, some spatial correlations may be trivial and there is then little point in modelling these pairs directly when the mass-action principle will suffice. This approach is taken by Keeling, Rand and Morris (1997) for the study of the measles equations: The SEIR pair equations are reduced to a fourth order system which concentrates on the dynamically important  $S$ - $I$  interactions (recall that the non-spatial SEIR equations are third order).

## 7.4 Summary

Much work remains to be done, but it is hoped that this thesis has shown that correlation models in general, and pair models in particular, have a valuable contribution to make in the search to understand the importance of spatial structure.



# Appendices

## A Binomial Theorem

The binomial theorem states that for any real numbers  $a$  and  $b$ , and any positive integer  $n$ ,

$$\sum_{i=0}^n \begin{bmatrix} n \\ i \end{bmatrix} a^i b^{n-i} = (a + b)^n \quad (\text{A } 1)$$

where the binomial coefficient is

$$\begin{bmatrix} n \\ i \end{bmatrix} = \frac{n!}{i!(n-i)!} \quad (\text{A } 2)$$

Useful results can be obtained by differentiating equation (A 1) with respect to  $a$  once, and then once again, each time multiplying through by  $a$  afterwards. (There is no problem with differentiation under the sum since it is a finite sum.)

$$\sum_{i=0}^n i \begin{bmatrix} n \\ i \end{bmatrix} a^i b^{n-i} = na(a+b)^{n-1} \quad (\text{A } 3)$$

$$\sum_{i=0}^n i^2 \begin{bmatrix} n \\ i \end{bmatrix} a^i b^{n-i} = na(na+b)(a+b)^{n-2} \quad (\text{A } 4)$$

The theorem is particularly important to probability theory when  $a + b = 1$  and  $a \in [0, 1]$  is interpreted as the probability of success on each attempt of  $n$  independent trials. Then

$$\begin{bmatrix} n \\ i \end{bmatrix} a^i (1-a)^{n-i}$$

is the probability of  $i$  successes in total, and equations (A 3) and (A 4) represent the expectation of  $i$  and  $i^2$ , the first two moments, from which the mean and variance are readily calculated to be  $na$  and  $nab$  respectively.

By applying the binomial theorem twice, a three-way multinomial equality is formed

$$\sum_{j=0}^n \sum_{i=0}^{n-j} \begin{bmatrix} n \\ ij \end{bmatrix} a^i b^j c^{n-i-j} = (a + b + c)^n \quad (\text{A } 5)$$

where this time

$$\begin{bmatrix} n \\ ij \end{bmatrix} = \frac{n!}{i!j!(n-i-j)!} \quad (\text{A } 6)$$

Differentiation (with respect to  $a$  and  $b$ ) now produces

$$\sum_{j=0}^n \sum_{i=0}^{n-j} i \begin{bmatrix} n \\ ij \end{bmatrix} a^i b^j c^{n-i-j} = na(a+b+c)^{n-1} \quad (\text{A } 7)$$

$$\sum_{j=0}^n \sum_{i=0}^{n-j} ij \begin{bmatrix} n \\ ij \end{bmatrix} a^i b^j c^{n-i-j} = n(n-1)ab(a+b+c)^{n-2} \quad (\text{A } 8)$$

As a probability distribution, where  $a + b + c = 1$ , equation (A 7) and its two sister equations again say that the three mutually exclusive (and exhaustive) events have means  $na$ ,  $nb$  and  $nc$ . The probability here

$$\begin{bmatrix} n \\ ij \end{bmatrix} a^i b^j c^{n-i-j}$$

of  $i$  event  $a$ ,  $j$  event  $b$  and  $n - i - j$  event  $c$  occurrences is identical to the probability of  $i$  event  $a$  occurrences and  $n - i$  non occurrences given by the original binomial distribution, so each event in a trinomial distribution is individually binomially distributed with the same probability.

Equations (A 1) to (A 8) are used throughout the text, usually in the form  $a + b = 1$  or  $a + b + c = 1$ , where either  $a$  and  $b$  are known directly, or when the mean and  $n$  are known, enabling  $a$  to be deduced.

## B Software and Computation

All computer simulations studied in this thesis were programmed by the author in the C language and run on Sun SPARC IPX, 10 and 20 UNIX workstations. All numerical integration of resulting ODE systems was performed with fourth order Runge-Kutta integration schemes.

Numerical simulations of the individual based models in this thesis (such as the square grid spatial game of Chapter 2) can be computationally expensive, especially when the population is large and several types of event must be considered. This is largely due to the time required for the computer to generate many random numbers. These simulations proceed by sequentially choosing and implementing a series of random events, but there is a trick which reduces the number of random numbers needed to do this. The obvious (but slow) method consists of i) choosing a (random) waiting time for each possible event that can occur in the system at the current time. ii) implementing the event with the shortest of these waiting times,  $T_{\min}$ , *i.e.* making appropriate changes to the individuals and incrementing time by  $T_{\min}$ . iii) returning to step i) for the next event. The short cut relies on the fact that any one event is likely to only directly affect a few individuals, and the waiting times are exponentially distributed (so the expected waiting time at any instant is independent of the length

of time already elapsed). This method begins in the same way as above: i) choose a waiting time for each possible event that can occur in the system at the current time. ii) implement the event with the shortest waiting time,  $T_{\min}$ . However, instead of returning directly to step i), we now iii) choose a new random waiting time only for the potential events which have been directly affected by the latest actual event. These are the events that now occur at a different rate than before, plus any new events which were not previously possible. For all other events, we do not select a new random expected waiting time, but instead subtract  $T_{\min}$  from each one's previously expected waiting time. (This will reduce all such times, but still leave them positive, because  $T_{\min}$  was the smallest such time). iv) return to step ii). Improvements in computing time can be significant because in each simulation cycle, many random number generations are replaced by (much quicker) subtractions.

Exponentially distributed waiting times,  $T(\lambda)$ , are randomly chosen by generating a floating point random variable  $X \in (0, 1)$  and transforming with the relation

$$T = \frac{-1}{\lambda} \log(1 - X)$$

where  $\lambda$  is the exponential distribution parameter, equal to the average waiting time.

Several freely available software packages, listed below, were used during the development and presentation of the work contained in this thesis.

DSTool (Guckenheimer, J., Meyers, M.R., Wicklin, F.J. and Worfolk, P.A. - Center for Applied Mathematics, Cornell University, New York, 1991) is a dynamical system toolkit with an interactive graphical interface. It was used extensively to numerically investigate the dynamical properties of the many different dynamical systems, (mainly coupled nonlinear ODEs), that appear in this thesis. It was also used to provide numerical data for use in some graphs and figures. All numerical integrations performed using Dstool also used a fourth order Runge-Kutta integration scheme.

Maple (release V, from Waterloo Maple Software, 1990) is a computer algebra package. It was used to algebraically solve for fixed points in the more complex ODE systems, and also to obtain the Jacobian matrix, characteristic equation and resulting eigenvalues and eigenvectors necessary for linear stability analysis.

Matlab (The MathWorks, Inc., 21 Eliot Street, South Natick, MA 01760, USA) is a powerful mathematical and graphical toolkit. It was heavily used for analysing, interpreting and viewing much of the data produced by both the author's simulations and also from DSTool. In addition, virtually all of the graphs in this thesis were produced using Matlab.

Other schematic diagrams and figures were produced with Xfig and edited using xv (version 3.10 by John Bradley, 1994).

This thesis was typeset using L<sup>A</sup>T<sub>E</sub>X.

## C Abbreviations

The following abbreviations are defined in and used throughout the text:

**CA** Cellular Automata

**CML** Coupled Map Lattice

**ESS** Evolutionarily Stable Strategy

**IPS** Interacting Particle System

**IPD** Iterated Prisoner's Dilemma

**ODE** Ordinary Differential Equation

**PA** Pair Approximation

**PDE** Partial Differential Equation

**RAS** Realistic Age Structure Measles Model

# References

- Andreasen, V. and Christiansen, F.B. (1995)  
SLOW COEVOLUTION OF A VIRAL PATHOGEN AND ITS DIPLOID HOST.  
*Phil. Trans. R. Soc. Lond. B* **348** : 341-354
- Anita, A., Koella, J.C. and Perrot, V. (1996)  
MODELS OF THE WITHIN-HOST DYNAMICS OF PERSISTENT MYCOBACTERIAL INFECTIONS.  
*Proc. R. Soc. Lond. B* **263** : 257-263
- Ardito, A. and Ricciardi, P. (1995)  
LYAPUNOV FUNCTIONS FOR A GENERALIZED GAUSE-TYPE MODEL.  
*J. Math. Biol.* **33** : 816-828
- Altmann, M. (1995)  
SUSCEPTIBLE-INFECTED-REMOVED EPIDEMIC MODELS WITH DYNAMIC PARTNERSHIPS.  
*J. Math. Biol.* **33** : 661-675
- Anderson, R.M. and May, R.M. (1992)  
INFECTIOUS DISEASES OF HUMANS: DYNAMICS AND CONTROL.  
Oxford Science Publications, O.U.P.
- Axelrod, R. and Dion, D. (1988)  
THE FURTHER EVOLUTION OF COOPERATION.  
*Science* **242** : 1385-1390
- Axelrod, R. and Hamilton, W.D. (1981)  
THE EVOLUTION OF COOPERATION.  
*Science* **211** : 1390-1396
- Bascompte, J. and Solé, R.V. (1995)  
RETHINKING COMPLEXITY: MODELLING SPATIOTEMPORAL DYNAMICS IN ECOLOGY.  
*Trends in Ecology and Evolution* **10** : 361-366
- Batali, J. and Kitcher, P. (1995)  
EVOLUTION OF ALTRUISM IN OPTIONAL AND COMPULSORY GAMES.  
*J. Theor. Biol.* **175** : 161-171

- Boerlijst, M.C. and Hogeweg, P. (1995)  
 ATTRACTORS AND SPATIAL PATTERNS IN HYPERCYCLES WITH NEGATIVE INTERACTIONS.  
*J. Theor. Biol.* **176** : 199-210
- Bolker, B. and Grenfell, B.T. (1993)  
 CHAOS AND BIOLOGICAL COMPLEXITY IN MEASLES DYNAMICS.  
*Proc. R. Soc. Lond. B* **251** : 75-81
- Bolker, B. and Grenfell, B.T. (1995)  
 SPACE, PERSISTENCE AND DYNAMICS OF MEASLES EPIDEMICS.  
*Phil. Trans. R. Soc. Lond. B* **348** : 309-320
- Bolker, B. and Pacala, S. (1996)  
 UNDERSTANDING STOCHASTICALLY DRIVEN SPATIAL PATTERN FORMATION IN ECOLOGICAL SYSTEMS USING MOMENT EQUATIONS.  
 Princeton Preprint.
- Boyd, R. and Lorberbaum, J.P. (1987)  
 NO PURE STRATEGY IS EVOLUTIONARILY STABLE IN THE REPEATED PRISONER'S DILEMMA GAME.  
*Nature* **327** : 58-59
- Connor, R.C. (1995)  
 ALTRUISM AMONG NON-RELATIVES: ALTERNATIVES TO THE PRISONER'S DILEMMA.  
*Trends in Ecology and Evolution* **10** : 84-86
- Cressman, R. (1990)  
 STRONG STABILITY AND DENSITY-DEPENDENT EVOLUTIONARILY STABLE STRATEGIES.  
*J. Theor. Biol.* **145** : 319-330
- DeRoos, A.M., McCauley, E. and Wilson, W.G. (1991)  
 MOBILITY VERSUS DENSITY-LIMITED PREDATOR-PREY DYNAMICS ON DIFFERENT SPATIAL SCALES.  
*Proc. R. Soc. Lond. B* **246** : 117-122
- Dickman, R. (1986)  
 KINETIC PHASE TRANSITIONS IN A SURFACE REACTION MODEL: MEAN FIELD THEORY.  
*Physics Review A* **34** 4246-4250
- Durrett, R. and Levin, S. (1994a)  
 THE IMPORTANCE OF BEING DISCRETE (AND SPATIAL).  
*Theor. Pop. Biol.* **46** : 363-394

- Durrett, R. and Levin, S. (1994b)  
 STOCHASTIC SPATIAL MODELS: A USER'S GUIDE TO ECOLOGICAL APPLICATIONS.  
*Phil. Trans. R. Soc. Lond. B* **343** : 329-350
- Dushoff, J. (1996)  
 INCORPORATING IMMUNOLOGICAL IDEAS IN EPIDEMIOLOGICAL MODELS.  
*J. Theor. Biol.* **180** : 181-187
- Edmunds, W.J., O'Callaghan, C.J. and Nokes, D.J. (1997)  
 WHO MIXES WITH WHOM? A METHOD TO DETERMINE THE CONTACT PATTERNS OF  
 ADULTS THAT MAY LEAD TO THE SPREAD OF AIRBOURNE INFECTIONS.  
*Proc. R. Soc. Lond. B* **264** : 949-957
- Farrell, J. and Ware, R. (1989)  
 EVOLUTIONARY STABILITY IN THE REPEATED PRISONER'S DILEMMA.  
*Theor. Pop. Biol.* **36** : 161-166
- Ferriere, R. and Michod, R.E. (1995)  
 INVADING WAVE OF COOPERATION IN A SPATIAL ITERATED PRISONER'S DILEMMA.  
*Proc. R. Soc. Lond. B* **259** : 77-83
- Ferriere, R. and Michod, R.E. (1996)  
 THE EVOLUTION OF COOPERATION IN SPATIALLY HETEROGENEOUS POPULATIONS.  
*The American Naturalist* **147** : 692-717
- Frean, M.R. (1994)  
 THE PRISONER'S DILEMMA WITHOUT SYNCHRONY.  
*Proc. R. Soc. Lond. B* **257** : 75-59
- Glendinning, P. (1994)  
 ISLAND CHAIN MODELS AND GRADIENT SYSTEMS.  
*J. Math. Biol.* **32** : 171-178
- Granovsky, B.L. and Rozov, L. (1994)  
 ON TRANSIENT BEHAVIOUR OF A NEAREST NEIGHBOUR BIRTH-DEATH PROCESS ON A  
 LATTICE.  
*J. App. Prob.* **31** : 549-553
- Grenfell, B.T., Bolker, B.M. and Kleczkowski, A. (1995)  
 SEASONALITY AND EXTINCTION IN CHAOTIC METAPOPULATIONS.  
*Proc. R. Soc. Lond. B* **259** : 97-103
- Grim, P. (1995)  
 THE GREATER GENEROSITY OF THE SPATIALIZED PRISONER'S DILEMMA.  
*J. Theor. Biol.* **173** : 353-359

- Guckenheimer J. and Holmes P. (1983)  
 NONLINEAR OSCILLATIONS, DYNAMICAL SYSTEMS AND BIFURCATIONS OF VECTOR FIELDS.  
 Springer Verlag
- Hamilton, W.D., Axelrod, R. and Tanese, R. (1990)  
 SEXUAL REPRODUCTION AS AN ADAPTATION TO RESIST PARASITES (REVIEW).  
*Proc. Nat. Acad. Sci. USA* **87** : 3566-3573
- Harada, Y., Ezoe, H., Iwasa, Y., Matsuda, H. and Satō, K. (1995)  
 POPULATION PERSISTENCE AND SPATIALLY LIMITED SOCIAL INTERACTION.  
*Theor. Pop. Biol.* **48** : 65-91
- Harada, Y. and Iwasa, Y. (1994)  
 LATTICE POPULATION DYNAMICS FOR PLANTS WITH DISPERSING SEEDS AND VEGETATIVE  
 PROPAGATION.  
*Res. Popul. Ecol.* **36(2)** : 237-249
- Herz, A.V.M. (1994)  
 COLLECTIVE PHENOMENA IN SPATIALLY EXTENDED EVOLUTIONARY GAMES.  
*J. Theor. Biol.* **169** : 65-87
- Hethcote, H.W. and van den Driessche, P. (1996)  
 AN SIS EPIDEMIC MODEL WITH VARIABLE POPULATION SIZE AND A DELAY.  
*Math. Biol.* **34** : 177-194
- Hofbauer, J. (1996)  
 EVOLUTIONARY DYNAMICS FOR BIMATRIX GAMES: A HAMILTONIAN SYSTEM?  
*J. Math. Biol.* **34** : 675-688
- Hofbauer, J. and Sigmund, K. (1987)  
 DYNAMICAL SYSTEMS AND THE THEORY OF EVOLUTION.  
 Cambridge University Press.
- Hofstadter, D.R. (1983)  
 MATHEMATICAL THEMAS: COMPUTER TOURNAMENTS OF THE PRISONER'S DILEMMA SUG-  
 GEST HOW COOPERATION EVOLVES.  
*Scientific American* **248** : 14-20
- Hsu, L., Hsu, T., Mortimer, J., Panju, M. and Schroeder, S. (1995)  
 DYNAMICALLY STABLE MULTIPLE STRATEGY STATES OF THE ITERATED PRISONER'S DILEMMA.  
*Physica D* **85** : 296-303
- Hutson, V.C.L. and Vickers, G.T. (1995)  
 THE SPATIAL STRUGGLE OF TIT-FOR-TAT AND DEFECT.  
*Phil. Trans. R. Soc. Lond. B* **348** : 393-404



- Jonansen, A. (1996)  
A SIMPLE MODEL OF RECURRENT EPIDEMICS.  
*J. Theor. Biol.* **178** : 45-51
- Keeling, M.J. (1995)  
THE ECOLOGY AND EVOLUTION OF SPATIAL HOST-PARASITE SYSTEMS.  
*Ph.D. Thesis*, Warwick University, U.K.
- Keeling, M.J. and Grenfell, B.T. (1997)  
DISEASE EXTINCTION AND COMMUNITY SIZE: MODELLING THE PERSISTENCE OF MEASLES.  
*Science* **275** : 65-67
- Keeling, M.J. and Rand, D.A. (1996)  
TWO METHODS TO MODEL THE PERSISTENCE OF MEASLES IN A POPULATION.  
Warwick Preprint.
- Keeling, M.J., Rand, D.A. and Morris, A.J. (1997)  
CORRELATION MODELS FOR CHILDHOOD EPIDEMICS.  
*Proc. R. Soc. Lond. B* **264** : 1-8
- Krakauer, D.C. and Pagel, M. (1995)  
SPATIAL STRUCTURE AND THE EVOLUTION OF COST-FREE SIGNALLING.  
*Proc. R. Soc. Lond. B* **260** : 365-372
- Kubo, T., Iwasa, Y. and Furumoto, N. (1996)  
FOREST SPATIAL DYNAMICS WITH GAP EXPANSION: TOTAL GAP AREA AND GAP SIZE DISTRIBUTION.  
*J. Theor. Biol.* **180** : 229-246
- Lemaître, A., Chaté, H. and Manneville, P. (1995)  
CLUSTER EXPANSION FOR COLLECTIVE BEHAVIOUR IN DISCRETE-SPACE DYNAMICAL SYSTEMS.  
Preprint
- Levin, S.A. and Durrett, R. (1996)  
FROM INDIVIDUALS TO EPIDEMICS.  
Princeton/Cornell Preprint.
- Lindgren, K. and Nordahl, M.G. (1994)  
EVOLUTIONARY DYNAMICS OF SPATIAL GAMES.  
*Physica D* **75** : 292-309
- Lloyd, A.L. and May, R.M. (1996)  
SPATIAL HETEROGENEITY IN EPIDEMIC MODELS.  
*J. Theor. Biol.* **179** : 1-12

- Lorberbaum, J. (1994)  
 NO STRATEGY IS EVOLUTIONARILY STABLE IN THE REPEATED PRISONER'S DILEMMA.  
*J. Theor. Biol.* **168** : 117-130
- Lotka, A.J. (1925)  
 THE ELEMENTS OF PHYSICAL BIOLOGY.  
 Williams and Williams Co., Baltimore.
- Malthus, T. (1798)  
 ESSAY ON THE PRINCIPLE OF POPULATION.  
 In: The Faber Book of Science, ed. John Carey. Faber and Faber, London.
- Matsuda, H., Ogita, N., Sasaki, A. and Satō, K. (1992)  
 STATISTICAL MECHANICS OF POPULATION - THE LATTICE LOTKA-VOLTERRA MODEL.  
*Prog. Theor. Phys.* **88** : 1035-1049
- May, R.M. (1974)  
 BIOLOGICAL POPULATIONS WITH NON-OVERLAPPING GENERATIONS: STABLE POINTS, STABLE CYCLES AND CHAOS.  
*Science* **186** : 645-647
- May, R.M. (1976)  
 SIMPLE MATHEMATICAL MODELS WITH VERY COMPLICATED DYNAMICS. (REVIEW)  
*Nature* **261** : 459-467
- May, R.M. (1987)  
 MORE EVOLUTION OF COOPERATION.  
*Nature* **327** : 15-17
- May, R.M. (1994)  
 SPATIAL CHAOS AND ITS ROLE IN ECOLOGY AND EVOLUTION.  
 Frontiers of Theoretical Biology (Lecture Notes in Biomathematics vol. 100). Springer, New York.
- Maynard Smith, J. (1974)  
 THE THEORY OF GAMES AND THE EVOLUTION OF ANIMAL CONFLICTS.  
*J. Theor. Biol.* **47** : 209-221
- Maynard Smith, J. (1982)  
 EVOLUTION AND THE THEORY OF GAMES.  
 Cambridge University Press
- Maynard Smith, J. and Price, G.R. (1973)  
 THE LOGIC OF ANIMAL CONFLICT.  
*Nature* **246** : 15-18

- Mesterton-Gibbons, M. (1992)  
ON THE ITERATED PRISONER'S DILEMMA IN A FINITE POPULATION.  
*Bull. of Math. Biol.* **54** : 423-443
- Molander, P. (1985)  
THE OPTIMAL LEVEL OF GENEROSITY IN A SELFISH, UNCERTAIN ENVIRONMENT.  
*J. Conflict Resolution* **29** : 611-618
- Murray, J.D. (1990)  
MATHEMATICAL BIOLOGY  
Springer-Verlag
- Nowak, M. (1990)  
STOCHASTIC STRATEGIES IN THE PRISONER'S DILEMMA.  
*Theor. Pop. Biol.* **38** : 93-112
- Nowak, M. and May, R.M. (1992)  
EVOLUTIONARY GAMES AND SPATIAL CHAOS.  
*Nature* **359** : 826-829
- Nowak, M., May, R.M. and Sigmund, K. (1995)  
THE ARITHMETICS OF MUTUAL HELP.  
*Scientific American* **June 1995** : 50-55
- Nowak, M. and Sigmund, K. (1992)  
TIT-FOR-TAT IN HETEROGENEOUS POPULATIONS.  
*Nature* **355** : 250-252
- Nowak, M. and Sigmund, K. (1993)  
A STRATEGY OF WIN-STAY, LOSE-SHIFT THAT OUTPERFORMS TIT-FOR-TAT IN THE PRISONER'S DILEMMA.  
*Nature* **364** : 56-58
- Nowak, M. and Sigmund, K. (1994)  
THE ALTERNATING PRISONER'S DILEMMA.  
*J. Theor. Biol.* **168** : 219-226
- Nowak, M., Sigmund, K. and El-Sedy, E. (1995)  
AUTOMATA, REPEATED GAMES AND NOISE.  
*J. Math. Biol.* **33** : 703-722
- Olsen, L.F. and Schaffer, W.M. (1990)  
CHAOS VERSUS NOISY PERIODICITY: ALTERNATIVE HYPOTHESES FOR CHILDHOOD EPIDEMIC.  
*Science* **249** : 499-504

- Poundstone, W. (1992)  
 PRISONER'S DILEMMA: JOHN VON NEUMANN, GAME THEORY, AND THE PUZZLE OF THE BOMB.  
 Oxford University Press.
- Rand, D.A. (1994)  
 MEASURING AND CHARACTERISING SPATIAL PATTERNS, DYNAMICS AND CHAOS IN SPATIALLY EXTENDED DYNAMICAL SYSTEMS AND ECOLOGIES.  
*Phil. Trans. R. Soc. Lond. B* **348** : 497-514
- Rand, D.A., Keeling, M., and Wilson, H.B. (1995)  
 INVASION, STABILITY AND EVOLUTION TO CRITICALITY IN SPATIALLY EXTENDED, ARTIFICIAL HOST-PATHOGEN ECOLOGIES.  
*Proc. R. Soc. Lond. B* **259** : 55-63
- Rand, D.A. and Wilson, H.B. (1991)  
 CHAOTIC STOCHASTICITY - A UBIQUITOUS SOURCE OF UNPREDICTABILITY IN EPIDEMICS.  
*Proc. R. Soc. Lond. B* **246** : 179-184
- Rand, D.A. and Wilson, H.B. (1995)  
 USING SPATIO-TEMPORAL CHAOS AND INTERMEDIATE-SCALE DETERMINISM TO QUANTIFY SPATIALLY EXTENDED ECOSYSTEMS.  
*Proc. R. Soc. Lond. B* **259** : 111-117
- Rhodes, C.J. and Anderson, R.M. (1996)  
 PERSISTENCE AND DYNAMICS IN LATTICE MODELS OF EPIDEMIC SPREAD.  
*J. Theor. Biol.* **180** : 125-133
- Roughgarden, J. (1979)  
 THEORY OF POPULATION GENETICS AND EVOLUTIONARY ECOLOGY: AN INTRODUCTION.  
 Macmillan Publishing Co. Inc., New York.
- Rozanov, Y.A., translated by Silverman, R.A. (1977)  
 PROBABILITY THEORY: A CONCISE COURSE.  
 Dover Publications Inc., New York.
- Ruxton, G.D. (1994)  
 LOW LEVELS OF IMMIGRATION BETWEEN CHAOTIC POPULATIONS CAN REDUCE SYSTEM EXTINCTIONS BY INDUCING ASYNCHRONOUS REGULAR CYCLES.  
*Proc. R. Soc. Lond. B* **256** : 189-193
- Satō, K. and Konno, N. (1995)  
 SUCCESSIONAL DYNAMIC MODELS ON THE 2-DIMENSIONAL LATTICE SPACE.  
*J. Phys. Soc. Japan* **64**(6) : 1866-1869

- Satō, K., Matsuda, H. and Sasaki, A. (1994)  
PATHOGEN INVASION AND HOST EXTINCTION IN LATTICE STRUCTURED POPULATIONS.  
*J. Math. Biol.* **32** : 251-268
- Scheuring, I. and János, I.M. (1996)  
WHEN TWO AND TWO MAKE FOUR: A STRUCTURED POPULATION WITHOUT CHAOS.  
*J. Theor. Biol.* **178** : 89-97
- Taylor, P.D. and Jonker, L.B. (1978)  
EVOLUTIONARY STABLE STRATEGIES AND GAME DYNAMICS.  
*Mathematical Biosciences* **40** : 145-156
- Tilman, D. (1994)  
COMPETITION AND BIODIVERSITY IN SPATIALLY STRUCTURED HABITATS.  
*Ecology* **75** : 2-16
- Tomé, T. and Drugowich de Felício, J.R. (1996)  
PROBABILISTIC CELLULAR AUTOMATON DESCRIBING A BIOLOGICAL IMMUNE SYSTEM.  
*Physical Review E* **53** : 3976-3981
- van Baalen, M. and Rand, D.A. (1997)  
THE UNIT OF SELECTION IN VISCOUS POPULATIONS AND THE EVOLUTION OF ALTRUISM.  
*Phil. Trans. R Soc. Lond. B (Submitted)*
- van Herwaarden, O.A. and Grasman, J. (1995)  
STOCHASTIC EPIDEMICS: MAJOR OUTBREAKS AND THE DURATION OF THE ENDEMIC PERIOD.  
*J. Math. Biol.* **33** : 581-601
- Volterra, V. (1926)  
FLUCTUATIONS IN THE ABUNDANCE OF A SPECIES CONSIDERED MATHEMATICALLY.  
*Nature* **118** : 558-560
- Weisser, W.W. and Hassell, M.P. (1996)  
ANIMALS 'ON THE MOVE' STABILIZE HOST-PARASITOID SYSTEMS.  
*Proc. R. Soc. Lond. B* **263** : 749-754
- Wilson, D.S., Pollock, G.B. and Dugatkin, L.A. (1992)  
CAN ALTRUISM EVOLVE IN PURELY VISCOUS POPULATIONS?  
*Evolutionary Ecology* **6** : 331-341
- Zeeman, E.C. (1981)  
DYNAMICS OF THE EVOLUTION OF ANIMAL CONFLICTS.  
*J. Theor. Biol.* **89** : 249-270

Zhou, J. and Hethcote, H.W. (1994)

POPULATION SIZE DEPENDENT INCIDENCE IN MODELS FOR DISEASES WITHOUT IMMUNITY.

*J. Math. Biol.* **32** : 809-834